Acta Morphologica Hungarica

VOLUME 35, NUMBERS 1–2, 1987

Akadémiai Kiadó, Budapest
ACTA MORPH. HUNG. HU ISSN 0236—5391

ACTA MORPHOLOGICA
HUNGARICA
A QUARTERLY OF THE HUNGARIAN ACADEMY OF SCIENCES

Acta Morphologica publishes original papers on experimental morphology and pathology in English.

Acta Morphologica is published in yearly volumes of four issues by

AKADÉMIAI KIADÓ
Publishing House of the Hungarian Academy of Sciences
H-1054 Budapest, Alkotmány u. 21.

Manuscripts and editorial correspondence should be addressed to

Acta Morphologica
Ist Institute of Pathology and Experimental Cancer Research, Semmelweis Medical University,
1085 Budapest, Üllői út 26, Hungary

Subscription information

Orders should be addressed to

KULTURA Foreign Trading Company
H-1389 Budapest P.O. Box 149

or to its representatives abroad

Acta Morphologica Hungarica is abstracted/indexed in Biological Abstracts, Chemical Abstracts, Chemie-Information, Current Contents–Life Sciences, Excerpta Medica, Gerontological Abstracts, Index Medicus

Acta Morphologica

Hungarica

INDEX

Volume 35

Akadémiai Kiadó, Budapest
1987

ACTA MORPHOLOGICA

VOLUME 35

CONTENTS

AUTHOR INDEX

CONTENTS

Normal and experimental morphology

Pathology

Acta Morphologica Hungarica, 35 (1—2) pp. 3—8 (1987)

MUTAGENICITY STUDIES ON TERBACIL, AN URACIL-ANALOGUE PESTICIDE

M. Börzsönyi, Zsuzsanna Kocsis, A. Pintér, Márta Csik, Zs. Kelecsényi, A. Surján, G. Török

NATIONAL INSTITUTE OF HYGIENE, BUDAPEST, HUNGARY

(Received 3 December 1985)

The possible mutagenic effect of the uracil analogue pesticide Terbacil was examined on *Drosophila melanogaster* and in mammalian cell culture.

Terbacil did not prove to be mutagenic in the sex-linked recessive lethal mutation test, and it did not cause an increase in sister chromatid exchange in CHO cells. It cannot be considered a chromosome-mutagenic compound.

Considering the procaryote studies known from the literature, it is assumed that Terbacil does not represent a genotoxic hazard for the persons involved either in its production or its use.

Introduction

The increased use of chemicals in agriculture makes it necessary to carry out thorough toxicological examinations of chemicals produced in large volumes. Detection of mutagenic or carcinogenic effects is of utmost importance.

Some uracil derivatives are used as non-specific herbicides in significant quantities in agriculture. The most famous of them are Terbacil (3-tertiary-butyl-5-chloro-6-methyl-uracil), Bromacil (5-bromo-3-tertiary-butyl-5,6-trimethylene-uracil), and Lenacil (3-cyclohexyl-5,6-trimethylene uracil). The structure of these compounds suggests a mutagenic activity if incorporated into DNA.

This possibility is substantiated by 5-fluorouracil which is used in human medicine as a cytostatic agent. The three herbicides (Terbacil, Bromacil and Lenacil) have been marketed for several years and studies were carried out to discover their eventual mutagenic effect in microbial systems. Moriya et al. [4] studied these three uracil-derivatives using 5 Salmonella strains, and found no mutagenic effect. Similarly negative results were found in *Bacillus subtilis* rev-assay [4]. Mutagenicity studies were carried out in higher organisms with Bromacil, with negative results. Terbacil has, however, not yet been examined in higher organisms.

Send offprint requests to: M. Börzsönyi, National Institute of Hygiene, Budapest, Gyáli 2—6, 1097 Hungary

In the present paper an account is given about the possible chromosome damaging effect of Terbacil, namely about its effect causing sister chromatid exchange in mammalian cell culture, as well as about its mutagenic effect in the gametes of *Drosophila melanogaster*.

Materials and methods

Technically pure Terbacil was [provided by Chemical Works of Gedeon Richter LTD, Budapest, Hungary.

Sister chromatid exchange

The examination of sister chromatid exchange was done on Chinese hamster ovary cells (CHO-Kl) [2]. The cells were obtained from dr. I. Raskó (Biological Centre of the Hungarian Academy of Sciences, Szeged). As a culture medium we used Ham's Fl2 of Serva, Heidelberg, FRG to which 5% fetal calf serum was added (Gibco, England). The cultures were kept at 37 °C in a humidified incubator in the presence of 5% CO_2.

The liver microsome fraction for the metabolic activation system was prepared according to Ames et al. [1], while the whole system was constructed according to Natarajan et al. [5].

The toxicity of Terbacil was established by studying cell survival (relative plating efficiency) after treatment.

The test was carried out as described by Natarajan et al. [5]. 1×10^6 cells were plated out on 90 mm Petri dishes, and after a period of 24 hours the treatment was done with the doses chosen on the basis of the toxicity test, i.e. with 400—200—100—40 μg/ml Terbacil. The treatment lasted 3 hours in the presence of the metabolic activation system, and 24 hours without it. The culture fluid contained 3 μg/ml bromodeoxyuridine (Sigma). For the last two hours 0.5 μg/ml colchicine (Sigma) was added. Metaphases were prepared in the usual way: after a hypotonic treatment in 0.075 M KCl, followed by triple fixation in 3 parts methanol and 1 part acetic acid, they were dried in air. The plates were stained with 0.5 μg/ml Hoechst 33258 fluorochrome stain (Merck) for 20 minutes, then exposed to UV-irradiation in McIlvaine buffer (pH 8.0) for 3 hours, at a temperature of 60 °C. As a radiation source two 15 W germicide lamps were used.

The preparations were stained with 4% Giemsa solution (pH 6.8) for 20 minutes. The test was carried out twice, and cyclophosphamide (15 μg/ml) and N-methyl-N'-nitro-N-nitrosoguanidine (1 μg/ml) were used as positive control compounds.

Sex linked recessive lethal test on Drosophila

The test was performed according to Würgler and co-workers [14] and the guidelines of UKEMS Part 1. Muller-5 females and males of (yw^{co}/Y) genotype were provided by Dr J. Szabad (Szeged Biological Centre of the Hungarian Academy of Sciences).

The males were 2—4 days old at the time of the toxicity test, and at the beginning of this test, while the females were 3—5 days old when mated with males.

Since Terbacil in standard food did not sufficiently toxic, it was mixed into food containing 5% ethanol and 5% Tween 80.

After establishment of toxicity (rendering about 50% lethality) male flies were kept on standard food containing 10% Terbacil, 5% ethylalcohol and 5% Tween 80 for 7 days. The surviving males mated with M-5 virgin females in a proportion 1 : 3. Because of the length of the time needed for poisoning, no brooding was carried out. In the course of the examination, 3088 Fl females were raised, each one carrying a "treated" x-chromosome.

Results

Results of the toxicity test of Terbacil on CHO cells are shown in Table I. On the basis of the toxicity examination 400—200—100—40 μg/ml Terbacil

Table I

Terbacil	No. of colonies*	Relative plating efficiency, per cent
400 μg/ml	15.6	22.2
200 μg/ml	32.3	46.1
100 μg/ml	51.3	73.2
40 μg/ml	83.3	110.0

* Mean number of colonies on 3 Petri dishes

Table II

Quantitative distribution of SCE in CHO cells after Terbacil treatment

	With metabolic activation			Without metabolic activation		
	Number of experiments	Number of metaphases	Mean (SD)	Number of experiments	Number of metaphases	Mean (SD)
Terbacil 400 μg/ml	1	30	7.9 ± 2.1	1	toxic	
	2	30	10.7 ± 2.4	2	toxic	
Terbacil 200 μg/ml	1	30	8.0 ± 1.9	1	30	7.9 ± 3.2
	2	NT		2	30	8.6 ± 1.0
Terbacil 100 μg/ml	1	30	10.2 ± 1.6	1	30	9.9 ± 1.6
	2	30	11.4 ± 2.8	2	30	7.6 ± 0.7
Terbacil 40 μg/ml	1	30	8.2 ± 2.2	1	30	7.5 ± 1.3
	2	30	10.7 ± 1.9	2	30	7.3 ± 0.9
Cyclophosphamide 15 μg/ml	1	30	37.7 ± 4.9*			
	2	30	29.5 ± 6.7*			
Methylnitrosoguanidine 1 μg/ml				1	30	31.3 ± 4.1*
				2	30	31.4 ± 6.0*
Dimethylformamide 1%	1	30	7.6 ± 1.8	1	30	9.1 ± 1.7
	2	30	10.2 ± 2.4	2	30	6.9 ± 0.9
Untreated control	1	30	8.5 ± 3.2	1	30	6.9 ± 1.3
	2	30	8.5 ± 3.8	2	30	7.0 ± 1.3

* $p < 0.01$

Table III

Terbacil concentration	5% ethanol + 5% Tween 80	Exposure time	Died/total
20%	—	5 days	2/74
10%	—	5 days	3/81
20%	—	8 days	2/68
10%	+	7 days	103/173
10%	+	7 days	23/84
—	+	9 days	11/143

Table IV

Treatment	Number of examined males	Number of examined chromosomes	Number of examined chromosomes	per cent**
10% Terbacil 5% ethanol 5% Tween 80	62	4	3088	0.13
5% ethanol 5% Tween 80	113	3	2988	0.1
Untreated control	82	5	3272	0.15
Positive control*	17	90	333	27

* The animals were given 0.25 volume per cent ethylmethane-sulphonate in 1% saccharose for a period of 8 hours following 12 hours of starving.

** Number of chromosomes with recessive lethal mutation expressed in the percentage of all chromosomes.

doses were used in both experiments. In each group 30 metaphases were evaluated, and the results were calculated by two-tailed-*t*-probe.

The results of the two examinations are shown in Table II.

Results of the toxicity test on *Drosophila melanogaster* are shown in Table III.

On basis of these results, in the M-5 test males fed with 10% Terbacil, 5% ethanol, and 5% Tween 80 in their food were used as experimental animals.

Results of the recessive lethal test are summarized in Table IV.

Discussion

Modern agriculture is dependent on the use of pesticides. For the wide application of these compounds it is, however, important to study their eventual genotoxic effect, as they may endanger a large number of people with their possible mutagenic/carcinogenic action.

According to our knowledge, the possible genotoxic effect of the herbicide Terbacil has only been examined in microbial systems [5]. The different sensitivity of higher organisms, and the differences between the metabolic activation systems, as well as between the detoxicating systems necessitate the study of xenobiotic agents in eucaryotic systems. The phenomenon of sister chromatid exchange appears as a result of an exchange between homologous parts of the original, and the new chain during DNA replication. Though its exact genetic backgorund and molecular mechanisms has not been cleared, the phenomenon is connected with DNA breakage and reunion. A great number of DNA damages may provoke SCE, and also certain known clastogens (agents causing chromosomal aberration) may give rise to SCE, often in concentrations below

the clastogenic dose [3]. This test has widely been used for screening potential mutagens/carcinogens [11].

The possible SCE inducing effect of Terbacil has been examined on CHO cells. Of the applied doses, 400 μg/ml occurred to be toxic without metabolic activation system, and no evaluable metaphase was won. With subtoxic doses no significant rise of SCE could be observed either with, or without metabolic activation system. The compounds used as positive control caused an important rise of SCE, which even proved to be significant statistically, with its values more than double the control values.

With the test of sex-linked recessive lethal mutation on *Drosophila melanogaster*, point mutations, or minor deletions may be detected. These genetic alterations may be inherited by the offspring, and be manifested. The method is based on detection of the recessive lethal mutation occurring on the x-chromosome. The x-chromosome contains about a thousand genetic loci, so with the help of this method alterations in about 20% of the total genome can be studied [4]. To achieve this, males and females carrying the appropriate genetic markers, i.e. in our case yellow bodied males with round, coral eyes (yw^{co}/Y) and narrow eye-shaped (Bar) white-apricot eyed females with an inversion on their x-chromosome (Muller-5) were mated.

A number of mutagenicity tests have proved it convincingly that the Muller-5 test can well be used for mutagenicity testing of environmental xenobiotic agents [12, 13, 14].

In our present studies Terbacil used in toxic doses has not caused an increase of recessive lethal mutations in comparison to the untreated controls and the controls treated with solvents only.

Terbacil caused neither a significant increase in the number of sister chromatid exchanges, or of recessive lethal mutations. Earlier examinations [5, 10], as well as the above two mutagenicity tests allow to assume that Terbacil does not represent a genotoxic danger either for those involved in its production, or for those using it.

REFERENCES

1. Ames BN, McCan J, Yamasaki E: Methods for detecting carcinogens and mutagens with the Salmonella mammalian microsome mutagenicity test. Mutat Res *31*: *347*, 1975
2. Kao FT, Puch, TT: Genetics of somatic mammalian cells. IV. Properties of Chinese hamster cell mutants with respect to the requirement for proline. Genetics *55*: 513, 1970
3. Latt SA: Sister chromatid exchanges, indices of human chromosome damage and repair: detection by fluorescence and induction by Mitomycin C. Proc Natl Acad Sci USA, *71*: 3162, 1974
4. Moriya M, Ohta T, Watanabe K, Miyazawa T, Kato K, Shirasu Y: Further mutagenicity studies on pesticides in bacterial reversion assay system. Mutat Res *116*: 185, 1983
5. Natarajan AT, Tates AD, van Buul PPW, Meijers M, Vogel N: Cytogenetic effect of mutagens/carcinogens after activation in a microsomal system in vitro. I. Induction of chromosome aberrations and sister chromatid exchanges by diethylnitrosamine (DEN) and dimethylnitrosamine (DMN) in CHO cells. Mutat Res *37*: 83, 1976

6. Perry PE, Thomson EJ: The methodology of sister chromatid exchanges. Elsevier, Amsterdam, p. 495. 1984
7. Rhodes RC, Reiser RW, Gardiner JA, Sherman H: Identification of the metabolites of Terbacil in dog urine. J Agric Food Chem *17*: 974, 1975
8. Sherman H, Kaplan AM: Toxicity studies with 5-bromo-3-tertiary-butyl-6-methyluracil. Toxicol Appl Pharmacol *34*: 183, 1975
9. Siebert D, Lemperle E: Genetis effects of herbicides: Induction of mitotic gene conversion in Saccharomyces cerevisiae. Mutat Res *22*: 11, 1974
10. Report of the UKEMS Sub-committee on guidelines for mutagenicity testing. Part I. United Kingdom Environmental Mutagen Society, 1984
11. Report of the UKEMS Sub-committee on guidelines for mutagenicity testing. Part II. United Kingdom Environmental Mutagen Society, 1984.
12. Vogel E, Zijlstra JA, Blijleven GH: Mutagenic activity of selected aromatic amines and polycyclic hydrocarbons in *Drosophila melanogaster*. Mutat Res *107*: 53, 1983
13. Wuu KD, Grant Wf: Chromosomal aberrations induced by pesticides in meiotic cells of barley. Cytologia *32*: 31, 1967
14. Würgler FE, Sobels PH, Vogel E: Drosophila as an assay system for detecting genetic changes. Elsevier, Amsterdam, p. 555. 1984

Acta Morphologica Hungarica, 35 (1–2), pp. 9–17 (1987)

DIFFERENT TYPES OF NERVE PROFILE IN THE WALL OF THE CANINE HEPATIC ARTERY: AN ELECTRON MICROSCOPIC STUDY

IDA E. TÓTH, GYÖNGYI GAÁL, G. VARGA, M. PAPP, E. S. VIZI

INSTITUTE OF EXPERIMENTAL MEDICINE, HUNGARIAN ACADEMY OF SCIENCES, BUDAPEST, HUNGARY

(Received 3 January 1986)

The fine structure of the hepatic artery of dogs was studied at electron microscopic level. The majority of nerve fibres innervating the artery was found at the adventitial-medial border of the vessel, but some of them entered the middle part of the media. The average distance of nerve to muscle fibre was found to measure 450 nm.

Three types of nerve profile could be observed, *viz.* adrenergic, cholinergic and cholinergic-peptidergic as suggested by the morphology of their vesicles. It is suggested that the cholinergic and cholinergic-peptidergic nerve endings probably modulate the release and the constrictor effect of the main neurotransmitter noradrenaline in the hepatic artery.

Introduction

The adrenergic nerve plexus and the adrenergic nature of the nerve terminals have been demonstrated in the hepatic artery of dogs [36, 37] and other species [20, 22, 33, 38] and also in a branch of the hepatic artery, the superior pancreatic–duodenal artery [13, 21].

Functional studies revealed that left splanchnic nerve stimulation [14], stimulation of the hepatic nerves [15], adrenaline and noradrenaline (NA) application [14, 15, 17, 28, 30, 31, 32] give rise to vasoconstriction of the hepatic artery, while acetylcholine [1, 2, 14] and some peptides such as glucagon, secretin, cholecystokinin and pentagastrin [28, 29] induce vasodilatation.

It was shown earlier [40] that NA was the main neurotransmitter acting on the α_1-adrenoceptors in the hepatic and pancreatic–duodenal arteries. A prazosin and yohimbine-resistant contraction (20%) was produced by an unknown transmitter. The muscarinic agonist oxotremorine and the purinergic agonist adenosine inhibited endogenous NA release without any direct effect on the smooth muscle cells. These results suggested that several types of nerve fibre regulate the calibre of the canine hepatic artery.

Send offprint requests to: M. Papp, M. D., D. Sc. Szigony u. 43, H-1083 Budapest, Hungary

In the present work we have studied the innervation of the hepatic artery at the fine structural level, and have examined the correlation between the morphological observations and the previously obtained functional evidence.

Materials and methods

Pieces (< 1 mm^3) of the hepatic artery of 3 male dogs were fixed in a mixture of 25 g/l glutaraldehyde and 20 g/l formaldehyde in sodium cacodylate buffer according to Karnovsky [18] for 90 minutes at 4 °C. They were then washed in the same buffer for several hours at 4 °C, and postfixed in 10 g/l buffered osmium tetroxide solution for 90 minutes. After dehydration in a graded series of ethanol, the samples were transferred to propylene oxide, and the tissue blocks were then embedded in Durcupan ACM (Fluka). Longitudinal or transverse sections were cut on a Reichert Om U2 ultramicrotome. Semithin sections (1 μm) stained with toluidine blue were used for orientation. Series of ultrathin sections, cut with either a glass or a diamond knife, were stained with uranyl acetate and lead citrate according to Reynolds [27]. Electron micrographs were taken with a JEOL TEMSCAN-100C electron microscope at an accelerating voltage of 80 kV.

Results

The hepatic artery is densely innervated. The terminal nerve plexus is situated near the adventitial-medial border of the vessel wall and penetrates into the middle part of the media (Fig. 1). The nerve endings approach the smooth muscle cells to provide a simple neuromuscular contact without membrane specialization. The distance between nerve to muscle fibre measures about 450 nm on the average ($n = 18$). The smallest measured neuromuscular distance was 200 nm, while the largest about 1 μm. The nerve fibres are enveloped by Schwann cell cytoplasm, but the terminals are devoid of it on the side facing the muscle fibres, being covered only by the basement membrane of the Schwann cell. There are no synaptic interactions between axon terminals. About ten nerve fibres of different types usually run together; their endings have been classified on the basis of their fine structural features as follows.

1. A considerable number of nerve terminals are bouton-like, about 1 μm across, or sometimes ovoid, with dimensions of $0.75 \times 3\mu$m. They contain two kinds of vesicle; some of them are granular and dense-core, 35—55 nm in diameter, and the rest with the same diameter but clear and agranular. Occasionally, one or two larger (90—110 nm) dense-core vesicles are seen. These varicosities may relate to the adrenergic innervation of the artery wall (Figs 2—5).

2. The second type of nerve endings is similar to the adrenergic terminals as regards their dimensions, but they differ from them in their vesicles. Here we find small, clear or agranular vesicles with a diameter of 30—55 nm, microtubules, small mitochondria and also profiles of smooth endoplasmic reticulum. This type of terminal may correspond to the cholinergic innervation (Fig. 6).

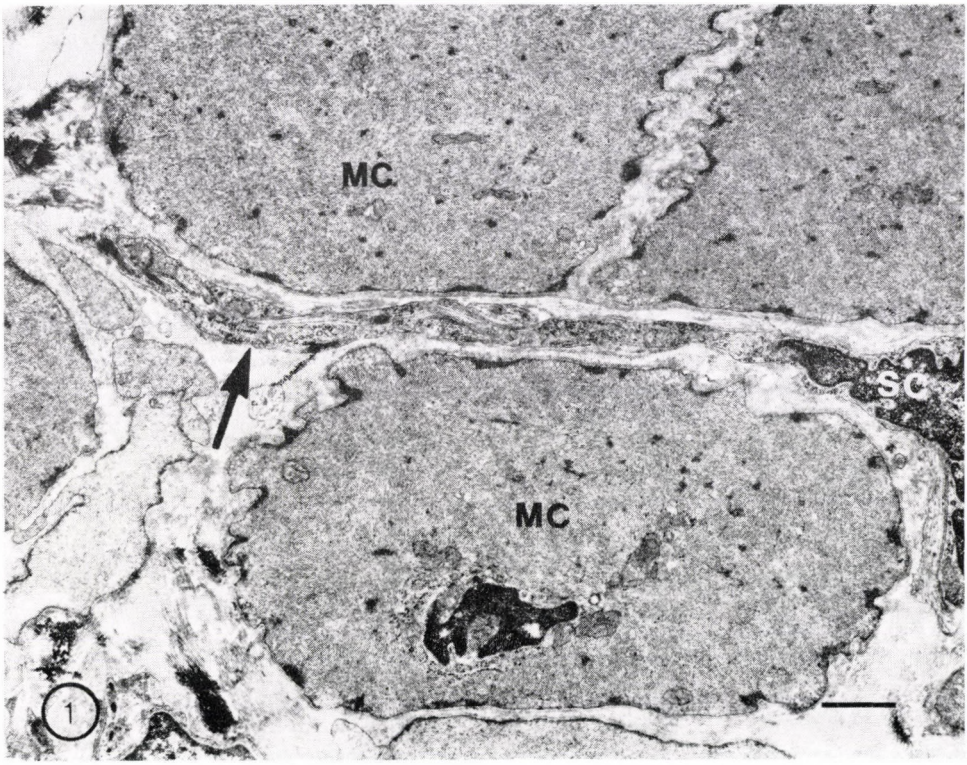

Fig. 1. Electron micrograph of medial layer of the canine hepatic artery, showing a nerve bundle (arrow) among the smooth muscle cells, enveloped by Schwann cell cytoplasm. MC = muscle cell, SC = Schwann cell. ×10 000, Bar = 1μm

3. The third type of nerve terminals reveals many large, dense-core granular vesicles about 90—120 nm in diameter, together with a smaller amount of clear vesicles, 30—55 nm in diameter. These terminals may represent mixed cholinergic-peptidergic nerve endings (Fig. 7).

The identity of the fine structural characteristics of the nerve profiles is usually preserved through their dimensions (Figs 8—11).

Discussion

A systemic study of the innervation of the canine hepatic artery has not previously been carried out at the electron microscopic level. We have investigated the innervation of the vascular smooth muscle in the hepatic artery wall of dogs with special regard to details of the neuromuscular relationships.

These experiments were based on earlier in vitro studies [40] in which we demonstrated that the main neurotransmitter in this artery was NA. The

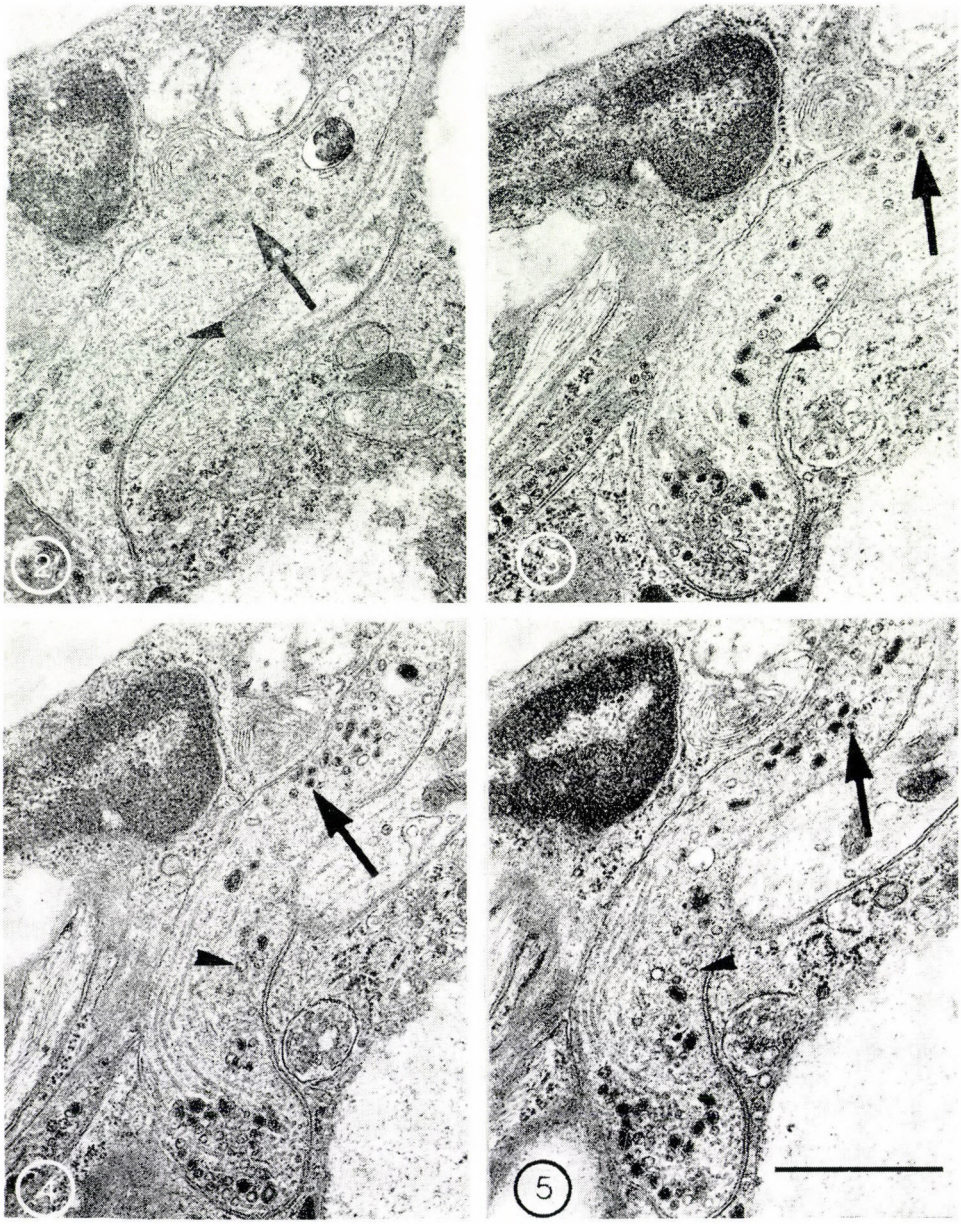

Figs 2—5. Serial sections of a presumably adrenergic nerve fibre. Dense-core vesicles (arrows) and clear agranular ones (arrowheads) are present in the nerve profile. ×22 000, Bar = 1 μm

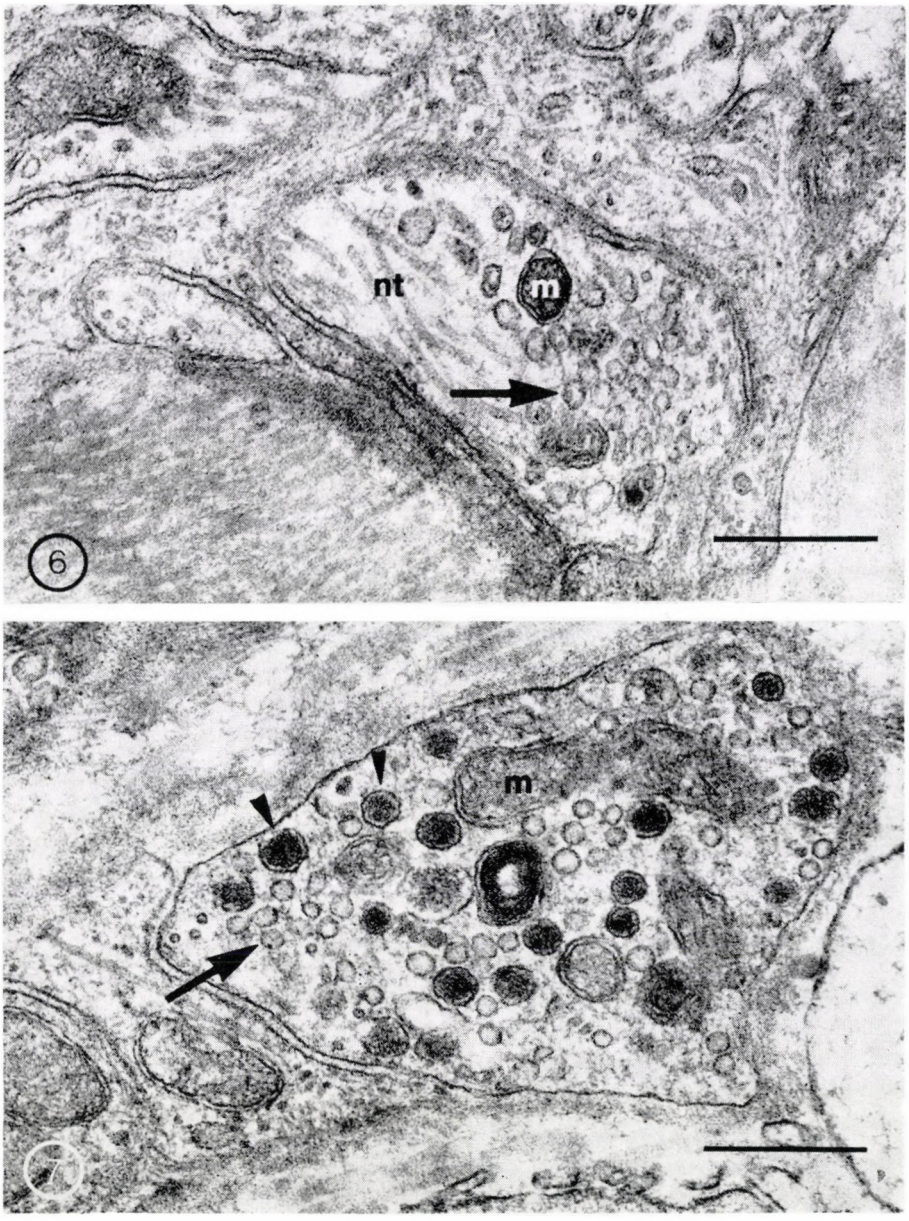

Fig. 6. Nerve ending, possibly cholinergic. Small clear vesicles (arrow), mitochondria (m) and neurotubules (nt). ×72 000, Bar = 0.3 μm

Fig. 7. A mixed cholinergic-peptidergic nerve ending. Small, clear vesicles (arrow) and large granular ones (arrowhead), besides mitochondria (m). ×72 000, Bar = 0.3 μm

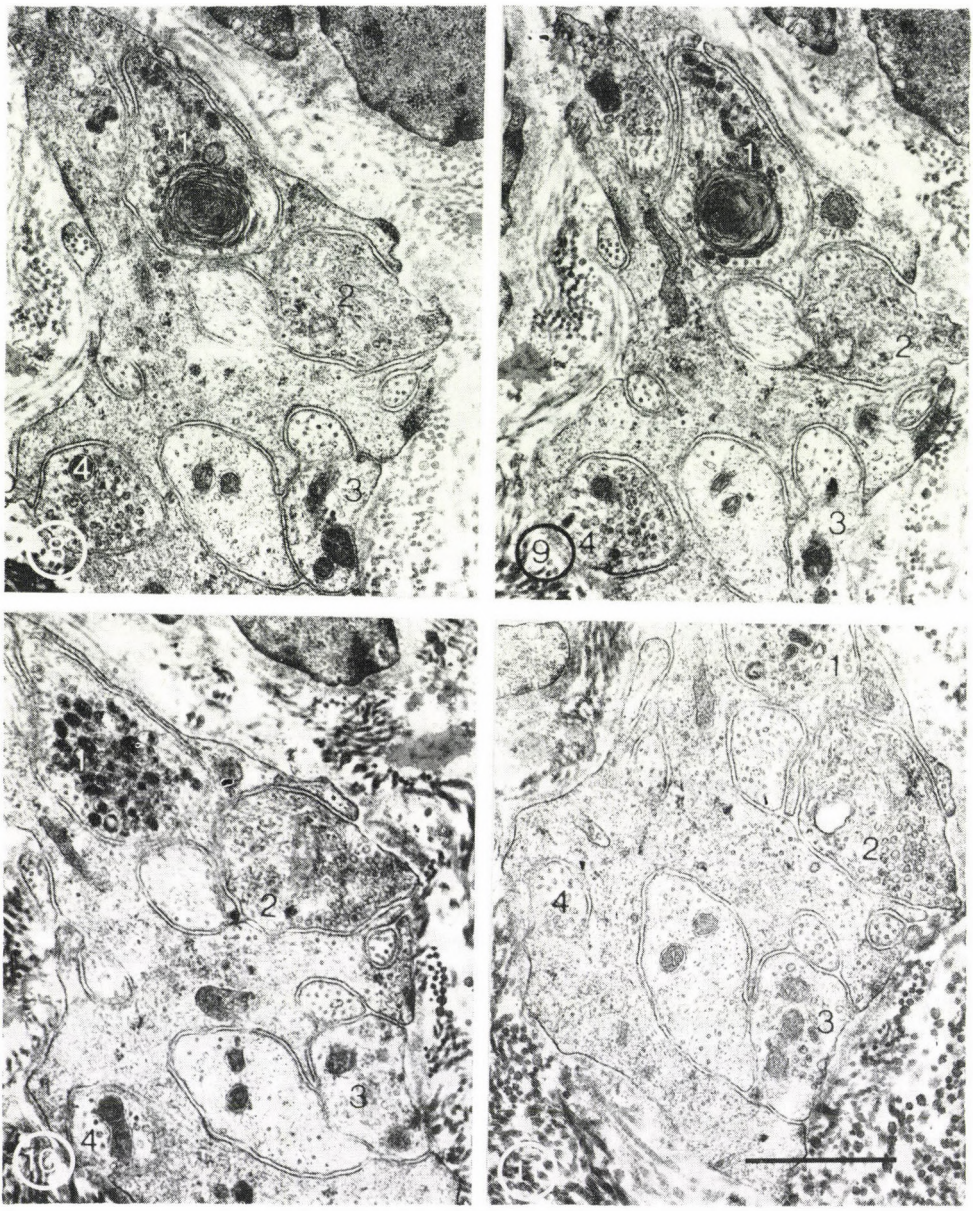

Figs 8—11. Serial sections of a nerve bundle situated near the adventitial-medial layer. The nerve profiles exhibit the same fine structural feature through several levels. Some identical profiles are numbered: 1 — cholinergic-peptidergic; 2 — cholinergic; 3 — adrenergic; 4 — adrenergic profile. ×20 000, Bar = 1 μm

muscarinic agonist oxotremorine was found to inhibit the release of NA from nerve terminals. Gastrointestinal peptide hormones (CCK, secretin and glucagon) had no direct effect on the blood vessel wall. In the present work we have sought the morphological background of the functional evidence.

We demonstrated the penetration of the nerve fibres into the muscular layer of the middle part of the media in the hepatic artery. In most arteries the nerve terminals are restricted to the area of the border between the adventitia and the media [7, 25]. There are, however, numerous exceptions where the nerve fibres penetrate into the media, for example in subcutaneous vines [9, 11, 24], human omental veins [34], dog pedal artery [35], rabbit and dog pulmonary arteries [8, 12], sheep common carotid artery [19], and the aorta of some mammalian species [10]. Due to the direct innervation of the muscle coat in the media, the path of the transmitter to distal effector muscle cells is shortened [24] and the vascular contractile response to a neural effect becomes maximum [3]. In a previous work [40] we found that the sensitivity of hepatic and pancreatic-duodenal arteries to the application of NA is lower than that of the vascular bed innervated at the border of the media and the adventitia. The former arteries might be less influenced by circulating catecholamines. In the present study the neuromuscular distance in the hepatic artery was found to be 200—1000 nm. According to data in the literature, the larger the vessel diameter, the greater the neuromuscular distance. This is about 80—120 nm in arterioles, and 200—500 nm in large arteries, while it may reach even 2 μm in some large elastic arteries [3, 5]. This distance influences the rate of transmitter release, its concentration, effectiveness, and its metabolic fate [3, 4, 5].

At the electron microscopic level we could demonstrate three types of nerve terminal which may represent the adrenergic, cholinergic and cholinergic-peptidergic innervation of the hepatic arterial wall. A similar classification was proposed by Burnstock [6] and Rechardt et al., [26] for other arteries. An andrenergic nerve plexus was previously demonstrated in the hepatic artery wall by means of a fluorescence histochemical method [36]. It was also shown that the catecholaminergic fibres in the hepatic artery degenerated after extirpation of the coeliac ganglion [36]. The existence of adrenergic nerve terminals in the vessel is in good agreement with the earlier neurochemical and functional findings that NA is the main transmitter in this artery [40]. There had been no direct evidence of the cholinergic innervation of the canine hepatic artery, although in vivo acetylcholine increased the hepatic blood flow due to dilatation of the arterial bed [16]. Our earlier finding that the muscarinic agonist oxotremorine inhibited NA release from nerve terminals showed that cholinergic nerves may play a role in the innervation of the hepatic artery.

The functional significance of mixed cholinergic-peptidergic endings has not been clarified. Any peptides in the nerve terminal may coexist with ace-

tylcholine and might interact with other transmitters or modulators participating in regulation of the blood flow through the hepatic artery. It is not known which peptide is present in these nerves.

There were no synaptic interactions between different nerve terminals. The neuromodulation of transmitter release is apparently non-synaptic [42]. The varicosities of different types of nerve terminals situated close to each other in the same bundle might modulate the release of NA from the adrenergic nerve terminals, influencing thereby the adrenergic neurotransmission and hence the functional vascular response of the hepatic artery.

In our laboratory, immunohistochemical attempts have been made to identify the peptide involved in the peptidergic-cholinergic innervation of the arterial wall and we observed vasoactive intestinal peptide-containing nerve fibres and varicosities at the light microscopic level [41]. Immunohistochemical localization of choline acetyltransferase and enzymes involved in the biosynthesis of noradrenaline remains to be carried out in order to verify the cholinergic and adrenergic nature of the fibres in the wall of the canine hepatic artery.

REFERENCES

1. Andrews WHH, Hecker R, Maegraith BG: The action of adrenaline, noradrenaline, acetylcholine and histamine on the perfused liver of the monkey, cat and rabbit. J Physiol (London) 132: 509, 1956
2. Bauer W, Dale HH, Poulsoon LT, Richards DW: The control of circulation through the liver. J Physiol (London) 74: 343, 1932
3. Bevan JA: Some functional consequences of variation in adrenergic synaptic cleft width and in nerve density and distribution. Fed Proc 36: 2439, 1977
4. Bevan JA, Su C: Variation of intra- and presynaptic adrenergic transmitter concentrations with width of synaptic cleft in vascular tissue. J Pharmacol Exp Ther 190: 30, 1974
5. Burnstock G: Cholinergic, adrenergic, and purinergic neuromuscular transmission. Fed Proc 36: 2434, 1977
6. Burnstock G.: Ultrastructural identification of neurotransmitters. Scand J Gastroent 16: 1 1981
7. Burnstock G, Gannon B, Iwayama T: Sympathetic innervation of vascular muscle in normal and hypertensive animals. Circ Res 26—27: (Suppl II) 5, 1970
8. Cech S, Dolezel A: Monoaminergic innervation of the pulmonary vessels in various laboratory animals (rat, rabbit, cat). Experientia 23: 114, 1967
9. Coimbra A, Ribeiro-Silva A, Osswald W: Fine structural and autoradiographic study of the adrenergic innervation of the dog lateral saphenous vein. Blood Vessels 11: 128, 1974
10. Dolezel S: Monoaminergic innervation of aorta. Folia Morphol 20: 14, 1972
11. Ehinger B, Flack B, Sporrong B: Adrenergic fibres to the heart and to peripheral vessels. Bibl Anat 8: 35, 1967
12. Fillenz M.: Innervation of pulmonary and bronchial blood vessels of the dog. J Anat (London) 106: 449, 1970
13. Graham JDP, Lever JD, Spriggs TLB: An examination of adrenergic axons around pancreatic arterioles of the cat for the presence of acetyl-cholinesterase by high resolution autoradiographic and histochemical methods. Br J Pharmacol Chemother 33: 15, 1968
14. Green HD, Hall LS, Sexton J, Deal CP: Autonomic vasomotor responses in the canine hepatic arterial and venous beds. Am J Physiol 196: 196, 1959
15. Greenway CV, Lawson A, Mellander S: The effects of stimulation of the hepatic nerves, infusions of noradrenaline and occlusion of the carotid arteries on liver blood flow in the anaesthetized cat. J Physiol (London) 192: 21, 1967
16. Ginsburg M, Grayson J: Factors controlling liver blood flow in the rat. J Physiol (London) 123: 574, 1954

17. Immink WFGA, Beijer HJM, Charbon GA: Hemodynamic effects of norepinephrine isoprenaline in various regions of the canine splanchnic area. Pflügers Arch 365: 107, 1976
18. Karnovsky MJ: A formaldehyde-glutaraldehyde fixative of high osmolarity for use in electron microscopy. J Cell Biol 27: 137A, 1965
19. Keatinge WR: Electrical and mechanical responses of arteries to stimulation of sympathetic nerves. J Physiol (London) 185: 701, 1966
20. Kyösola K: Comparative formaldehyde-induced and glyoxylic acid-induced fluorescence histochemical studies on the intrinsic adrenergic innervation of the intestine and the liver of normal and vagotomized cats. Acta Histochem 62: 188, 1978
21. Lever JD, Spriggs TBL, Graham JDP: A formol-fluorescence, fine-structural and autoradiographic study of the adrenergic innervation of the vascular tree in the intact and sympathectomized pancreas of the cat. J Anat 103: 15, 1968.
22. Moghimzadeh E, Nobin A, Rosengren G: Fluorescence microscopical and chemical characterization of the adrenergic innervation in mammalian liver-tissue. Cell Tissue Res 230: 605, 1983
23. Osswald W, Guimaraes S, Coimbra A: The termination of action of catecholamines in the isolated venous tissue of the dog. Naunyn-Schmiedeberg's Arch Pharmacol 269: 15, 1971
24. Osswald W, Guimaraes S: Adrenergic mechanisms in blood vessels, morphological and pharmacological aspects. Rev Physiol Biochem Pharmacol 96: 54, 1983
25. Owman C: Neurogenic vasodilatation mediated by the autonomic nervous system. Triangel 18: 89, 1979
26. Rechardt L, Kyösola K, Aalto-Setala K, Hervonen H: Ultra-structure of the nerve terminals in human heart muscle. Neurosci Letter (Suppl) S 300, 1983
27. Reynolds ES: The use of lead citrate at high pH as an electron-opaque stain in electron microscopy. J Cell Biol 17: 208, 1963
28. Richardson PDI, Withrington PG: The inhibition by glucagon of the vasoconstrictor actions of noradrenaline, angiotensin and vasopressin on the hepatic arterial vascular bed of the dog. Br J Pharmacol 57: 93, 1976
29. Richardson PDI, Withrington PG: The effects of glucagon, secretin, pancreozymin and pentagastrin on the hepatic arterial vascular bed of the dog. Br J Pharmacol 59: 147, 1977
30. Ross G, Karrash M: Adrenergic responses of hepatic circulation. Am J Physiol 216: 1380, 1969
31. Di Salvo J, Peterson AP, Hofer DR: Drug-evoked adrenergic responses in the hepatic circulation. Proc Soc Exp Biol Med 142: 833, 1973
32. Scholtholt J, Lochner W, Renn H, Shiraishi T: Wirkung von Noradrenalin, Adrenalin, Isoproterenol and Adenosin auf die Durchblutung der Leber und des Splanchnicusgebietes des Hundes. Arch Ges Physiol 293: 129, 1967
33. Skaaring, P, Bierring F: On the intrinsic innervation of normal rat liver. Histochemical and scanning electron microscopical studies. Cell Tiss Res 171: 141, 1976
34. Thureson-Klein A, Stjarne L, Brudin J: Ultrastructure of nerves in veins from human omentum. Neuroscience 1: 333, 1976
35. Tsunekawa K, Morhri K, Ikeda M, Ohgushi N, Fujiwara M: Histochemical demonstration of adrenergic fibres in the smooth muscle layer of media of dorsal pedal artery in dog. Experientia 23: 842, 1967
36. Ungváry Gy: Functional Morphology of the Hepatic Vascular System. Akadémiai Kiadó, Budapest 1977
37. Ungváry Gy, Donáth T: On the monoaminergic innervation of the liver. Acta Anat (Basel) 72: 446, 1969
38. Ungváry Gy, Donáth T: Neurohistochemical changes in the liver of guinea pigs following ligation of the common bile duct. Exp Molec Pathol 22: 29, 1975
39. Vanhoutte PM: Cholinergic inhibition of adrenergic transmission. Fed Proc 36: 2444, 1977
40. Varga G, Papp M, Hársing LG, Tóth IE, Gaál G, Somogyi GT, Vizi ES: Neuroeffector transmission of the hepatic and pancreatic-duodenal isolated arteries of the dog. Gastroenterology 87: 1056, 1984
41. Vizi ES: Proceedings: Interaction between adrenergic and cholinergic systems: presynaptic inhibitory effect of noradrenaline on acetylcholine release. J Neurol Transm 11: 61, 1974
42. Varga G, Papp M, Kiss JZ, Vizi ES: VIP-containing nerve terminals in arteries supplying the pancreas in dogs. Digestion 32: 221, 1985

Acta Morphologica Hungarica, 35 (1—2), pp. 19—30 (1987)

EFFECT OF EMBRYONIC AND/OR NEONATAL DIETHYLSTILBESTROL AND ALLYLESTRENOL TREATMENT ON POSTNATAL DEVELOPMENT OF THE CHICK TESTIS

P. T. Sótonyi, G. Csaba

INSTITUTE OF BIOLOGY, SEMMELWEIS UNIVERSITY OF MEDICINE BUDAPEST

(Received 28 January 1986)

The synthetic steroid diethylstilbestrol (DES) and the steroid-like allylestrenol (AE) have been used for years in human medicine for the protection of pregnancy. The hazards to the fetus of gestational DES treatment are well established [2, 17, 18]. Knowledge of a similar effect of AE is still fragmentary. Therefore, further studies are required of the after-effects of embryonic and perinatal AE exposure. In our earlier experiments with polypeptide hormones [4, 5, 6] we have observed that perinatal age is a critical period in the maturation of hormone receptors. In this period the presence of hormone induces the development of its specific receptors. The phenomenon is termed hormonal imprinting [4, 5, 6]. During its maturation the receptor is flexible and the presence of non-specific hormones capable of binding to it may alter its normal development Accordingly, even a single hormone injection in the perinatal period may alter the hormone-sensitivity of the target organ.

Introduction

The role of the endocrine system in the intrauterine, perinatal and neonatal phases of ontogeny is poorly understood. It is unclear to what extent may endogenous and exogenous hormones influence development of the endocrine system. Although several papers have been published on the normal pre- and postnatal development of genital organs in birds, little is known about the effect of prenatal hormone treatment on the differentiation and development of genital organs. There are some data on the development of male and female sexual organs after estrogen (including DES) treatment prior to their differentiation. These early treatments were shown to produce marked alterations: feminization in genetic males, the formation of ovotestis, inhibition of gonads, persistence of Müller-ducts and significant changes in gonadal hormone secretion [9, 11, 16, 25, 40, 41, 42, 43]. Recent studies have shown that in the embryonic gonads estrogens may influence the binding capacity of estrogen hormone receptors and acceptors [31, 32, 33, 34].

In earlier experiments in chicken after DES and AE treatments we found signs of functional teratogenicity, various malformations [26], suppu-

Send offprint requests to: G. Csaba, Inst. of Biology, Semmelweis University of Medicine, Budapest, Nagyvárad tér 4, H-1445, P. O. Box 370, Hungary

rative inflammation of the oviduct [27], and a change in free histones in chicken and rats [28, 29]. In the rat, DES and AE treatment resulted in a decrease of binding capacity of uterine estrogen receptors [7].

In the present work we investigated the effect of embryonic steroid treatment performed after sexual differentiation, i.e. when differentiation of the gonads had already been completed, but that of the Müller-ducts was in an initial stage. We were interested in the weight and histology of the testes on the 5th day and on the 6th week after hatching. We also studied the effect of a single embryonic treatment on that of repeated postnatal treatments.

Materials and methods

In the yolk sac of Hubbard broyler chick embryos a single dose of 0.5 mg allylestrenol (AE, Richter, Budapest, 5 mg/ml) or 0.25 mg diethylstilbestrol (DES, Richter, Budapest, 2.5 mg/ml) was injected on the 9th day of incubation. Both agents were dissolved in absolute ethanol, then after the addition of two drops of Tween 80 they were further diluted in physiologic saline solution. Controls received 0.1 ml of the solvent. Eggs were incubated according to routine technology. Immediately after hatching, a group of animals was treated again by an intramuscular injection of 0.25 mg AE (2.5 mg/ml) and 0.125 mg DES (1.25 mg/ml). AE and DES were dissolved in benzyl alcohol, then diluted with sunflower oil. Controls received 0.05 ml of the solvent. The animals were divided into 7 groups.

I.	Control	
II.	DES-treatment	on the 9th day of incubation
III.		on the 9th day of incubation and at hatching
IV.		at hatching
V.	AE-treatment	on the 9th day of incubation
VI.		on the 9th day of incubation and at hatching
VII.		at hatching

The animals were killed either 5 days or 6 weeks after hatching. The testicles were removed, weighed and fixed in Bouin's fixative. Materials were embedded in paraffin and 5 μm sections were prepared in the mid-plane of the testes and stained with haematoxilin-eosin.

Quantitative histological evaluation of the testicular tissue was performed according to the cock testis test of Ishii et al. [19]. This method was complemented with quantitative analysis of the cellular composition of seminiferous ducts. In each animal 40 ducts were measured under an eyepiece micron-scale to determine the mean duct diameter. In addition, in each animal 10 ducts were analysed concerning cellular composition. Their means were regarded as characteristic of the group. Within the same group the average number of each cell type was correlated to the average total cell number and expressed in percentage of the total. Moreover, the ratios of spermatogenic cells (spermatogonia and primary spermatocytes) versus Sertoli cells, and spermatogonia versus primary spermatocytes were calculated. The number of cells per unit area was also determined. Differences between groups were evaluated by the two-sample t test.

Results

Postnatal day 5

A decrease of both testes was observed in the treated animals (Table I). The degree of decrease was roughly similar in both testes, but more pronounced after DES than after AE treatment. The decrease was the greatest ($p < 0.01$)

Table I

Testicular weight and seminiferous duct diameter on day 5

	DES			Control	AE		
	9	9 + 1	1		9	9 + 1	1
Testicular weight, mg							
left	6.2 ±0.92	5.8 ±0.73	8.3 ±1.02	11.6 ±1.52	8.7 ±0.91	7.1 ±0.94	9.4 ±1.87
right	5.3 ±0.64	3.9 ±0.51	6.6 ±1.27	8.7 ±1.18	6.4 ±0.59	6.2 ±1.38	7.3 ±0.78
Duct diameter, μm	29.8 ±3.64	27.4 ±5.55	38.3 ±4.78	44.7 ±5.30	33.2 ±4.37	32.9 ±6.81	40.1 ±5.37
Number of animals	18	19	15	23	17	16	18

when treatment was performed on the 9th day of incubation *plus* at hatching (in the case of DES the testicular weight decreased to the half of the control). The difference against the group having received treatment on the 9th gestational day only, was not significant. Treatment immediately after hatching caused a small decrease in testicular weight.

Seminiferous duct diameter was found to change in the treated animals with testicular weight (Table I) i.e. it decreased after treatment as compared to the control. Also in this case, the greater decrease occurred after DES treatment. There was no significant difference between the control and the group treated at hatching, and between the groups treated on the 9th gestational day and the 9th gestational day *plus* at hatching. A significant difference ($p < 0.01$) was however, found between the control and the embryonally treated groups.

The cellular composition of seminiferous ducts and its alterations after treatments are summarized in Table II.

Histology of the control testes showed a pattern corresponding to age (Fig. 1). They were found to be surrounded by a well-developed tunica albuginea and to contain contorted cords (ducts were not yet present) with interposed connective tissue. Lumen formation was sporadic. In the germinal epithelium constituting the cords, many undifferentiated, so-called peritoneal cells were seen with only a few differentiated, identifiable cells. The latter as follows were. Spermatogonia: large, round cells with a nucleus containing evenly distributed chromatin and prominent nucleolus. They occurred close to the basement membrane. Primary spermatocytes: those were smaller than the spermatogonia; they had a small, chromatic nucleus and were found at a distance from the basement membrane. Sertoli cells: slender, cylindrical cells contacting the basement membrane. Their nucleus is euchromatic, oval, with a characteristically large nucleolus. In fact, these are precursors rather than fully differentiated Sertoli cells.

Table II

Cellular composition of seminiferous ducts on day 5

		No. of animals	Cell no. counted	Total cell no.	%	No. of Spermatogonia	%	No of primary spermatocytes	%	No. of Sertoli cells	%	Sg/Sc*	SG/pSC**	Cell packing density no/μm$\times 10^{-2}$
	9	18	1337	74.3 ± 6.02	100	31.8 ± 1.33	42.8	0	0	42.5 ± 3.93	57.2	0.75	0	10.7
DES	9+1	19	1123	59.1 ± 6.78	100	26.3 ± 2.20	44.5	0	0	32.8 ± 4.31	55.5	0.80	0	10.0
	1	15	1419	94.6 ± 7.43	100	38.4 ± 1.08	40.6	4.3 ± 0.86	4.5	51.9 ± 6.30	54.9	0.82	8.93	8.21
Control		23	3606	156.8 ± 9.42	100	54.2 ± 3.46	34.6	18.1 ± 1.84	11.5	84.5 ± 3.76	53.9	0.86	2.99	9.99
	9	17	2062	121.3 ± 4.37	100	46.2 ± 2.35	38.1	7.8 ± 0.79	6.4	67.3 ± 0.83	55.5	0.80	5.92	14.0
AE	9+1	16	1736	108.5 ± 5.18	100	41.2 ± 0.95	38.0	5.1 ± 1.07	4.7	62.2 ± 2.35	57.3	0.74	8.08	12.8
	1	18	2064	114.7 ± 4.05	100	39.4 ± 1.5	34.4	6.8 ± 1.43	6.0	68.5 ± 4.11	59.7	0.67	5.79	9.08

* Spermatogonium + primary spermatocyte/Sertoli cell
** Spermatogonium/primary spermatocyte

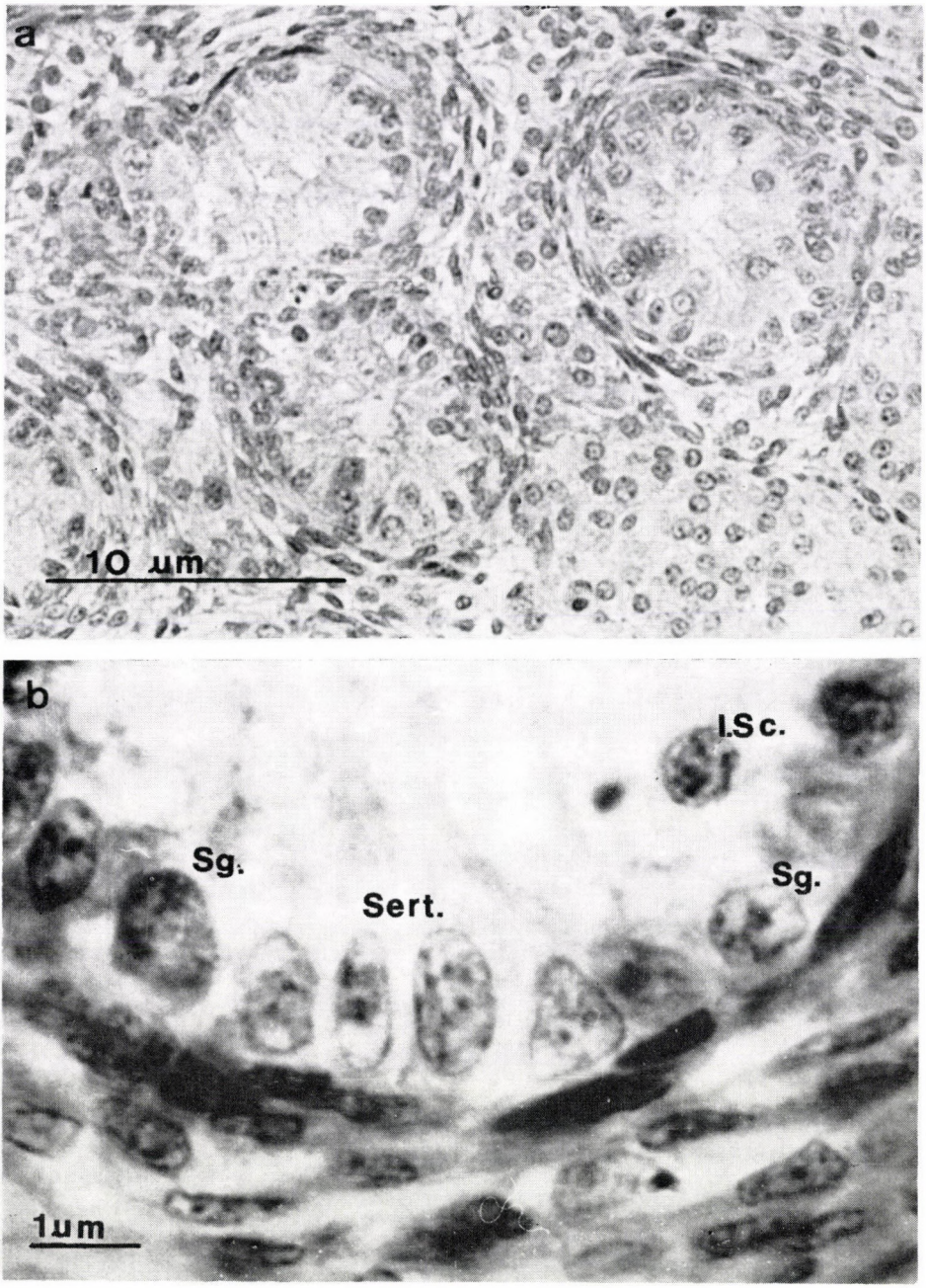

Fig. 1. In the testicles of 5-day-old cocks, convoluted cords (A) constituted by cell types of the germinal epithelium. Sg = spermatogonia, I. Sc = primary spermatocytes, Sert = Sertoli cells (B)

Upon DES and AE treatment, irrespective of its timing, the above light microscopic structure remained unaltered. The number of identifiable cells showed however, a marked reduction and that of the peritoneal matrix cells increased as compared to the control. In the treated groups lumen formation was not encountered. The mean cell number within the cords (Table II) changed with testicular weight and seminiferous duct diameter. Reduction in cell number was greater after DES than after AE. The greatest decrease, to one third of the control, occurred when treatment on the 9th embryonic day was repeated at hatching, but there was a significant ($p < 0.01$) decrease also in the group treated only at hatching. With DES, there was a significant difference ($p < 0.01$) also between the experimental groups. In the AE-treated groups the difference was significant ($p < 0.01$) as compared to the control but not between the treated groups. The number of spermatogonia and Sertoli cells decreased like the average cell number, but their percentage distribution showed no difference between the experimental groups. Nor did the ratio of spermatogenic and Sertoli cells change. On the other hand, there was a decrease in the number and percentage of primary spermatocytes and in their ratio versus spermatogonia. No primary spermatocytes were found after embryonic DES treatment, while in the control group they constituted 10% of the whole population. After AE treatment too, their number decreased significantly ($p < 0.01$); their percentage decreased to 5%, half of that in the control.

Postnatal week 6

The change in testicular weight in the treated animals (Table III) corresponded to that of the 5-day-old group but in a higher degree. In the animals treated with DES on the 9th embryonic *plus* hatching days the left testis decreased to its third, the right to its quarter, while following AE treatment

Table III

Testicular weight and seminiferous duct diameter at 6 weeks of age

	DES			Control	AE		
	9	9 + 1	1		9	9 + 1	1
Testicular weight, mg							
left	82 ± 10.32	54 ± 8.75	107 ± 9.81	176 ± 14.32	96 ± 8.34	88 ± 11.43	137 ± 10.58
right	58 ± 8.46	39 ± 7.06	82 ± 13.67	151 ± 12.03	84 ± 10.38	73 ± 8.12	121 ± 9.48
Duct diameter, μm	39.3 ±5.02	34.1 ±4.67	57.8 ±6.21	68.4 ±5.62	54.3 ±4.88	50.6 ±4.07	62.2 ±5.37
No. of animals	16	14	17	19	16	19	15

Table IV

Cellular composition of seminiferous ducts at 6 weeks of age

		No. of animals	Cell no. counted	Total cell no.	%	No. of spermatogonia	%	No of spermatocytes	%	No. of Sertoli cells	%	Sg/Sc*	SG/pSC**	Cell packing density no/$\mu m \times 10^{-2}$
	9	16	2204	138.4 ± 4.17	100	34.3 ± 3.03	24.8	8.7 ± 0.97	6.3	95.4 ± 2.57	68.9	0.45	3.94	11.4
DES	9+1	14	1621	115.8 ± 3.47	100	32.8 ± 2.62	28.3	3.6 ± 0.78	3.1	79.4 ± 3.42	68.6	0.46	9.11	12.7
	1	17	3634	214.3 ± 6.39	100	41.5 ± 1.34	19.4	17.2 ± 0.93	8.0	155.6 ± 6.30	72.6	0.38	2.41	8.16
Control		19	6083	320.2 ± 9.18	100	56.4 ± 4.28	17.6	31.3 ± 1.76	9.8	232.5 ± 5.45	72.6	0.38	1.80	8.71
	9	16	3620	226.3 ± 4.08	100	42.7 ± 3.47	18.9	21.4 ± 0.86	9.4	162.2 ± 4.10	71.7	0.40	2.00	9.77
AE	9+1	19	3893	204.9 ± 4.70	100	42.6 ± 4.52	20.8	22.1 ± 1.66	10.8	140.2 ± 3.87	68.4	0.46	1.93	10.2
	1	15	4395	293 ± 5.36	100	48.7 ± 2.27	16.6	24.8 ± 1.82	8.5	219.5 ± 4.81	74.9	0.33	1.96	9.64

* Spermatogonium + primary spermatocyte/Sertoli cell
** Spermatogonium/primary spermatocyte

the weight of both testes was reduced to half. The degree of decrease was significant at the 0.01 level.

Decrease of the seminiferous duct diameter after treatment (Table III) was also similar to that observed at postnatal day 5, but was more conspicuous, particularly after DES treatment when the diameter decreased to half of that of the control ($p < 0.01$) in the embryonally *plus* perinatally treated animals.

The cellular composition and its post-treatment alterations were also similar (Table IV.) as those observed on day 5. In this age the controls already showed a pronounced canaliculization of the contorted cords as a result of which most cross-sections had a lumen. Cells were readily identifiable with only a few undifferentiated peritoneal cells. The average cell number increased along with the number of Sertoli cells as well as the ratio of the latter versus spermatogenic cells.

In the treated animals the total cell number decreased equally affecting the different cell types, thus their ratio remained unchanged. An exception was the number of primary spermatocyte which fell after DES to 10% of the control and its percentage compared to the total cell number decreased to the third of that in the controls. AE decreased their number but not their percentage.

Discussion

Several data are available concerning the effect on gonadal development of different prenatal estrogen treatment. These treatments were performed in the early gestational period prior to sexual differentiation, which takes place in the chick by the 6th day of incubation. Between gestational days 5 and 8 however, the chick urogenital system, in particular the Müller ducts are in a resting phase in both male and female embryos. In the male embryo both Müller ducts start to regress on day 9 and this process is complete by embryonic day 13. In female embryos, involution of the right Müller duct also begins on day 9 and is seen at hatching as a tiny rudiment. The left duct develops gradually to form the oviduct [22, 44]. In the male embryo the gonads differentiate into testes, while in the female the right gonad degenerates and the left gives rise to the ovary [3, 8]. In the gonads of the chick embryo the synthesis and secretion of sexual steroids starts in the early developmental stage. In this stage, in females both gonads are capable of producing estrogens and androgens under gonadotropin control [12, 14, 35, 38]. Gonadal secretion of these sexual steroids [39, 49] and some other hitherto unidentified factors [21] are held responsible for the growth or degeneration of the Müller ducts.

The effects of estrogen given prior to the differentiation of genital organs are well established. These effects are rather pronounced: for example, DES transforms in males the left testis to ovotestis, while the right one degenerates and the Müller duct persists [44].

The mechanism by which DES, and estrogens in general, inhibit the involution of Müller ducts is unclear. Following DES treatment, an inhibition of early gonadal secretion has been observed in cells of the medullary tissue [23]. It may be assumed that DES inhibits the differentiation of these cells, inactivating thereby their secretory activity. It is also possible that high DES levels counteract the effect of testosterone on the Müller ducts [24] but an effect through the hypophysis cannot be ruled out either [48]. A full persistence of Müller-ducts has been observed when in both sexes DES treatment was performed between embryonic days 3 and 5, but was incomplete when the hormone was given after day 5 [37, 47]. These observations suggest the operation of some gonadal factor(s) which cause degeneration of the Müller ducts.

Early DES treatment has been shown to inhibit the development of gonads. Ovarian DNA synthesis was blocked by 36 to 41%, RNS synthesis by 52 to 53%, protein synthesis by 45 to 47%. A similar inhibition (57, 40 and 45%, respectively) has been observed in the testis, 37% of which was manifest as early as 3 h after treatment. This type of hormonal inhibition of gonadal growth and function has been verified in rodents after neonatal estrogen treatment [10, 30, 49]. In bird embryos the change of sex as a result of estrogen has long been known [20, 42, 43].

Histologically, proliferation of cortical tissue has been demonstrated and the development of ovocytes in the cortex of intersex males has been observed up to 3 months after hatching [15]. Less is known about the endocrine functions of these sexually altered males. With DES treatment, estrogen secretion could be induced in the left testis with an inhibiton of testosterone secretion. The decrease of testosterone secretion is proportionate to the loss of medullary substance, as described by Wolff and Ginglinger [45].

In the present studies, steroid treatment was performed on the 9th day of incubation, i.e. after sexual differentiation. These late treatments obviously did not produce rough anomalies, although some of them were described in our earlier papers (26, 27). Changes seen during this work were less conspicuous and could be revealed mainly by quantitative morphometric analysis. The change and their irreversible nature provided evidence of the effect on testicular development of late embryonic and perinatal steroid treatments. This effect manifested with changes of testicular weight, diameter of seminiferous ducts and cellular composition. The roughly similar decrease in the number of Sertoli and spermatogenic cells suggested that DES and AE inhibited equally the generation of both cell types. The similarity of changes at 4 days and 6 weeks postnatally argued for the lasting effect even of a single embryonic treatment to which neonatal treatments may add.

Between DES and AE effects the differences were mainly quantitative, but in qualitative terms they were similar. Although it would be premature

to extrapolate our results to human situations, it is remarkable that AE is used to protect human pregnancy.

The mechanism by which these steroids influence the gonads is not clear. In agreement with the literature, we postulate an irreversible interference with the gonadotropic regulation of the hypothalamo-hypophyseal system which, in turn, would inhibit gonadal growth and function [1, 13]. It may also induce some unknown alteration in early gonadal secretory activity which may act upon the gonads themselves.

REFERENCES

1. Barraclough CA: Modifications in the CNS regulation of reproduction after exposure of prepubertal rats to steroid hormones. Recent Progr Horm Res *22:* 503, 1966
2. Bibbo M, Gill W, Azizi F: Follow-up study of male and female offsprings of DES-exposed mothers. Obstet Gynecol *49:* 1, 1977
3. Burns RK: Role of hormones in the differentiation of sex. In: Sex and Internal Secretion, ed. WC Young, Williams and Wilkins, Baltimore *76:* p. 158, 1961
4. Csaba G: Phylogeny and ontogeny of hormone receptors: the selection theory of receptor formation and hormonal imprinting. Biol Rev *55:* 47, 1980
5. Csaba G: Ontogeny and phylogeny of hormone receptors. Monographs in Developmental Biology Vol 15, Karger, Basel 1981.
6. Csaba G: The present state in the phylogeny and ontogeny of hormone receptors. Horm Metabol Res *16:* 329, 1984
7. Csaba G, Inczefi-Gonda Á, Dobozy O: Hormonal imprinting by steroids: a single neonatal treatment with diethylstilbestrol (DES) or allylestrenol (AE) gives rise to lasting decrease in the number of rat uterine receptors. Acta Physiol Hung *5:* 67, 207 1986
8. Domm LV: New experiments on ovariectomy and the problem of sex inversion in the fowl. J Exp Zool *48:* 31, 1927
9. Domm LV: Recent advances in knowledge concerning the role of hormones in the sex differentiation of birds. In: Recent Studies in Avian Biology. University of Illinois Press, Urbana, Ill. 1955 pp. 309—325
10. Frick J, Chang CC, Kinol FA: Testosterone plasma levels in adult male rats injected neonatally with estradiol benzoate or testosterone propionate. Steroids *13:* 21, 1969
11. Gaarenstroom JH: Action of sex hormones on the development of the Mullerian duct of the chick embryo. J Exp Zool *82:* 31, 1939
12. Galli F, Wasserman GF: Steroid biosynthesis by gonads of 7- and 10-day-old chick embryos. Gen Comp Endocrinol *21:* 77, 1973
13. Gorski RA: Localization and sex differentiation of the nervous structures which regulate ovulation. J Reprod Fertil *1:* (Suppl.): *67*, 1966
14. Guichard A, Cedard L, Haffen K: Aspect comparatif de la synthese de stéroides sexuels par les gonades embryonnaires de poulet a différents stades du dévelopment. Gen Comp Endocrinol *20:* 16, 1973
15. Haffen K: Quelques aspects de l'intersexualité experimentale chez le poulet (Gallus gallus) et la caille (Coturnix coturnix japonica). Bull Biol Fr Belg *103:* 401, 1969
16. Hamilton TH: Studies on the physiology of urogenital differentiation in the chick embryo. 1. Hormonal control of sexual differentiation of Mullerian ducts. J. Exp Zool *146:* 625, 1961
17. Herbst AL, Ulfelder H, Poskanzer DC: Adenocarcinoma of the vagina: association of maternal stilbestrol therapy with tumor appearance in young women. N Engl J Med *284:* 878, 1971
18. Herbst AL, Poskanzer DC, Robboy SJ, Friedlander L, Scully RE: Prenatal exposure to stilbestrol. N Engl J Med *292:* 334, 1975
19. Ishii S, Furuya T: Effect of purified chicken gonadotropin on the chick testis. Gen Comp Endocrinol *25:* 1, 1975
20. Lutz-Ostertag Y: Action du stilboestrol sur les canaux de Müller de l'embryon de caille (Coturnix coturnix japonica). CR Acad Sci (Paris) *259:* 879, 1964

21. Maraud R, Stoll R, Couland H: Données nouvelles sur le role du testicule et d'hypophyse dans la differenciation sexuelle du poulet. Bull Assoc Anat *148:* 442, 1970
22. Price D, Zaaijer JJJP, Ortiz E, Brinkmann AO: Current views on embryonic sex differentiation in reptiles, birds, and mammals. In: Trends in Comparative Endocrinology, ed. JW Barrington. Am Zool *15*, Suppl. 1: 173, 1975
23. Scheib D, Haffen K: Sur la localization histoenzymologique de la 3β-hydroxysteroide deshydrogénase dans les gonades de l'embryon de poulet; apparition et specificité de l'activité enzymatique. Ann Embryol Morph *1:* 61, 1968
24. Scheib D: Mécanismes cellulaires et determinisme hormonal de la regréssion de canaux de Müller chez l'embryon de poulet: Étude cytologique et biochemique. In: Mécanismes de la rudimentation des organes chez les embryons de vertébrés. Colloques Internationaux Centre National de la Recherche Scientifique, Paris 1976
25. Snedecor JG: A study of some effects of sex hormones on the embryonic reproductive system and comb of the white Leghorn chick. J Exp Zool *110:* 205, 1949
26. Sótonyi PT, Dobozy O, Csaba G: The impairing effect of diethylstilbestrol and allylestrenol in chick embryo. Acta Morph Hung. In press.
27. Sótonyi PT, Dobozy O, Csaba G: Late effect of embryonal allylestrenol treatment in chicken. Acta Morph Hung *34:* 87, 1986
28. Sótonyi PT, Dobozy O, Csaba G: The changes of the free histones in the chicken's testis and ovaries after diethylstilbestrol or allylestrenol treatment. Acta Morph Hung *34:* 23, 1986
29. Sótonyi PT, Csaba G, Treit P: Changes in free histone level in the cells of rat womb after single neonatal diethylstilbestrol or allylestrenol treatment. Acta Morph Hung *34:* 47, 1986
30. Takasugi N: Testicular damages in neonatally estrogenized adult mice. Endocrinol Jpn *17:* 277, 1970
31. Teng CS, Teng CT: Studies on sex-organ development: Isolation and characterization of an oestrogen receptor from chick Müllerian duct. Biochem J *150:* 183, 1975
32. Teng CS, Teng CT: Studies on sex-organ development: ontogeny of cytoplasmic oestrogen receptor in chick Mullerian duct. Biochem J *150:* 191, 1975
33. Teng CS, Teng CT: Studies on sex-organ development: oestrogen receptor translocation in the developing chick Mullerian duct. Biochem J *154:* 1, 1976
34. Teng CS, Teng CT: Studies on sex-organ development: changes in chemical composition and oestradiol-binding capacity in chromatin during the differentiation of chick Mullerian ducts. Biochem *172:* 361, 1977
35. Teng CS, Teng CT: Studies on sex-organ development: the hormonal regulation of steroidogenesis and adenosine 3 : 5-cyclic monophosphate in embryonic-chick ovary. Biochem J *162:* 123, 1977
36. Teng CT, Teng CS: The effect of diethylstilbestrol on the embryonic gonadal steroid production and its responsiveness to gonadotropic hormone. J Cell Biol *75:* 190a, 1977
37. Teng CS, Teng CT: Prenatal effect of estrogenic hormone on embryonic genital organ differentiation. In: Ontogeny of Receptors and Reproductive Hormone Action, eds TH Hamilton, JH Clark, WA Sadler. Raven Press, New York 1979
38. Weiger JP, Zeis A: Biosynthesis d'oestrogenes par les ébauches gonadiques de poulet. Gen Comp Endocrinol *16:* 391, 1971
39. Willier BH: The embryonic development of sex. In: Sex and Internal Secretions, eds E Allen, CH Danforth, EA Doisy,, Williams and Wilkins, Baltimore 1939 p. 64
40. Willier BH, Gallagher TF, Koch FC: The modification of sex development in the chick embryo by male and female sex hormones. Physiol Zool *10:* 101, 1937
41. Witschi E: Modification of the development of sex in lower vertebrates and in mammals. In: Sex and Internal Secretions, eds E Allen, CH Danforth, EA Doisy, Williams and Wilkins, Baltimore 1939 p. 145
42. Wolff E: L'évolution aprēs l'éclosion des poulets males transformés en intersexués par l'hormone femelle injectée aux jeunes embryons. Arch Anat Histol Embryol *23:* 1, 1936
43. Wolff E: Action du diethylstilboesterol sur les organes génitaux de l'embryon de poulet. CR Acad Sci (Paris) *208:* 1532, 1939
44. Wolff E: L'evolution des canaux de Muller de l'embryon d'oiseau aprēs castration précoce. CR Soc Biol *143:* 1239, 1949
45. Wolff E, Ginglinger A: Sur la transformation des poulets male en intersexués par injection d'hormone femelle-folliculine-aux embryons. Arch Anat Histol Embryol *20:* 219, 1935
46. Wolff E, Lutz-Ostertag Y, Haffen K: Sur la régression et la nécrose in vitro des canaux de Muller de l'embryon de poulet sous l'effet de substances hormonales. CR Soc Biol *146:* 1793, 1952

47. Woods JE, Simpson RM, and Moore PL: Plasma testosterone levels in the chick embrio. Gen Comp Endocrinol *27:* 543, 1975
48. Woods JE, Weeks RL: Ontogenesis of the pituitary-gonadal axis in the chick embryo. Gen Comp Endocrinol *13:* 242, 1969
49. Wrenn TR, Wood JR, Bitman J: Oestrogen responses of rats neonatally sterilized with steroids. J Endocrinol *45:* 415, 1969

Acta Morphologica Hungarica 35 (1—2), pp. 31—35 (1987)

INTERSPECIFIC INTERACTION OF AORTIC ENDOTHELIAL AND SMOOTH MUSCLE CELLS

ÉVA CSONKA, A. S. KOCH, P. I. BAUER, K. G. BÜKI

SECOND INSTITUTE OF PATHOLOGY AND SECOND INSTITUTE OF BIOCHEMISTRY, SEMMELWEIS UNIVERSITY MEDICAL SCHOOL, BUDAPEST, HUNGARY

(Received 19 March 1986)

The proliferation stimulating or inhibitory effect of aortic endothelial cells on aortic smooth muscle cells and vice versa was studied in cell culture by using a newly developed co-cultivation technique. The effect was registered as the incorporation of labelled thymidine detected by liquid scintillation counting. The experiments were performed in intra and interspecific combinations, using bovine, pig or rat aortic cell cultures. The endothelial cells stimulated smooth muscle cell proliferation in a species specific way. In interspecies combinations either inhibition or no effect was observed. The smooth muscle cells usually had an inhibitory effect on the proliferation of endothelial cells except for the pig smooth muscle cells which had a stimulatory effect in both inter and intraspecies combinations. Co-cultivation of smooth muscle or endothelial cells with cells of the same type resulted mostly in inhibition or no effect in both intra and interspecies combinations. This phenomenon was particularly conspicuous with endothelial cells .The different stimulatory and inhibitory effects produced by these cells may play an important role in the regulation of neovascularization and in reendothelization of denuded intimal areas.

Keywords: cultured aortic cells, co-cultivation, inter-, and intraspecific interactions in culture, cell proliferation.

Introduction

The cells of a multicellular organism mutually influence each other's functions in a regulated manner. Since this is a general rule it should function also between endothelial and smooth muscle cells of the vessel wall under both normal and pathologic conditions.

There are reports on the stimulatory effect of endothelial cells on the growth of smooth muscle cells [3] but we found only few studies on the mutual effect on each other of endothelial and smooth muscle cells in intra and interspecies co-cultivation experiments [5, 9].

In previous co-culturing experiments we have investigated the possible aortic endothelium — smooth muscle cell interaction, partly with the classical method of applying the different conditioned media in various arrangements to different cultured cells to check the effects on their proliferative activity, partly by using a newly developed co-cultivation technique [1].

Send offprint requests to Dr. E. Csonka Üllői út 93. H-1091, Budapest, Hungary

In the present study we have examined the proliferation stimulating effect of endothelial cells on the smooth muscle cells and vice versa in intra and interspecific combinations, using bovine, pig or rat aortic cell cultures. The effect was registered as the incorporation of labelled thymidine detected by liquid scintillation counting.

Materials and methods

Cell culture

The BAEC (Budapest Aortic Endothelial Cell culture)-806 bovine aortic endothelial; the BASC (Budapest Aortic Smooth Muscle Cell culture)-809 bovine aortic smooth muscle; the BAEC-812 mini-pig aortic endothelium; the BASC-813 mini-pig aortic smooth muscle; the 2PE rat aortic endothelium and the 2PS rat aortic smooth muscle cell cultures were used. All cell cultures were established in our laboratory and were cultured in modified Dulbecco MEM with 10% fetal calf serum. The cells used in the experiments were in the first to sixth passages in vitro.

Co-culture experiments

The different cell types were grown separately on glass coverslips in Leighton tubes (10^5 cells/ml) and on the bottom of the counting vials ($2 \cdot 10^5$ cells/2ml). After 4 hours of incubation the cells attached to the glass. Co-cultivation was started at this time by putting the coverslip cultures diagonally into the vials carrying the other type of cells. The original amount (2 ml) of medium in the vials was adjusted with 10 ml of fresh medium so as to cover also the cells on the diagonally inserted coverslip (Fig. 1). By this method any pairs of cell types could be co-cultivated in a system where only the medium was common while the cells were spatially separated.

Measurement of proliferation

Proliferation of the different cell types as controls and the proliferation stimulating effect of either endothelial cells on smooth muscle cells or vice versa in intra, as well in interspecific combinations was assessed by measuring ^{3}H-thymidine (^{3}H-TdR) incorporation after 24 hours of co-cultivation. The coverslips with the other cell types were removed and the cells grown in the vials were labelled by 2 ml culture medium containing a final concentration of $3.7 \cdot 10^{-3}$ Bq/ml (^{3}H-TdR). Four hours after labelling, the cell monolayers were washed as described previously [2] and solubilized in 5 ml mixture of Toluol-Triton $100 \times (3 : 1)$. Radioactivity was determined with a Beckmann M-25 spectrometer.

Results

The figures represent labelled thymidine incorporation in the 24th hour of co-cultivation. The absolute counts were variable because of individual differences of the culture used in the different experiments. Since, however, only the relative effects were of interest in this study, the data were normalized to 1 and represented as a plane square lattice in the three dimensional coordinate. The left side of triangles perpendicular to the lattice represented the relative stimulation (upwards) or inhibition (downwards) as referred to the controls.

Figures 2A and B show the intra and interspecific effects of endothelial and smooth muscle cells on smooth muscle cell cultures of different species.

As demonstrated also by others, the endothelial cells in logarithmic phase stimulated the growth of smooth muscle cells of the same species. Endothelial cells of different species had inhibitory or no effect (Fig. 2A). The same was found on interspecific co-cultivation of smooth muscle cells (Fig. 2B). It appeared that the proliferation stimulating effect of endothelial cells is species specific and no "cross reaction" occurs.

Figure 3A shows the results obtained with endothelial cells. On co-cultivation of smooth muscle and endothelial cells the effect observed was inhibitory. The aortic smooth muscle cells of pig origin stimulated, however, the growth of endothelial cells of the same and of the other species tested.

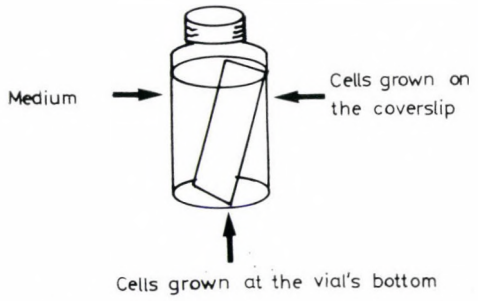

Fig. 1. Scheme of co-cultivation method

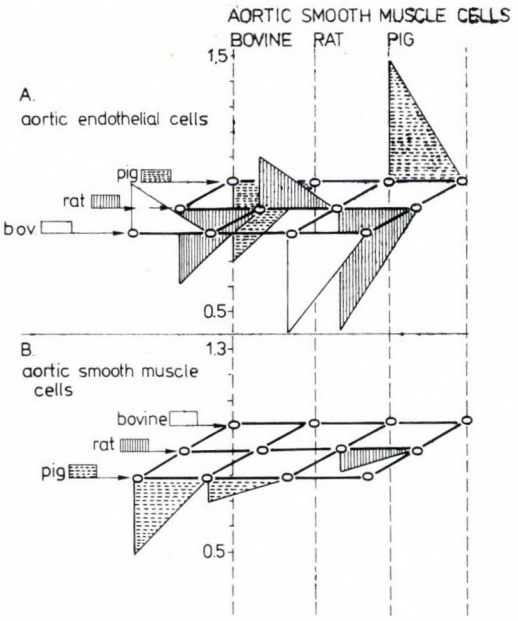

Fig. 2. Labelled thymidine incorporation in different aortic smooth muscle cells after co-cultivation with aortic endothelial or smooth muscle cells from different species

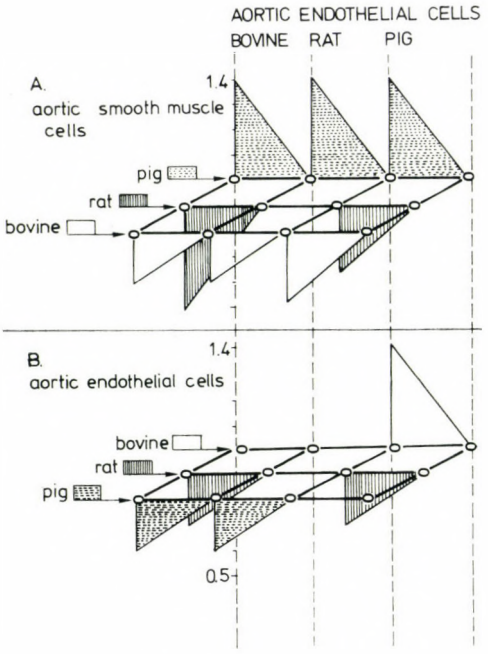

Fig. 3. Labelled thymidine incorporation in different aortic endothelial cells after co-cultivation with aortic smooth muscle or endothelial cells from different species

Endothelial cells of different species had an inhibitory effect on each other when co-cultivated (Fig. 3B). The only exception was the bovine endothelium which stimulated remarkably the proliferation of pig endothelium.

Discussion

In vitro grown endothelial cells in the exponential phase are known to produce a mitogenic factor active on smooth muscle cells [3]. The same was observed in our co-cultivation system (Fig. 2A) containing cells of the same animal species (intraspecific). Slight inhibition or no effect was seen if interspecific combinations of these cell types were studied.

Smooth muscle cells of different animal species (Fig. 2B) had no effect on each other when co-cultivated, except for some slight inhibition in 3 of the combinations studied.

As regard the effect of smooth muscle cells on endothelial cells, few data are available. Schumacher et al. [6] isolated from smooth muscle cells a substance inhibitory to endothelial cells. The inhibitory effect of smooth muscle cells on the proliferation of endothelial cells in intraspecific co-cultiation experiments with rat and cal cells may be explained on the same basis. Smooth

muscle cells of the pig were, however, found to stimulate considerably the growth of endothelial cells coming from the same as well as from the other species. In this case the existence of a non-specific stimulant may be supposed.

Co-cultivation of endothelial cells from the same and from different species resulted in no effect and in inhibition (in all but one case), respectively. The inhibitory effect of endothelial cells on the other endothelial or smooth muscle cells may be related to the inhibitor described by Sorgente [7]. This substance was isolated from cultured bovine endothelial cells.

Both the literary data and the present results suggest that the equilibrium regulatory interactions of stimulatory and inhibitory substances produced by one and the same cells may be of considerable biological importance. The endothelial cells produce in their logarithmic phase and in the phase of confluence a smooth muscle cell stimulatory and an inhibitory substance, respectively [4]. Opinions on this finding are, however, equivocal [8].

The different stimulatory and inhibitory substances may play an important role in the regulation of neovascularization and/or in the reendothelization of denuded intimal areas. The bovine endogenic endothelial cell growth inhibitor seems to be involved in regulation of neovascularization [6, 7].

The co-cultivation procedure proposed by us appeared to be useful in the study of direct stimulatory and/or inhibitory interactions of different homo and/or heterospecific cells in various combinations.

REFERENCES

1. Csonka E, Jellinek H: Aortic endothelial and smooth muscle cell interactions in culture. Acta Morphol Acad Sci Hung 34: 157, 1986
2. Dénes R, Mey J, Lehman R, Hauss WH: Vascular smooth muscle cells in culture after experimental diabetes. Abhandl Rhein-Westf Akad. Wissensch Westdeutscher Verlag, Opladen 1978, Vol. 63 p. 249
3. Gajdusek C, DiCorleto P, Ross R, Schwartz StM: An endothelial cell-derived growth factor. J Cell Biol 85: 467, 1980
4. Karnovsky MJ: Endothelial-vascular smooth muscle cell interactions. Rous-Whipple Award Lecture. Am Ass Pathol 105: 200, 1981
5. Merrilees MJ, Scott L: Interaction of aortic endothelial and smooth muscle cells in culture. Effect on glycosaminoglycan levels. Atherosclerosis 39: 147, 1981
6. Schumacher BL, Grant D, Eisenstein R: Smooth muscle cells produce an inhibitor of endothelial cell growth. Arteriosclerosis 5: 110, 1985
7. Sorgente N, Bullard DL, Jakovljevic L, Dorey K: Endogenous regulation of endothelial cell proliferation. Cell Tissue Kinet 17: 573, 1984
8. Willems CH, Astaldi GCB, DeGroot PhG, Janssen MC, Gonsalvez MD, Zeilmaker WP, vanMourik JA, vanAken WG: Media conditioned by cultured human vascular endothelial cells inhibit the growth of vascular smooth muscle cells. Exp Cell Res 139: 191, 1982
9. Wissler RW: Conference on the Biology of Inflammation, Cell-cell Interactions, Connective Tissue, and Endothelial Reactions. Potential new approaches to atherosclerosis research. Arteriosclerosis 3: 398, 1983

Acta Morphologica Hungarica, 35 (1–2), pp. 37–46 (1987)

FURTHER STUDIES ON THE INTRAVENOUSLY ADMINISTERED FAT ARTERIOSCLEROSIS MODEL

ÉVA TAKÁCS, JUDIT HÁRSING, SZLÁVA FÜZESI, H. JELLINEK

SECOND INSTITUTE OF PATHOLOGY, SEMMELWEIS UNIVERSITY MEDICAL SCHOOL, BUDAPEST, HUNGARY

(Received 4 May 1986)

30 rats were devided into 3 experimental groups. These included 8 days of Lipofundin treatment + 8 days recovery period (Group I), 16 days of Lipofundin treatment (Group II), and 16 days of Lipofundin treatment + 8 days recovery period (Group III). After sacrifice semi-thin and ultra-thin sections prepared from the aorta segments were examined light and electron microscopically.

In addition to the development of alterations characteristic of the Lipofundin-model, the accumulation of collagen fibres was also observed. After 16 days of Lipofundin treatment the alterations were much more advanced than after 8-day treatment. Subsequent migration of smooth muscle cells through the newly formed internal elastic lamina was apparent and led to thickening of the sclerotic plaque. When the 16-day Lipofundin treatment was followed by a recovery period of 8 days prior to sacrifice, no signs of regression were seen. The alterations were present in unchanged form and the only difference was in the extent of accumulation of collagen fibres.

Keywords: fibrous plaque, proliferation, arteriosclerotic regression, smooth muscle cell, ghost body.

Introduction

In previous papers [8, 14, 16, 17, 23] we reported that after 8-day treatment with Lipofundin-S 20% (Braun, Melsungen) aortic smooth muscle proliferation could be observed in rats. Smooth muscle cell migration through internal elastic lamina resulted in accumulation of basement membrane-like material followed by the appearance of elastic granules and elastic membrane-like structures in the subendothelial space.

In these studies it was also shown that the pattern of vascular alterations in the model was much closer to that seen in human atherosclerosis than after cholesterol feeding [1, 2, 6, 7, 13, 15, 25, 26, 30, 31]. The advantage and significance of Lipofundin-treatment lies in the fact that responses appear rapidly and sclerotic changes can be observed as soon as 8 days after treatment.

In the present study we have investigated the Lipofundin-induced changes after a prolonged period of treatment, and further, how the well-known histological picture was modified by a 8-day recovery period elapsing from the end of the short-term or long-term Lipofundin treatments until sacrifice.

Send offprint requests to: Éva Takács Üllői út 93, 1091 Budapest, Hungary

Materials and methods

Lipofundin-S (20%) (Braun, Melsungen) is a soy-bean oil extract stabilized to a particle size of 1 μm (chylomicron size), used for parenteral nutrition. Lipofundin-S was administered intravenously (i.v.) in a dose of 1 ml/100 g bodyweight/2 min, two times daily over a period of 8 days. Food and water were provided ad libitum.

30 Wistar male rats with 180—200 g bodyweight were divided into 3 groups:

Group I. Lipofundin treatment for 8 days followed by a recovery period of 8 days until sacrifice (10 rats)

Group II. Lipofundin treatment for 16 days and sacrifice (10 rats)

Group III. Lipofundin treatment for 16 days followed by a recovery period of 8 days until sacrifice (10 rats).

Before sacrifice the animals were anaesthetized with pentothal-Na and the aorta was prepared. Segments of the thoracic and abdominal aorta about 2—3 mm long were fixed in 4.5% glutaraldehyde in 0.1 M phosphate buffer (pH 7.2) for 2 h. After washing, the specimens were postfixed in 1% OsO_4 solution for 2 h, then following repeated washing they were dehydrated in an ascending alcohols series and embedded in Durcupan ACM. Semi-thin sections were stained with methylene blue-azure II and basic fuchsin. Ultra-thin sections were contrasted with uranyl acetate and lead citrate and examined in a JEM 100 B electron microscope.

Results

In the *semi-thin sections* a multilayer thickening of the intima was occasionally observed over the internal elastic lamina. In some areas over the novel cell layer and endothelium, thin elastic fibres appeared in foci whereas in other zones they were confluent.

Electron microscopic findings

Group I. Aortic preparations of rats subjected to 8-day Lipofundin treatment followed by 8-day recovery period prior to sacrifice, exhibited alterations as published earlier [14, 16, 17]. In the original enlarged subendothelial space around the immigrated smooth muscle cells elastic granules and developing elastic fibres appeared. In the new subendothelial space formed between the parts of the "new" elastic lamina and endothelial cells, granular basement membrane-like material and details of further migrating smooth muscle cells were seen. Smooth muscle cell processes were occasionally observed even within the cleft between the new elastic lamina. There was an apparent accumulation of collagen fibres, and some of them were in close contact with the elastic lamina (Fig. 1).

Group II. Aortic specimens of rats killed immediately after 16-day Lipofundin treatment exhibited the following electron microscopic alterations. In the enlarged space between the "old" internal elastic lamina and the endothelium, numerous smooth muscle cells and elastic granules appeared with occurrence of light, mature elastic lamina. The "new" subendothelial space between the new elastic lamina and endothelium was enlarged and contained granular basement membrane-like material. A few immigrated smooth muscle cells, or smooth muscle cell processes just penetrating the new elastic stroma were also

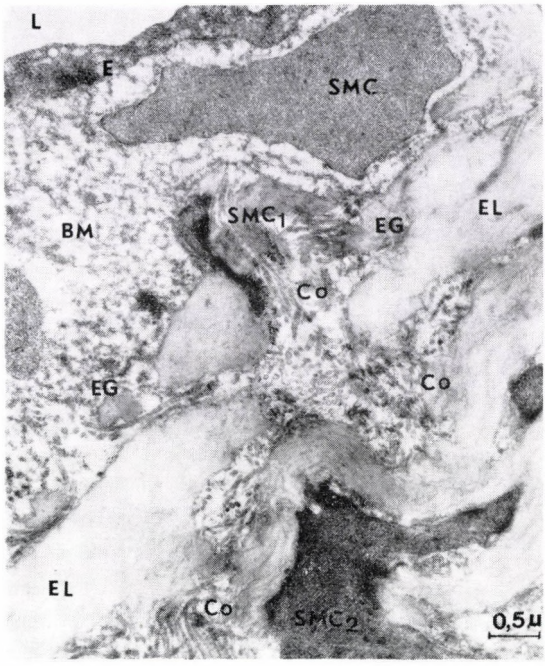

Fig. 1. Electron micrograph prepared from rat subjected to 8-day Lipofundin treatment and 8-day recovery period prior to sacrifice. Under the endothelium (E) in the subendothelial space the accumulation of basement membrane-like material (BM) and details of smooth muscle cells (SMC) are seen. The former internal elastic lamina is not present. The elastic lamina (EL) formed from the elastic granules (EG) seemed to be mature on the basis of loss of their staining affinity. Within the cleft between the elastic lamina new smooth muscle cell (SMC_1) processes penetrate into the subendothelial space. Numerous collagen fibres (Co) are present forming close contact with the elastic fibres. SMC_2 = process of an immigrated smooth muscle cell residing over the elastica. Some smooth muscle cells display signs of degeneration. L = lumen

seen (Fig. 2). The structure of these smooth muscle cells was preserved, in the granular substance there was apparent accumulation of collagen fibres (Fig. 3), moreover under the endothelial cell layer in close contact with it, pale, not identifiable cells were present (Fig. 3) which were believed to be young cells on the basis of their structure. Some of the smooth muscle cells migrating into the subendothelial space showed signs of degeneration (Fig. 4) and where an abundance of collagen fibres was apparent. In the subendothelial space among the smooth muscle cells, elastic granules and maturing elastic fibres also a migration of smooth muscle cells was readily seen (Figs 4 and 5). Their processes in the subendothelial space established a close contact with the endothelial cells (Fig. 6). The progression of events was indicated by the appearance of newly formed elastic granules around the smooth muscle cells migrating toward the surface between the elastic lamina formed over the internal elastic lamina (Figs 5 and 7).

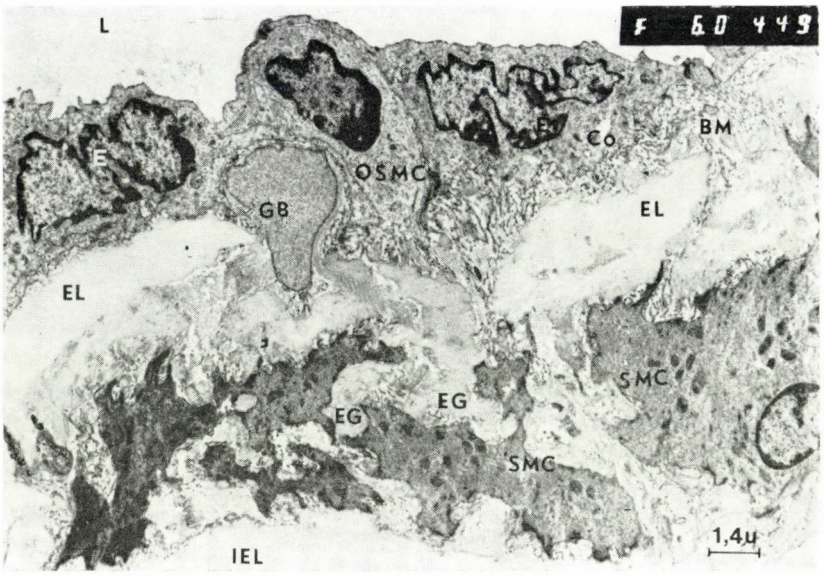

Fig. 2. Electron micrograph prepared from rat killed after 16 days of Lipofundin treatment. Between the endothelial cells (E) and the internal elastic lamina (IEL) smooth muscle cells (SMC), elastic granules (EG) and newly formed, mature elastic lamina (EL) are present. Through these lamina smooth muscle cell processes penetrate into the subendothelial space, which shows signs of slight congestion (GB). Smooth muscle cells (OSMC) are also seen in the subendothelium. A marked accumulation of basement membrane (BM) and formation of collagen fibres (Co) are apparent. L = lumen

Group III. Electron microscopic findings in aortic preparations of rats killed after 16 days of Lipofundin treatment + 8 days of recovery period were as follow. In the enlarged area containing elastic lamina-like structures over the elastic fibres, cells appeared with accumulation of granular substance. In the layer between the endothelium and the internal elastic lamina, the heavy staining of a few smooth muscle cells was prominent, indicating signs of osmiophilic degeneration and the presence of numerous mature collagen fibres was apparent (Fig. 8). In a few specimens the number of Weibel-Palade bodies an the endothelial cells was enhanced.

Discussion

The purpose of the present study was to describe and characterize the alterations developed after Lipofundin administration to rats by varying the period of treatment and including a recovery period of 8 days before sacrifice. It appeared that inclusion of a 8-day recovery period following 8-day Lipofundin treatment (Group I) resulted in a histological picture which was similar to that observed in the Lipofundin-model with standard protocol except that

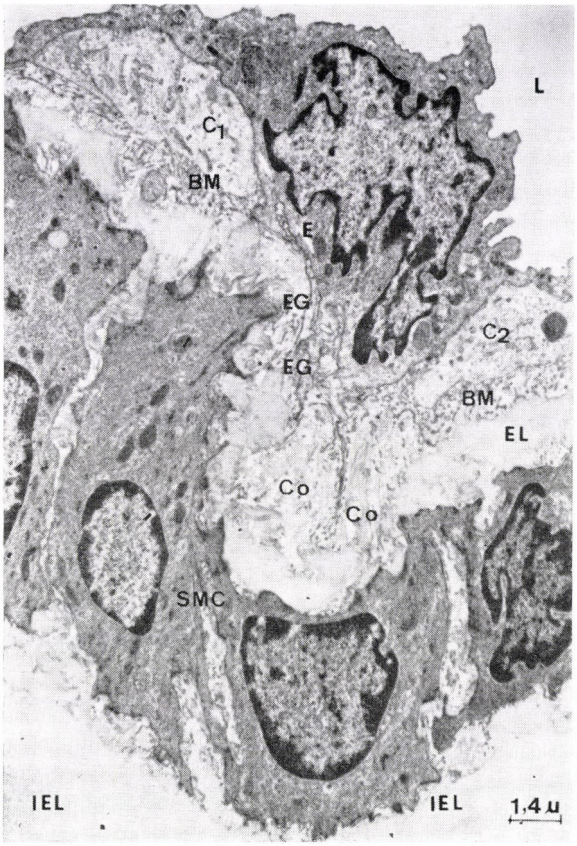

Fig. 3. Electron micrograph prepared from rat treated with Lipofundin for 16 days. Between the endothelial cell (E) and internal elastic lamina (IEL) smooth muscle cells (SMC) appear with elastic granules (EG) and early elastic fibres (EL) around them. The newly formed subendothelial space is enlarged, containing basement membrane-like material (BM), processes of two light, unidentified cells (C_1, C_2) and numerous collagen fibres (Co) which are in close contact with the elastic fibres. L = lumen of the vessel

the accumulation of collagen fibres was more enhanced. Once the Lipofundin-induced alterations had developed no signs of regression were seen.

Electron microscopic examination of aortic specimens of rats killed after 16 days of Lipofundin treatment (Group II) revealed that the elastic granules were in a more mature state than in rats sacrificed after 8 days treatment + 8 days of recovery period (Group I), as compared to findings in rats treated according to the standard protocol. Aortic preparations of rats in Group II showed an early formation of elastic lamellae. In terms of function and structure these lamellae resembled the internal elastic lamina; they were light in colour, though their stomata smooth muscle cell processes had penetrated from the former subendothelium into the new subendothelial space where they were surrounded by a great amount of granular, basement membrane-like material.

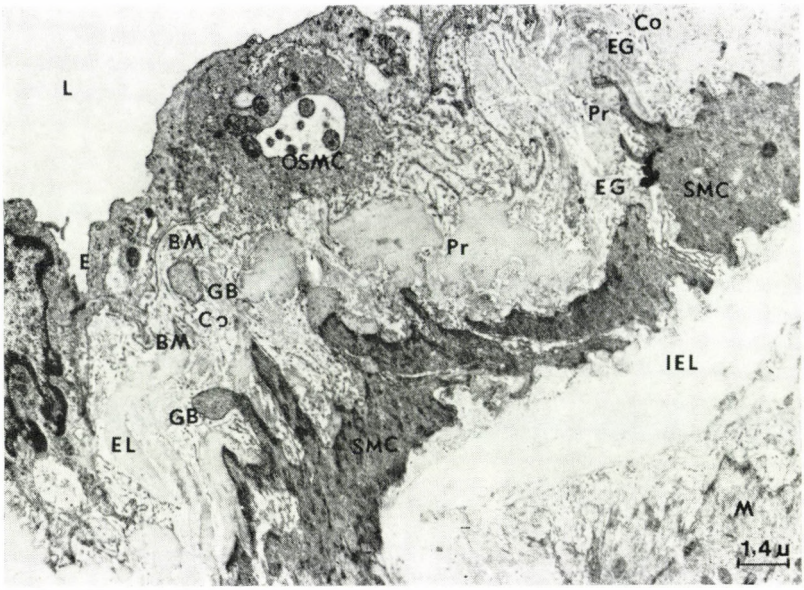

Fig. 4. In the subendothelial space formed after 16 days of Lipofundin treatment, among the smooth muscle cells (SMC) immigrated between the endothelial cell (E) and internal elastic lamina (IEL), the formation of elastic granules (EG) and new elastic lamina (EL) is apparent. Between the new elastic lamina in the subendothelial space, processes (Pr) of new smooth muscle cells are seen, some of them being edematous exhibiting ghost-body-like (GB) formations. Note also the presence of a degenerated smooth muscle cell (OsMC) in the subendothelial space. In the new enlarged subendothelial space basement membrane (BM) and collagen fibres (Co) are accumulated

The abundace of collagen fibres was noteworthy. Smooth muscle cell processes migrating through the new elastic lamellae occasionally became pale and detached (ghost body) (Fig. 8). In some areas these processes established contact with the endothelial cells as described by Cavallero et al. [4].

In the animal preparations in Group II it was also apparent that certain smooth muscle cells which migrated into the subendothelium, displayed signs of degeneration. Thus, alterations induced by 16-day Lipofundin treatment were more prominent than after 8 days of treatment; the formation of the new elastic lamina-like structures was more advanced, whereas the lamina serving as barriers to the new smooth muscle cell proliferation showed the characteristic transmigration pattern of smooth muscle cells. The accumulation of collagen fibres in turn appeared to indicate the progression and ageing of the process.

Alterations that developed in rats treated with Lipofundin for 16 days and then subjected to a 8-day recovery period (Group III) were essentially the same as after 16 days of treatment. Smooth muscle cells had migrated into the subendothelial space and were surrounded by granular substance. The accumulation of collagen fibres was even more apparent and their contact

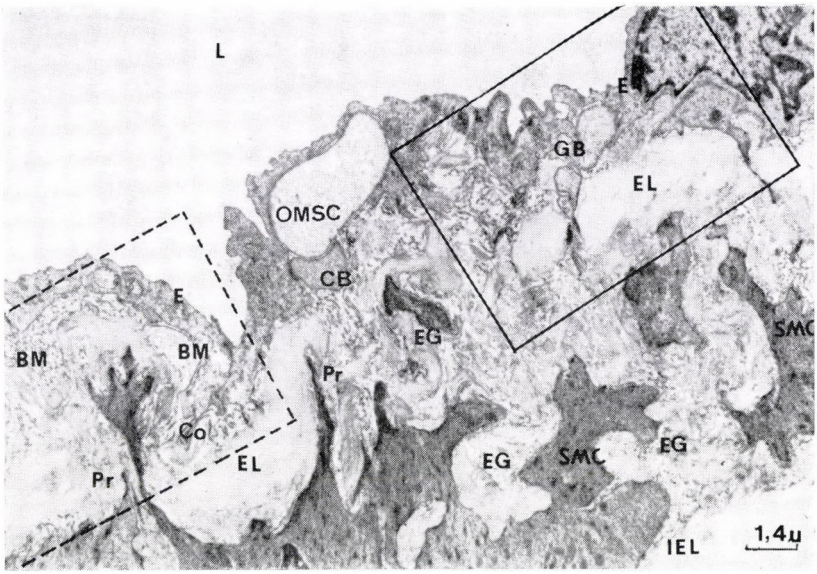

Fig. 5. In the enlarged aortic subendothelial space of a rat subjected to 16 days of Lipofundin treatment, between the endothelial cell (E) and internal elastic lamina (IEL) there are numerous smooth muscle cells (SMC), elastic granules (EG) and newly formed elastic lamina (EL). In the new subendothelial space basement membrane-like material (BM) is accumulated. A detail of an edematous smooth muscle cell (OSMC) and ghost body (GB) formation is seen. Smooth muscle cells residing in the subendothelial space send out new processes (Pr) through the new elastic laminae toward the new subendothelium.
L = lumen

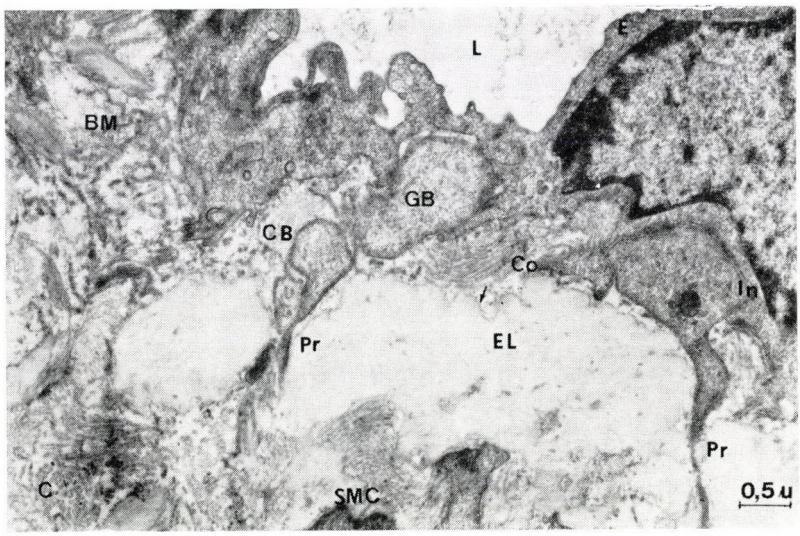

Fig. 6. Enlargement of the framed area in Fig. 5. The endothelial cell (E) and the newly formed elastic lamina (EL) can well be recognized. The microfibrils (→) being incorporated into the EL stain readily. Through the new elastic lamina smooth muscle cells (SMC) send out processes (Pr) into the subendothelial space, some of them are edematous with signs of ghost body (GB) formation. The other smooth muscle cell process forms an apparent junction (Ju) with the endothelial cell. The presence of numerous collagen fibres (Co) is evident. BM = accumulated basement membrane-like material; L = lumen

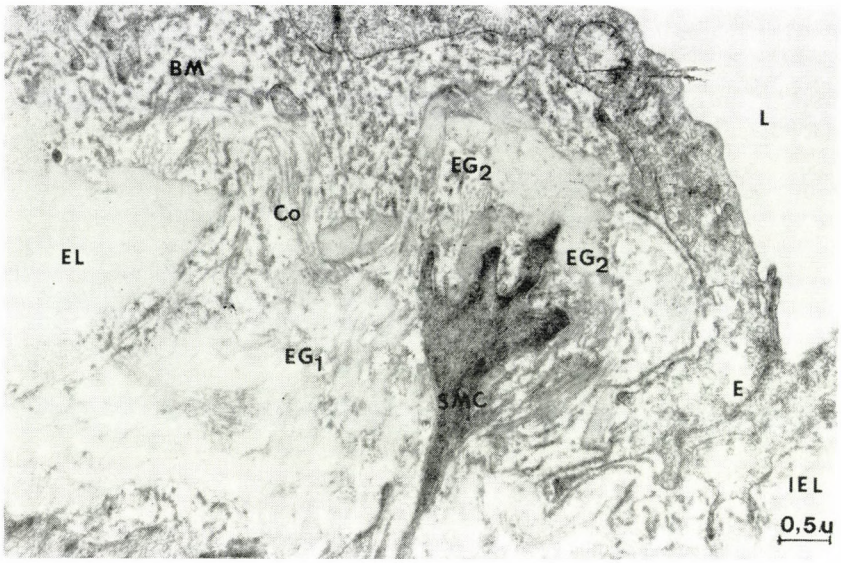

Fig. 7. Area of Fig. 5 framed by dotted line. Around the smooth muscle cell process (SMC) sent out through the old elastic granules (EG_1) and elastic lamina (EL), newly formed elastic granules (EG_2) appear. In addition to the accumulation of basement membrane-like material (BM) there are numerous collagen fibres (Co). E = endothelial cell; L = lumen

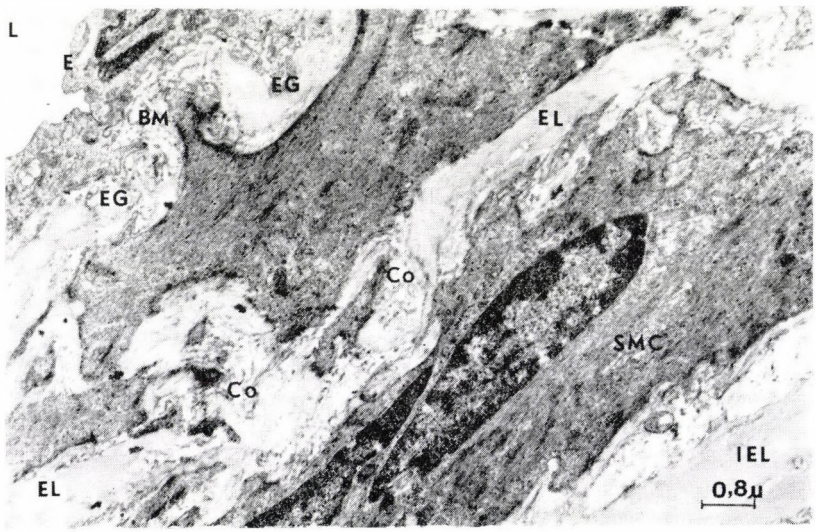

Fig. 8. Aortic preparation of rat subjected to 16 days of Lipofundin treatment and a recovery period of 8 days prior to sacrifice. A smooth muscle cell (SMC_1) had migrated into the new subendothelial space through the newly formed mature elastic fibres (EL) of the enlarged subendothelial space. Under the endothelial cell (E) basement membrane-like material (BM) had accumulated. Between the endothelial cell and the basement membrane the detail of an immigrated smooth muscle cell appears. Formation of new elastic granules (EG) is seen. Smooth muscle cells (SMC) of previous proliferations reside on the internal elastic lamina (IEL). There is a marked accumulation of collagen fibres (Co). L = lumen

with the elastic fibres was occasionally more intense. Thus these findings indicate that the process had progressed until a certain time, but as soon as the stimulus for proliferation was withdrawn no further progression occurred. The presence of lipid droplets in some endothelial cells also supported the occurrence of degeneration as described in various forms of proliferation [3, 4, 5, 6, 8, 9, 10, 11, 12, 13, 14, 16, 18, 19, 20, 21, 22, 27, 28, 29, 30, 31].

On the basis of the above findings, it is concluded that the vascular alterations induced by Lipofundin treatment were more advanced and severe with time. Thus they provide evidence for the aortic sclerosis and arteriosclerosis-inducing potential of the Lipofundin-model. Reasons favouring the use of this model are its cheapness and the short duration of treatment.

REFERENCES

1. Anitschkow N, Chalatov S: Über experimentelle Cholesteratose und ihre Bedeutung für die Entstehung einiger pathologischen Prozesse. Zbl Allg Pathol *24:* 1, 1913
2. Bálint A, Veress B, Nagy Z, Jellinek H: Role of lipophages in the development of rat atheroma. Atherosclerosis *15:* 7, 1972
3. Betz E, Hämmerle H: Arterienwandproliferate und Zellkulturen als Indikatoren für Hemmstoffe der Atherogenese. Funkt Biol Med *3:* 46, 1984
4. Cavallero C, Villaschi S, Pace F, Spagnoli LG: Role of acute serum sickness in the response of arterial wall to endothelial injury. In: Immunity and Atherosclerosis. Proc. Serono Symposia. eds P Constantinides, F Pratesi, C Cavallero, T DiPerri; Academic Press, New York, 1980
5. Chobanion AB, Brescott MF, Haudenschild CC: Recent advances in molecular pathology. The effects of hypertension on the arterial wall. Exp Molec Path *41:* 153, 1984
6. Detre Z, Jellinek H: Role of the altered transmural permeability in the pathomechanism of arteriosclerosis I. Path. Res Pract *181:* 693, 1986
7. Detre Z, Jellinek H: Role of the altered transmural permeability in the pathomechanism of arteriosclerosis II. Path. Res Pract *181:* 693, 1986
8. Füzesi Sz, Hársing J, Jellinek H: Characteristic features of the smooth muscle cell migration in vascular wall injury. Exp Pathol *21:* 94, 1982
9. Geer JC: Fine structure of human aortic intimal thickening and fatty streaks. Lab Invest *14:* 1764, 1965a
10. Hauss WH: Die Rolle der Reaktion der Arterienwandzellen ("unspezifische Mesenchymreaktion") in der Sklerogenese. In: Atherogenese. I. Initiale Zelluläre Vorgänge bei Atherosklerose und Hypertension. Ed. WH Hauss Maudrich, Wien 1976, p. 37.
11. Haust MD, More RH, Movat ZH: The role of smooth muscle cells in the fibrogenesis of arteriosclerosis. Am J Pathol *37:* 377, 1960
12. Haust MD, More RH: Significance of the smooth muscle cell in atherogenesis. In: Evaluation of the Atherosclerotic Plaque. ed. RJ Jones Univ Chicago Press 1963, Vol. 1, p. 51.
13. Jellinek H: Arterial Lesions and Arteriosclerosis. Plenum Press — Akadémiai Kiadó Budapest 1974
14. Jellinek H, Hársing J, Füzesi Sz, Bihari-Varga M: Lipofundin administration and vessel damages in diet and drugs in atherosclerosis, eds G, Noseda B, Lewis R Paoletti: Raven Press, New York 1980, p. 131.
15. Jellinek H, Kerényi T, Detre Z, Veronesi PL: Atlante grafico della arteriosclerosi. Experimental Arterial Injuries on the Rat and Arteriosclerosis. SKEMA Editions, Bologna 1979
16. Jellinek H, Hársing J, Füzesi Sz: A new model for arteriosclerosis. An electron microscopic study of the lesions induced by i.v. administered fat. Atherosclerosis *43:* 7, 1982
17. Jellinek H, Detre Z, Veress B: Transmural Plasma Flow in Atherogenesis. Akadémiai Kiadó, Budapest 1983
18. Kádár A, Veress B, Jellinek H: Ultrastructural elements in experimental intimal thickening. II. Study of the development of elastic elements in intimal proliferation. Exp Molec Pathol *11:* 212, 1969

19. May J, Grünwald J, Schaper W, Schulte H, Hauss WH: About the effect of risk factors on the structure and the proliferation of arterial wall cells. Part 2. Changes in structure and proliferation of cultivated aortic endothelial cells from hypertensive minipigs. Exp Pathol *25*, 163 1984
20. Reidy MA, Silver M: Endothelial regeneration VII. Lack of intimal proliferation after defined injury to rat aorta. Am J Pathol *118:* 173, 1985
21. Reinila A: Ultrastructure of arteries in rats fed a high-fat cholesterol diet. Intimal thickening of a small muscular artery. Arch Pathol *108:* 295, 1984
22. Ross R, Glomset JA: The pathogenesis of atherosclerosis. N Engl J Med *295:* 420, 1976
23. Schrecker O, Weckermann D, Weckermann J, Jellinek H: Lipoprotein changes induced by i.v. administered lipid-emulsion leading to arteriosclerotic lesions in rat. Appl Pathol *4:* 211, 1986
24. Scott RF, Kim DN, Schmee J: Endothelial lesion and cell growth patterns of early smooth muscle cell atherosclerotic lesions in swine. Arch Pathol *109:* 450, 1985
25. Seidel D, Cremer P, Thiery J: Plasmalipoproteine und Atherosklerose. I. Biochemie, Physiologie und Pathophysiologie der Lipoproteine. FK. Schattauer, Stuttgart 1985, p. 114.
26. Seidel D, Cremer P, Thiery J: Plasmalipoproteine und Atherosklerose. II. Lipoproteindiagnostik. Therapie der Fettstoffwechselstörungen. FK Schattauer, Stuttgart] 1985, p. 159.
27. Staubesand J: Entstehung und Bedeutung der sog. Matrix Vesikel bei Umbauvorgängen in der Gefässwand. Verh Anat Ges *72:* 492, 1978
28. Staubesand J: Sind Krampfadern tonisierbar? Eine elektronenmikroskopische und experimentelle Studie zur Ultrastruktur varikös veränderter Venen des Saphena-System. I. Venen Symposion, Wiesbaden 1981. Acron Verl Berlin 1981
29. Staubesand J: Mediadysplasie und Arteriosklerose. Elektronenmikroskopische und biochemische Untersuchungen. Gödecke, Berlin 1981
30. Weber G, Fabrini P, Resi L: Scanning- and transmission electron microscopic observations on the surface lining of aortic intimal plaques in rabbit on a hypercholesterolic diet. Virchows Arch Path Anat *364:* 325, 1974
31. Wissler RW, Vesselinovich D: Evaluation of animal models for the study of the pathogenesis of atherosclerosis. In: State of Prevention and Therapy in Human Arteriosclerosis in Animal Models. eds: WH, Hauss R, Lehmann; Westdeutscher Verl Münster 1978, p. 13.

Acta Morphologica Hungarica, 35 (1—2), pp. 47—57 (1987)

LARGE CELL DYSPLASIA OF HEPATOCYTES, IS IT A PREMALIGNANT CONDITION?

L. Kovács, G. Elek

HUNGARIAN RAILWAY HOSPITAL, BUDAPEST, HUNGARY

(Received 10 December 1985)

Incidence and character of large cell dysplasia (LCD) of liver were examined by histological, statistical and morphometric methods in an aged Middle European population. The necropsy material of 487 patients with micronodular cirrhosis and cirrhosis with primary liver tumour was studied. In addition, 50 primary tumours developed in non-cirrhotic livers, 34 metastatic tumours and 90 normal livers were examined. According to the findings, LCD often developed in aged patients. The high occurrence is presumably due to the high age. The frequency of LCD was significantly higher in active than in inactive cirrhosis. LCD could mostly be found around metastatic tumours, especially those with large, destructive foci. Sex differences occurred in a part of cases but an age dependence could not be demonstrated, Normal and dysplastic cells did not differ significantly in most morphometric parameters but there was a significant difference between tumorous and normal or dysplastic parameters.

The data suggested that LCD is a secondary, reactive phenomenon occurring in various pathological processes.

Keywords: liver-cell, liver cancer, liver cirrhosis,, displasia morphometry

Introduction

Large cell dysplasia (LCD) as a premalignant condition was described by Anthony et al [2] among young Ugandan patients suffering from macronodular cirrhosis and primary liver tumour. The present work analyses the occurrence of LCD in active and inactive micronodular cirrhosis, cirrhosis and hepatocellular carcinoma, primary carcinoma of the liver as well as metastatic tumours.

Materials and methods

Histological section obtained from autopsy of 667 patients admitted between 1963—1985 to our hospital were examined: 487 patients died with micronodular cirrhosis and primary liver tumour.

Liver specimens were fixed in 4% neutral formol, embedded in paraffin. 5 μ sections were cut and stained with haemalaun-eosin, Prussian blue, basic fuchsin for HBsAg, Masson and picrosirius-red. The term micronodular cirrhosis was used if the diameter of nodules was less than 3 mm, it was easily measurable on picrosirius stained preparations. As to the activity of cirrhosis, the presence of piecemeal necrosis, intensive lymphotic, plasmocytic in-

Send offprint requests to: L. Kovács Hungarian Railway Hosp. Budapest, Rudas L. u. 111, 1062 Hungary

filtration, wast connective tissue framework, bile duct prolitferation were the signs of active cirrhosis. In inactive cirrhosis these signs were much less remarkable.

We took into consideration the entity of steatocirrhosis widely used earlier in German literature [9], which we regard as an early phasis of alcoholic cirrhosis, developing in alcoholic fatty livers. The number of primary tumours developed in non-cirrhotic livers was 50. Metastatic liver tumours were analysed in 34 cases.

In this way the liver tumours were subdivided into three groups: a) primary liver tumour developed on the ground of micronodular cirrhosis, b) primary liver tumour without cirrhosis, c) metastatic liver tumour. In the control group 90 normal organs without liver disease were investigated.

For morphometric analysis, 30 cases were studied including 10 cases of hepatocellular carcinoma and 10 cases of liver cell dysplasia. Ten histologically normal livers were used as controls. In the HE stained sections 20 to 50 representative fields were selected and two to three photographs were made of these areas (final magnification approximately $\times 2500$). The cells, their nuclei and nucleoli having clear contours on the photographs were traced. Each group of chromatin exceeding an area of 1 μm^2 with a homogeneous density and more or less regular contour was considered to be a nucleolus. 100 cells from each group (normal, dysplasia and carcinoma) were randomly selected and their contour, nuclei and nucleoli were numbered to make them identifiable.

Measurements were done on a HP digitizing pad of a Hewlett—Packard 9830 microcomputer. The photographs were affixed to the tablet of the digitizing pad and boundaries of cross sectioned cytoplasm, nuclei and nucleoli were traced by the cursor of the device. The two dimensional information entered the computer in the form of X and Y coordinates. From the coordinates of the contour the computer calculated and printed out the cytoplasmic, nuclear and nucleolar area, perimeters and X—Y coordinates of centres of gravity. (For computer facilities and programs we are indebted to B. Turcsányi, Central Research Institute of Chemistry, Hungarian Academy of Sciences, Budapest).

Cytoplasm to nucleus ratio; nucleolar, nuclear and cytoplasmic contour index; the relative nuclear and nucleolar excentricity and their standard deviations were calculated by hand microcalculator. The contour index is a size independent shape index defined as perimeter/square root of the area. Its minimum value is 3.54 and is a perfect circle [10]. The relative excentricity is the distance between the centres of gravity of a small area in a larger area divided by the square root of the larger area in order to make it a size independent parameter for the small area [18, 19]. For example, the relative excentricity of the nucleus is the distance between the centres of gravity of cytoplasm and nucleus divided by the square root of the cytoplasmic area. A zero excentricity denotes a perfectly central nucleus or nucleolus, while one of almost 0.5 denotes a marginal nucleus or nucleolus.

For calculation of significance, Student's t test (algorithms 11 and 12) were used [14].

Results

Occurrence

Table I demonstrates liver diseases and the prevalence of LCD found by us. Among 369 micronodular cirrhosis case 152 LCD (41%) were found.

Table I

Large cell dysplasia (LCD) in different changes of the liver

Diseases	No. of cases	No. of dysplasia	Per cent
Cirrhosis	369	152	41
Cirrhosis and primary liver tumour	118	65	55
Primary tumour without cirrhosis	50	15	30
Metastatic tumour	34	15	44
Normal	90	7	8

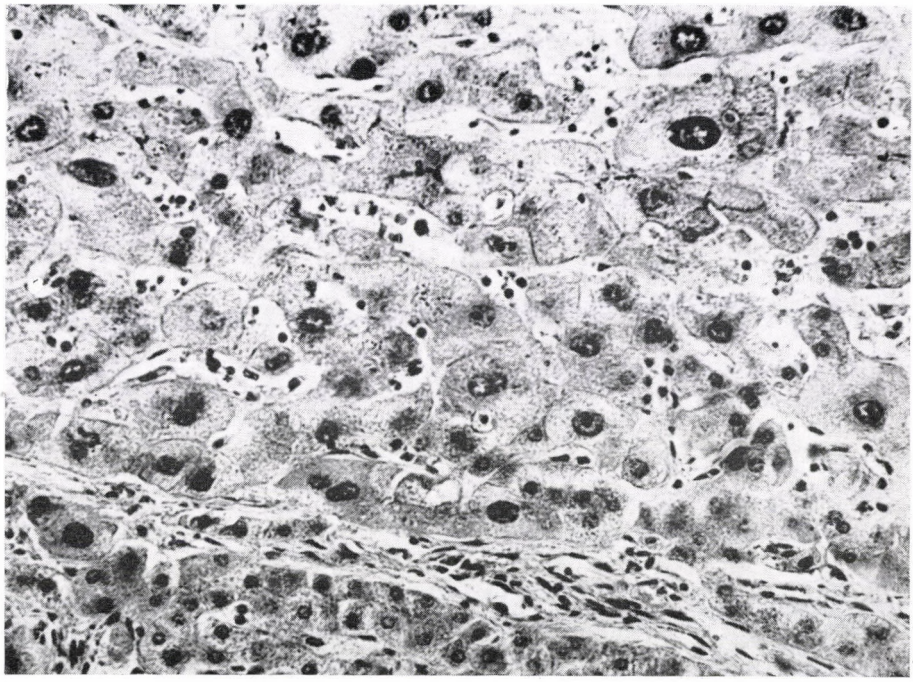

Fig. 1. Large cell dysplasia in liver 25×3.2

118 cirrhosis and tumours were found together. In this group the number of dysplastic cases was 65 (55%), significantly higher than in the previous group ($p < 0.001$, Fig. 1). Primary tumour developed in 50 non-cirrhotic livers. The occurrence of LCD was 15 (30%). Among 34 metastatic liver tumours 15 were associated with LCD (44%). In 90 livers showing no signs of primary disease LCD occurred in 7 cases (8%).

Aetiology

HBsAg positivity was found in 5% of cases (24 patients). It appeared in different groups and there was no correlation between it and the malignant transformation. Mallory bodies were found in 14% of cirrhotic livers. High alcohol consumption (over 100 g alcohol/day) was observed in 61% of cases. In 34% the exact aetiology was not detectable.

Activity of cirrhosis

Table II. shows the frequency of LCD in active and inactive micronodular cirrhosis.

Significantly more LCD occurs in active cirrhosis (51%) than in the inactive form (31%, $p < 0.001$). In steatocirrhosis the active and inactive

Table II

LCD in active and inactive cirrhosis

Diseases	No. of cases	No. of dysplasia	Per cent
Active cirrhosis	159	81	51
Inactive cirrhosis	120	37	31
Steatocirrhosis			
active	33	10	30
inactive	57	6	11
Cirrhosis and tumour			
active	66	44	67
inactive	52	22	42

forms are less distinct entities but differences could be recognized even in this group.

If primary tumours developed on the ground of active micronodular cirrhosis, the occurrence of LCD was the highest (67%). If LCD appeared on the basis of inactive cirrhosis, LCD was significantly lower (42%, $p < 0.001$). The data on LCD were in increasing incidence: normal liver 7%, inactive steatocirrhosis 11%, active steatocirrhosis 30%, inactive cirrhosis 31%, inactive cirrhosis + primary tumour 42%, active cirrhosis 51%, active cirrhosis and primary tumour 67%.

Histological type of tumours

Among 44 hepatocellular tumours observed in non-cirrhotic livers 15 LCD were found (34%, Table III). There was no LCD around the 6 cholangiocellular carcinomas. Among 34 metastatic tumours there were 26 carcinomas; in this group we found LCD in 15 cases (58%).

Malignant Hodgkin and non-Hodgkin lymphomas were identified in 8 cases; around these lymphomas there was no sign of LCD.

Table III

Distribution of LCD among primary and metastatic liver tumours

Diseases	No of cases	No of dysplasia	Per cent
Primary liver tumours without cirrhosis hepatocellular carcinoma	44	15	34
Cholangiocellular carcinoma	6	0	0
Metastatic tumours carcinomas	26	15	58
Lymphomas	8	0	0

Sex distribution

In our series there were 330 male and 137 female patients, the ratio was 2.1 : 1. In the subgroups we found the following male-female ratios: simple cirrhosis 1.92 : 1, steatocirrhosis 1.52 : 1, active cirrhosis with tumour 4.58 : 1,

Table IV

Sex distribution of LCD in pathological conditions of liver

Diseases	No.	Male	Occurrence of LCD, per cent	Female	Occurrence of LCD, per cent
Cirrhosis	369	235		134	
without LCD	235	144		91	32
with LCD	134	91	39	43	
Cirrhosis + primary liver cancer	118	95		23	
without LCD	52	38		14	39
with LCD	66	57	60	9	
Total	487	330		157	
without LCD	287	182		105	33
with LCD	200	148	45	52	

inactive cirrhosis with tumour 3.63 : 1. The sex distribution was significantly different in the above subgroups ($p < 0.05$).

The occurrence of LCD in male and female subjects was different in the subgroups. Taking into consideration all the cirrhotic as well as cirrhotic + primary tumourous cases it appeared that in males LCD appeared significantly more often than in women ($p < 0.05$). In the cases with cirrhosis by itself LCD appeared nearly in the same percentage in both sexes, the difference being insignificant (Table IV). In the group of primary liver tumours developed on the basis of cirrhosis the occurrence of LCD was significantly more frequent among males than in females ($p < 0.01$).

Age

Table V shows that mean age for males was 62.5 years, for females 70.2 years. We compared the age of dysplastic and non-dysplastic cases of both sexes. The scatter of ages being high, significance was calculated in each group. In the group of males a significant difference was found only for simple inactive cirrhosis ($p < 0.05$). In the females a significant age difference was found in both active and inactive micronodular cirrhosis in regard of LCD. In the other groups with both sexes, there was no significant difference between the age of dysplastic and non-dysplastic cases.

Table V

Age distribution of LCD in liver diseases

Diseases	Sex							
	Male				Female			
	With dysplasia		Without dysplasia		With dysplasia		Without dysplasia	
	Year	± SD	Year	± SD	Year	± SD	Year	± SD
Active cirrhosis	62	11	62	12	71*	12	62	13
Inactive cirrhosis	71*	12	65	11	70*	10	66	15
Steatocirrhosis								
active	61	11	51	11	75	3	66	12
inactive	57	19	59	12	76	17	62	11
Cirrhosis and tumour, active	64	10	63	9	68	11	69	9
Cirrhosis and tumour, inactive	65	9	68	8	87	1	73	16
Primary liver tumour without cirrhosis	60	15	68	13	70	6	70	11
Metastatic liver tumour	64	10	55	13	73	10	68	14
Normal	73	7	64	13	72	11	73	12

* = significant

Histochemical observations

The Prussian blue method revealed that large dysplastic cells nearly always contained more or less haemosiderin. HBsAg was observed only in 51% of the observed micronodular cirrhosis cases. Mallory bodies occurred often, in 14% of the cirrhotic cases.

Morphometry

The mean area of tumour cell sections was smaller than that of normal hepatocytes but tumorous nuclei and nucleoli were larger than the normal ones (Table VI). The cytoplasm to nucleus ratio of dysplastic and normal cell was significantly larger ($p < 0.001$) than that of tumour cells. This ratio for dysplastic cells was even higher than for normal cells, but the standard deviation was considerable. The larger nucleus of the tumour cell was placed more centrally in a smaller cytoplasm and its excentricity was therefore smaller than that of normal nuclei. The nuclear excentricity of dysplastic cells was between the value for normal and tumorous ones. Mean nuclear excentricity for normal-dysplastic and dysplastic-tumorous pairs was significantly different ($p < 0.001$ and $p < 0.05$). Normal, dysplastic and tumorous cells and nuclei did not differ significantly in shape (contour index) but this index of the nucleoli increased in the same order of sequence. In the mean contour index only normal and tumorous nucleoli differed significantly ($p < 0.001$), indicating that the shape of tumorous nucleoli was more irregular than that of normal ones.

Table VI

Morphometric data of 100—100 normal, dysplastic and tumorous hepatocytes

	Normal	Dysplastic	Tumorous
Cytoplasmic area (μm^2)	263.54 ± 102.58	1550.89 ± 906.18	223.71 ± 103.78
Cytoplasmic contour index	4.11 ± 0.52	4.28 ± 0.49	4.18 ± 0.48
Average number of nuclei per cytoplasm cross section	1,02	1.23	1.1
Nuclear area (μm^2)	36.95 ± 10.68	157.89 ± 103.13	53.23 ± 23.86
Nuclear contour index	3.83 ± 0.25	3.71 ± 0.23	3.88 ± 0.21
Nuclear excentricity	0.228 ± 0.148	0.197 ± 0.127	0.156 ± 0.109
Number of nucleoli per nuclear cross section	0.99	1.23	0.97
Cytoplasm to nucleus ratio	7.24 ± 3.17	9.84 ± 5.06	3.91 ± 1.7
Nucleolar area (μm^2)	3.54 ± 2.28	15.97 ± 10.45	7.38 ± 4.6
Nucleolar contour index	3.84 ± 0.26	3.92 ± 0.49	4.03 ± 0.43
Nucleolar excentricity	0.329 ± 0.113	0.233 ± 0.128	0.319 ± 0.141

The mean area of dysplastic cells, nuclei and nucleoli was nearly four--five times the normal value. The standard deviation of dysplastic cell-component areas were however six to nine times of the normal. The high standard deviation of areas and cytoplasm to nucleus ratio suggested heterogeneity, that is there were divergent subpopulations among the multitude of dysplastic cells. Treating separately the two most important subpopulations of dysplastic

Table VII

Morphometric data of subpopulation of normal, dysplastic and tumorous hepatocytes

	Normal		Large cell dysplasia		Tumour	
	Mono-nuclear Mono-nucleolar	Multi-nuclear	Mono-nuclear Mono-nucleolar	Multi-nuclear	Mono-nuclear Mono-nucleolar	Multi-nuclear
Number of cells among 100 hepatocytes	75	2	61	17	63	8
Cytoplasmic area (μm^2)	271.69 ± 110.32	195.86 ± 7.44	1441.75 ± 753.0	1608.02 ± 742.16	213.89 ± 93.95	270.08 ± 99.96
Nuclear area (μm^2)	38.28 ± 10.91	24.53 ± 9.0	143.88 ± 89.7	112.7 ± 74.33	58.37 ± 20.91	32.56 ± 19.28
Nuclear excentricity	0.226 ± 0.134	0.241 ± 0.117	0.204 ± 0.134	0.229 ± 0.124	0.138 ± 0.107	0.220 ± 0.110
Cytoplasm to nucleus ratio	7.35 ± 2.87	4.02 ± 0.58	11.04 ± 5.38	6.87 ± 2.9	3.88 ± 1.77	3.83 ± 1.22
Nucleolar area (μm^2)	3.88 ± 1.97	3.39*	16.06 ± 9.91	10.47 ± 7.33	7.47 ± 4.51	6.37 ± 4.72

* single nucleolus

cells (Table VII), multinuclear and mononuclear (and nucleolar) subpopulations differed significantly in cytoplasm to nucleus ratio ($p < 0.001$). This ratio for mononuclear populations was higher, indicating clearly a hyperdiploidity. No significant difference existed in the cytoplasm to nucleus ratio of uni-, and multinuclear tumour cells. The ratio of both dysplastic subpopulations were significantly different from the ratio of the tumour cell population, the latter having been homogenous. Normal and dysplastic subpopulations did not differ significantly in nuclear excentricity but their values were significantly different ($p < 0.001$) from those of tumour cells. The dysplastic cell population therefore reminds more of normal than tumorous cells.

Discussion

Anthony et al [2] described the LCD as a premalignant condition defining the phenomenon as cellular enlargement, nuclear pleomorphism with hyperchromasia and multinucleation inside a focus. The nuclear-cytoplasmic ratio is normal. The cells occur in smaller or larger groups. They found the phenoenon often in young Ugandan patients who suffered from posthepatitic or postnecrotic cirrhosis and primary liver tumour. The importance of the phenommenon has been analysed widely [1, 3, 4, 8, 13, 15, 16] and some authors did not consider it to be a premalignant change [1, 4, 8, 12, 16]. Altman [1] for example pointed out that LCD occurred too often, it appeared in regenerative processes and the multinuclear cells are not tending to mitose.

At first we wanted to know whether there is any correlation between LCD and nutritional cirrhosis in a Middle-European population. According to Athony et al [2] the frequency of LCD in normal liver is 1% and 3.4% in nutritional cirrhosis. In our series these values were 8% and 41% respectively. The age of Anthony's patients was between 25—41 years, while in our series the mean age of males was 62.5 years and that of women 70.25 years. This means that in our cases the average age was about 30 years higher than in Anthony's series.

Here we have to call attention to age. As it is well known [6, 7, 20, 21] the ploidity and with that cell size increase as a function of age. We think that the difference of LCD frequency was due to the differences in age.

These data strongly suggested a connection between LCD and nutritional cirrhosis. In our material the occurrence of LCD was much higher in active cirrhosis than in inactive one. Somewhat similar observation was made by Uchida [17].

In the entity of steatocirrhosis we found LCD in a significantly higher percentage in the active form than in inactive cases. The activity of cirrhosis had the same effect on the frequency of LCD if primary liver cancer had joined

to micronodular cirrhosis: the percentage of LCD was the highest around tumours associated with active cirrhosis. Does this mean that LCD is a premalignant condition?

In our series its foci occurred around metastatic tumours. The fact that primary liver tumours develop extremely rarely around secondary (metastatic) tumours shows that LCD found around metastatic tumour-islets presumably may not be a premalignant change. Nieburgs et al [11] also observed LCD beside metastatic tumours.

Analysis of metastatic neoplasms gave further informations. In metastatic carcinomas, where the large tumour cell islets destroyed the acinar structure, we found numerous foci of LCD. Around lymphomas there was no deep structural transformation and we could not observe LCD either. These data seemed to support our assumption that LCD was induced by structural changes and it was not the LCD that had led to malignant tumours.

According Anthony et al [2], if LCD joins to cirrhosis the age of patients is higher than in non-dysplastic cases. They found the highest ages in cirrhosis born liver tumours. Our data did not seem to support the assumption that LCD and tumours would develop in higher age than does simple liver cirrhosis, and as said above, the number of males was always higher in every subgroup of cirrhosis and tumour.

Summarizing all cirrhotic and cirrhotic tumourous cases, LCD occurred more often in males than in females. This was in good agreement with the findings of Anthony et al [2]. LCD frequency of males and females was however not different in simple cirrhosis. Moreover, the occurrence of LCD was much higher among men than women in the primary tumour + cirrhosis group. These data are not in accordance with those of Anthony et al [2], suggesting that their and our examined populations were different. The low percentage and diffuse distribution of HBsAg positivity underlined this difference.

Similarly to Henmi et al [7] in the dysplastic cells we found iron that did not prove their proliferative activity assumed by other authors [4].

Morphometric data did not support the premalignant nature of LCD either. The high standard deviation of dysplastic cytoplasmic, nuclear or nucleolar areas was underlined also by others [7, 21]. Although nuclear excentricity and nucleolar contour index of dysplastic cells are between normal and tumoronus values, the pleomorphism of LCD is caused by a heterogeneity of the population, by the large number of multinuclear cells. Having separated the most numerous subpopulations, normal and dysplastic cells did not differ significantly either in nuclear excentricity or nucleolar contour index. On the other hand, the cytoplasm to nucleus ratio of both dysplastic subpopulations was significantly different from that of tumour cells. The high value of the cytoplasm to nucleus ratio of mononuclear dysplastic cells pointed to polyploidity, somewhat like in age related changes in the liver [20].

Finally, is the LCD a premalignant condition? The fact that the activity of cirrhosis, the extent of tumour islets in metastatic tumours deeply influence the occurrence of LCD suggests that the phenomenon is induced by other pathological processes and is thus a secondary change.

The lack of age differences observed by others suggests that this cellular abnormality is not part of a progressive process leading to tumour. The high incidence of LCD in our population and the cell pleomorphism revealed by morphometric analysis was presumably due to the relatively high age of the patients.

These data however relate to our population and they do not disclose the possibility that in other countries, under the effect of other hepatotoxic agents the biological importance of the phenomenon is different.

REFERENCES

1. Altman HW: Pathology of human liver tumors. In: Primary Liver Tumors, eds, H Remmer, HM Bolt, P Bannasch, H Popper, MTP. Press, Lancaster 1977, 53—71
2. Anthony PP, Vogel CL, Barker LF: Liver cell dysplasia. A premalignant condition. J Clin Pathol *26:* 217, 1973
3. Bartók I, Remenàr É, Tóth I, Duschanek P, Kanyár B: Clinicopathological studies of liver cirrhosis and hepatocellular carcinoma in a general hospital. Human Pathol *12:* 794, 1981
4. Cohen C, Berson SD, Geddes EW: Liver cell dysplasia. Association with hepatocellular carcinoma, cirrhosis and hepatitis B antigen carrier status. Cancer *44:* 1671, 1979
5. Gerber MA, Orr W, Denk H, Schaffner F, Popper H: Hepatocellular hyalin in cholestasis and cirrhosis, its diagnostic significance. Gastroenterology *64:* 89, 1973
6. Grisham JW: Cellular proliferation in the liver, In: Normal and Malignant Cell Growth eds, RJM Fry, ML Griem, WH Kirsten Springer Verlag, Heidelberg, New York 1969, pp. 28—43
7. Henmi A, Uchida T, Shikata T: Karyometric analysis of liver cell dysplasia and hepatocellular carcinoma. Cancer *55:* 2594, 1985
8. Higginson J: Primary carcinoma of the liver in Africa. Br J Cancer *10:* 609, 1956
9. Kaufmann E: Lehrbuch der Speziellen Pathologischen Anatomie II/2. Walter De Gruyter, Berlin 1958, pp. 1146—1147
10. Litovitz TL, Lutzner AM: Quantitative measurements of blood lymphocytes from patients with chronic lymphoid leukaemia and Sezary syndrome. J Natl Cancer Inst *53:* 75, 1974
11. Nieburgs HE, Parets AD, Perez V, Boudreau C: Cellular changes in liver tissues adjacent and distant to malignant tumors. Arch Pathol *80:* 262, 1965
12. Okita K, Oda M, Yasunaga M, Takemoto T: Possible premalignant lesion directed to the induction of hepatocellular carcinoma. Hepatology *4:* 797, 1984
13. Peters RL: Pathology of hepatocellular carcinoma. In: Hepatocellular Carcinoma eds, K Okuda, RL Peters John Wiley, New York 1976, pp. 10—168
14. Plohinsky NA: Algorithms in biometry. (in Russian) University of Moscow
15. Roncalli M, Borzio M, De Biogi G, Servida E, Cantaboni A, Sironi M, Toccagni GL: Liver all dysplasia and hepatocellular carcinoma, A histological and immunohistochemical study. Histopathology *9:* 209, 1985
16. Steiner PE, Davies JNP; Cirrhosis and primary liver cancer in Uganda Africans. Br J Cancer *11:* 523, 1957
17. Uchida T: Viral Hepatitis, Histology and Differential Diagnosis Chugaiigakusha Tokyo (in Japanese) cit. by Henmi et al Cancer *55:* 2594, 1985
18. Van der Valk P, Hermans J, Brand R, Cornelisse CJ, Spander PJ, Meijer CJLM: Morphometric characterisation of diffuse large cell (histiocytic) lymphomas. Am J Pathol *107:* 327, 1982

19. Van der Valk P, Ball P, Mosch A, Meijer CJLM: Large cell lymphomas. Differential diagnosis of centroblastic and B immunoblastic subtypes by morphometry on histologic preparations. Cancer *54:* 2082, 1984
20. Watanabe S, Shimada H, Tanaka T: Human hepatocytes and ageing. A cytophotometrical analysis in 35 sudden-death cases. Virchows Arch Cell Pathol *27:* 307, 1978
21. Watanabe S, Okita K, Harada T, Kodama T, Numa Y, Takemoto T, Takahashi M: Morphologic studies of the liver cell dysplasia. Cancer *51:* 2197, 1983

Acta Morphologica Hungarica, 35 (1–2), pp. 59–69 (1987)

CHANGES IN THE AORTA OF GUINEA PIGS EXPOSED TO KEROSENE

MIRIAM NOA, J. ILLNAIT

DEPARTMENT OF PHARMACOLOGY AND TOXICOLOGY,
NATIONAL CENTRE OF SCIENTIFIC RESEARCH, HAVANA, CUBA

(Received 10 January 1986)

Guina pigs were exposed to kerosene aerosols or to smoke produced from kerosene under conditions approximating those in a kitchen. They were compared to controls exposed to saline aerosols or to atmospheric air. Both types of kerosene exposure engendered aortic plaques, resembling those seen in atherosclerosis, and changes in levels of blood lipids. The results suggest that chronic exposure to kerosene, a domestic fuel widely used in many countries, may have important toxic effects in addition to the pulmonary effects that have been reported by others.

Keywords: kerosene, atherosclerosis, guinea pigs, aorta

Introduction

Kerosene is a petroleum byproduct very much used for cooking, illumination and heating in underdeveloped countries. A high correlation has been demonstrated between the use of kerosene and the frequency of asthmatic crises in housewives and other workers who use it [1]. The mechanism of this effect has been scarcely studied, and even less is known of other possible toxic effects.

Pulmonary changes have been reported in children who ingested kerosene accidentally [2, 3] and in experimental animals [4, 5, 6, 7]. In 1980, Rai and Singh observed cardiovascular changes in mongrel dogs exposed to kerosene smoke [8].

We are engaged in a systematic study of the effects of kerosene on experimental animals, especially guinea pigs [9, 10, 11, 12, 13, 14]. In the course of these studies we have noted alterations in the aorta and in the blood lipids of animals exposed to kerosene aerosols or to kerosene smoke at levels typical of a kitchen. Our findings suggest that chronic exposure to kerosene may have serious cardiovascular consequences that deserve further study.

Send offprint requests to Miriam Noa, Department of Pharmacology and Toxicology, National Centre of Scientific Research, Post Box 6990, Havana. Cuba

Materials and methods

Kerosene was obtained from the Nico López refinery. It is principally composed of saturated and unsaturated aliphatic (straight chain) hydrocarbons (alkanes/paraffins, alkanes/-olefins, alkadienes/diolefins, alkanes/acetylenes) with small amounts of cyclalkanes (cycloparaffins) and aromatic hydrocarbons, and minute quantities of sulphurous and nitrogenous impurities.

Animals

Group l. Twenty three male guinea pigs (180—200 g) were exposed to kerosene aerosol for 15 minutes daily over twenty one days. The animals were placed in a closed plastic box ($1 \times 1 \times 0.80$ m) in which they inhaled droplets of kerosene not more than 8 micrometers in diameter. The initial concentration during the exposure was approximately 20.4 mg aerosol/L air, during the exposure this increased to 34 mg/L. Concentrations were determined by gas chromatography (Chrom IV System: Laboratorni Prisroje, Praha). The aerosol was produced with a Wright nebuliser.

Group 2. Twenty five male guinea pigs (180—200 g) were exposed for two hours daily over 21 days, to kerosene smoke produced by a kerosene stove. The exposure was in a room $2 \times 2 \times 3$ 1/2 m, with a chimney and ventilatory fan. The conditions approximated those in a kitchen of many households.

Group 3. — Twenty animals were kept in atmospheric air.

Group 4. — Ten guinea pigs were exposed to a saline aerosol for fifteen minutes a day under conditions similar to those used for group 1.

Analysis and tissue preparation

Animals were sacrificed by cervical dislocation or by ether anaesthesia. Blood for serum cholesterol and high density lipoprotein analyses was taken from the vena cava (for these lipid determinations we used only animals sacrificed by cervical dislocation) and the determinations were done using Boehringer (Mannheim, GFR) kits.

At necropsy the thoraco-abdominal cavity was opened and the aorta was cut at its origin and removed. Several portions of all the aortas were studied by light microscopy. For paraffin sections, tissue was fixed by routine procedures in 10% buffered formalin: this material was stained with hematoxylin and eosin, van Gieson's procedure for elastic fibres (orcein), and Alcian Blue for mucopolysaccharides.

Tissue from 10 animals of each group was prepared for electron microscopy and for examination of plastic embedded semi-thin sections. These aortas were fixed by perfusion with 3.2% glutaraldehyde in 0.1 M phosphate buffer and then were cut. Parts of thoracic aorta with atherosclerotic plaques were postfixed for one hour in 1% phosphate-buffered osmium tetroxide. Following dehydration, the tissue was embedded in Epon 812. Semithin sections were stained with Stevenel's Blue [15, 16]. Thin sections were stained with uranyl acetate and lead citrate and examined in a JEOL 100 S electron microscope.

Results

In preliminary studies, we observed changes in the aorta as early as 15 days after initiation of the experimental treatment. We chose 21 days for our initial detailed studies, because by that time all the experimental animals showed well developed lesions, readily detectable by gross observation. Macroscopically, aortas of guinea pigs submitted to kerosene aerosol or to kerosene smoke were similar in appearance, we could see small, disk-like, gray, raised patches of intimal thickening, most often in the thoracic aorta (Fig. 1). Controls of both types showed no such patches.

Microscopically (Fig. 2), kerosene-exposed animals of both groups showed changes typical of those associated with atherosclerotic lesions and with changes

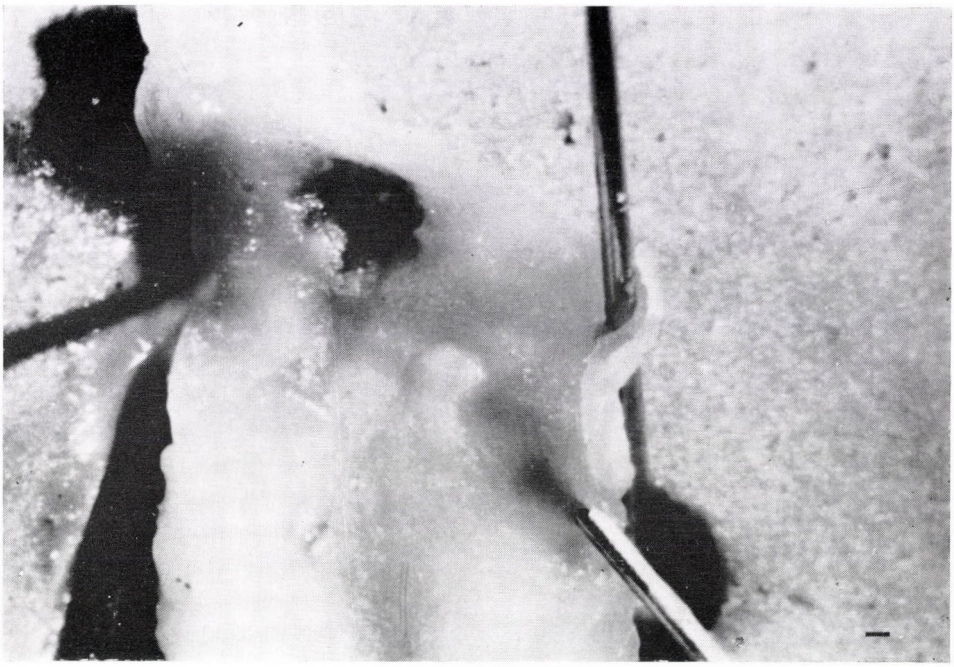

Fig. 1. Aorta of guinea pig exposed to kerosene aerosol. Raised plaque as described in text. ×3

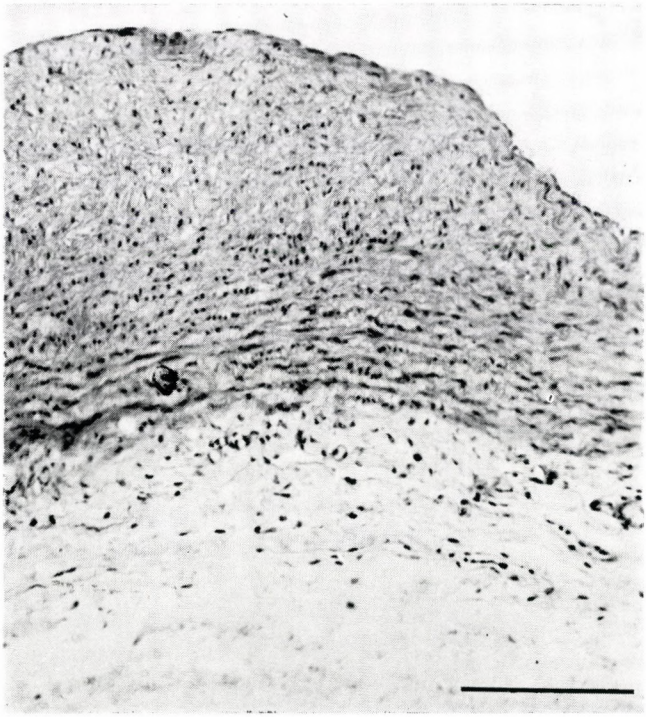

Fig. 2. Aorta of guinea pig exposed to kerosene smoke. Section through one of the plaques. Haematoxylin and eosin. ×225

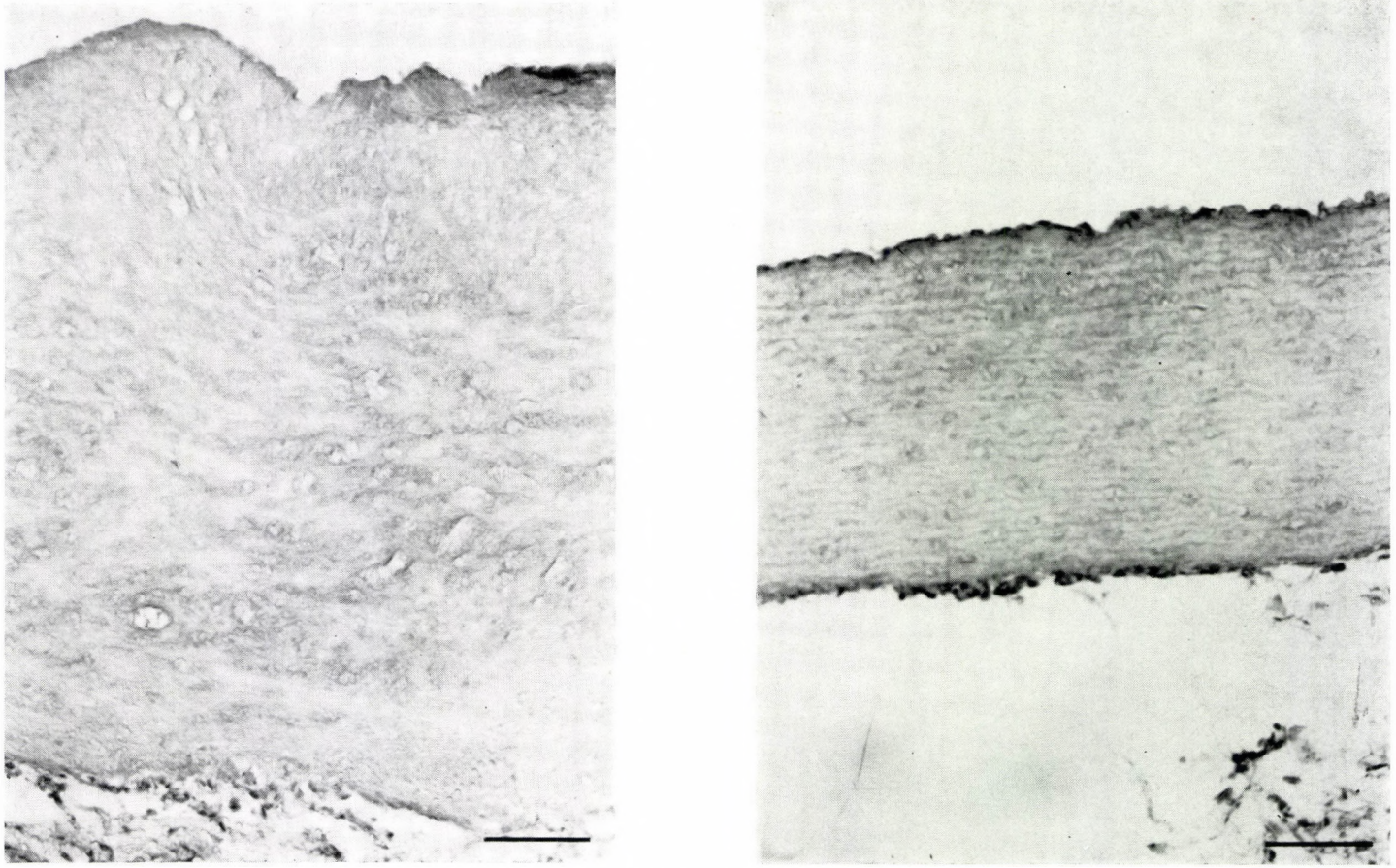

Figs 3, 4. Aortas stained with van Gieson's Orcein stain for elastic fibres. Fig. 3 is from a control (air) Fig. 4 from an animal exposed to kerosene smoke. Extensive fragmentation of fibres in the experimental preparations ×140

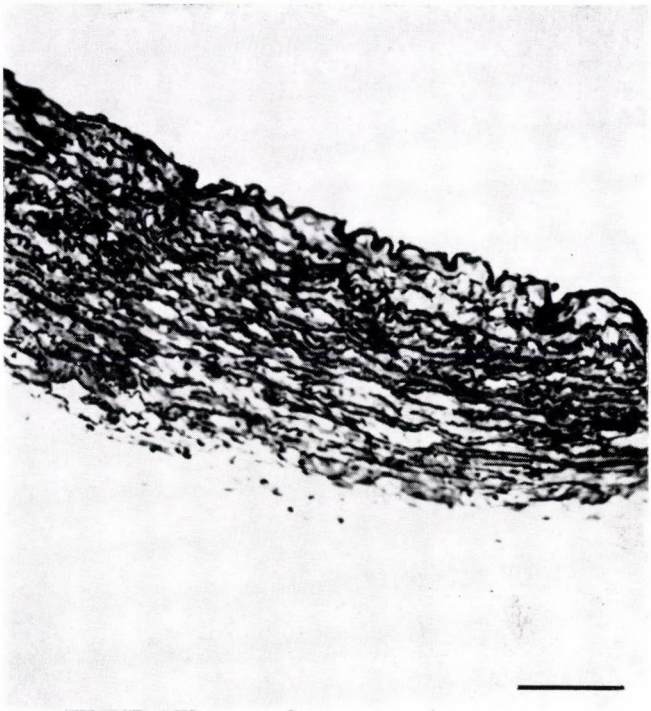

Figs 5, 6. Preparations of aortas stained with alcian blue. Fig. 5. is from a control (air) and

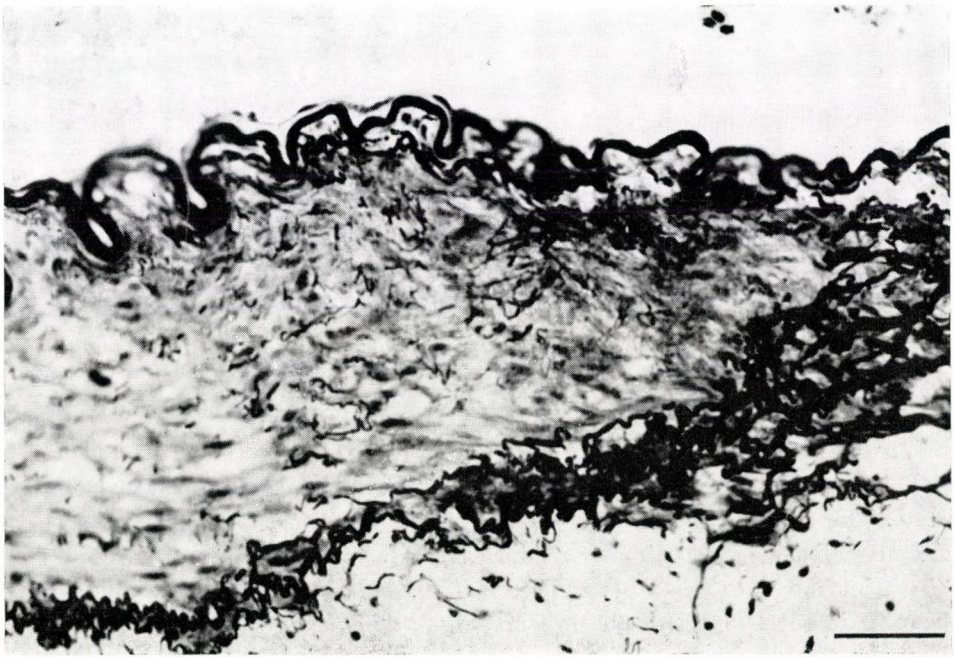

Fig. 6 from a plaque of an animal exposed to kerosene smoke. Alcian blue stained material is presumably mucopolysaccharides. Note accumulation of this material in the experimental preparation. ×140

that could be related to permeability disturbances (Figs 3—6). There was thickening of the intima, with fibrous plaques containing elongate smooth muscle cells. Paraffin sections stained with van Gieson's Orcein procedure showed disorganization of the elastic tissue of the media; this varied from minimal loosening and fragmentation of lamellae to extensive disorganization.

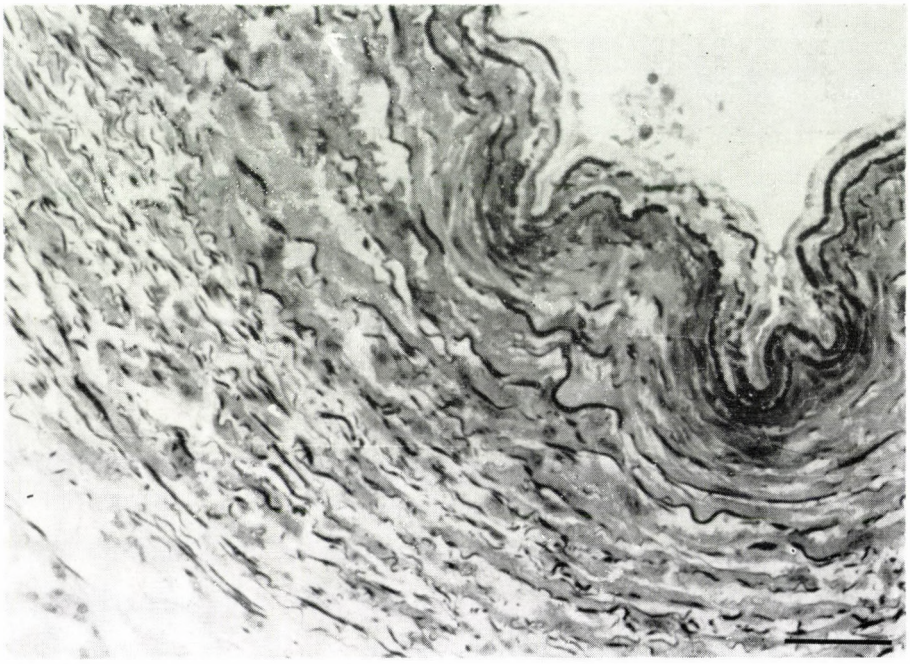

Fig. 7. One micrometer Epon section of aorta of animal exposed to kerosene smoke. Stained with Stevenel's Blue, which stains a number of tissue components. Oedema of the subendothelial space, rupture of internal elastic lamina. ×140

The media exhibited accumulation of Alcian Blue positive materials, presumably acid mucopolysaccharides (glycosaminoglycans) of the connective tissues.

In semithin sections stained with Stevenel's Blue, we found changes such as subendothelial vacuoles and oedema, presence of smooth muscle cells in the subendothelial space, and fragmentation of the internal elastic membrane. There was accumulation of material with the staining characteristics of mucopolysaccharides in the media (Fig. 7).

Electron microscopic examination (Figs 8, 9) revealed in the plaques of the experimental material the presence of modified smooth muscle cells. These cells were readily distinguished from fibroblasts as they had a centrally located

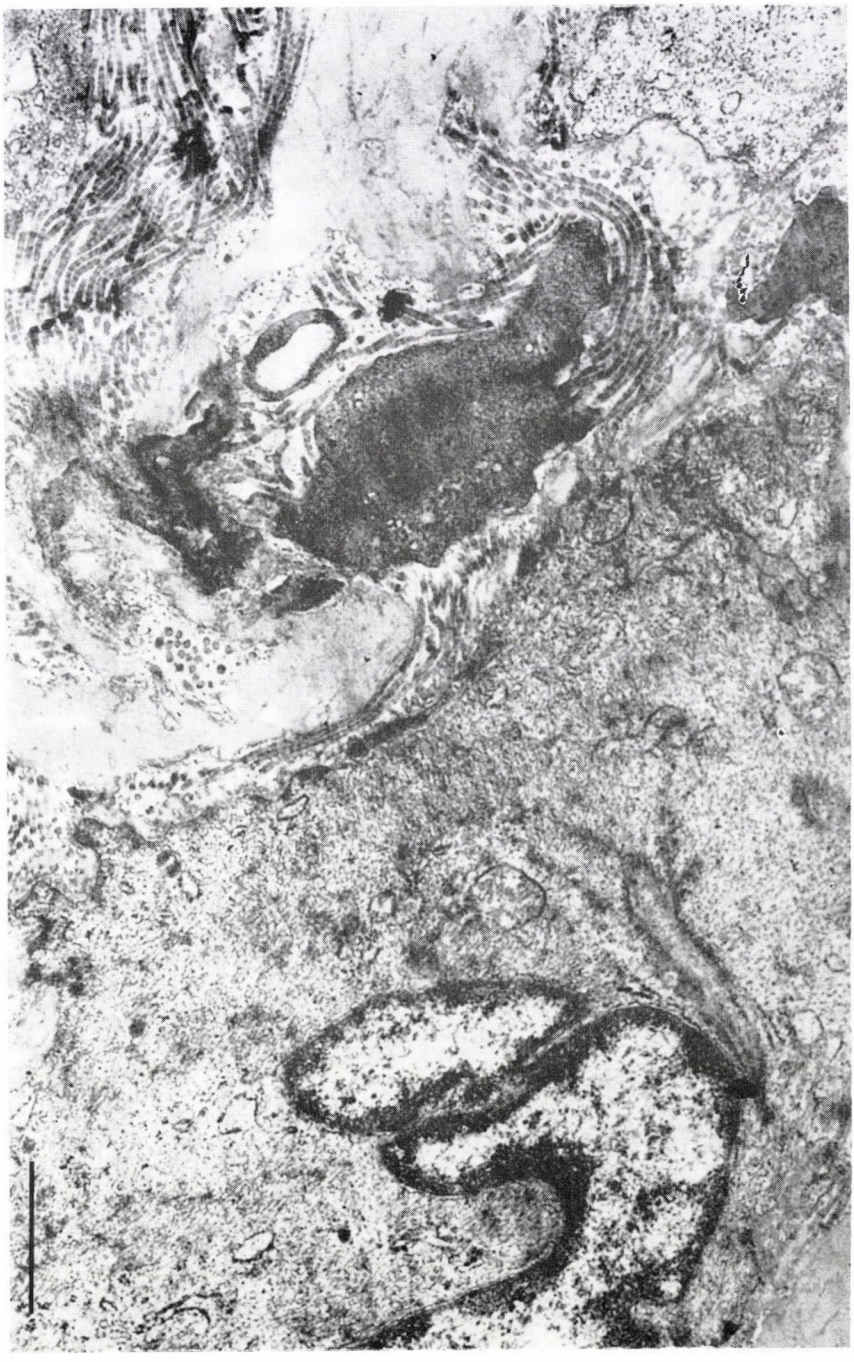

Fig. 8. Electron micrograph of one of the principal cell types seen in plaques of animals exposed to kerosene aerosol. The cell shows the morphological characteristics of smooth muscle, such as an abudance of cytoplasmic filaments. ×20 000

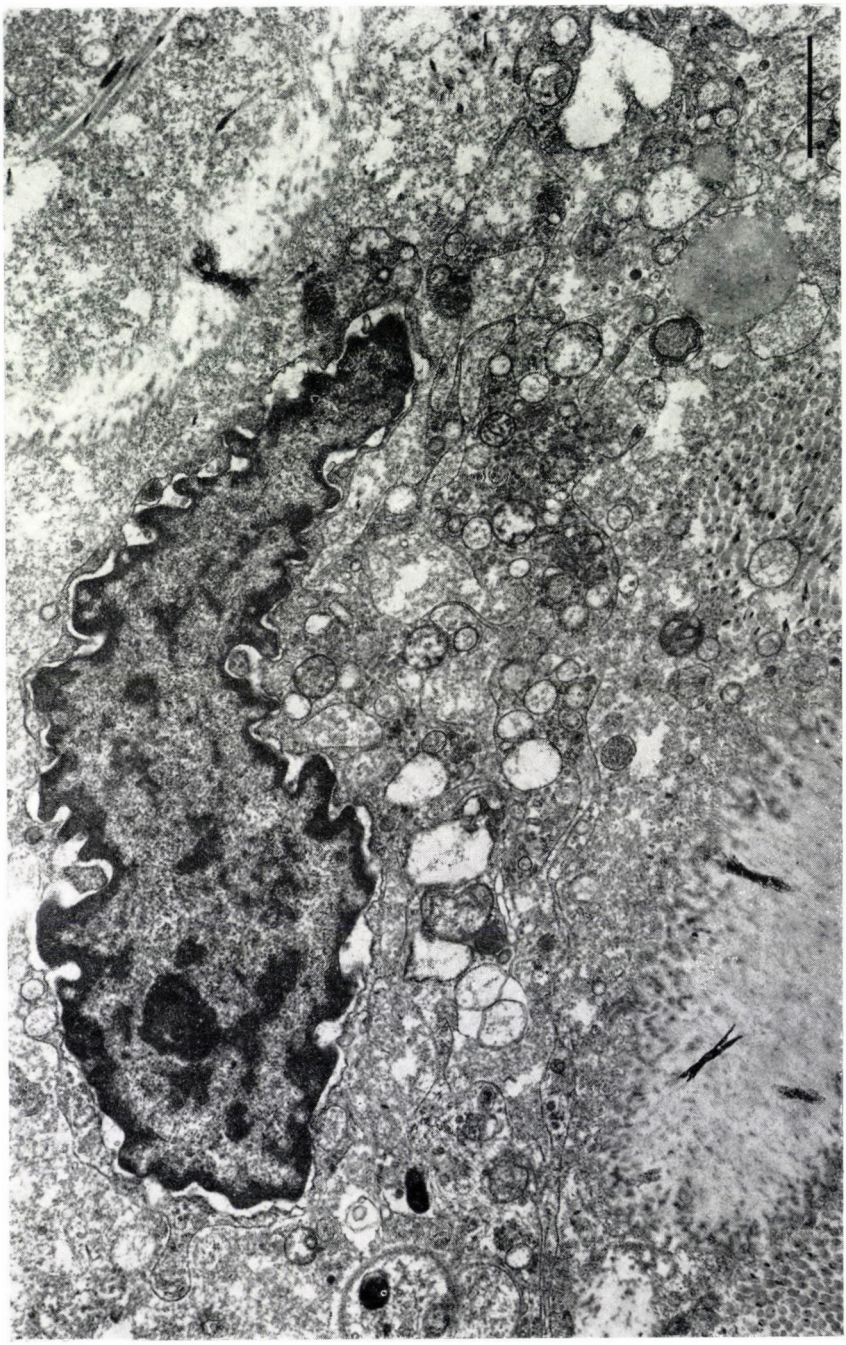

Fig. 9. Electron micrograph of another cell type frequently seen in plaques. This one is from an animal exposed to kerosene aerosol. From the presence of numerous cytoplasmic vacuoles, and the extensively folded plasma membrane, this cell type seems to be active in endocytosis. A lipid droplet is seen. ×16 000

Table I

	Cholesterol	HDL cholesterol	$\frac{\text{HDL cholesterol}}{\text{Total cholesterol}} \times 100$
Experimental guinea pigs	62.6 ± 7.2^b	11.7 ± 3.4^b	22.5 ± 6.7
Controls	53.8 ± 9	15.5 ± 3.2	33.6 ± 15.6

Values are means ($\pm$SD) for 23 kerosene exposed animals and 11 control animals.
[b] These values differ significantly from controls ($p < 0.001$). Student's *t*-Test.

nucleus; the abundance of cytoplasmic organelles such as mitochondria, varied from cell to cell, but the cells showed numerous filaments, packing their cytoplasm. The cells were surrounded by filamentous material, probably corresponding to fibres of connective tissue origin, or to basement membrane material, which often was discontinuous. Elastic fibres were associated with some of the cells.

In neither of the control groups were any of these changes observed and we could easily distinguish control and experimental material in blind comparisons.

The experimental animals showed moderate but significant increases in overall serum cholesterol, and decrease in HDL cholesterol. HDL Cholesterol/Total cholesterol ratio did not decrease significantly (Table I).

Discussion

The results indicated that kerosene and kerosene smoke cause changes in the organization of the wall of the aorta and in levels of blood lipids, like those associated with atherosclerosis. Controls, including animals subjected to extensive handling, movement in and out of small chambers, and other manipulations required for the saline aerosol experiments, showed no such changes, indicating that the observations reflected exposure to kerosene rather than accidental factors such as possible stresses due to handling or hypoxia.

In the experiments with kerosene aerosol, hypoxia did not seem to have played an important role in the development of lesions, because when we studied the group of animals with saline aerosol under the same experimental conditions we did not find any changes in the aortas.

In the experiments with kerosene smoke, beside carbon monoxide, that has an important role in vascular damage [17], some of the components of kerosene proper may have an effect on atherosclerotic plaque formation. The effect of kerosene was observed at levels of exposure to kerosene smoke similar to those commonly experienced in kitchens where kerosene is used in cooking. Direct ingestion of unburnt kerosene and aspiration into the pulmonary tract

also occurs, particularly among children [2, 3]. More work is needed to determine which components of kerosene are responsible for the damage and to establish how they are related to the pulmonary effects.

We have made a study on these animals with two different types of kerosene (chemically treated), one without aromatic hydrocarbons and another without compounds; in these cases we did not find atherosclerotic plaques [18]. So we suppose that these compounds are responsible for the changes presented in this paper.

In general the alterations observed in the aortas of guinea pigs exposed to kerosene, are first due to permeability changes of the endothelium promoting migration of smooth muscle cells, fibrosis, and so on. We found changes of the permeability of the endothelial cells of the aorta dyed with Evans blue and studied with X-ray diffraction (unpublished results).

The only prior investigation into the present issues was that of Rai and Singh [8] who observed changes in heart function and vascular strucutere in dogs exposed to high levels of kerosene smoke for three months. All these findings suggest that, in addition to the pulmonary effects of exposure to kerosene [9—14], there may be other toxic effects that could pose serious health hazards on chronic exposure. Especially in view of the wide use of kerosene as a domestic fuel in many countries, this matter would seem to merit additional experimental and epidemiological studies.

Acknowledgement

We thank Professor E. Holtzman for discussions and help in preparing the manuscript, and also to Dr. A. Somogyi.

REFERENCES

1. Rodriguez de la Vega A, Rojas O, Batule M. Sparis P: Factores ambientales en relacióon con la evolución del asma bronquial con especial referencia al keroseno. Rev Cub Med *6:* 605, 1981
2. Steiner M: Syndromes of kerosene poisoning in children. Am J Dis Child *74:* 32, 1947
3. Baldachin BJ, Melmed RN: Clinical and therapeutical aspects of kerosene poisoning. A series of 200 cases. Br Med J *2:* 28, 1964
4. Carpenter CP, Geary DL, Myers R, Nechreiner D, Sullivan L, King J: Petroleum hydrocarbon toxicity studies: XI: Animal and human responses to vapors of deodorized kerosene. Toxicol Appl Pharmacol *36:* 443, 1976
5. Gerarde HW: Toxicological studies on hydrocarbons. IX. The aspiration hazard and toxicity of hydrocarbons and hydrocarbon mixtures. Arch Environ Health *6:* 329, 1963
6. Richardson JA, Pratt, TH: Toxic effects of varying doses of kerosene administered by different routes. Am J Med Sci *221:* 531, 1951
7. Woldsdort J: Kerosene intoxication: an experimental approach to the etiology of the CNS manifestation in primates. J Pediatr *88:* 1037, 1976
8. Rai U. Singh T: Cardiopulmonary changes in mongrel dogs after exposure to kerosene smoke. Ind J Exp Biol *18:* 1236, 1980
9. Noa M, Sanabria K: Tracheal ultrastructure in kerosene treated guinea pigs. A preliminary report. Allergol Immunopath *12:* 33, 1984

10. Sanabria J, Noa M, Casacó A, Gonzalez, R: Alteraciones morfológicas del árbol respiratorio de cobayos sometidos a aerosol de keroseno. Allergol Immunopath *14:* 213, 1984.
11. Noa M, Illnait J, de la Rosa MC: Efecto de la exposición del aerosol de keroseno en la aterogénesis de cobayos. Patologia *21:* 366, 1983
12. Noa M, Sanabria J, Casacó A, Gonzalez R, de la Rosa MC, Aguilar C: Alteraciones morfológicas de las traqueas de cobayos inducidas por aerosol de keroseno. Patologia *21:* 366, 1983
13. Noa M, Illnait J, Aguilar C, Capote A: Cambios citológicos y bioquimicos en lavados pulmonares de cobayos tratados con aerosol de keroseno. Patologia *21:* 384, 1983
14. Casacó A, Gonzalez R, Arruyazabala L, Garcia M, de la Vega A: Studies of the effects of kerosene aerosols on the airways of rabbits. Allergol Immunopath *10:* 364, 1982
15. Del Cerro M, Cogen J, del Cerro C: Stevenel's Blue, an excellent stain for optical microscopical study on plastic embedded tissue. Microsc Acta *83:* 177, 1980
16. Del Cerro M, Standler N, del Cerro C: High resolution optical microscopy of animal tissue by the use of submicrometer thick section and a new stain. Microsc Acta *83:* 217, 1980
17. Wanstrup J, Kjeldsen K, Astrup P: Acceleration of spontaneous intimal-subintimal changes in rabbit aorta by a prolonged moderate carbon monoxide exposure. Acta Path Microbiol Scand *75:* 353, 1969
18. Noa M, Illnait J, Casacó A: Estudio del efecto producido en las aortas por dos tipos de keroseno modificado. IX. Seminario Centro Nacional Investigaciones Cientificas, La Habana 1985

Acta Morphologica Hungarica, 35 (1—2), pp. 71—76 (1987)

ABDOMINAL MESOTHELIOMA INDUCED BY OCCUPATIONAL ASBESTOS EXPOSURE

KINGA KARLINGER*, J. GERE***, L. NÉMETH,* G. GALGÓCZY**

DEPARTMENT OF RADIOLOGY* AND PULMONOLOGY** OF THE NATIONAL INSTITUTE OF OCCUPATIONAL HEALTH, AND DEPARTMENT OF PATHOLOGY*** OF TÉTÉNYI CITY HOSPITAL, BUDAPEST, HUNGARY

(Received 6 February 1986)

Asbestos bodies were demonstrated within an abdominal mesothelioma, proving the tumour-inductive role of asbestos fibres. Asbestos fibres were also found earlier in a case of bile duct carcinoma (17).

Keywords: asbestos exposure, asbestos bodies, abdominal mesothelioma

Report of a Case

A 63 years old male had been exposed to asbestos for 26 years sawing mostly dry asbestos plates. Thirty four years after the beginning of exposure he had developed abdominal complaints in November, 1984. He had used to smoke 8 cigarettes a day from the age of 19 years for 8 years, but since then he had not smoked any more. X-ray, screening revealed a slight fibrosis in the lower parts of the lungs and pleural thickening which could well be seen in oblique films (Fig. 1b). X-ray films did not show the hyaline plaque in the parietal diaphragmatic pleura only the calcifications in it. On the basis of these findings and knowing his high exposure, the asbestosis was considered an occupational disease in spite of the fact that the chest CT did not show pleural hyalinosis. An uneven, undefinable tumour of the hardness of cartilage was palpable in the coecal region, sonography showed a solid tumour and moreover ascites. Abdominal exploration was carried out, and it revealed a peritoneal carcinosis. The ascites and meteorism increased and he died on 16 th May 1985.

Necropsy revealed in the left parietal pleura, between the VIII-X ribs 60×60 mm and on the left side of the diaphragm 50×50 mm sized bulky, hard, yellowish hyaline plaques and the diaphragmatic visceral and parietal pleuras coalesced (Figs 1a and 1c).

The omentum maius was bulky and rough. Numerous white and hard nodules were scattered on the mesenterium. The gut was unobstructed. There were no signs of metastases in the organs.

Send offprint requests to: Dr Kinga Karlinger MD, National Institute of Occupational Health, P O B 22 Budapest 9, Hungary 1450

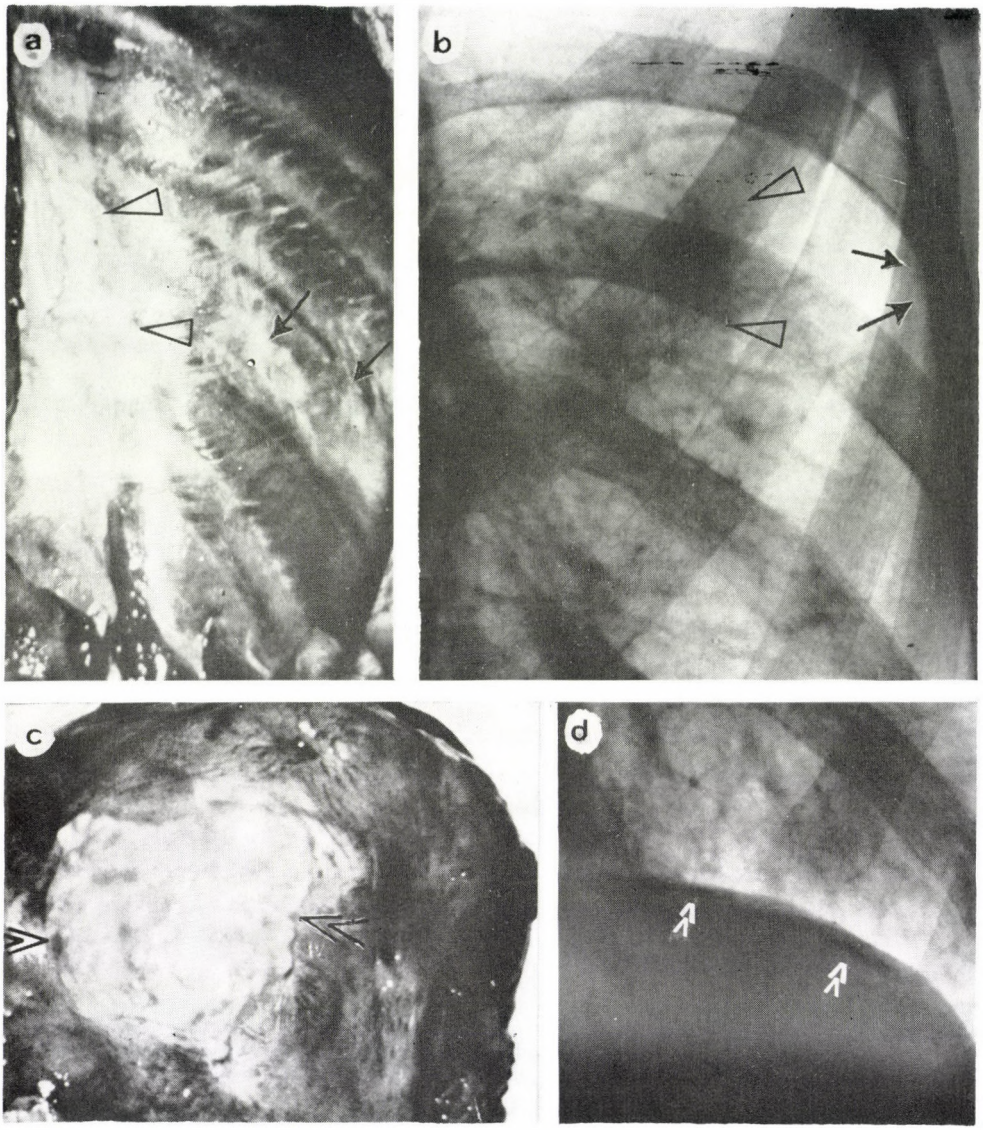

Fig. 1. a—b—c—d Pleural hyalinosis displaying a shining yellowish-white elevation with sharp borders (Fig. 1a) best shown tangentially with oblique X-rays (Fig. 1b). Diaphragmatic surface exhibits bulky, circumscribed, disklike plaques (Fig. 1c) but in the X-rays irregular areas of calcification can only be seen (Fig. ld « arrows). (ILO 1980 Geneva Short Classification: s1 a2—s1 a2)

Microscopically, (Figs 3a, b) asbestos bodies have been seen to be surrounded and partly covered with flakes of soot, within the slight fibrotically widened alveolar septa (grade 2a, according to the Grading Scheme proposed by AMA 1982). In the parietal diaphragmatic peritoneum features of a mixed

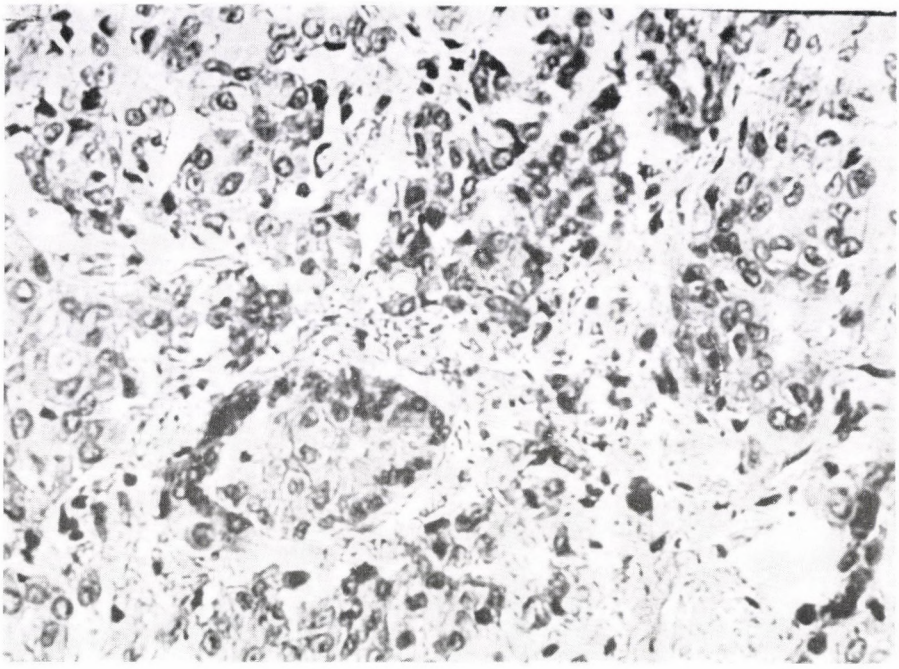

Fig. 2. High magnification of mesothelioma (H and E stain). Original magnification, ×200

cell peritoneal mesothelioma could be seen consisting partly of clear, polygonal cells with dark nuclei, partly darker, smaller fibrobastic cells and scattered psammous bodies. In haematoxylin-eosin stained specimens within the mesothelioma infiltrating the diaphragm, some fragments of asbestos bodies were seen. Pieces of the tumour tissue were digested [17] and divided into two parts. One of them was filtered on a Whatman GF/V glass-fibre membrane, the other on a Sartorius membrane (pore size: 0.45 μm). The acetone vapour cleared Sartorius filtrate and the dried glass filtrate were investigated by light microscope.

In the formalin fixed tumour tissue (weight 90 mg) we found 4—5 asbestos bodies (Figs 3c and 3d).

Discussion

Mesothelioma arises from multi-potential mesothelial cells of the pleura, peritoneum, pericardium and testicles. In the sixties and seventies, retrospective studies proved that in subjects who had had either industrial or residential contact with asbestos more than twenty-thirty years earlier, mesotheliomas occurred. Besides the 21% prevalence of lung tumour of asbestos exposed

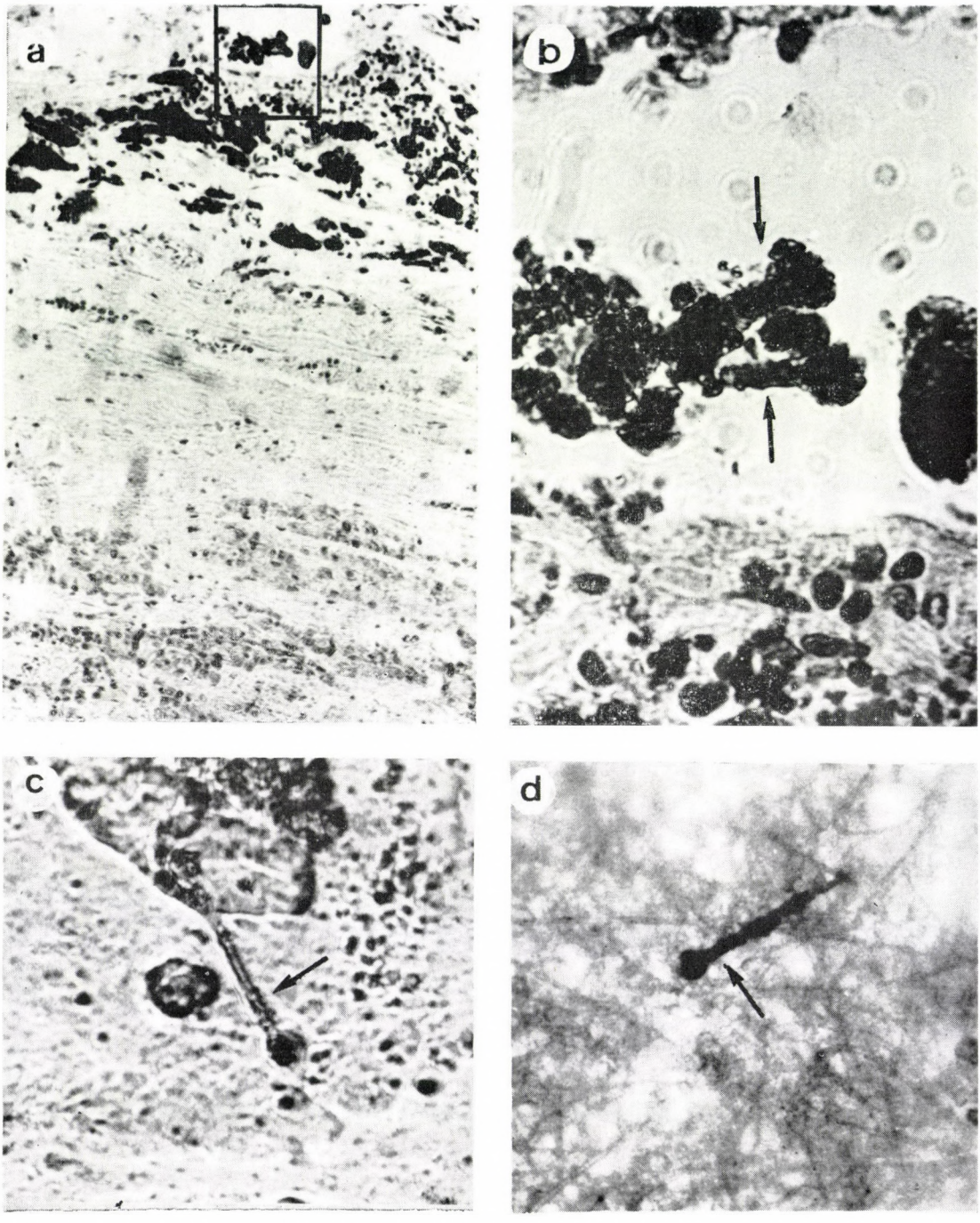

Fig. 3. a—b—c—d Photomicrograph of a mixed type mesothelioma (Fig. 3a, H and E stain, ×100). Enlargement of framed area (in Fig. 3a) shows asbestos bodies (Fig. 3b arrows, ×400). Asbestos body on Sartorius membrane (Fig. 3c ×400) and among the fibres of the glass filtrate (Fig. 3d, ×400)

subjects the occurrence of mesothelioma was only 5—8%, but in 10—15% of these cases no earlier asbestos exposure could be proved [18]. The most important in asbestos industry is chrysotile which represents some 90% of the world's asbestos production, the other types of asbestos share the remaining 10%. Crocidolite is particulary associated with the development of malignant mesothelioma of the pleura and peritoneum [11], its stimulating effect on the mesothelial cells has been proved experimentally [14].

In the experiments of Lafuma et al. [8] chrysotile was the most toxic; it elicited as many mesotheliomas as crocidolite. They supposed a synergistic effect of other cancerogens besides the mineral fibres. Pooley [12] showed that the more predominant fibre type detected in the mesothelioma cases is of amphibole asbestos, the number of which increased in direct ratio to the intensity of exposure. Pott et al. [13] observed 15 mesotheliomas in rats after the intraperitoneal injection of asbestos.

Concerning the rise of human peritoneal mesotheliomas it is important that fed asbestos fibres were found to cross the gut wall [16] and to circulate in the abdominal lymph 2—24 hours after feeding [9]. Godwin and Jagatic [6] showed some asbestos bodies in specimens of an abdominal mesothelioma. It is well-known that there is no strict association between the fibrosis and tumour-inductive biological effects of asbestos, therefore an abdominal mesothelioma may occur without any sign of respiratory asbestosis or slight asbestosis [1, 2, 3] just like in the case of our patient who suffered only from a slight respiratory asbestosis. This case was thought worth publishing

— by showing the presence of asbestos bodies in the peritoneal mesothelioma; by proving the close relation between the mesothelioma and occupational asbestos exposure, indicating that peritoneal mesothelioma may be considered an occupational disease with at least 20 years latency after the commencement of exposure, the tumour, inductive effect of the asbestos is probably independent of its fibrosis, causing effect in respiratory organs, and

— we found that films were able to show well the gross appearance of respiratory disease caused by asbestos (lung fibrosis, pleural hyalinosis) even in early stages.

Acknowledgements

The authors are indebted to Prof. P. Vittay MD for the chest CT, L. Bohár MD for the US investigations in the Radiological Department of the Postgraduate Medical School, and to Mrs. Zs. Haskó, radiological technician, for valuable help.

REFERENCES

1. Anspach M, Roitzsch E, Clausnitzer W: Ein Beitrag zur Ätiologie des diffusen malignen Pleura-Mesothelioms. Arch Gewerbepath Gewerbehyg *21:* 392, 1965
2. Craighead JE: Asbestos-associated diseases. Arch Pathol Lab Med *106:* 541, 1982
3. Elmes PC: The Natural History of Diffuse Mesothelioma. In: Biological Effects of Asbestos. IARC Sci Publ, Lyon 1973 No 8 pp. 267—272
4. Enticknap JB, Smither WJ: Peritoneal Tumours in asbestosis. Br J Ind Med *21:* 20, 1964
5. Evans RW: Histological Appearances of Tumours. 2nd ed. E and S Livingstone Edinburgh and London 1966 pp. 119
6. Godwin MC, Jagatic J: Asbestos and mesotheliomas. Environ Hlth *3:* 391, 1970
7. Kannerstein M, Churg J, McCaughey WTE: Asbestos and mesothelioma. A rewiew. Path Ann *13:* 81, 1978
8. Lafuma J, Morin M, Poncy JL, Masser R, Hirsch A, Bignon J, Monchaux G: Mesothelioma induced by intraperitoneal injection of different types of fibres in rats; synergistic effect of other carcinogens. In: Biological Effects of Mineral Fibres. IARC Sci Publ Lyon Vol 1, No 30 1980 pp. 311—320
9. Masse R, Sebastien P, Monchaux G, Bignon J: Experimental demonstration of the penetration of asbestos fibres into the gastrointestinal tract. In: Biological Effects of Mineral Fibres. IARC Sci Publ Lyon Vol 1, No 30, 1980 pp 321—328
10. Németh L, Tolnai K, Hoványi E, Egerváry M, Győri S: Frequency, Sensitivity and Specificity of Roentgenographic Features of Slight and Moderate Asbestos — Related Respiratory Diseases. Fortschr Röntgenstr *144:* 9, 1986
11. Parkes WR: Occupational Lung Disorders. Butterworth and Co, Ltd, London 1974 pp 311—321
12. Pooley FD: Mesothelioma in relation to exposure. In: Biological Effects of Asbestos, IARC Sci Publ Lyon 1973 pp 222—225
13. Pott F, Huth F, Spurny K,: Tumour induction after intraperitoneal injection of fibrous dusts. In: Biological Effects of Mineral Fibres. IARC Sci Publ Vol 1, No 30 1980 pp 337—342
14. Rajan KT, Evans PH: Experimental methods-organ culture. In: Biological Effects of Asbestos, IARC Sci Publ Lyon 1973 No 8, pp 94—98
15. Selikoff IJ, Hammond EC, Churg J: Carcinogenicity of amosite asbestos. Arch Env Hlth *25:* 183, 1972
16. Storeygard AR, Brown AL: Penetration of the small intestinal mucosa by asbestos fibres. Mayo Clin Proc *52:* 809, 1977
17. Szendrői M, Németh L, Vajta G: Asbestos bodies in a bile duct cancer after occupational exposure. Environ Res *30:* 270, 1983
18. Wagner JC: Asbestos cancers. J Nat Cancer Inst *46:* 5, 1971

Acta Morphologica Hungarica, 35 (1–2), pp. 77–88 (1987)

STRIATED MICROFILAMENT BUNDLES (SMF) IN THE GLOMERULAR CELLS OF HUMAN KIDNEYS

K. Szepesházi*, K. Lapis

1ST INSTITUTE OF PATHOLOGY AND EXPERIMENTAL CANCER RESEARCH, SEMMELWEIS MEDICAL UNIVERSITY BUDAPEST, HUNGARY

(Received 16 July 1986)

Rhizoplast or striated rootlet is a rarely described cytoplasmic organelle in non-ciliated mammalian cells. We observed the centrosome related rhizoplast like structures relatively often in the human renal glomerular cells. Of 226 kidney biopsies striated microfilament bundles (SMF) have been found in 41 cases in a total of 64 cells. More than half of these organelles were found in podocytes, about a quarter in endothelial cells, fewer in mesangial cells and they rarely occurred in the parietal epithelium.

The majority of SMF are connected with the centrosome, but not in direct connection with the centriole. The longer bundles have often been located near the Golgi complex. The thickness of the SMF varies, their cross striation has a periodicity of 88 ± 13,4 nm.

The occurrence of SMF does not show any connection with the age of the patients, the type of disease, the morphological changes or therapy. It is difficult to say whether they are normal or pathological organelles. Their presence can be regarded as a metaplastic process in functionally overloaded cells.

Keywords: kidney ultrastructure, glomerular cells, striated microfilaments, rhizoplast, rootlet

Introduction

Microtubules and microfilaments are found in almost every cell, but their amount and distribution vary [7]. The microtubules are attributed a role in the formation of the cystoskeleton, the organisation of organelles, the intracellular transport processes as well as in the movement of cell surface receptors. The microfilaments have a role in both the external and internal movement of the cell [3, 8, 16, 23, 25].

Less knowledge has been gained on the striated microfilaments related to the centrosome. The centrosome consists of centriole pairs and surrounding pericentriolar material. During the interphase it is situated near the nucleus. In the dividing cell it plays a role in the formation of the mitotic apparatus [14].

The pericentriolar material consists of four components: dense amorphous material, pericentriolar satellites, centriole feet and *striated rootlets* [34]. Structures corresponding to the latter have only rarely been observed in animal cells [4, 6, 22, 34]. In protozoa and invertebrates the structure that has analo-

* Send offprint requests to: K. Szepesházi Department of Pathology, Jahn Hospital Budapest, Köves út 2–4, 1204 Hungary

gous morphology to the centriole is the basal body of cilia and flagella. As their accessory, the striated rootlet (rhizoplast) is a well-known structure, and beside its motive or anchoring function it may be the organizer of the microtubules [30]. Furthermore in certain protozoa, instead of the centriole, the rhizoplast serves as the place of adhesion for the mitotic spindle [5].

In ciliates the striated microfilament bundles are situated between two neighbouring kinetosomes, as well as between the kinetosomes and the nucleus, with one side facing the Golgi, and the other adhered by the microtubules [5]. A similar structure in animals is the part of the basal apparatus of the ciliated cells, the rootlet anchoring the basal body [12].

We observed rhizoplast-like structures occurring around the centriole relatively often in various cell types of the glomeruli in human kidney biopsies. In this paper we present an analysis of their morphology.

Materials and Methods

226 specimens from various kidney biopsy cases (122 children) were studied by electron microscopy. Beside the usual light microscopic and immunohistochemical investigations 0,5—1 mm^3 parts of the fresh biopsy material were fixed in 2% osmium tetroxide solution (Palade buffer 0.1 m, pH 7.4) for 1 h at 4 °C, and following alcoholic dehydration the samples were embedded in Durcupan ACM (Fluka). The ultrathin sections were contrasted with uranyl acetate and lead hydroxide according to *Karnowsky* and examined under JEM 100 B electron microscope. Glutaraldehyde (in 2.5% pH 7.4 cacodylate buffer) fixation was carried out in one case. In average, 10 photographs were prepared in each case from the glomeruli.

Results

Occurrence, localisation

Striated microfilament bundles were found in the glomerular cells in the kidneys of 41 patients (18% of the cases). 21 were adults, 20 were children. In 10 cases SMF were found in more than one cell of the glomeruli, thus occurring in a total of 64 cells.

The occurrence according to diagnosis of the kidney disease in which striated microfilament bundles were found is shown in Table I (see No of cases, child cases are in parentheses). The incidence of SMF was diverse according to the different cell types. The following connections could be found between the type of the 64 cells containing this structure and the nature of the disease.

The localisation of the SMF occurring in several cells of one case was the following: podocyte + endothelial cell in 3 cases, several podocytes in 2 cases, endothelial + mesangial cell in 2 cases, and in single cases podocyte + mesangial cell, podocyte + parietal epithelial cell, and podocyte + endothelial + peritubular capillary endothelial cell.

Table I

Occurrence of SMF according to diagnosis of the kidney disease

No of cases	8 (6)	3 (1)	18 (10)	2 (0)	2 (0)	1 (0)	7 (3)	41 (20)
Disease	m.ch.	m.gn.	mes.gn.	mp.gn.	f. s.	s.gn.	else	total
Podocyte	8	1	16	4	2		6	37
Endothel	3	2	4	1	1		4	15
Mesangial cell	2	2	3			1	1	9
Parietal epithel	1							1
Peritubular capillary endothel			2					2
Total	14	5	25	5	3	1	11	64

(Abbreviations: minimal changes: m.ch., membranous glomerulonephritis: m.gn., mesangial proliferative glomerulonephritis: mes.gn., membranoproliferative glomerulonephritis: mp.gn., focal-segmental glomerular lesions: f.s., sclerosing glomerulonephritis: s.gn.)

The morphology and relationship to other organelles of the SMF

The majority of the microfilament bundles was connected with the centrosome. Among the 64 structures only 8 were such that the centriole was not visible on the same photograph (Fig. 1). Despite this, direct connection was not demonstrable with the centriole itself. No connection or continuation could be seen with the centriole feet either, though it is rarely observable that the microtubules originate from these (Fig. 2). The SMF are mostly followable to the pericentriolar dense material (Figs 3, 4, 7, 8), sometimes it seems as though they project from satellite-like structures (Fig. 5).

The bundles situated in the neighbourhood of the centriole vary in number. Sometimes only 1 can be seen, other times even several can be observed, spreading radially towards the surroundings (Figs 7, 8, 9). In some cases striated fibre bundles can be found between the centriole pairs (Figs 3, 10), or the bundles are seen passing by the centriole (Figs 11, 12).

The centrosome itself is generally located in the field of the Golgi complex, often in the neigbourhood of the nucleus. The bundles frequently extend between the Golgi vesicles (Fig. 1), or seem to encircle the Golgi (Figs 7, 13, 15). Their distal ends are not connected to any kind of organelles, sometimes, however, their ramification into unique microfilaments and spreading into the cytoplasm can be observed (Fig. 14).

Generally 5—6 longitudinal filaments can be well recognized in the structure itself (Fig. 14). In some cases, however, only fewer longitudinal filaments are observable, and the structure more likely resembles striated tubules (Figs 1, 11, 13). The striation periodicity within the fibers is relatively constant, but may be somewhat different in various bundles. Measuring an average of

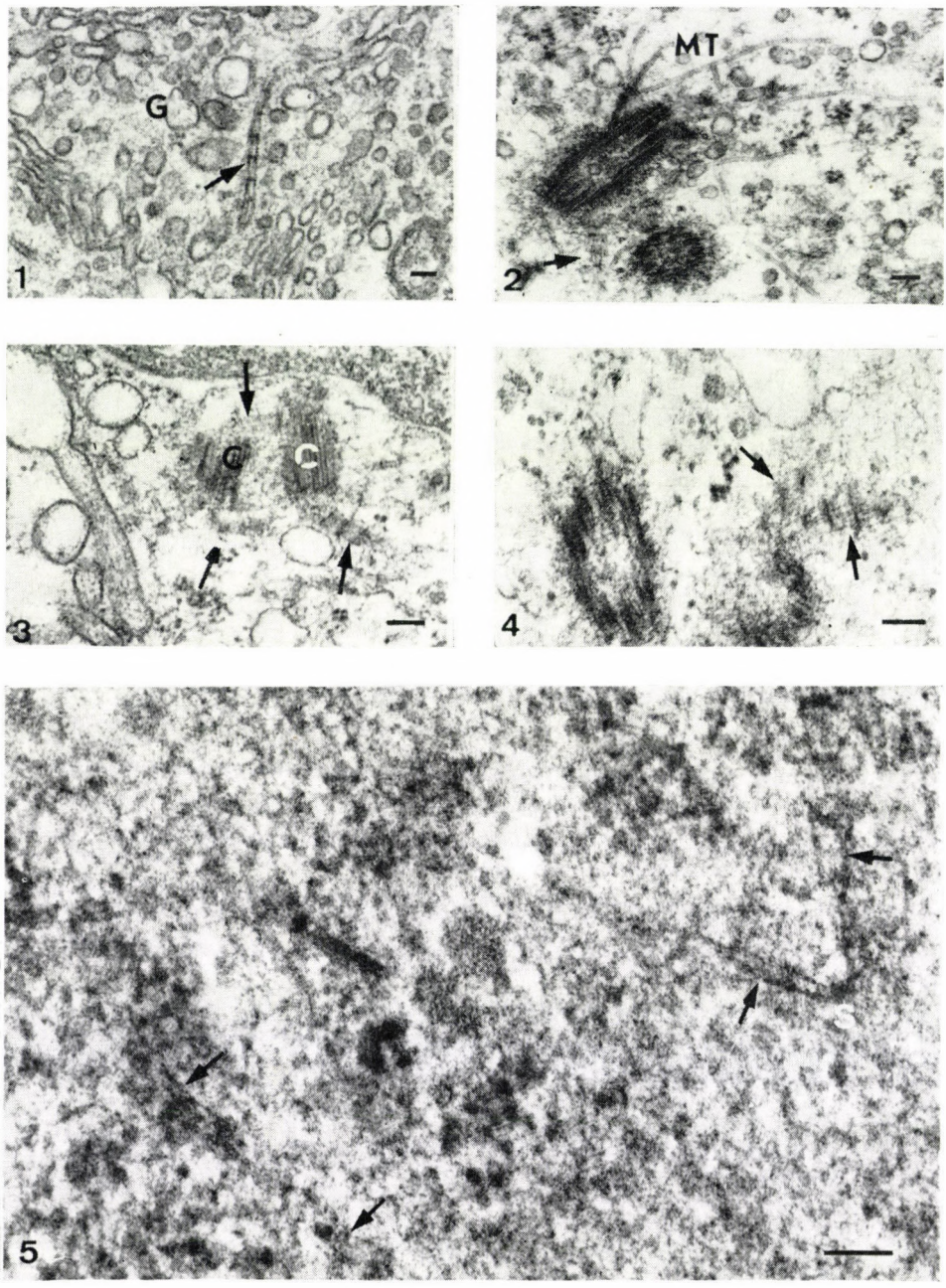

Fig. 1. Endothelial cell, SMF among the Golgi vesicles 33 000×(105 198)

Fig. 2. Mesangial cell. Some microtubules originate from the centriole foot. 33 000×(144 948)

Fig. 3. Podocyte. Centriole pair near the nucleus, short SMF in various directions. 50 000×(136 361)

Fig. 4. Messangial cell. SMF-s starting from the pericentriolar dense material. 55 000××(116 347)

Fig. 5. Podocyte. SMF related to the pericentriolar satellite. Glutaraldehyde fixation. 88 000××(145 662)

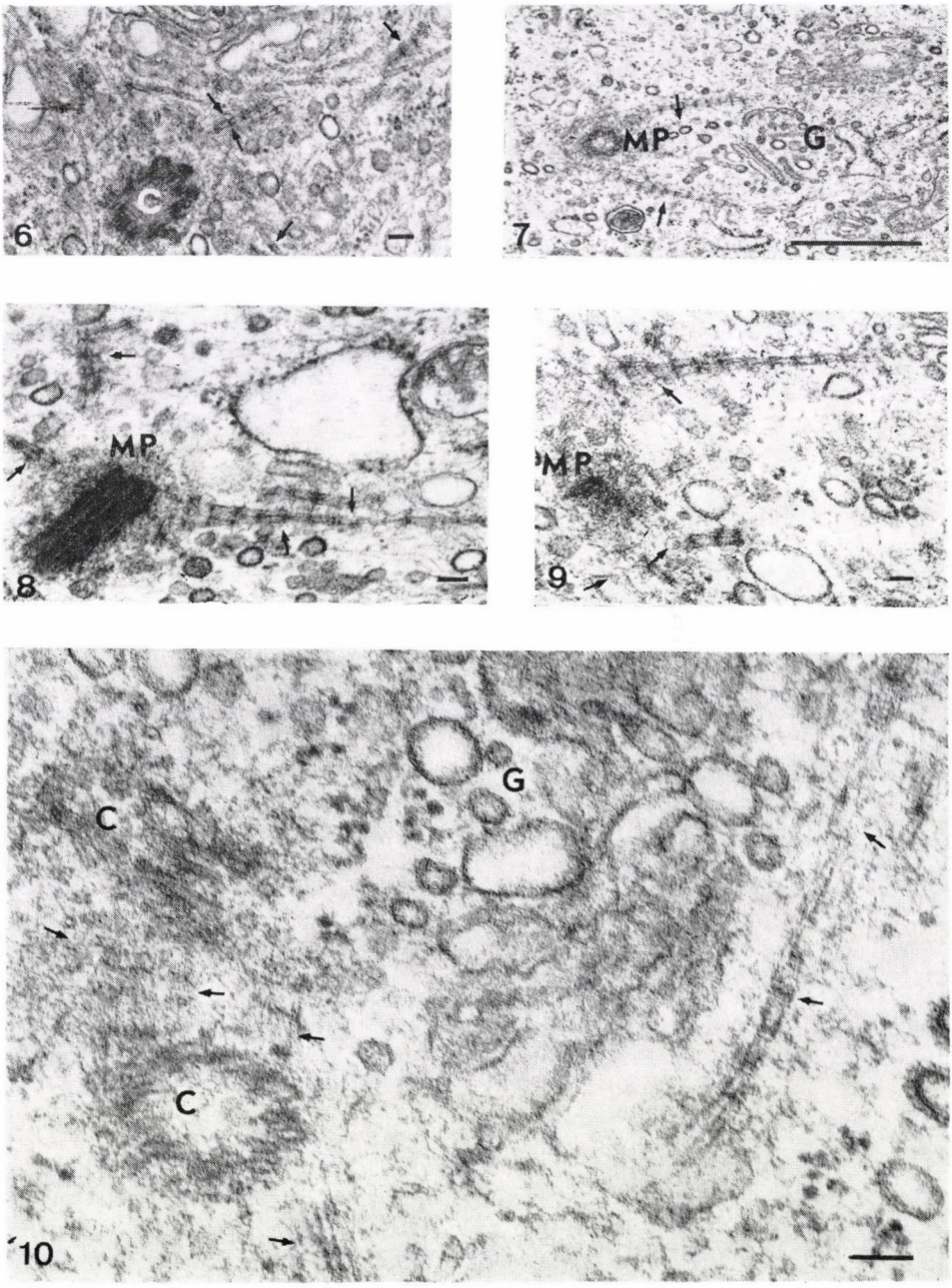

Fig. 6. Podocyte. Several SMF of various directions. 33 000×(140 629)
Fig. 7. Podocyte. SMF radiating in a horn-like manner from the pericentriolar dense material. 17 000×(109 050)
Fig. 8. SMF-s extending radially from the centriole in a podocyte. Some of them are widening beneath the pericentriolar dense material. 33 000×(84 435)
Fig. 9. Podocyte. SMF starting from the pericentriolar dense material, widening in the beginning. 30 000×(84 431)
Fig. 10. dothelial cell. Short SMF-s (shor t arrows) between the centriole (c) pair. The longer ones (long arrows) extend towards the cell periphery. 74 000×(140 625)

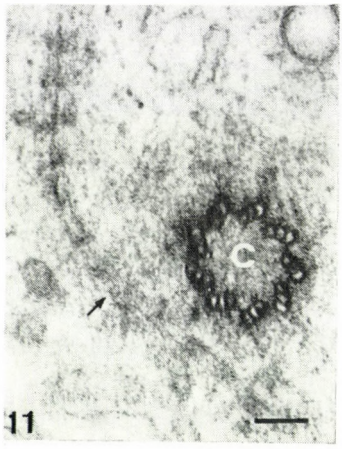

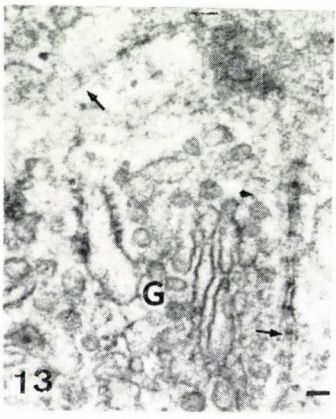

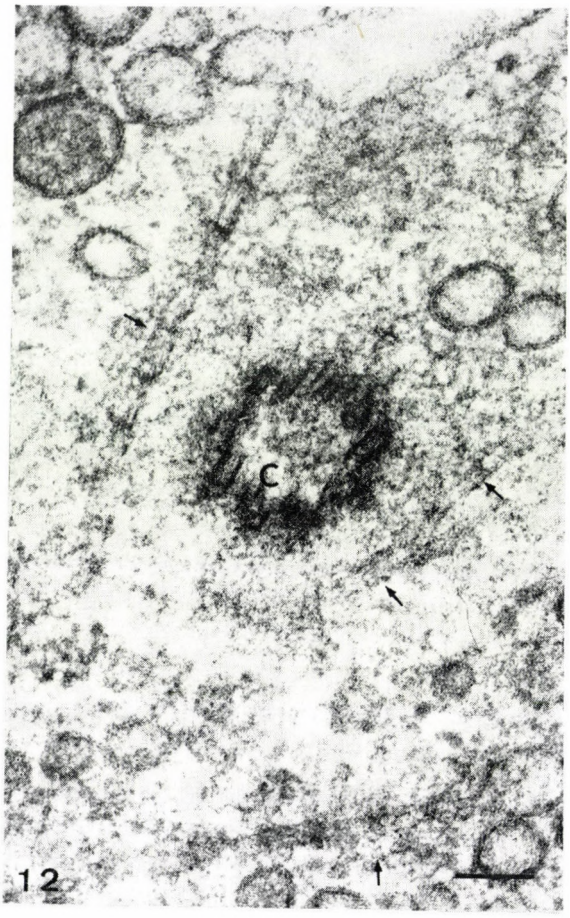

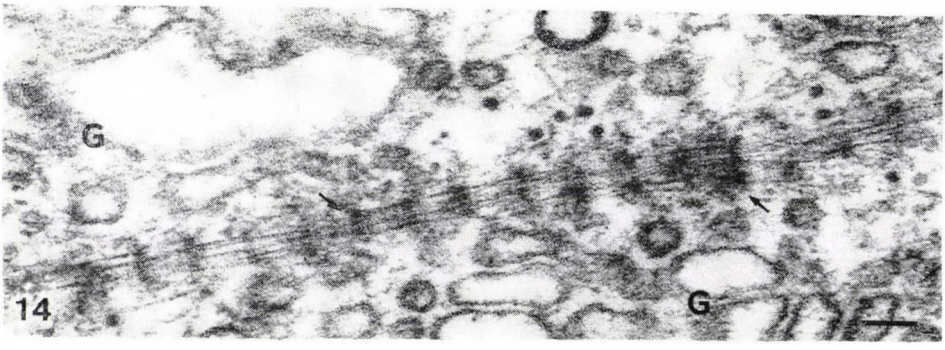

Fig. 11. Podocyte. SMF extending beside the centriole. 66 000×(102 505)
Fig. 12. Endothelial cell. SMF-s running beside the centriole. 99 000× ×(131 053)
Fig. 13. Endothelial cell. SMF-s surround the Golgi. 31 000×(84 165)
Fig. 14. Podocyte. A bundle consisting of 5—6 microfilaments can be seen among the Golgi vesicles. Its end shows spreading like a broom. 62 000×(82 569)
Fig. 15. Endothelial cell. SMF running by the margin of the Golgi. 20 000×(102 500)

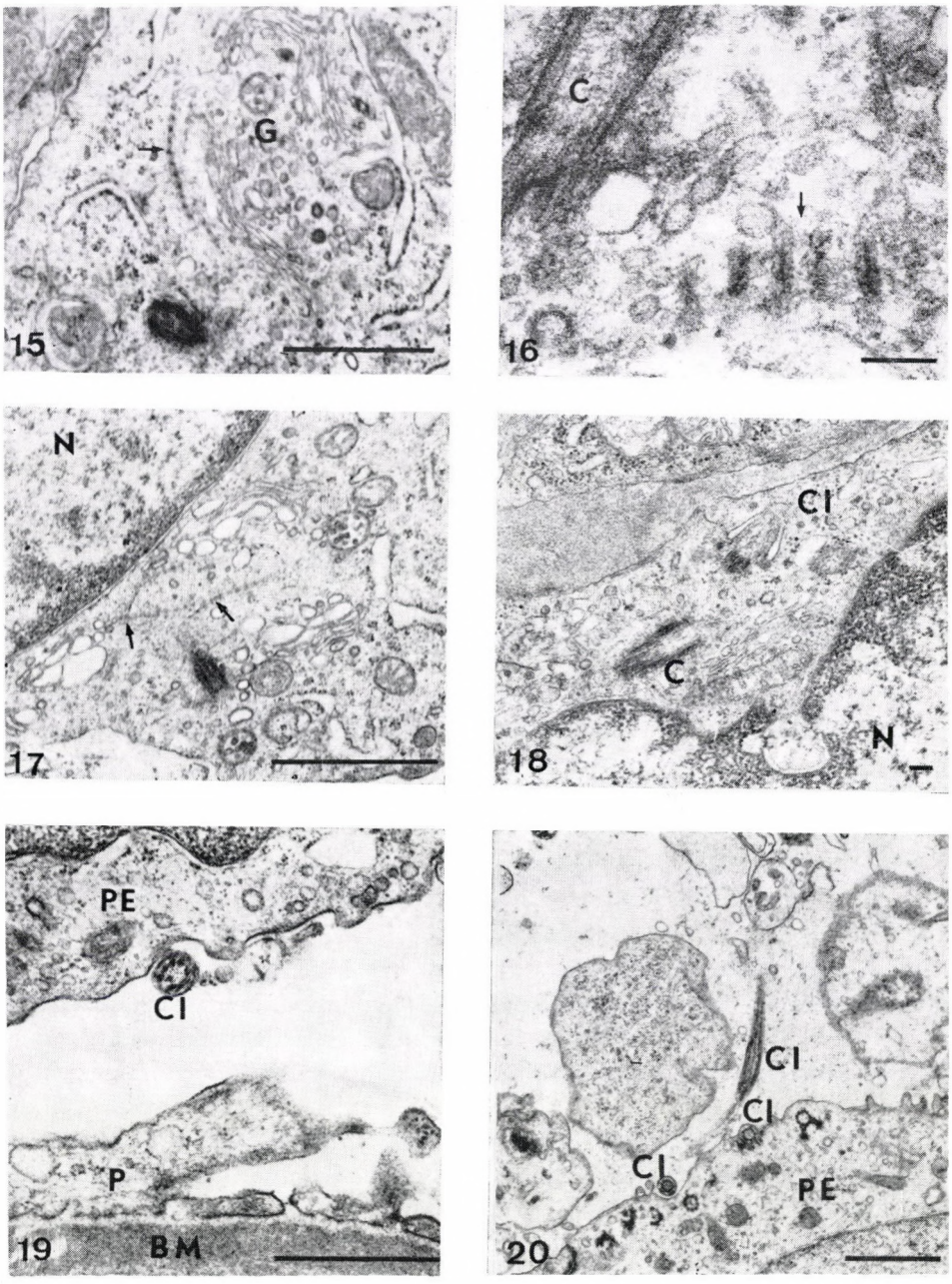

Fig. 16. Podocyte. A rather wide SMF. The cross striations have denser inner and lighter outer bands. 99 000 × (139 679)

Fig. 17. Podocyte. SMF seeming to ramify. 22 000 × (4661)

Fig. 18. Mesangial cell. Intracytoplasmic abortive cilium-formation. 25 000 × (116 226)

Fig. 19. Cilium on the surface of a parietal epithelial cell. 22 000 × (116 330)

Fig. 20. Several cilia on parietal epithelial cell. 12 000 × (103 557)

Abbreviations in the figures: arrows show SMF, BM — basement membrane, C — centriole, CI — cilium, G — Golgi, MT — microtubule, N — nucleus, P — podocyte, PE — parietal epithelial cell, PM — pericentriolar dense material, S — satellite

6 periods on 20 SMF we found periodicity of 88 ± 13.4 nm. The cross striations are not homogeneous, but consists of a central dense strip with less sharply outlining lighter bands on the two sides (Figs 14, 16). The thickness of the filament bundles varies. Sometimes it is observable that they widen in the neighbourhood of the centriole (Figs 8, 9). Their average thickness in the more even parts further from the centriole is app. 40—60 nm.

The length of the SMF cannot be determined, they are of various lengths, and generally only a shorter part of them is observable on the pictures. At times only 2—3 cross striations containing short structure is visible near the centriole. The longest one found was 2.0 μm. In some cases the bundles show branching (Figs 6, 17). After glutaraldehyde fixation their structure is similar to that observed with osmium tetroxide fixation (Fig. 5).

Other alterations concerning the centrosome

In the majority of the glomerular cells the centrioles have normal structure. Hypertrophic, larger than usual centrioles were only rarely observable. In the kidneys of two patients triple centrioles could be seen, 1 in a podocyte and 1 in a mesangial cell.

In a few cases, and mainly in the mesangial cells, the centriole was encircled in a cilium-like manner by an arched U-shaped vesicle (Fig. 18). In two cases a cilium, and the development of cilia, respectively, could be observed on the surface of the parietal epithelial cells (Figs 19, 20).

Discussion

There is a relatively rich microfilament network in the kidney glomerular cells, and actin-like proteins are also demonstrable in the podocytes and mesangial cells [1]. Structures similar to striated microfilament bundles, connected to the centrosome occur in 3 forms in other cell types: 1. kinetosome-related rhizoplast (rootlet) in protozoa (ciliata, flagellata), 2. kinetosome-related rhizoplast (rootlet in the ciliary cells of animals [12, 31], 3. centriole-related striated microfilament bundles independent of cilium or flagellum.

The latter has been observed in the lymphatic endothelial cells of rabbit lung [22], human and chicken liver tumors [4], HeLa and L_2 tumor cells [6], but in the latter it was only observable after precipitation and isolation of the microtubules.

According to Zeligs et al [34] the striated rootlets are one of the components of the pericentriolar material, which is only detectable in the interphase and disappears under mitosis. Morphologically the rootlet belonging to the basal body and the striated microfilament bundles belonging to the centriole

have a similar structure. The cross striation periodicity is 70 nm (12), 60—90 nm (22), and 88±13.4 nm in our cases. The thickness of the SMF is minute related to the size of the cell, their length was 0.2—2.0 μm in our figures. Dingle [9] reports two short (0.5 μm) and two long (1.3. μm) rootlets in Xenopus, and the formers are nearly twice as wide as the longer ones. From its size it is not very probable that it can be visible on the section of a cell. As it expands radially from the centriole into the cytoplasm, with all probability it can be found in the neighbourhood of the centriole. Its recognition is hampered by the fact that it can only be identified in longitudinal sections; in cross sections it is not recognizable.

In about half of our kidney biopsies the SMF were searched for retrospectively on the pictures taken earlier, while in the other half of the cases we attempted to discover them systematically already during the microscopic examination. Of course the bundles were more frequently found in the latter cases. In the first group of 124 cases they occurred in 16 (12.9% of the cases), and in the second half of the cases they were found in 25 of 102 (24.5%).

When judging the frequency of occurrence the following points should be considered. The microscopic examination had first of all diagnostic aims. About 5—6 ultrathin sections were prepared from each tissue block usually containing 1—3 glomeruli. The size of the bundles compared to the cell should also be taken into consideration. To analyse the frequency of occurrence in the different cell types we must know the incidence rate of the cell types on the pictures. Thus 103 podocyte nuclei and 95 mesangial cell nuclei per 100 endothelial cell nuclei were counted on the photographs of 30 different cases, without selection. It can be said therefore, that in the studied pictures the cell types occur at nearly the same frequency. On this base the conclusion is reasonable that more than half of the striated microfilament bundles occur in the podocytes; almost a quarter in the endothelial cells and about 1/7 in the mesangial cells.

To a certain extent the structure may resemble long spacing collagen, which rarely occurs in the kidney [27], however on the basis of its localisation and morphology it can be distinguished from it.

Despite the relatively frequent occurrence it cannot be stated that the SMF are normal organelles in every glomerular cell. This is also inferred by the fact that its incidence in the three cell types varies significantly. In several cases they could not be discovered even with thorough searching, despite the fact that the centrioles were visible.

Some authors raise the possibility that the appearance of the SMF may be a sign of the disturbance in the histological differentiation [4], or they may be the rootlets of rudimentary cilia [22].

The occurrence of oligocilia in the various tissues has been reviewed in detail by Ghadially [12]. We ourselves observed the development of cilia in

the glomeruli in 2 cases and only on the parietal epithelial cells. The basal bodies of these did not have any relationship with the rootlet. In a few cases vacuole-formation and cell membrane invagination around the centriole was observable mainly in the mesangial cells; these phenomena may refer to differentation towards cilium.

Several authors have observed the alterations and cilia-formation of centrioles of various cells in different pathological states: e.g in hypophysis anterior-lobe adenoma [18], hypophysis posterior-lobe stimulation [15] and in certain, mainly endocrine tumours the increase in centrioles [17]. These alterations may be connected to each other, since the formation of cilium and basal body, respectively, may also be of centriolar origin [2, 10].

In protozoa the kinetosome-related rootlet is generally a striated structure [5, 28], but may also be an other type [30]. In animals the striated rootlet can be found in most of the cilia [12]. In other cases, however, there is no rootlet system: e.g. in mammary myoepithelial cells [32], mouse oviduct [10]. In other cases it may be found, but it is not of striated structure: e.g. rhesus monkey oviduct [2], human adenocarcinoma [24].

From our results it may be concluded that the occurrence of centriole-related SMF is not connected to cilium formation in human glomerular cells. Though the rhizoplast connected to the basal body corresponds morphologically to the centriole-related similar structure, they cannot be regarded as identical, and the designation rootlet or rhizoplast is not correct for labelling the latter. In contrast to the opinion of Zeligs et al [34] the centriole-related SMF cannot be considered as the component of the pericentriolar material. Although it arises from the pericentriolar area, it spreads far from it, even to a distance of several μm — and on this basis the microtubules should also be classed among the pericentriolar material.

There was no relationship in the occurrence of the SMF with the age of the patient, the nature of the kidney disease, the clinical symptoms or the character of the morphological picture. Some of the patients received corticosteroid and cytostatic immunosuppressive treatment, respectively, at various intervals before biopsy. There also seemed to be no relationship between the occurrence of the SMF and therapy. However, it seems that their appearance was accompanied by other signs of an increase in the activity of the cell, the increase of other cell organelles — first of all the hypertrophy of the Golgi. The formation of these structures cannot be observed better in the glutaraldehyd-fixed material than in that fixed in osmium tetroxide.

We have no knowledge at present regarding the function of the striated microfilament bundles. In the case of the cilia, the rhizoplast and the rarely occurring similar fibers of finer periodicity are presumed to play mechanoreceptor, movement, and movement-coordinating roles, respectively [13]. According to others the rhizoplast has a function of mechanical supporting [11]

or anchoring function with the centriole [34] and in connection with the basal body [31]. The beat of the flagellum in flagellata can only be effective in the motion of the cell, if the rootlet system is anchored to an organelle large enough (to the nucleus) [29]. The direction of the ciliary beating appears to be controlled through the orientation of the stable anchoring striated rootlet system [9].

The contractile nature of other microfilaments, the striation periodicity resembling the structure of the skeleton muscle fibers, a certain variability in periodicity indicate a function of contractility or elasticity [28]. The active motile function of these organelles in protozoa has been accepted in the last years, their ion-sensitive contractile nature having been detected [26]. The actin [21] as well as ATP-ase activity [33] demonstrable in the rootlet proves the contractile, locomotive character of this structure. Hyams and King [19] have isolated and identified the rhizoplast fibre protein as a 47 kDa molecule.

The various cell types of the kidney glomeruli are cells of complicated function with characteristic structure, having a role in the filtration process, the production of the basement membrane, the processing of certain elements of blood etc. Their complex metabolic and movement processes are in connection with these tasks. The occurrence of the SMF in the glomerular cells may be regarded as an adaptive metaplastic process. They may play a role in the movement processes of these cells and in the intracellular material-transport. However, further studies are necessary for the elucidation of their function.

REFERENCES

1. Accini L, Natali, PG Vassallo L: Immunoelectron microscopic evidence of contractile proteins in the cellular and acellular components of mouse kidney glomeruli. Cell Tissue Res *162:* 297, 1975
2. Anderson RGW, Brenner RM: The formation of basal bodies (centrioles) in the rhesus monkey oviduct. J Cell Biol *50:* 10, 1971
3. Bardele CF: Struktur Biochemie und Funktion der Mikrotubuli. Cytobiol. (Stuttg) *7:* 442, 1973
4. Bencsáth M, Strausz J, Schaff Zs, Lapis K: Rhizoplastjellegű struktúrák megjelenése kísérletes és humán májtumorokban. Orvostudomány *29:* 241, 1978
5. Bouck GB, Brown DL: Microtubule biogenesis and cell shape in Ochromonas. I. The distribution of cytoplasmic and mitotic microtubules. J Cell Biol *56:* 340, 1973
6. Dales SK, Hsu, C Nagayama A: The fine structure and immunological labelling of the achromatic mitotic apparatus after disruption of cell membranes. J Cell Biol *59:* 643, 660 (1973)
7. David H: Cellular Pathobiology. In: Electron Microscopy in Human Medicine ed. J. V. Johannessen Vol 2 Mc GrawHill Int. Book Co. 1978
8. De Brabander M, De Mey J, Van De Veire R: Microtubules in mammalian cell shape and surface modulation: An alternative hypothesis. Cell Biol Int Rep *1:* 453, 1977
9. Dingle AD: Striated rootlet fibres and the orientation of the ciliary beat. J Cell Biol *99:* 188a 1984
10. Dirksen ER: Centriole morphogenesis in developing ciliated epithelium of the mouse oviduct. J Cell Biol *51:* 286, 1971
11. Flood PR: Ciliary rootlet-fibres as tail fin-rays in larval Amphyoxus (Branchiostoma lanceolatum, Pallas) J Ultrastruct Res *51:* 218, (1975)
12. Ghadially FN: Ultrastructural pathology of the cell. Butterworths, London and Boston, 1975

13. Goodenough UA, Weiss RL: Interrelationship between microtubules, a striated fiber and the gametic mating structure of chlamidomonas Reinchardi. J Cell Biol *76:* 430—438, 1978
14. Gould RR, Borisy GG: The pericentriolar material in Chinese hamster ovary cells nucleates microtubule formation. J Cell Biol *73:* 601—615, 1977
15. Herbert JP, Flament Durand J, Dustin P: Centrioles and cilia multiplication in the pituitary of the rat after furosemid and colchicin treatment. I. The posterior lobe. Cell Tissue Res *149:* 349—361, 1974
16. Hoffstein S, Goldstein, IM Weissmann G: Role of microtubule assemblay in lysosomal enzyme secretion from human polymorphonuclear leukocytes. A reevaluation. J Cell Biol *73:* 242—256, 1977
17. Horvath E, Kovacs K: Mitochondrial derivation of centrioles in some endocrine adenomas. Experientia *32:* 742—744, 1976
18. Horvath E, Kovács K, Ezrin C: Centrioles and cilia in non tumorous anterior lobes and adenomas of human pituitary. Path Europ (London) *11:* 81—86, 1976
19. Hyams JS, King CA: Identification of proteins of the striated rootlet of *Tetrahymena* by immunofluorescence microscopy and immunoblotting with an anti-rootlet serum. Europ J Cell Biol *38:* 102—107, 1985
20. Karnovsky M: Simple method for "staining with lead" at high pH in electron microscopy. Biophys Biochem Cytol *11:* 729—732, 1961
21. Kleve MG, Clark WH: Association of actin with sperm centrioles: Isolation of centriolar complexes and immunofluorescent localisation of actin. J Cell Biol *86:* 87—95, 1980
22. Lauweryns JM, Boussauw L: Striated filamentous bundles associated with centrioles in pulmonary lymphatic endothelial cells. J Ultrastruct Res *42:* 25—28, 1973
23. Lother H, Blitstein-Willinger, E Diamantstein T: Studies on the relevance of microtubules and of microfilament -dependent processes for triggering lymphocyte activation. Z Immun-Forsch *155:* 346—358, 1979
24. Marcus PB, Martin, JH Green, RH Krouse MA: Glycocaliceal bodies and microvillus core rootlets. Arch Pathol Lab Med *103:* 89—92, 1979
25. Pollard TD: Cytosceletal functions of cytoplasmic contractile protein. J Supramolec Struct *5:* 317—334, 1976
26. Salisbury JL, Baron A, Surek Barbara, Melkonian M: Striated flagellar roots: isolation and partial characterisation of a calcium-modulated contractile organelle. J Cell Biol *99:* 962—970, 1984
27. Schubert GE, Adam A: Glomerular nodules and long spacing collagen in kidneys of patients with multiple myeloma. J Clin Path *27:* 800—805, 1974
28. Simpson PA, Dingle AD: Variable periodicity in the rhizoplast of Naegleria flagellates. J Cell Biol *51:* 323—328, 1971
29. Spiegel FW: Role of nucleus/flagellar rootlet attachment in swimming ability of Protosporangium articulatum J Cell Biol *99:* 187a 1984
30. Stearns ME, Brown DL: Microtubule organizing centers (MTOCs) of the Alga Polytomella exert special control over microtubule initiation in vivo and in vitro. J Ultrastruct Res *77:* 366—378, 1981
31. Stephens RE: The basal apparatus. Mass isolation from the molluscan ciliated gill epithelium and a preliminary characterisation of striated rootlets. J Cell Biol *64:* 408—420, 1975
32. Stirling JW, Chandler JA: Ultrastructural studies of the female breast. I 9 + 0 cilia in myoepithelial cells. Anat Res *186:* 413—416, 1976
33. White RB, Brown DL: ATP-ase activities associated with the flagellar basal apparatus of *Polytomella*. J Ultrastuct Res *75:* 151—161, 1981
34. Zeligs JD, Wollman SH: Mitosis in rat thyroid epithelial cells in vivo. II. Centrioles and pericentriolar material. J Ultrastruct Res *66:* 97—108, 1979

Acta Morphologica Hungarica, 35 (1—2), pp. 89 (1987)

Book Review

MICHAEL RICKMANN and JOACHIM R. WOLFF: *Prenatal Gliogenesis in the Neopallium of the Rat.*

Advances in Anatomy, Embryology and Cell Biology, Vol. 93. — Springer-Verlag, Berlin, Heidelberg, New York, Tokyo (1985). Price: DM 58,—

This monograph deals with the morphological characteristics and early differentiation of non-radial glial cells in the prenatal cerebral cortex. The book which has 104 pages is divided into 4 main chapters (Introduction, an informative Material and Methods, a most detailed, and richly illustrated Results, and the following, Discussion + concluding brief Summary). A comprehensive list of References concludes the monograph.

The methods utilized include standard light- and electron microscopy, ^{3}H-thymidine and ^{3}H-GABA autoradiography, Golgi impregnation 3-d reconstruction of EM-graphes and last, but not least, GFAP and C, immunocytochemistry.

The main message of the monograph is, that embryonic glial cells exhibit a very specific polarity established through contacts with (1) mesenchymal surfaces and (2) by a system of interglial contacts. Interglial contacts and communication structures form a spongious framework, into which differentiating nerve cells are layed down during cortical development. In addition, the authors provide evidence, that glial cells of various positions and of various shape are present at very early developmental stages, coexisting with preneurons, and other, radial glial cells.

The monograph is recomended to those interested in developmental neurobiology, and in cellular differentiation problems.

J. HÁMORI

PRINTED IN HUNGARY

Akadémiai Kiadó és Nyomda, Budapest

INSTRUCTIONS TO AUTHORS

Form of manuscript

Contributors are requested to supply two complete copies of the manuscript including all tables and illustrations. Manuscripts should be typed double-spaced with margins of at least 4 cm. Pages should be numbered consecutively.

The *headline* should include the title of the paper, authors' names, and name and short postal address of the institute where the work was done.

An *abstract* of not more than 200 words should be supplied typed before the text. It should briefly describe the purpose of the investigations, the methods utilized, the results obtained, and the authors' principal conclusions.

Abbreviations and symbols

Abbreviations should be spelled out when first used in the text or, alternatively, a list of abbreviations might be given. The *International System of Units (SI)* should be used for all measurements. Symbols for physical quantities are to be printed in italics and should, therefore, be underlined in the manuscript. Unusual symbols should be identified on the margin.

References

References should be numbered in alphabetical order, and these numbers only should be inserted in the text (in parentheses). In the reference list each item should include the names and initials of all authors; the title of the article; the title of the journal abbreviates according to the style used in *Index Medicus* (a list of the journals indexed is printed annually in the January issue); the volume number; the first page number; and the year of publication.

Kaplan AP, Kay AB, Austen KF: A pre-albumin activator of prekallikrein. J Exp Med 135:81, 1972

Titles of books should be followed by the publisher; place of publication; and the year.

Oláh I, Röhlich P, Törő I: Ultrastructure of Lymphoid Organs. Akadémiai Kiadó, Budapest 1975

Halász B: The endocrine effects of isolation of the hypothalamus from the rest of the brain. In: Frontiers in Neuroendocrinology, eds Ganong WF, Martini L, Oxford University Press, Oxford 1969, p. 307

Tables and illustrations

Tables should be comprehensible to the reader without reference to the text. The headings should be typed above the table. Tables should be numbered with Roman and illustrations with Arabic numerals.

Figures should be identified by number and authors' name written lightly in pencil on the back. The top should be indicated on the back of prints. The letters a, b etc. should be placed in the lower left-hand corner of prints. Staining techniques and the original magnification of photomicrographs should be stated. Figure captions should be typed on a separate sheet. The approximate place of figures and tables in the text should be indicated in the manuscript on the left-hand margin.

Proofs and reprints

Reprints and proofs will be sent to the first author unless otherwise indicated. A hundred reprints of each paper will be supplied free of charge.

Periodicals of the Hungarian Academy of Sciences are obtainable at the following addresses:

AUSTRALIA
C.B.D. LIBRARY AND SUBSCRIPTION SERVICE
Box 4886, G.P.O., *Sydney N.S.W. 2001*
COSMOS BOOKSHOP, 145 Ackland Street
St. Kilda (Melbourne), Victoria 3182

AUSTRIA
GLOBUS, Höchstädtplatz 3, *1206 Wien XX*

BELGIUM
OFFICE INTERNATIONAL DES PERIODIQUES
Avenue Louise, 485, *1050 Bruxelles*
E. STORY-SCIENTIA P.V.B.A.
P. van Duyseplein 8, *9000 Gent*

BULGARIA
HEMUS, Bulvar Ruszki 6, *Sofia*

CANADA
PANNONIA BOOKS, P.O. Box 1017
Postal Station "B", *Toronto, Ont. M5T 2T8*

CHINA
CNPICOR, Periodical Department, P.O. Box 50
Peking

CZECHOSLOVAKIA
MAD'ARSKA KULTURA, Národni třida 22
115 66 Praha
PNS DOVOZ TISKU, Vinohradská 46, *Praha 2*
PNS DOVOZ TLAČE, *Bratislava 2*

DENMARK
EJNAR MUNKSGAARD, 35, Nørre Søgade
1370 Copenhagen K

FEDERAL REPUBLIC OF GERMANY
KUNST UND WISSEN ERICH BIEBER
Postfach 46, *7000 Stuttgart 1*

FINLAND
AKATEEMINEN KIRJAKAUPPA, P.O. Box 128
00101 Helsinki 10

FRANCE
DAWSON-FRANCE S.A., B.P. 40, *91121 Palaiseau*
OFFICE INTERNATIONAL DE DOCUMENTATION ET LIBRAIRIE, 48 rue Gay-Lussac
75240 Paris, Cedex 05

GERMAN DEMOCRATIC REPUBLIC
HAUS DER UNGARISCHEN KULTUR
Karl Liebknecht-Straße 9, *DDR-102 Berlin*

GREAT BRITAIN
BLACKWELL'S PERIODICALS DIVISION
Hythe Bridge Street, *Oxford OX1 2ET*
BUMPUS, HALDANE AND MAXWELL LTD.
Cowper Works, *Olney, Bucks MK46 4BN*
COLLET'S HOLDINGS LTD., Denington Estate,
Wellingborough, Northants NN8 2QT
WM DAWSON AND SONS LTD., Cannon House
Folkstone, Kent CT19 5EE
H. K. LEWIS AND CO., 136 Gower Street
London WC1E 6BS

GREECE
KOSTARAKIS BROTHERS INTERNATIONAL BOOKSELLERS, 2 Hippokratous Street, *Athens-143*

HOLLAND
FAXON EUROPE, P.O. Box 167
1000 AD Amsterdam
MARTINUS NIJHOFF B. V.
Lange Voorhout 9-11, *Den Haag*
SWETS SUBSCRIPTION SERVICE
P.O. Box 830, 2160 Sz Lisse

INDIA
ALLIED PUBLISHING PVT. LTD.
750 Mount Road, *Madras 600002*
CENTRAL NEWS AGENCY PVT. LTD.
Connaught Circus, *New Delhi 110001*
INTERNATIONAL BOOK HOUSE PVT. LTD.
Madame Cama Road, *Bombay 400039*

ITALY
D. E. A., Via Lima 28, *00198 Roma*
INTERSCIENTIA, Via Mazzé 28, *10149 Torino*
LIBRERIA COMMISSIONARIA SANSONI
Via Lamarmora 45, *50121 Firenze*
SANTO VANASIA, Via M. Macchi 58
20124 Milano

JAPAN
KINOKUNIYA COMPANY LTD.
Journal Department, P.O. Box 55
Chitose, *Tokyo 156*
MARUZEN COMPANY LTD., Book Department
P.O. Box 5050 Tokyo International, *Tokyo 100-31*
NAUKA LTD., Import Department
2-30-19 Minami Ikebukuro, Toshima-ku, *Tokyo 171*

KOREA
CHULPANMUL, *Phenjan*

NORWAY
TANUM-TIDSKRIFT-SENTRALEN A.S.
Karl Johansgata 43, *1000 Oslo*

POLAND
WĘGIERSKI INSTYTUT KULTURY
Marszalkowska 80, *00-517 Warszawa*
CKP I W, ul. Towarowa 28, *00-958 Warszawa*

ROUMANIA
D. E. P., *Bucuresti*
ILEXIM, Calea Grivitei 64-66, *Bucuresti*

SOVIET UNION
SOYUZPECHAT — IMPORT, *Moscow*
and the post offices in each town
MEZHDUNARODNAYA KNIGA, *Moscow G-200*

SPAIN
DIAZ DE SANTOS Lagasca 95, *Madrid 6*

SWEDEN
ESSELTE TIDSKRIFTSCENTRALEN
Box 62, *101 20 Stockholm*

SWITZERLAND
KARGER LIBRI AG, Petersgraben 31, *4011 Basel*

USA
EBSCO SUBSCRIPTION SERVICES
P.O. Box 1943, *Birmingham, Alabama 35201*
F. W. FAXON COMPANY, INC.
15 Southwest Park, *Westwood Mass. 02090*
MAJOR SCIENTIFIC SURSCRIPTIONS
1851 Diplomat, P.O. Box 819074,
Pallas, Tx. 75381-9074
READ-MORE PUBLICATIONS, INC.
140 Cedar Street, *New York, N. Y. 10006*

YUGOSLAVIA
JUGOSLOVENSKA KNJIGA, Terazije 27, *Beograd*
FORUM, Vojvode Mišića 1, *21000 Novi Sad*

Index: 26.017

Acta Morphologica Hungarica

VOLUME 35, NUMBERS 3–4, 1987

Akadémiai Kiadó, Budapest
ACTA MORPH. HUNG. HU ISSN 0236–5391

ACTA MORPHOLOGICA
HUNGARICA
A QUARTERLY OF THE HUNGARIAN ACADEMY OF SCIENCES

Acta Morphologica publishes original papers on experimental morphology and pathology in English.

Acta Morphologica is published in yearly volumes of four issues by

AKADÉMIAI KIADÓ

Publishing House of the Hungarian Academy of Sciences
H-1054 Budapest, Alkotmány u. 21.

Manuscripts and editorial correspondence should be addressed to

Acta Morphologica

Ist Institute of Pathology and Experimental Cancer Research, Semmelweis Medical University, 1085 Budapest, Üllői út 26, Hungary

Subscription information

Orders should be addressed to

KULTURA Foreign Trading Company
H-1389 Budapest P.O. Box 149

or to its representatives abroad

Acta Morphologica Hungarica is abstracted/indexed in Biological Abstracts, Chemical Abstracts, Chemie-Information, Current Contents–Life Sciences, Excerpta Medica, Gerontological Abstracts, Index Medicus

---

CONTENTS

Normal and experimental morphology

Pathology

Acta Morphologica Hungarica, 35 (3—4), pp. 91—104 (1987)

EXPERIMENTAL INVESTIGATION OF THE EFFECT OF CARDIAC GLYCOSIDES ON THE ISCHEMIC CORONARY CIRCULATION

P. Sótonyi, V. Kékesi, E. Somogyi

DEPARTMENT OF FORENSIC MEDICINE AND RESEARCH UNIT OF DEPARTMENT OF CARDIOVASCULAR SURGERY, SEMMELWEIS UNIVERSITY OF MEDICINE, BUDAPEST

(Received 21 February 1986)

The paper presents new evidence of the vasoactivity of cardiac glycosides in the myocardium. Experiments were performed on the in situ dog heart. The present study primarily focuses on the analysis of K-strophantoside induced topo-optical and thermographic alterations in acute myocardial ischemia. The strong binding of K-strophantoside to the coronary vessel wall and the endothelial cells was found to be accompanied by vasoconstriction in the regionally ischemic heart muscle. The potential clinical impact of these findings on therapy is briefly evaluated.

Keywords: Cardiac glycosides, ischemia, coronary circulation thermographia

Introduction

Sufficient morphological evidence exists to document the affinity of cardiac glycosides to the coronary vessels: Determined with Romhányi's aldehyde-bisulphite-toluidine blue (ABT) technique (22) the intensity of birefringence in the vascular wall indicating the strengtht of binding was found to be similar to that of the myocardial sarcolemmal reaction [26, 27]. This histological pattern has its functional equivalent: although a secondary metabolic vasodilator response resulting from cardiostimulation would be expected to follow cardiac glycoside administration, in earlier experiments a primary direct vasoconstrictor effect has been found in the coronary bed of the intact dog heart [26]. These findings strongly suggest that the direct coronary action of cardiac glycosides also competes with hypoxic vascular adaptation (vasodilation) during myocardial ischaemia. However, in the past, it was difficult to examine this possibility with conventional techniques. With the advent of the functional morphologic method of cardiac thermography, the detailed inquiry into the problem seems convenient. Papp and his co-workers have proved that the power by thermography of resoluting coronary vascular changes in the dimensions of both space and time far exceeds the power

Send offprint requests to P. Sótonyi, Dept. of Forensic Medicine, Semmelweis University of Medicine, 1091 Budapest, Üllői út 39, Hungary

possessed by alternative methodologies aimed at similar purposes [17, 18, 19, 21]. Since thermographic mapping freezes rapidly changing physiological activity to well defined morphologic patterns, the technique is suitable to examine rapidly acting drugs such as strophantine. These patterns can be compared with the binding of the drug as determined with the aid of the polarization microscope. The present study therefore focuses on the analysis of K-strophantoside-induced topo-optical and thermographic alterations in acute myocardial ischaemia by utilizing the methods described by Romhányi et al. [22] and Papp et al. [19, 21], respectively.

Materials and methods

Experiments were done using 15 mongrel dogs of either sex, weighing between 9.5 and 27 kg, and anaesthetised with pentobarbital sodium, 30—35 mg/kg, given intravenously. Supplemental doses (30—60 mg) were injected as needed. The animals were incubated intratracheally and ventilated with room air by means of a volume-cycled respirator (RO-5). The heart was exposed through a bilateral transsternal thoracotomy in the 4th intercostal space and the pericardium was incised. The heart was firmly suspended in a pericardiac cradle. The left anterior descending (LAD) coronary artery was prepared free distal to the septal branch, usually in an upper mid-position and a thread was placed loosely around it. Arterial blood pressure was measured with a P 23 Bd Statham transducer through a heparine-filled polyethylene cannula inserted into a femoral artery. Pressure tracings were continuously displayed on a Hellige recorder. After the surgery had been completed a 25—30 min period was allowed for the stabilization of the preparation. Nine dogs (Group I) were used only for studying by the ABT technique of the binding and distribution of glycosides in acute myocardial ischaemia. In six dogs (Group II) thermographic analysis was also performed. The experimental protocol was similar in both groups: when the blood pressure and/or the thermographic image of the heart (v.i.) appeared to be stabilized, the LAD artery against the flanged end of a rigid polyethylene tube, and maintained for the remaining part of the experiment. After 60 min the dogs were given 50 μg/kg K-strophantoside in slow intravenous injection. The drug was administered either as a single dose (Group I), or in the form of two equal subsequent doses (Group II). The haemodynamic effect of the glycoside was characterized by the change of the mean arteria pressure, and the change in the number of ectopic beats. At the termination of the experiment the beating heart was removed rapidly and placed on crushed ice for histochemical analysis. Comparative investigation of cardiac glycoside binding to the coronary vessels was studied with the ABT (aldehyde-bisulphite-toluidine blue) topo-optical staining reaction. The tissues were cut for thick sections (Cryo-Cat-Microtome. American Opt. Co.). The slices were treated with 1.0 periodic acid for 30 min then with saturated solutions of sodium bisulphate also for 30 min. After short rinsing with water, the slices were stained for 5 min with toluidine blue (Sigma) at pH 0.1 toluidine blue in 0.1N HCl). After staining, the dye solution was blotted with a good quality of filter paper. Then 1.0% potassium ferrycyanide solution was dropped onto the slides. Without being rinsed in water the slices were mounted on gum arabic containing 1.0% potassium ferrycyanide. Polarization optical examinations were carried out with a Leitz Ortholux microscope. Quantitative measurements were made with rotating compensators. For more details on topo-optical reactions see Romhányi et al [22]. A minimum of three sections from each heart was cut having a thickness of 5 to 10 μm and stained with haemotoxylin-eosin (HE) or phosphotunstic-acid-haemotoxylin (PTAH).

The investigated ischemic territory was always distal from the LAD ligature. The control was the area supplied by the circumflex artery.

Cardiac thermograms, as described formerly [21, 19] were recorded with an AGA 750 Thermovision camera which senses the infrared waves in the 2.0 to 5.6 μm wavelength range. The method is based on the principle that these rays, projected by rotating prism on an indium-antimonide crystal cooled with liquid N_2 to -196 °C, are converted into electric signals: Colour-coded thermographic images are displayed by a unit of the equipment working on the

principle of a closed television chain. In the false-coloured images the warm and cold ranges are represented by white-red and blue-green colours, respectively. The sensitivity of the equipment was set to cover a 5 °C temperature range: accordingly, each colour of scale, which is divided into 10 bands, represented a 0.5 °C step in temperature. With the aid of a standard reference heat source the temperature pertaining to a given colour could be detected and calibrated at regular intervals. Pictures were taken from the appropriate monitoring unit of the device with a Canon AT-1 photographic camera.

Results

I. Polarization microscopic investigations

In one of nine dogs, occlusion of the LAD artery caused irreversible ventricular fibrillation. Seven of the survivers received 50 μg/kg of K-strophantoside, in a single dose, while the remaining animal served as histologic control. The haemodynamic stability of the experimental subgroup is shown in the Table I. The effect of LAD occlusion failed to elicit a statistically significant drop in blood pressure, and the increase of the number of extrasystoles was also slight. Cardiac glycoside administration elicited significant hypertension and a moderately augmented frequency of ectopic beats.

After the occlusion of the LAD artery the signs of acute myocardial ischemia were shown in the effected myocardial cells with PTAH staining

Table I

Haemodynamic consequence of experimental interventions*

Time (min)	Control	Myocardial ischaemia (LAD) occlusion		
	0	5	00	70 (strophantoside**)
Mean arterial blood pressure (mmHg)	124.6 ± 9.8	113.7 ± 10.6	123.4 ± 11.3	142.3 ± 11.8[a]
Incidence of arrhythmias (ES/min)	0.4 ± 0.4	3.1 ± 2.2[b]	3.1 ± 1.8[b]	7.0 ± 3.4[b]

* Mean values ± SEM, n = 7
** 10 min after the i.v. administration of 50 μg/kg K-strophantoside
[a] Significant change ($p < 0.01$) from the preceeding phase (60 min)
[b] Significant change ($p < 0.05$) from control

method. The ABT reaction was practically negative: only some sections showed small basophilia and birefringence of the small vessels and sarcolemma membrane. The retardation of birefringence was 5—10 nm. In the non-damaged myocardial area the topo-optical reaction induced a very intensive effect of the sarcolemma membrane and capillaries. Negative birefringence to the surface was found. The strong binding of cardiac glycoside was indicated by the appearance of dichroism and the characteristic green colour of polarization

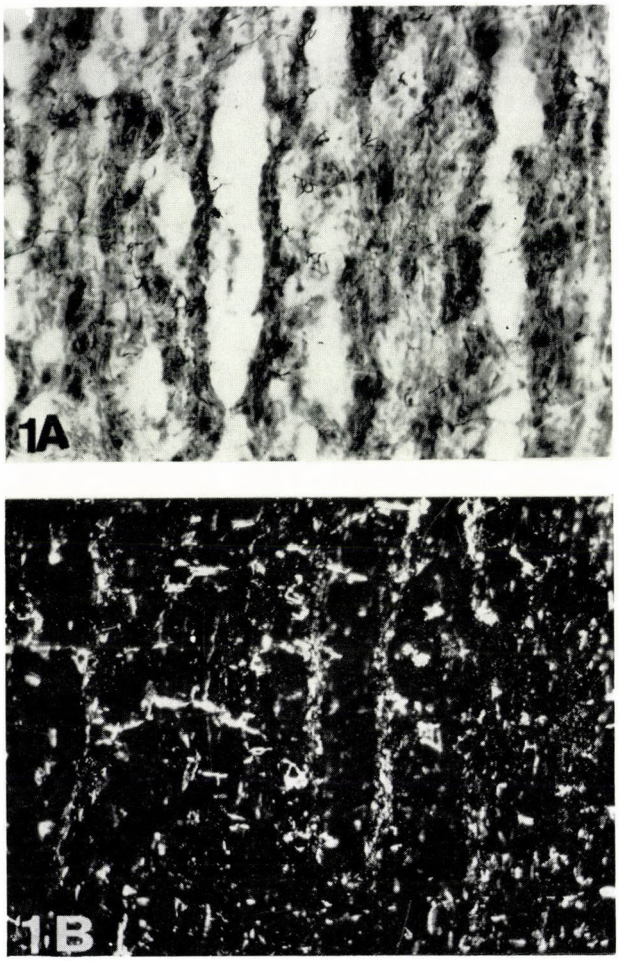

Fig. 1. Demonstration of K-strophantoside administered intravenously in doses of 50 μg/kg. Light microscopic (A) and polarization microscopic (B) pictures of the same preparations. The arrows show localization of the strong binding of cardiac glycoside in the wall of small coronary artery. ABT reaction. (240×, 240×)

(Fig. 1). Negative birefringence of the surface of the sarcolemma membrane and capillaries, pointed to perpendicularly oriented dye molecules and to linear polysaccharide chains. The retardation of birefringence was 20—30 nm. The border of damaged and non-damaged region presented an increased topo-optical reaction (Fig. 2). The retardation of the birefringence was 30—40 nm. The polarization colour was green. The glycogen had granulated birefringence with red polarization colour. Glycogen granules were rendered strongly basophilic and slightly methachromatic due to the ABT reaction. The retardation of birefringence was 5—10 nm.

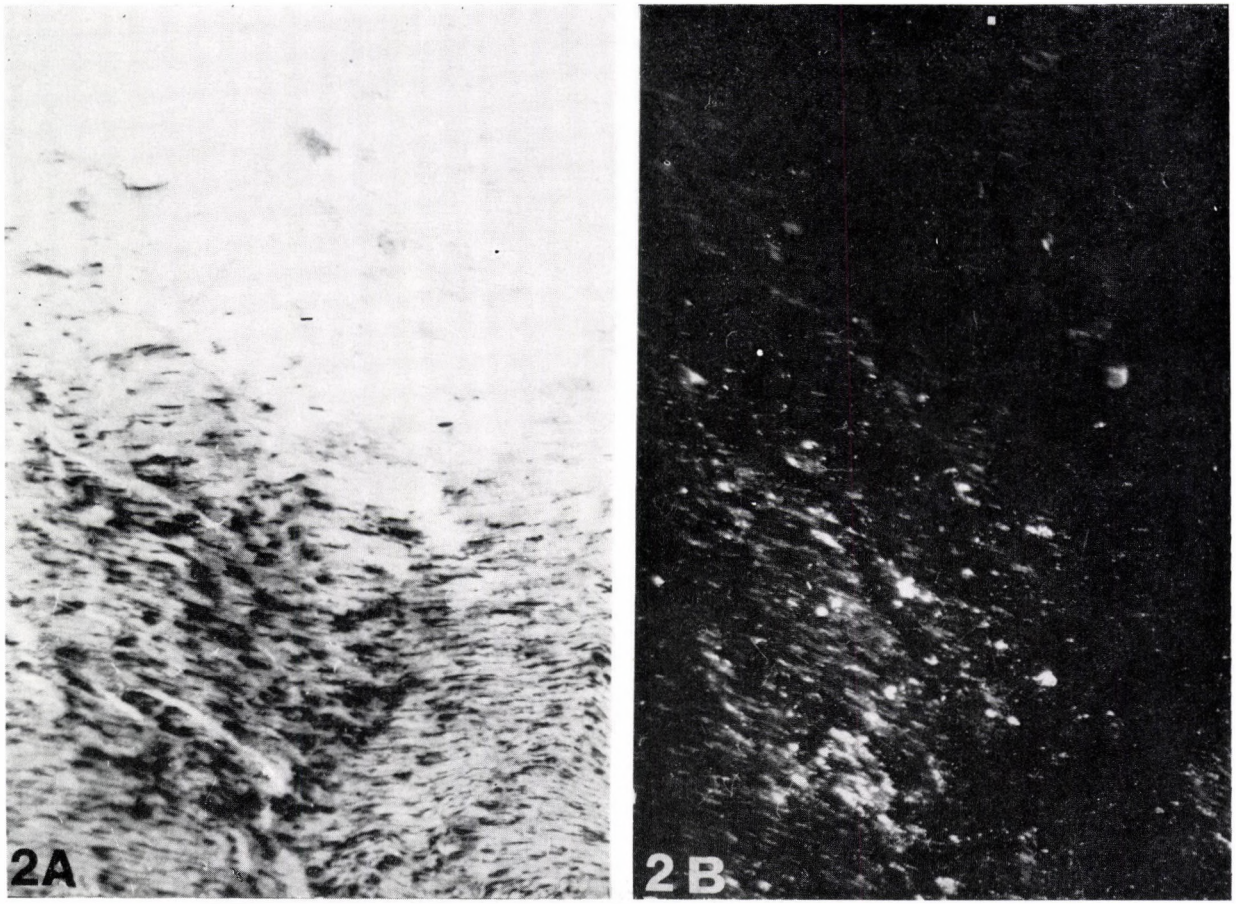

Fig. 2. K-strophantoside administration intravenously in doses of 50 μg/kg after LAD occlusion. Light microscopic (A) and polarization microscopic (B) pictures of the same preparations. The arrows show the border of the damaged myocardial area with increased binding of cardiac glycoside and deficiency of binding on the coronary vessels. ABT reaction (240×, 240×)

II. Thermographic investigations

Haemodynamic behaviour of these preparations was similar to that of the former group. The most typical thermographic pattern induced by two subsequent intravenous doses of K-strophantoside in the ischaemic heart is shown in Fig. 3. Before coronary occlusion, heat emission from the epicardial surface displayed a remarkable homogeneity (A). Occlusion of the LAD artery with a snare produced a rapid local temperature decrease which appeared to be fairly stable after 5 min (B). However, although at a much slower rate, heat irradiation from the ischaemic area continued to fall for the whole 60 min observation period (C). This type of reaction of the thermographic demarcation of the ischaemic damage was noted by Papp et al. [19], and will be referred to as such in this paper. K-strophantoside given intravenously in two subsequent doses (D, E) elicited considerable dose-dependent decreases of subepicardial temperature, a spreading image of the localized cooling in the ischaemic region, and an appreciable sharpening of temperature-gradient between the intact and affected areas, i.e. a further demarcation of the ischaemic damage. Moreover, after the larger glycoside dose (50 μg/kg) there appeared a still cooler centre inside the injured zone. This phenomenon was coupled with the generalized shift to the cooler range of the whole cardiac image, i.e. a restricted heat emission from the unaffected part, too.

In some respect this dramatic demarcation is in contrast to what has been observed in experiments illustrating thermographic signs of flow compensation (Fig. 4). The latter type of reaction is characteristic of the abundance of the performed collateral coronary network possessing a good fluid-carrying capacity. According to the observations of Papp et al. [19], in the compensatory types of ischaemic events the thermographic image of the damaged zone is much smaller then the size of the vascular area that the heart is deprived of by occlusion (compare B—E and F in Fig. 4). As shown in Fig. 4, the homogeneous thermographic pattern of the left ventricle supplied by the LAD artery (A) tends to exhibit a characteristic mixed pattern of cool and warm islets after LAD occlusion (B). The effective, averaged cooling is much smaller than in Fig. 3. Even after a 60 min observation the affected myocardial tissue appears to be divided into distinct warmer and cooler sub-areas within the jeopardized zone (C) and did not exhibit any sign of the demarcation of the imminent „infarct". Thus, the history of ischaemic events was dissimilar to that of the preceding heart. Nevertheless, K-strophantoside evoked an appreciable cooling not only in major segments of the affected area, too (E). At the same time, the size of the coolest spots inside the ischaemic zones diminished, i.e. inhomogeneity of the affected parts became less apparent. This indicated the partial cessation of the compensatory tendency of the vaso-

dilation within the ischaemic zone and of the adaptive reactions within the intact zone supplying the collaterals.

Figure 5 depicts the characteristic thermographic image produced by close arterial injection of K-strophantoside. Sudden, direct contact of the coronary vessel wall with the glycoside resulted in a substantial cooling in the

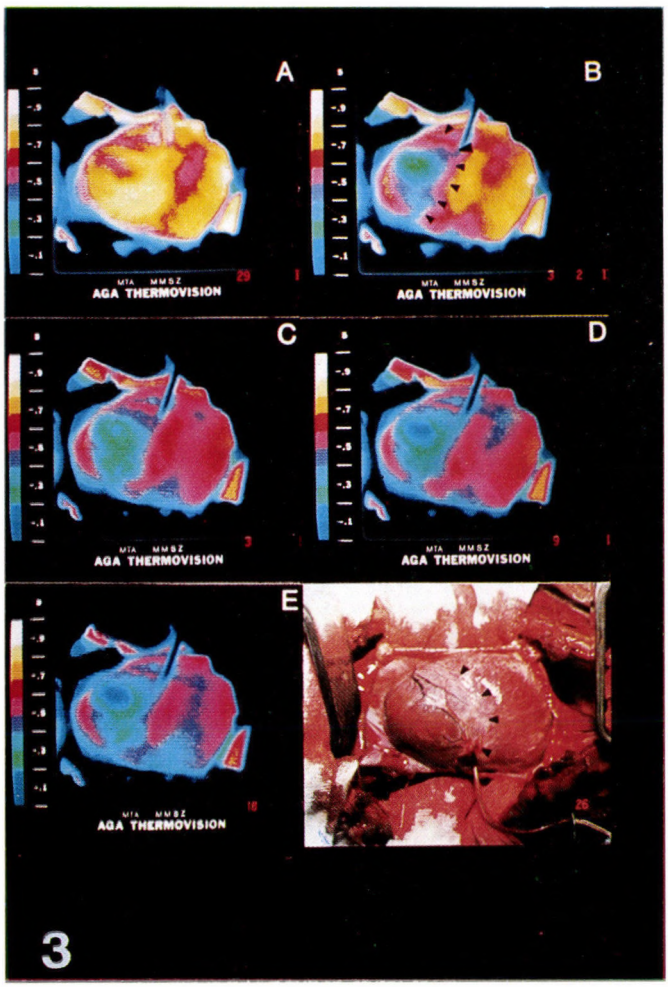

Fig. 3. Accentuated thermographic demarcation of ischaemic cooling after K-strophantoside. Original thermograms. The colour-scale in each thermogram (left) shows 0.5 °C temperature steps (from above downwards: cooling). Borders of the myocardial area supplied by the occluded LAD artery are indicated by arrow-heads (upper right thermogram) as compared to normal photo (lower right insert). The largest arrow-head denotes the point of occlusion. Note the mirror image of the heart in the thermograms (left and right sides are reversed). Characteristic phases of the experiment (mean arterial pressure, mmHg, in parentheses): (A) control (95), (B) 5 min after LAD occlusion (90), (C) 60 min after LAD occlusion (86), (D) after the first dose of 25 μg/kg K-strophantoside (97), (E) after the second dose of 25 μg/kg K-strophantoside (100)

affected area, but not in the heart muscle supplied by other coronary branches. Since this form of selective thermographic reaction was qualitatively similar to reactions elicited by intravenous injections of the drug in the normal heart, the observations indicated the direct vascular character of thermographic actions obtained with latter way of drug administration.

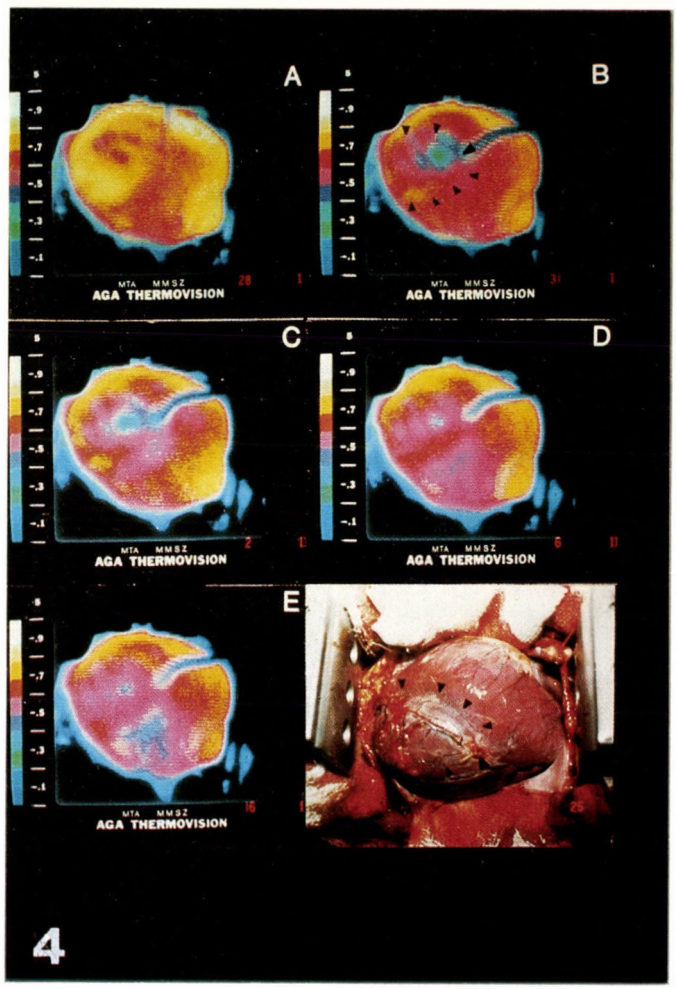

Fig. 4. Thermographic features of K-strophantoside administration in moderate ischaemic cooling. Note the effective cooling is much smaller than size of the affected area, and that cooling is not progressive (compare (B) and (C). Same arrangement as in Fig. 3. (A) (12), (B) (116), (C) (122), (D) (132), (E) (135)

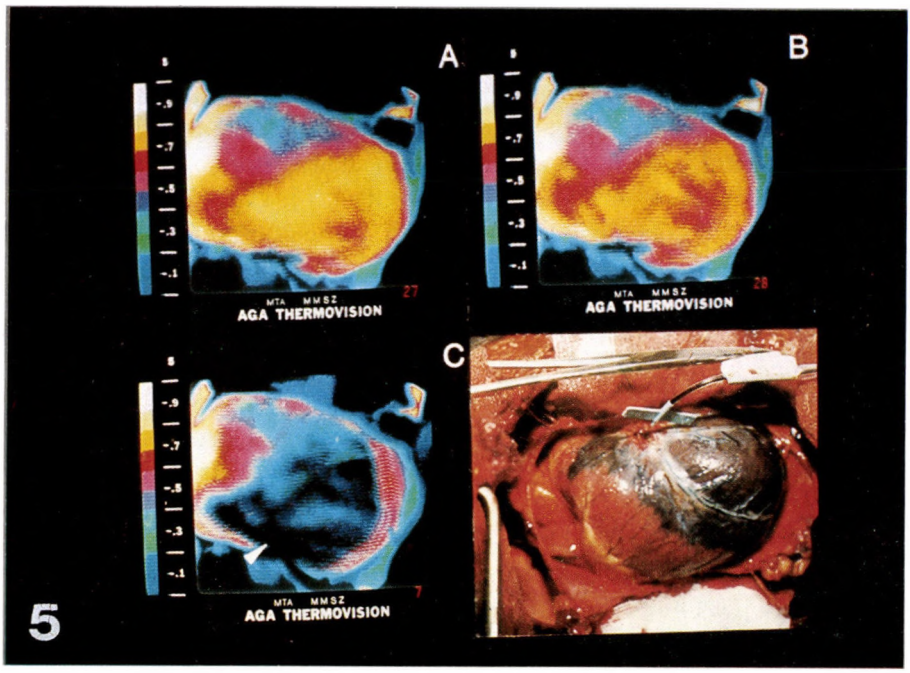

Fig. 5. Effect of intracoronary K-strophantoside (20 μg) in the non-ischaemic heart. (A) control (95 mmHg), (B) glycoside-induced rapid cooling of the left ventricle (20 s), (C) thermogram taken after injection of ice-cool methylene-blue into the LAD (white arrow-head indicates the point of the "winged" needles inserted into the artery), (D) normal photo of the intervention depicted in (C). Note the sharp boundaries of the stained area

Discussion

The direct coronary vasoconstrictor effect of cardiac glycosides was postulated as early as 1913 by Voegtlin and Macht who reported vigorous smooth muscle contractions when several digitalis preparations were added to the bathing medium of isolated coronary strips. Since that time, the possible augmentation by digitalis and ouabain of the coronary vascular tone has been the subject of numerous investigations on the *in situ* coronaries. [3, 4, 5, 6, 7, 8, 15, 25, 26, 32, 33, 36]. In spite of the fact that most studies implicated an (unfavourable) reduction in the myocardial blood flow atfer the administration of cardiac glycosides, especially when these drugs were applied at higher doses, the direct coronary action has often been neglected as compared to the well known arrhythmogenic effect. Since many cardiac disease patients, including those suffering from coronary heart disease, receive an overdosed cardiac glycoside therapy, the toxicological aspects of the drug actions on myocardial blood supply also have a potential clinical significance. When

studying post-mortem signs of digitalis toxicity in humans, a surprising degree of digitalis binding to the coronary vessel wall has been documented [29, 30]. This morphological observation, which became available with the adaptation of Romhányi's topo-optical method for detecting cardiac glycosides [27], stimulated research aimed at elucidating related physiological phenomena supposed to be involved in coronary reactivity [26]. The results suggested a strong functional antagonism between the vasomotor actions induced by cardiac glycosides and transmitters of metabolic adaptation (adenine nucleosides) under *in vivo* conditions, thus indicating probable correlations between glycoside uptake and autoregulatory impairment of the coronary smooth muscle on one hand, and contribution of blood flow reduction to the toxicological manifestations in myocardial ischaemia, on the other.

The blood flow reduction in the myocardium after occlusion of a major coronary branch is never complete because subepicardial collateral connections, which are particularly abundant in the dog heart, ensure about one-third to one-half of the average level of resting blood supply to the outer and middle layers of the heart muscle [10, 23]. In the subendocardium the situation is less favourable [24], but even in this layer the collateral flow far exceeds zero. Through the collateral network practically any regional pharmacological influence by systemic drug administration is possible, although at a reduced local delivery. At the same time, both the binding to and the elimination from membrane receptors of the cardiac glycosides are modified by myocardial ischaemia [1, 9, 11, 12]. The equilibrum of all these factors: reduced drug delivery, modified uptake, and hindered washout characteristics is reflected evidently by the present findings obtained with the ABT technique which showed characteristic change in glycoside binding induced by myocardial ischaemia. The ABT topo-optical reaction elaborated by Romhányi et al. [22] and widely applied in polarization microscopy has opened new scopes in polysaccharide research. The reaction mechanism is well known. During ABT-reaction the vicinal OH groups are transformed into dialdehydes by periodic acid then transformed into negatively charged groups by the bisulphite addition reaction. In this way they are rendered capable of binding toluidine blue at pH 1.0. which results in strong metachromatic basophilia and birefringence. The reaction offer information about their order in different biological structures. The ABT topo-optical reaction [22] is suitable for molecular analysis and localization of cardiac glycoside [14, 28, 29, 30]. The sugar component of cardiac glycoside has an expressed basophilia and methachromasia. The birefringence was strong. The negative birefringence points to vertical oriented toluidine blue and to linear polysaccharide chains. The green colour of polarization points to a high orientation of dye molecules. Myocardial ischemia produced by the ligation of branch of the coronary artery caused a significant decrease of the cardiac glycoside binding. The ABT-reaction was

negative or strongly reduced in basophilia and birefringence on the other hand. The binding of cardiac glycoside increased on the border of normal and hypoxic damaged cells. The ABT reaction presented a higher birefringence and basophilia of the sarcolemma membrane and small vessels than the control territory.

In the present study the functional significance of the cardiac glycoside binding to the coronary wall was assessed by infrared thermography. The results confirm earlier investigations which have indicated the sensitivity and reliability of this method for studying not only gross anatomical defects in myocardial blood supply, but much subtler functional alterations, such as drug actions, too. [18, 19, 20]. Changes of heat radiation from the surface of the exposed heart reflect essentially changes in blood flow. The efforts of Papp and his co-workers interpreting cardiac thermographic alterations in the terms of blood supply proved to be extremely successful [17, 20]. They have shown that rapid warming and cooling on the heart surface are quantitatively correlated with increased and decreased blood flow rates, respectively. The cardiac calorigenic action of interventions were found to be only secondary and protracted in this respect. This explains the seemingly paradoxial situation that *increased* heart activity after strophantine administration was found to be associated with the *decrease* of heat irradiation of the epicardial surface. Evidently, the reduced blood flow and not the enhanced metabolic rate was the predominant factor in the thermographic response. Considering the vascular regulatory aspects of the phenomenon, it seems likely that secondary metabolic stimuli affecting the coronary vessels may not have been great enough to mask the glycoside-induced direct smooth muscle contraction. Since thermographic signs of coronary vasoconstriction occurred in spite of a concomitant hypertension which, otherwise, would tend to increase flow both by the increased driving pressure across the coronary bed and the augmented O_2 demand of the heart muscle, the results are likely to underestimate the actual vasoconstrictor potency of cardiac glycosides. It is assumed that this potency serves as a basis for the actions seen in myocardial zones subjected to ischaemia.

In acute regional myocardial ischaemia a maximally or nearly maximally dilated (low-resistance) vascular bed is known to be connected distal to the occluded branch with intact (thus ischaemically unaffected) remote coronary segments via relatively high-resistance collaterals which preserve possibly their vasomotor activity. These latter channels bordering upon arterial segments, ischaemic in the proper sense, may rightly be considered, therefore, the strategic place of drug actions. The high affinity of strophantoside to the border zones supplying these channels as shown by the topo-optical reaction, explains the unequivocal flow decrease, in general, within the ischaemic area itself. Since strophantoside binding to the core of the ischaemic area was found

to be greatly reduced (or even negligable) in our study, the direct vasoconstrictor action of glycosides inside the central infarct seems less probable. However, even the latter possibility cannot be *a priori* excluded because ischaemically altered vessels also may exhibit reversely altered functional sensitivity parallel with their diminished binding capacity.

According to the differing course of the ischaemic events thermographic responses of a similar general character but differing qualitatively from each other were found in these experiments. For explaining different thermographic features, important corroboration comes from the pioneer work of Papp and his co-workers who described, in terms of quantitative thermography, two basic types of acute regional myocardial ischaemia in the dog heart [19]. In one of these types, characterized by an early demarcation, the combination of an underdeveloped collateral network with an augmented sensitivity to (unknown) "natural" vasoconstrictor stimuli can be postulated — albeit even this unfavourable situation can be influenced favourably by experimental interventions [18]. It was this type of the experimental infarct where the most pronounced and uniform vasoconstrictor effect of strophantoside was observed (Fig. 2). In the other type of Fig. 1, compensatory tendencies that diminish the ischaemic damage are reportedly prevailing [19]. Cardiac glycoside actions which seem less spectacular in the latter type of ischaemia are explained possibly by the same circumstances which determine flow inhomogeinity in this particular situation. Since the distribution of ischaemic (collateral) blood supply depends upon the actual vascular resistance changes very close to the ischaemic core itself and the steepness of the intracoronary pressure drop occurring from the intact parts of the myocardial circulation to the centre of the ischaemic area, moderate vasoconstrictor effects that influence both factors simultaneously, may decrease (a), equalize (b), or increase (c) the heat emission from a given smaller spot subserving to the affected area as a whole. In other words, the *relation*, of the effective local driving pressure to the localized vasoconstrictor effect and not simply the development of the latter phenomenon is the determining factor concerning subtle elements of the thermographic pattern. At the same time, albeit the situation necessitates an appropriate caution in evaluating sophisticated details, the main finding (i.e. the generalized cooling) validitated the inherent vasoconstrictor potency of cardiac glycosides.

Our present findings may have some possible clinical importance: It is obviously hazardous to administer digitalis preparations to seriously ill coronary disease patients, although as shown by the above considerations when these drugs are given in moderate doses, consequent to a milder degree of vasoconstriction the appearance or the disappearance of coronary steal phenomena may occur with equal possibility. Nevertheless, flow reductions, however slight, may precipitate ischaemic damage leading to the death of cells with a

delicate metabolic balance as well as to ectopic beats and/or intractable arrhythmias in highlight zones. These effects may contribute to an increased digitalis-induced mortality among infarcted patients — a controversial subject of violent discussions in the recent cardiological literature [2, 13, 32, 35].

Acknowledgement

We thank Dr. A. Juhász-Nagy (Clinic of Cardiovascular Surgery Semmelweis Univ Med. School) for his expert advice concerning pathophysiological interpretation of the results

REFERENCES

1. Beller GA, Conroy J, Smith TW: Ischaemia-induced alterations in myocardial (Na^+-K^+)-ATPase and cardiac glycoside binding. J Clin Invest 57: 341, 1976
2. Bigger JT, Fleiss JL, Rolniczky LM, Merab JP, Ferrick KJ: Effect of digitalis treatment on survival after acute myocardial infarction? Am J Cardiol 55: 623, 1985
3. Bloor CM, Walker DE, Pensinger RP: Ouabain induced primary vasoconstriction. Proc Soc Exp Biol Med 140: 1409, 1972
4. Dearing WH, Essex HE, Herrick JF, Barnes AR: Experiments with calculated therapeutic and toxic doses of digitalis. III. Effect on coronary blood flow. Am Heart J 25: 719, 1943
5. Gilbert NS, Fem GK: Effect of digitalis on the coronary flow. Arch Intern Med 50: 668, 1932
6. Ginsberg AM, Stoland OO, Siler KA: Studies on coronary circulation VI. The effect of some members of the digitalis group on the coronary circulation. Am Heart J 16: 663, 1938
7. Gross GJ, Waltier DC, Hardman HF, Somani P: The effect of ouabain on nutritional circulation and regional myocardial blood flow. Am Heart J 93: 487, 1977
8. Hamlin NP, Willerson JT, Garan H, Powell WJ Jr: The neurogenic vasoconstrictor effect of digitalis on coronary vascular resistance. J Clin Invest 53: 288, 1974
9. Hopkins BE, Taylor RR: Digoxin distribution in the dog's left ventricle in the presence of coronary artery ligation. J Mol Cell Cardiol 5: 197, 1973
10. Juhász-Nagy A, Szentiványi M, Grosz G: Effect of adrenergic activation on collateral coronary blood flow. Jpn Heart J 15: 290, 1974
11. Ku DD: Subcellular (^3H) Digoxin distribution after temporary myocardial ischaemia in dogs. Eur J Pharmacol 88: 329, 1983
12. Maclean D, Davis MA, Maroko PR: Influence of coronary artery occlusion on the myocardial distribution of digoxin. Am J Cardiol 39: 279, 1977
13. Moss AJ, Davis HT, Conrad DL, De Camilla JJ, Odoroff CL: Digitalis associated cardiac mortality after myocardial infarction. Circulation 65: 1150, 1981
14. Németh Á, Bayer E, Sótonyi P, Fischer J: Cytochemical demonstration of cardiac glycosides in the heart muscle tissue using lectins and ABT reaction. Lectins 4: 109, 1985
15. Page RG, Foltz EL, Sheldon WF, Wendel H: Effect of ouabain on the coronary circulation and other circulatory functions in intact anesthetized dogs. J Pharmacol Exp Ther 101: 112, 1951
16. Papp L: Significance of thermography in heart surgical research. In: Szabó Z (ed): Current Problems of Cardiovascular Surgery: A Scientific Approach. Akadémiai Kiadó, Budapest, 1986a p. 29.
17. Papp L, Álló G, Kékesi V, Juhász-Nagy A: Correlation between coronary flow and epicardial temperature determined by quantitative infra-red thermography. IRCS Med Sci: 13: 621, 1985c
18. Papp L, Álló G, Kékesi V, Szabó Z, Juhász-Nagy A: Computer-aided thermographic evaluation of disturbance of the coronary adaptive reserve: An experimental study. Acta Morph Hung 33: 179, 1985b
19. Papp L, Álló G, Szabó Z, Juhász-Nagy A: Natural history of acute regional myocardial ischaemia revealed by infra-red thermography in the canine heart. Acta Morph Hung 33: 123, 1985a

20. Papp L, Kékesi V, Osváth B, Juhász-Nagy A, Szabó Z: The effect of pressure controlled intermittent coronary sinus occlusion during reperfusion. In: Mohl W, Faxon D, Wolner E (eds): Clinics of Coronary Sinus Interventions, Steinkopff, Darmstadt, 1986 b p. 399.
21. Papp L, Mezei B, Osváth B, Szabó Z: Thermography in artificially induced coronary circulatory disorders. Acta Chirurg Hung 23: 75, 1982
22. Romhányi Gy, Deák Gy, Fischer J: Aldehyde-bisulphite-toluidine blue (ABT) staining as a topooptical reaction for demonstration of linear order of vicinal OH groups in biological structures. Histochemistry 43: 333, 1975
23. Schaper W: The Collateral Circulation of the Heart. North Holland, Amsterdam 1971
24. Schaper W, Pasyk S: Influence of collateral flow on the ischaemic tolarence of the heart following acute and subacute coronary occlusion. Circulation 53: Suppl I, 57, 1976
25. Somberg JC, Kuhlman JE, Smith TW: Localization of the neurally mediated coronary vasoconstrictor properties of digitalis in the cat. Circ Res 49: 226, 1981
26. Sótonyi P, Juhász-Nagy A: Effect of cardiac glycosides on the coronaries: Physiologic and morphologic studies in the dog heart. Acta Physiol Hung 63: 153, 1984
27. Sótonyi P, Somogyi E, Romhányi Gy: Comparative electron microscopical and polarization optical investigation of myocardial digitalis localization. Elektronmikroskopie. Leipzig, Vol. I: 1981, p. 25.
28. Sótonyi P, Somogyi E, Oberna M, Kerényi NA: Electron cytochemical investigation of acute digitalis intoxication of heart muscle. Acta Med Leg (Liege) 32: 421—426, 1982
29. Sótonyi P, Somogyi E: Cytochemical demonstration of the molecular forms of cardiac glycosides in the heart muscle. Acta Histochem 72: 117—122, 1983a
30. Sótonyi P, Somogyi E: Comparative topooptical investigation of cardiac glycoside localization. J Leg Med 90: 87—94, 1983b
31. Tanz RD: Possible contribution of digitalis-induced coronary constriction to toxicity. Am Heart J 111: 812, 1986
32. Tanz RD, Fairfax CA: Insurmountable antagonism of ouabain induced coronary constriction by prazosin. Eur J Pharmacol 112: 111, 1985
33. Vatner SF, Higgins CB, Franklin D, Braunwald E: Effect of a digitalis glycoside on coronary and systemic dynamics in conscious dogs. Circ Res 28: 471, 1971
34. Voegtlin C, Macht DI: The action of nitrites and drugs of the digitalis group on the isolated coronary artery. J Pharmacol Exp Ther 5: 77, 1913
35. Yusuf S, Wittes J, Bailey K, Furberg C: Digitalis a new controversy regarding an old drug. Circulation 73: 14, 1986
36. Zimpfer M, Schutz W, Raberger G: Haemodynamics and coronary actions of ouabain during coronary infusion. Naunyn-Schmiedebergs Arch Pharmacol 229: 61, 1977

Acta Morphologica Hungarica, 35 (3—4), pp. 105—110 (1987)

LOCALIZATION OF AMINO ACID HORMONES (ADRENALIN, SEROTONIN, HISTAMINE AND A HORMONE PRECURSOR (5-HYDROXYTRYPTOPHANE) IN ASCIDIA CELLS

F. SUDÁR, G. CSABA

DEPARTMENT OF BIOLOGY, SEMMELWEIS UNIVERSITY OF MEDICINE, BUDAPEST, HUNGARY

(Received 22 May 1986)

All tritiated amino acid hormones added to the maintenance medium of *Ascidia mentulosa* entered the cells of the coat and gut, and all appeared in intranuclear localizations. The quantitative differences in incorporation did not indicate a specific affinity for any hormone tested.

Keywords: Ascidia, amino acid hormones, internalization, nuclear localization

Although formerly only the steroid hormones had been believed to penetrate across the cell membrane, recently evidence has been presented on the internalization of polypeptide hormones, and even on their binding to the nuclear membrane [7, 8, 10—13]. Amino acid hormones have also been shown to enter not only the cytoplasm, but also the nucleus of the cells of higher vertebrates [1, 2, 3, 14] and of the unicellular Tetrahymena as well [4, 5, 6]. Since previous studies into the internalization of amino acid hormones had been performed mainly on independent cells or unicellular organisms (Tetrahymena), we investigated the intracellular localization of such hormones inside cells belonging to coherent populations at a low level of phylogenesis, to obtain information on possible quantitative differences between the incorporation of different amino acid hormones, or of a single hormone and its precursor.

Materials and methods

Experiments were performed on *Ascidia mentulosa* (Urochordata, Tunicata). From the medium region of the body of Ascidia an about 1 cm wide segment was excised; this transversal section contained details of the gut, coat and tunica. The excised specimen was placed in 5 ml seawater, to which 20 μCi/ml ^{3}H-adrenalin (10.8 Ci/mmol), ^{3}H-histamine (8.0 Ci/mmol), ^{3}H-serotonin (8.2 Ci/mmol) or ^{3}H-5-hydroxytryptophane (9.0 Ci/mmol) was added. All radiolabeled hormones were products of the Amersham Ltd. (England). Incubation in presence of the hormones lasted 30 min, and was followed by three washes in seawater. The specimens were fixed in Karnovsky's solution for 2 h, post-fixed in 1 per cent OsO_4-solution for 1 h, and

Send offprint requests to G. Csaba, Dept. of Biology, Semmelweis University of Medicine, 1445 Budapest, P.O.B. 370, Hungary

were embedded in Spurr's resin. The sections were coated with Ilford L4 emulsion, and were developed in Microdol X after an exposure time of 12—16 weeks. Finally, preparations were counter-stained with uranyl acetate and lead citrate and examined under a Philips 300 electron microscope. Grain counting was performed in electron micrographs.

Results and discussion

All amino acid hormones tested entered the cells of the coat and the gut. Grains also appeared above the cellular nuclei, although in different numbers depending on the hormone used (Figs 1—4).

The highest amount was incorporated of histamine (Fig. 2a, b). The grains were readily observed over the microvilli of the lining cells of the gut, inside the cells, and above the nuclei of the cells forming the gut wall. Many grains could also be seen over the cells of the coat and their nuclei.

Grain counts were considerably lower over the cells exposed to adrenalin, but the label appeared above both cytoplasm and nucleus of the coat and gut cells.

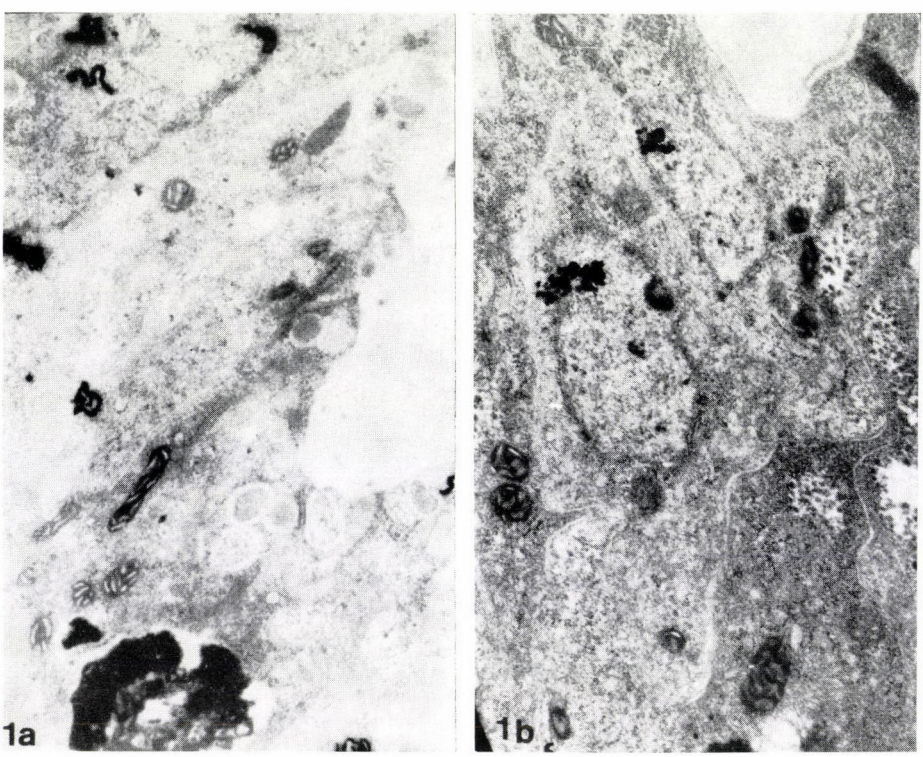

Fig. 1. Localization of ^{3}H-adrenalin induced silver grains over the cell membrane, inside the cytoplasm (a), above the nuclear membrane and inside the nucleus (b). (a) ×12 900; (b) × 19000

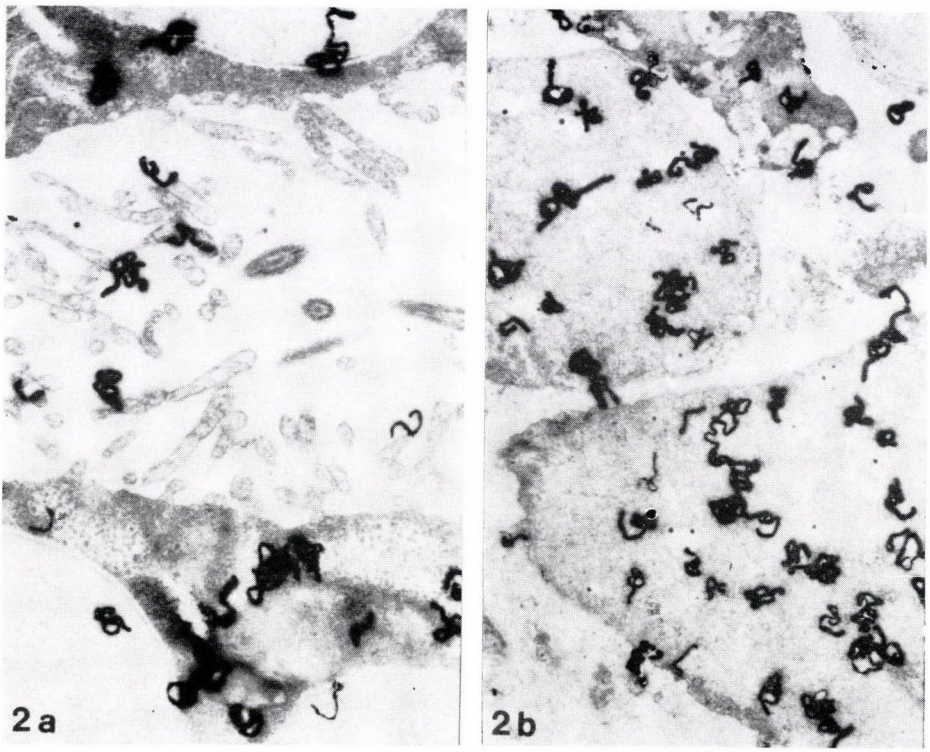

Fig. 2. ^{3}H-histamine incorporation is indicated by presence of many grains on the membrane process (a) and over the nucleus (b). (a) ×12 900; (b) × 10 000

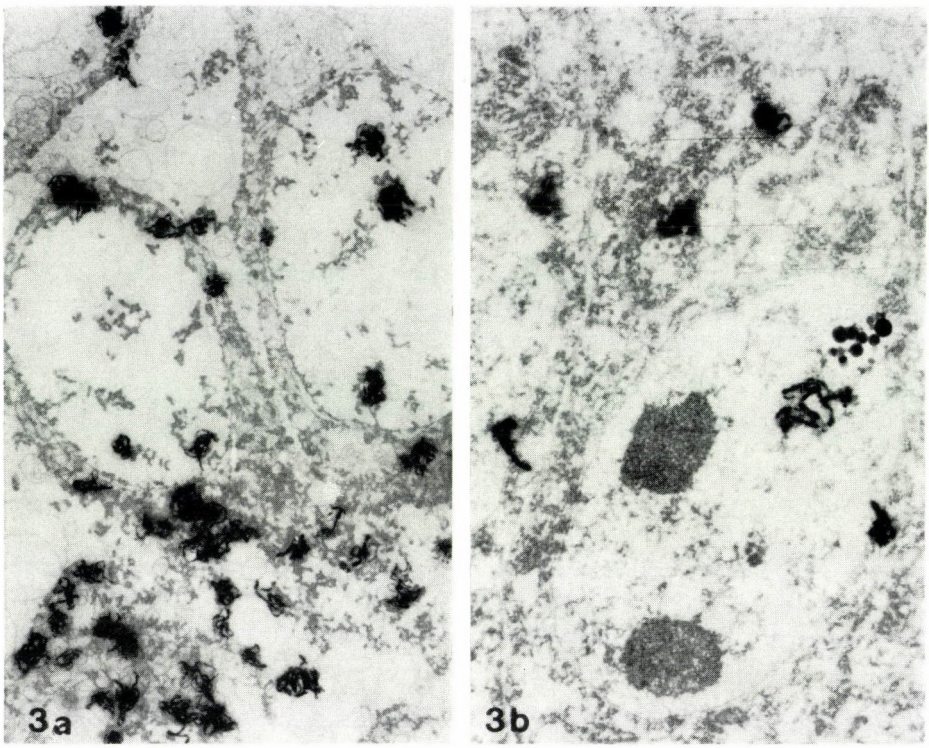

Fig. 3. The grains indicating incorporation of ^{3}H-serotonin can be seen over the membranes of vesicles and inside the cellular nuclei (a), as well as over the nuclear membrane and the euchromatic regions (b). (a) × 12 900; (b) × 16 300

The grains indicating incorporation of serotonin appeared above the microvilli and cilia of the coat, and above the cells of the coat and gut (Fig. 3a, b). A similar pattern of labeling was observed with 5-HTP (Fig. 4a, b).

Grain counts found in the specimens exposed to the different labeled hormones are shown in Fig. 5.

Results suggest that, although in different quantities, all hormones entered the cells and the cell nuclei. The highest affinity to the nucleus was shown by histamine. It is known that at the low levels of evolution, the cells possess amino acid receptors which serve according to the observations of Lenhoff [9], as precursors of the future hormone receptors. This may explain the entry of the hormones tested into the cells, for amino acid hormones are able to bind to amino acid receptors. The entry of the hormones into the nucleus strongly suggests a gene level action, as has already been substantiated for the amino acid type vertebrate hormone thyroxine. The fact that also the precursors are able to enter the cell to the same extent as the finished hormone (5-HTP-5-HT) also suggests the involvement of amino acid receptors.

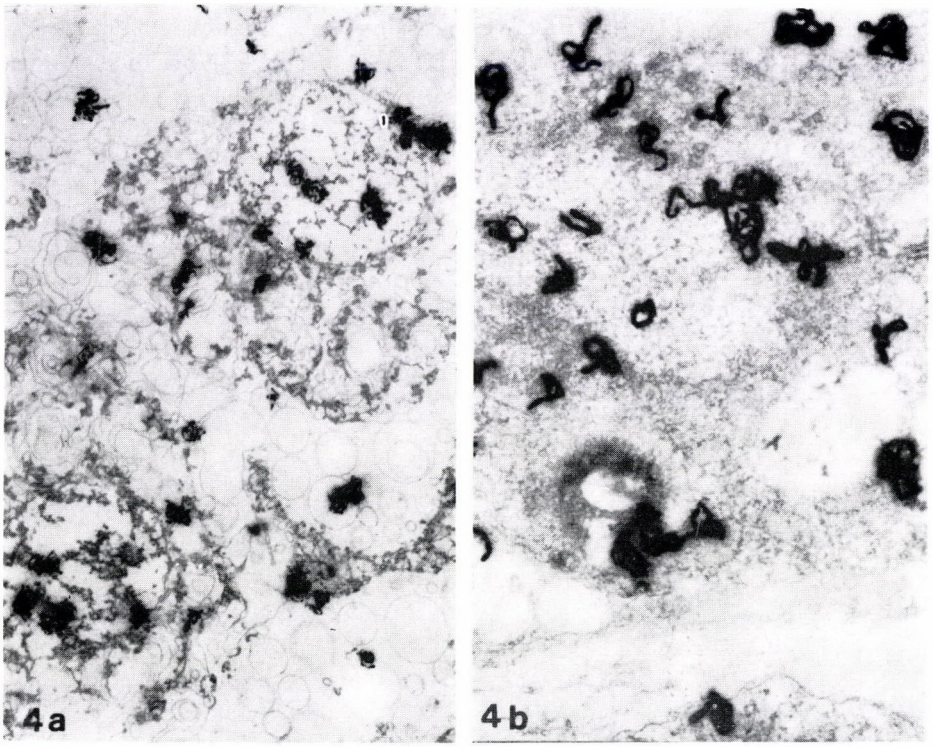

Fig. 4. Intra-cytoplasmic and intra-nuclear localization of ^{3}H-5-HTP. Grains are also present over the cytoplasmic and vesicular membranes (b). (a) ×10 050; (b) ×16 350

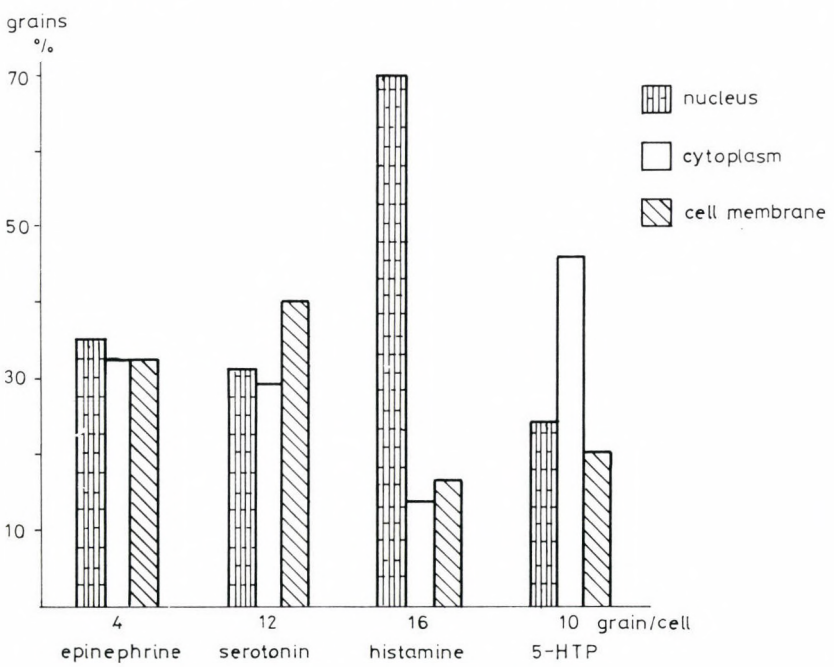

Fig. 5. Number and distribution of grains over cells

The grain counts established above the coat and gut cells did not appreciably differ during the period of study. It therefore seems highly possible that the cells of both tissues are capable of a direct incorporation of amino acid hormones, without mediation of the adjoining tissue.

REFERENCES

1. Csaba G, Sudár F, Dobozy O: Triiodothyronine reception in lymphocytes of newborn and adult rats. Horm Metab Res 9: 499, 1977
2. Csaba G, Sudár F: Localization of radioactively labelled serotonin in the nucleus of adrenal medulla cells. Acta Anat (Basel) 100: 237, 1978
3. Csaba G, Sudár F: Differentiation dependent alteration in lymphocytic triiodothyronine reception. Horm Metab Res 10: 365, 1978
4. Csaba G, Sudár F: Localization of ^{3}H-histamine in the nucleus of Tetrahymena. Acta Morph Hung 27: 89, 1979
5. Csaba G, Sudár F, Pados R: Binding and internalization of ^{3}H epinephrine in Tetrahymena. Endokrinologie 76: 340, 1980
6. Csaba G, Sudár F, Ubornyák L: Comparative study of the internalization and nuclear localization of amino acid type hormones in Tetrahymena and rat lymphocytes. Exp Clin Endocrinol 82: 61, 1983
7. Horvat A: Insulin binding sites on rat liver nuclear membranes: biochemical and immunofluorescent studies. J Cell Physiol 97: 37, 1978
8. Horvat A, Katsoyannis PG: Cellular binding sites for insulin in rat liver. Biochim Biophys Acta 382: 609, 1975
9. Lenhoff HM: Behavior, hormones and hydra. Science 161: 434, 1968
10. Pastan I, Willingham MC: Receptor mediated endocytosis: coates pits, receptosomes and the Golgi. TIBS 8: 250, 1983
11. Rao CV: Receptor for gonadotropins in human ovaries. In: Recent Advances in Fertility Research Part: A. Alan R Liss, New York, 1982 p. 123.
12. Rao CV, Chegini N: Nuclear receptor for gonadotropins and prostaglandins. In: Evolution of Hormone Receptor Systems. Alan R Liss, New York, 1983 p. 413.
13. Steinman RM, Mellmann WA, Cohn ZA: Endocytosis and the recycling of plasma membrane. J Cell Biol 96: 1, 1983
14. Sudár F, Csaba G: Localization of ^{3}H-serotonin in the adrenal medullary cells of newborn rats. Acta Morph Hung 27: 83, 1979

Acta Morphologica Hungarica, 35 (3—4), pp. 111—124 (1987)

MORPHOLOGICAL STUDIES ON THE ARTICULAR CARTILAGE OF OLD RATS

J. GYARMATI,** I. FÖLDES,** MÁRIA KERN,*** I. KISS*

*RADIOLOGICAL CLINIC, **DEPARTMENT OF ANATOMY, HISTOLOGY AND EMBRYOLOGY AND ***ORTHOPEDIC CLINIC, UNIVERSITY MEDICAL SCHOOL, DEBRECEN, HUNGARY

(Received 18 July 1986)

Age-dependent morphological alterations of the tibial articular cartilage were studied in 26-month-old Wistar rats of both sexes. Young and adult rats (6 and 10 months of age, respectively) served as a basis for comparison. Light microscopic histology, polarization optical analysis (toluidine-blue staining with or without the addition of 0.2, 0.4 or 0.8 M $MgCl_2$, as well as after phenol reaction) as well as transmission electron microscopy were applied. The main observations are: (1) According to the histological findings, the proportion of the zones changes with age; the subchondral bone layer becomes wider and separated to a certain extent, while the fibres become demasked. (2) Polarization microscopy revealed a disorientation of both the proteoglycane (PG) and collagen molecules; considering the available biochemical data, this phenomenon involves both quantitative and structural changes, as well as differences in the localization of the PG and collagen molecules. (3) Electron microscopy also supports the structural alterations of the collagen (thin and thick, as well as non-striated, fragmented fibres). Cellular alterations are also observed parallel with the changes of the matrix (cell organelles occur less frequently, signs of degeneration and disintegration, rupture of the plasma membrane, as well as accumulation of lipid-bodies can be seen [4]. On the basis of the findings, one can consider the articular cartilage in the old rats as a tissue which is still in equilibrium, however, aged chondrocytes with decreased function become predominant in it. This state can be modified into a pathological one by various mechanical, endocrinological, iatrogenic, post-traumatic, etc., influences through the alterations of the cell-matrix interactions.

Keywords: Glycosaminoglycan, collagen, polarizing and electron microscope

Introduction

The age-dependent alterations of the articular cartilage have been in the focus of interest since long time. A deeper knowledge in this respect would allow us to distinguish between the physiological or biological age-dependent alterations and the pathological, degenerative ones, i.e., a more safe functional basis would be available for a better understanding of the pathological processses of the articular cartilage [8]. Studies have been concentrated mostly to one of the main macromolecular components of the cartilage matrix, the proteoglycane (PG), and it has been established first of all by biochemical methods that the concentration and chemical structure of PG and glycosamino-

Send offprint requests to J. Gyarmati, Department of Anatomy, University Medical School, Debrecen, H-4012, Hungary

glycane (GAG) molecules becomes altered with advancing age [2, 7, 12, 23, 24, 30, 32, 36, 38, 43, 53]

The water content and the synthesis of collagen [53] as well as of DNA [4] also decrease with age. Relatively sporadic data are available as regards the age-dependent morphological alterations, and even the available ones describe only minor lesions [9, 54]. It is a valuable histochemical observation that the keratan-sulfate (KS) content increases with age; it is localized mainly in the territorial area above the 4th decade of age, whereas in the younger ages it is found mainly in the inter-territorial area [50]. Scanning electron microscopic studies also indicated changes in the cell to matrix and in the intra-matrix proportions [19, 29]. Electron microscopic data may serve for the cellular explanation of the observed alterations [5, 20, 41, 42].

Starting from the above situation, the present paper describes some microscopic morphological observations obtained in old rats by comparative studies. The polarization optical investigations allow us to reveal the structural alterations of the GAG and collagen molecules and to compare the latter with the EM results. We describe some recent morphological observations regarding the age-dependent cellular and matrix-alterations and their interrelationships.

Materials and methods

The studies were performed on 3 age groups of Wistar rats of both sexes: Young (10 rats), adult (7 rats) and old (10 animals) ones, 6, 10 and 26 months of age, respectively. All the rats were fed ad libitum with an identical standard food. They were killed by bleeding out. The tibia was removed from both sides for histological purposes. The bones were cut in proximal and distal halves, and then cut again in two parts along their longitudinal axis.

For light microscopic studies one half of the proximal tibia-part was fixed (and decalcified) in Susa solution, and embedded in paraffin. Sections of 5—7 μm were cut, stained with haematoxylin-chromotrope, Azan and Goldner methods.

For polarization optical studies the other half of the proximal tibia was fixed in a 1 : 4 mixture of formaldehyde and absolute ethanol, decalcified in a 1 : 1 mixture of formic acid and 70% ethanol, and embedded in paraffin. The following stainings were performed:

(a) 0.1% toluidine-blue at pH 3.5 according to Romhányi [37].

(b) 0.1% toluidine-blue at pH 3.5 in the presence of 0.2, 0.4 or 0.8 M $MgCl_2$, respectively, according to Scott and Dorling [39] and Módis [34], in order to reveal the sulfated GAG molecules.

(c) Phenol reaction according to Ebner [15] in order to reveal the collagen.

An external and internal zone can be distinguished in the articular cartilage according to the optical characteristics. The optical reactions were evaluated separately in these zones; optical path differences were measured by means of a Brace-Köhler compensator, i.e., the alterations could be described in quantitative terms. The data obtained are summarized in Tables I—III.

For electron microscopy, the articular cartilage of several tibias were excised, fixed in Karnovsky-fixative and embedded in Durcupan ACM. Sections were cut by using a diamond knife on a Reichert OmU 2 ultramicrotome, contrasted by uranyl-acetate and lead citrate. Micrographs were taken by a JEOL JEM 100B electron microscope.

It should be noted here that the young and adult animals served as controls; no differences were observed in these two age groups by either of the methods used.

Results

Light microscopy. The histological structure of the articular cartilage of the 26-month-old rats (Fig. 1) differs considerably from that of the younger animals (Fig. 2). The thickness of the cartilage did not decrease (or did only slightly), however, its structure changed. One can see fissures at the cartilage-bone border, almost parallel to the surface. The widened subchondral bone displays some trabecular microfractures (Fig. 1). The proportion of the zones of the cartilage surface changes, too: the superficial cellular layer became thinner considerably, and as a consequence, one encounters rounded, hypertrophic cells immediately below the surface. The cell sizes do not increase from the surface toward the subchondral zone, but are practically the same everywhere. One cannot see a true hypertrophic cell zone, and the cell to matrix proportion is shifted characteristically in favour of the latter. The fibres of the matrix became frequently visible, i.e., they are demasked.

Polarization microscopy. Aging causes a decrease in the path-difference after phenol reaction in the internal zone of the articular cartilage, whereas in the external zone these values are identical with those of the controls (Table I).

Table I

Optical path differences measured in polarizing microscope after phenol reaction in the zones of the articular cartilage of the tibia in Wistar rats

Group	External zone	Internal zone
26-month-old	27.50 ± 3.34	26.51 ± 7.57
Control	25.25 ± 4.54	38.62 ± 4.69

When applying toluidine-blue staining at pH 3.5, the path differences proved to be smaller in both layers of the cartilage, however, the extent of this decrease was larger in the external zone (Table II). If 0.2 M $MgCl_2$ was added to the toluidine blue, the path differences were equal in both layers to the control values; 0.4 M of this salt revealed identical path differences in the external layer of both young and old rats, and smaller ones in the internal

Table II

Optical path differences measured in polarizing microscope after toluidine-blue staining at pH 3.5 in the zones of the articular cartilage of the tibia in Wistar rats

Group	External zone	Internal zone
26-month-old	25.68 ± 3.28	32.14 ± 2.27
Control	39.40 ± 2.50	39.72 ± 3.40

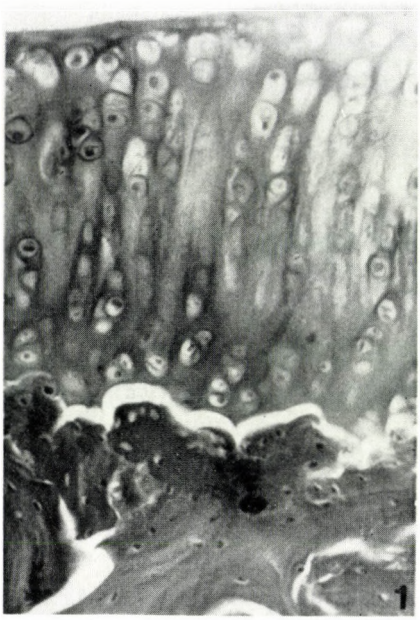

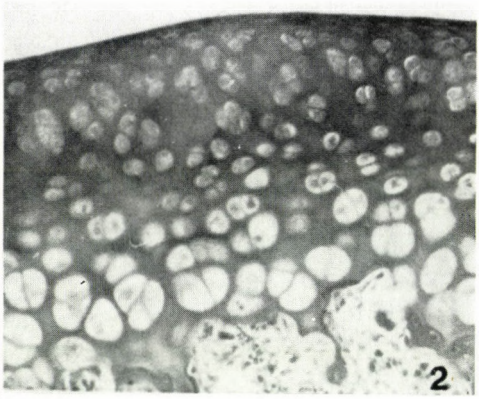

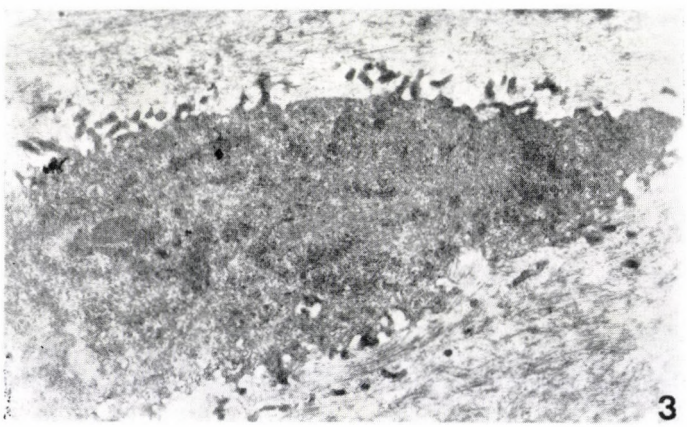

Fig. 1. Articular cartilage of tibia from a 26-month-old rat. One can see the altered proportions of the zones, the absence of hypertrophic cells and a well defined fissure between the cartilage and the subchondral bone. Haematoxylin-chromotrope staining. ×220

Fig. 2. Articular cartilage of tibia from a 10-month-old rat showing the regular pattern. Haematoxylin-chromotrope staining, ×220

Fig. 3. EM micrograph of a cell near to the surface which is poor in cell organelles. × 10 000

layer of the old animals. In case of the addition of 0.8 M $MgCl_2$, we observed larger path differences in the external layer of the old animals, whereas these values were considerably smaller in the internal layer as compared to the younger ages (Table III). These data indicate a lower degree of orientation of the collagen in the internal layer of the old cartilage, whereas this orienta-

Table III

Optical path differences measured in polarizing microscope after toluidine-blue staining at pH 3.5 in the presence of various $MgCl_2$ concentrations in the zones of the articular cartilage of the tibia in Wistar rats

Group	0.2 M $MgCl_2$		0.4 M $MgCl_2$		0.8 M $MgCl_2$	
	Ext.	Int.	Ext.	Int.	Ext.	Int.
26-month-old	31.53±2.23	31.64±2.67	25.96±4.05	23.66±2.44	16.80±2.84	12.74±1.46
Control	30.17±2.08	35.74±2.91	25.61±3.08	32.22±2.88	14.48±1.16	23.72±2.49

tion is maintained in the external layer (Table I). In the external zone of the cartilage, aging causes a decrease of the orientation of the GAG and a slight increase of the orientation of the keratan-sulfate molecules.

Electron microscopy. The electron microscopic structure of both the cells and the matrix of the old animals differs considerably in all zones from that of the younger rats. In the old rats, the cytoplasm of the cells having processes and laying near to the surface displays a higher density and is poorer in organelles; occasionally one can see some round-shaped, crysta-type mitochondria, the accumulation of a fibrous substance as well as tubular endoplasmic reticulum (ER) (Fig. 3).

More deeply below the surface one encounters rounded cells; their cytoplasm contains Golgi complex of lamellar structure, ER tubuli and lipid droplets (Fig. 4). In some cells lysosomes can be observed frequently (Fig. 5). Only few mitochondria with rare crystae can be observed.

The matrix is compact under the surface, rich in fibres. At several places one can see an amorphous substance of high electron density in the cell lacunae, which may represent the rest of a cellular necrobiosis (Fig. 6). In the central cellular zone one can encounter also apparently intact cartilage cells of medium secretory activity. These cells display an undulated nuclear membrane surface, the nuclei are rich in chromatin, their cytoplasm contains, apart from the ER tubules also cysternae of the rough surfaced ER (Fig. 7). The mitochondria are larger and of lower density in these cells, as well as poor in crystae.

The fibres of the matrix are of various diameters; apart from the thick, mature collagen fibres displaying the typical striated pattern, one can observe

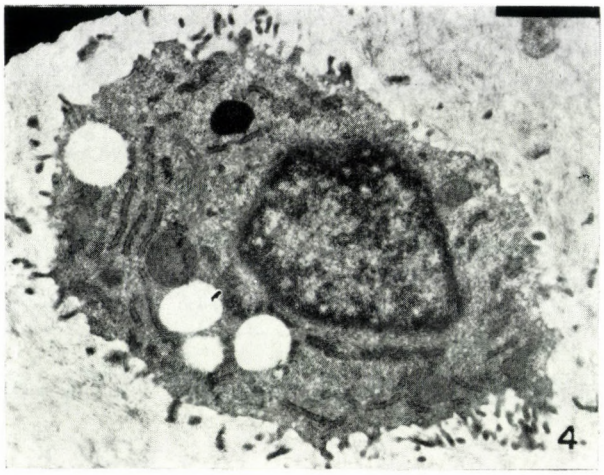

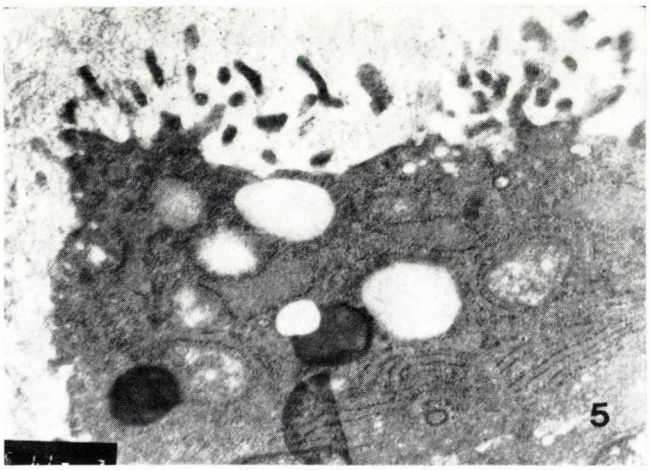

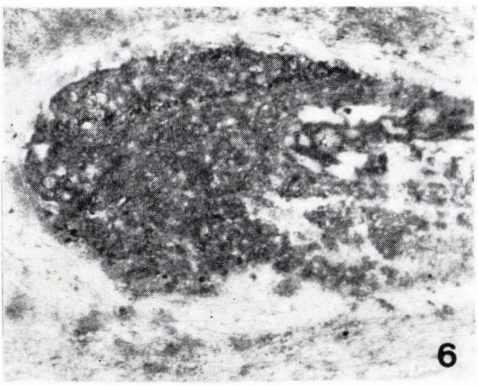

Fig. 4. EM micrograph of a cell containing large lipid droplets and flattened, lamellar form of the Golgi complex. × 10 000
Fig. 5. A cell which is more rich in lysosomes than usual. × 17 000
Fig. 6. A necrotic chondrocyte. × 6700

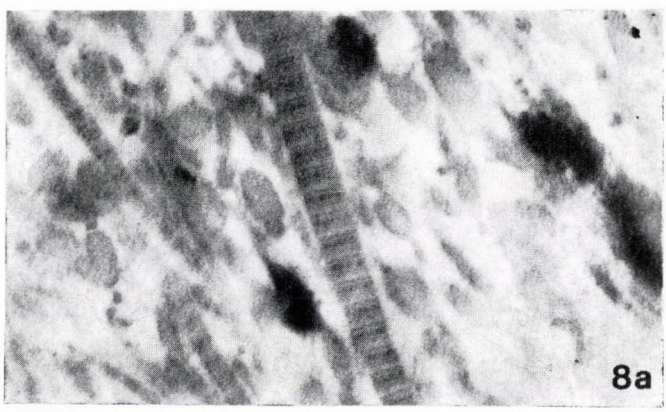

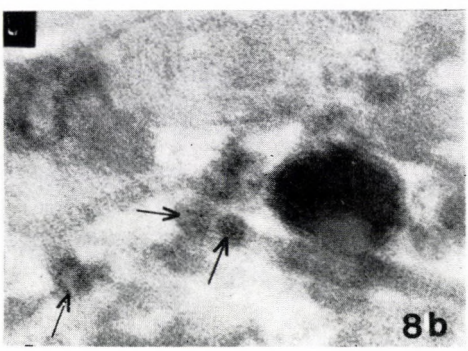

Fig. 7. ER cysternae and enlarged mitochondria in a cell of the middle zone. ×6700
Fig. 8a. Collagen fibres of various diameter and striation. ×50 000
Fig. 8b. Bonucci-granules (arrow) between collagen fibres. ×100 000

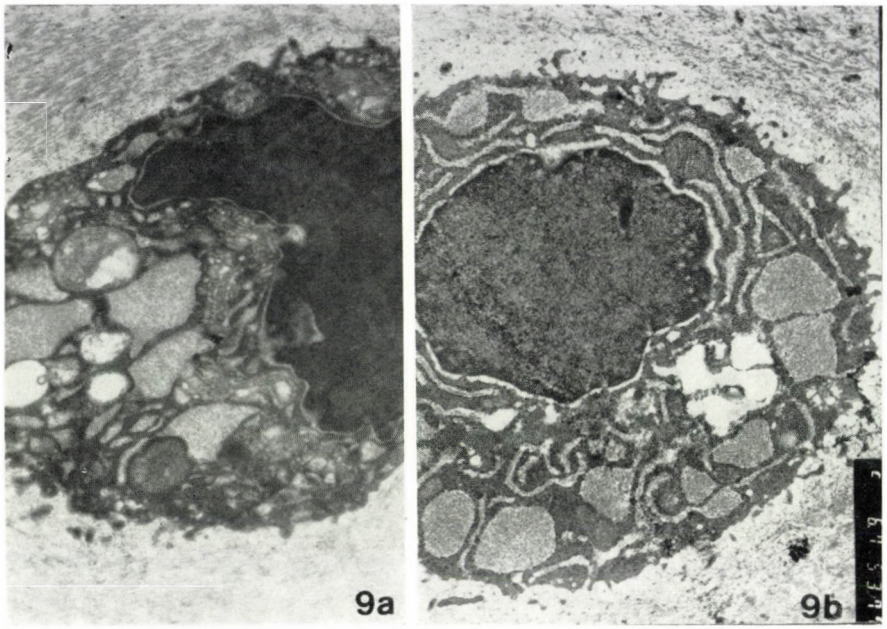

Figs. 9a and 9b. Degenerated cells in the internal zone with irregularly homogeneous cell nuclei, widened ER cysternae with a granular substance. ×6700
Fig. 10. Glycogen accumulation in the cell. ×20 000

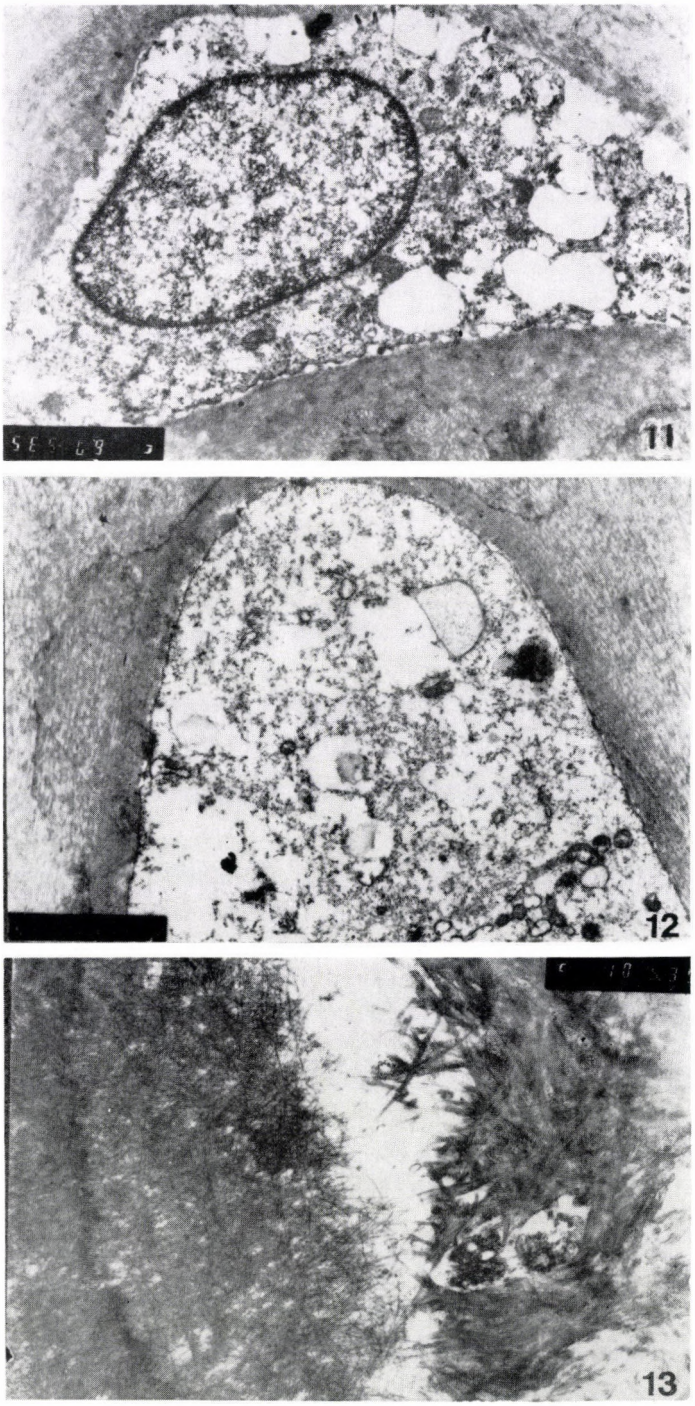

Fig. 11. A disintegrated, necrotic cell with small mitochondria and large lipid droplets. ×6700

Fig. 12. Some cell debris in an empty lacuna. ×3300

Fig. 13. Fissure at the cartilage-bone border with several connecting fibrils. ×10 000

numerous thinner fibres, too (Fig. 8a). The striated pattern disappeared at frequently occurring places, and one encounters also fragmentation of the fibres. When using higher magnifications, one can observe dense structure surrounded by a smooth membrane; these are the so-called Bonucci granules (Fig. 8b). Toward the subchondral zone, a significant portion of the hypertrophic chondrocytes display degenerative alterations; these occur also in the younger animals, however, the structural alterations are more frequent and more extensive in the old age. In some cells the nucleus becomes homogeneous, the density of the cytoplasm considerably increases, large vesicles appear which are filled in with a granular and/or fibrillar substance, and the ER cysternae are widened. The content of the latter is of lower density than the hyaloplasm itself (Figs. 9a and 9b).

One can observe even glycogen accumulation (Fig. 10). In addition, in the calcification zone some further disintegrating cells can be seen, which derive from the normal cells of the upper layer: the cell membrane is disrupted, the cytoplasm looses its characteristic structure, small, round mitochondria occur with ER tubuli and cysternae as well as with lipid droplets (Fig. 11).

Numerous lacunae contain already only cell debris (Fig. 12). The fissures at the cartilage-bone border which were observed histologically, can be seen also by EM; at certain places one can see a fibrous system connecting the cartilage to the bone; this does not seem to be an artifact (Fig. 13).

Discussion

The light, polarization and electron microscopic results complete each other into a well defined morphological picture regarding the age-dependent alterations of the articular cartilage. The results obtained are consistent with the fact (established mainly by using biochemical methods) that aging influences considerably the two main components of the matrix, the PG and the collagen.

The alterations of the PG molecules are in part structural, in part quantitative and qualitative. Our polarization optical studies with toluidine blue staining at pH 3.5 revealed a decrease of the optical path differences in both layers of the articular cartilage; this indicates a decrease of the orientation of the GAG molecules, i.e., a qualitative, structural alteration. This may correspond to the biochemical data, according to which aging causes a decrease of the PG and GAG [2, 37, 53], the ChS chain-length [18, 23, 52], and of the aggregation capacity of the PG molecules [7]. This is accompanied by an increase of the protein content, the Ch6S content in the GAG [12, 25, 36, 43, 51], the sulfation level of the ChS [30] and the turnover time [32]. Champion et al [11] suggested the synthesis of an "accessory" PG species during

aging on the basis of immunological studies. The increased demasking of the fibres observed histologically and the decrease of the interfibrillar matrix area seen in the electron microscope indicate a quantitative decrease of the PG molecules. The effect of 0.8 M $MgCl_2$ revealed an increase of the optical path difference in the external zone of the cartilage, i.e., the orientation of the KS molecules increased. Similar observations were published on the basis of light microscopic alcian blue staining [50]. This finding supports the biochemical results of several authors [26, 28] indicating a relative increase of the proportion of KS-content in the GAG molecules.

The polarization optical studies performed after phenol reaction showed a decreased path difference (i.e., collagen orientation) in the internal layer of the articular cartilage of the old rats, whereas this parameter in the external zone remained unchanged. The EM observations revealed the presence of fibres with various thicknesses and frequently occurring thin as well as non-striated, fragmented fibres in the central zone. According to Miller and Lust [33], the procollagen content is considerably higher in the extract of degenerated cartilage, than of the normal one, which was attributed to a failure of the transformation. The collagen heat-solubility decreases with age [44]. Our EM and polarization optical results support each other, since both of them indicate the decrease of the regular, mature collagen fibres in the old cartilage. This agrees with the findings of Venn [53] showing a decrease of the collagen content with aging, however, it is quite difficult to judge this parameter, since the molecular alterations of the collagen are quite slow [45, 46].

Our findings indicate that the PG and collagen alterations are of different localization: in the external zone of the articular cartilage only the changes of PG and GAG molecules were observed (in quantitative, compositional and structural sense), whereas in the internal zone mainly the collagen displayed quantitative and qualitative (thicker and thinner fibres) alterations as well as a changed orientation. This observation means that the proportion of various PG molecules and PG to collagen is altered by aging; the interrelationships and integrity of these two types of molecules are also shifted [3, 27], and as a consequence, the architecture and the mechanical resistance of the matrix becomes altered [17] in the superficial zone. It is well established that the tensile strenght of this tissue is due to the collagen, whereas the more labile PG molecules are responsible for the elastic properties of it. It should be noted also that the water content assuring the plasticity of the cartilage [10] decreases with the advancing age. These alterations can be considered as regressive signs which were observed also in the old costal cartilage [21] losing its ability to support the pressive load. On the other hand, these alterations can explain the age-dependent differences in the mechanical properties which may be quite near to the pathological limits.

The matrix alterations reflect obviously changes of the cellular components. Our EM observations on the chondrocytes agree in many aspects with those of others obtained in the articular cartilage [5, 20, 41, 42]. The decreased frequency of the cell organelles, degenerative phenomena, ruptures of the cell membrane and the accumulation of glycogen and mainly of lipids indicate an altered structure and function of the chondrocytes. According to Stockwell [48], the phospholipid content of the central zone increases with advancing age, and this is accompanied by a lipid infiltration. These structural alterations may explain why the chondrocytes are unable to perform the 5 steps of the PG synthesis [51], or the collagen synthesis. Data showing decreased enzyme activities of the old cells [6, 51] are in agreement with these findings. At the same time, it has been shown that some proteases, first of all metalloproteases can get out into the extracellular space and may decompose the PG molecules [1, 14, 35, 47] and also the collagen [40]. This process stimulates the PG synthesis of the cells, due to the matrix-cell interactions [22, 31]. However, because of the increased need and the lower number of cell organelles, not completely mature PG molecules will be secreted by these cells (this is indicated by the decreased subunit size, 38). This is, however, still a biological aging process [9] without pathological alterations, i.e., it is a self-controlled process, which is able to produce new cells, being able to synthesize new, perfect macromolecules and to maintain a certain equilibrium, too. Nevertheless, this represents a special state of predisposition, in which certain mechanical, endocrine, iatrogenic or post-traumatic influences may result in the acceleration of the degenerative process, i.e. arthrosis. For example, synovitis producing certain factors which stimulate the matrix degradation in the condrocytes [16] or inactivate the protease inhibitors [13], etc., may contribute very seriously to this process.

REFERENCES

1. Albright JA, Misra RP: Mechanisms of resorption and remodeling of cartilage. In: Hall Br K (ed.) Cartilage Vol. 3. Biomedical aspects. Academic Press New York, London. 1983 p. 49,
2. Anderson B, Hoffman P, Meyer K: The O-serine linkage in peptides of chondroitin 4 or 6 sulfate. J Biol Chem 240: 156, 1965
3. Armstrong CG, Mow VC: Variation in the instrinsic mechanical properties of human articular cartilage with age, degeneration, and water content. J Bone Jt Surg 64A: 88, 1980
4. Ashton IK, Matheson JA: Change in response with age of human articular cartilage to plasma somatomedin activity. Calcif. Tissue Int 29: 89, 1979
5. Barnett CH, Cochrane W, Palfrey AJ: Age changes in articular cartilage of rabbits. Ann Rheum Dis 22: 389, 1963
6. Barnett CH, Stockwell RA: The aetiology of osteoarthrosis. In: Hill AGS (ed.) Modern Trends in Rheumatology, Butterworths, London, 1966, p. 247.
7. Bayliss MT, Ali SY: Age-related changes in the composition and structure of human articular cartilage proteoglycans. Biochem J 176: 683, 1978
8. Bozsóky S: Az arthrosis. Orvosi Hetilap 123: 1463, 1982

9. Byers PD, Contepomi CA, Farkas TA: Postmortem study of the hip joint. Histological basis for limited and progressive cartilage alterations. Ann Rheum Dis 35: 114, 1976
10. Caplan AI: Cartilage. The molecules that make up cartilage enable it to play key structural roles in the human body. Sci Am 251: 84, 1984
11. Champion BR, Reiner Á, Roughley PJ, Poole AR: Age-related changes in the antigenicity of human articular-cartilage proteoglycans. Collagen Rel Res 2: 45, 1982
12. Cole MB: Morphology of the interlacunar network in four sites of hyaline cartilage of neonatal, juvenile, and adult rats. Clin Orthopaed Relat Res 170: 277, 1982
13. Dingle JT: Recent studies on the control of joint damage: The contribution of Strangeways Research Laboratory. Ann Rheum Dis 38: 201, 1979
14. Dingle JT, Dingle TT: The site of cartilage matrix degradation. Biochem J 190: 431, 1980
15. Ebner VV: Über die optische Reaktion der Bindesubstanzen auf Phenole S. Ber Acad Wiss Wien math-nat Kl 103: 162, 1894
16. Fell HB, Jubb RW: Effect of synovial tissue on the breakdown of articular cartilage in organ culture. Arthritis Rheum 20: 1359, 1977
17. Gardner DL, Elliott RJ, Armstrong CG, Longmore RB: The relationship between age, thickness, surface structure, compliance and composition of human femoral head articular cartilage. In: Pitman Nuki, G. (ed.) The Aetiopathogenesis of Osteoarthrosis. Medical. Publ. 1979 p. 65.
18. Garg HG, Swann DA: Age-related changes in the chemical composition of bovine articular cartilage. The structure of high density proteoglycans. Biochem J 193: 459, 1981
19. Gattone WH, Saul FP, O'Connor BL, McNamara MC: Scanning electron microscopic study of age-related surface changes in rat femoral head articular cartilage. J Submicrosc Cytol 14: 99, 1982
20. Ghadially FN, Roy S: Ultrastructure of synovial joints in health and diease. Butterworth, London. 1969
21. Hass GM: Pathological calcification. In: Bourne GH. (ed.) The Biochemistry and Physiology of Bone. Academic Press, New-York, 1956, p. 767
22. Hewitt A, Tyl Varner HH, Silver MH, Martin GK: The role of chondronectin and cartilage proteoglycan in the attachment of chondrocytes to collagen. In: Kelley RO, Goetinck PF, MacCabe JA. (eds.) Limb Development and Regeneration Part B. Alain R Liss, Inc New-York. 1983, p. 25
23. Hjertquist SO, Wasteson A: The molecular weight of chondroitin sulfate from human articular cartilage. Effect of age and of osteoarthritis. Calc Tiss Res 10: 31, 1972
24. Inerot S, Heinegård D, Audell L, Olsson SE: Articular cartilage proteoglycans in ageing and osteoarthritis. Biochem J 169: 143, 1978
25. Inerot S, Heinegård D: Articular cartilage proteoglycans in aging and osteoarthritis. In: Horowitz MI. (ed.) The Glycoconjugates, Vol. IV. Glycoproteins, Glycolipids, and Proteoglycans Part B. Academic Press. New-York, London. 1982, p. 335
26. Kaplan D, Meyer K: Ageing of human cartilage. Nature (London) 183: 1267, 1959
27. Kempson GE, Tuke MA, Dingle JT, Barett AJ, Horsfield PH: The effects of proteolytic enzymes on mechanical properties of human articular cartilage. Biochem Biophys Acta 428: 741, 1976
28. Lash JW, Whitehouse MW: Variation in the polysaccharide composition of cartilage with age. Biochem Biophys Acta 90: 159, 1960
29. Longmore RB, Gardner DL: The surface structure of ageing human articular cartilage: a study by reflected light interference microscopy (RLIM). J Anat 126: 353, 1978
30. Madsen K, Moskalewski S, von Der Mark K, Friberg U: Synthesis of proteoglycans, collagen, and elastin by cultures of rabbit auricular chondrocytes. Relation to age of the donor. Devel Biol 96: 63, 1983
31. Von der Mark K, Mollenhauer J, Kühl U, Bee J, Lesot H: Anchorins: A new class of membrane proteins involved in cell-matrix interactions. In: The role of extracellular matrix in development. Alan R Liss, Inc. New-York, 1984, p. 67
32. Maroudas A: Physico-chemical properties. In: Freeman MAR, (ed.) Adult Articular Cartilage. 2nd ed. Pitman, London. 1979, p. 215
33. Miller DR, Lust G: Accumulation of procollagen in the degenerative articular cartilage of dogs with osteoarthritis. Biochem Biophys Acta 583: 218, 1979
34. Módis L: Topo-optical investigations of mucopolysaccharides (acid glycosaminoglycans). Handbuch der Histochemie. II. 4. Fischer, Stuttgart, 1974
35. Muir IHM: The chemistry of the ground substance of joint cartilage. In: Sokoloff L (ed.) The Joints and Synovial Fluid. II. Academic Press. Inc. New-York, London, 1980, p. 27
36. Murata K, Bjelle AD: Age dependent constitution of chondroitin sulfate isomers in cartilage proteoglycans under associative conditions. J Biochem (Tokyo) 86: 371, 1979

37. Romhányi G: Über die submikroskopische strukturelle Grundlage der metachromatischen Reaktion. Acta Histochem 15: 201, 1963
38. Roughly PJ, White RJ: Age related changes in the structure of the proteoglycan subunits from human articular cartilage. J Biol Chem 255: 217, 1980
39. Scott JE, Dorling J: Differential staining of acid glycosaminoglycans (mucopolysaccharides) by alcian blue in salt solution. Histochemie 5: 221, 1965
40. Sellers A, Reynolds JJ, Meikle MC: Separation in latent forms of distinct enzymes that when activated degrade collagen, gelatin and proteoglycans. Biochem J 171: 493, 1978
41. Silberberg R, Silberberg M, Vogel A, Wettstein W: Ultrastructure of articular cartilage of mice of various age. Am J Anat 109: 251, 1961
42. Silberberg R, Silberberg M, Feir D: Life cycle of articular cartilage cells. An electron microscopic study of the hip joint of the mouse. Am J Anat 114: 17, 1964
43. Simunek Z, Muir H: Changes in the protein-polysaccharides of pig articular cartilage during prenatal life, development and old age. Biochem J 126: 515, 1972
44. Snowden JM, Eyre DR, Swann DA: Vitreous structure VI. Age related changes in the thermal stability and cross links of vitreous, articular cartilage and tendon collagens. Biochem Biophys Acta 706: 153, 1982
45. Sokoloff L: The pathology of osteoarthrosis and the role of ageing. In: Pitman Nuki G (ed.) The Aetiopathogenesis of Osteoarthrosis. Med. Publ. 1979, p. 1
46. Sokoloff L: Aging and degenerative diseases affecting cartilage. In: Hall BK (ed.) Cartilage Vol. 3. Biomedical Aspects. Academic Press New-York, London. 1983, p. 109
47. Starkey PM, Barett AJ, Burleight MC: The degradation of articular collagen by neutrophil proteinases. Biochem Biophys Acta 483: 386, 1977
48. Stockwell RA: Lipid in the matrix of ageing articular cartilage. Nature (Lond.) 207: 427, 1965
49. Stockwell RA, Barnett CH: Changes in permeability of articular cartilage with age. Nature (Lond.) 201: 835, 1964
50. Stockwell RA, Scott JE: Observations on the acid glycosaminoglycan (mucopolysaccharide) content of the matrix of ageing cartilage. Ann Rheum Dis 24: 341, 1965
51. Stuhlsatz HW, Greiling H: Proteoglycans and glycosaminoglycans of human joint cartilage in health, senescence, and disease. In: Glycosaminoglycans and Proteoglycans in Physiological and Pathological Process of Body Systems. Karger, Basel 1982, p. 276
52. Sweet MBE, Thonar EJMA, Marsh J: Age related changes in proteoglycan structure. Arch Biochem Biophys 198: 439, 1979
53. Venn MF: Variation of chemical composition with age in human femoral head cartilage. Ann Rheum Dis 37: 168, 1978
54. Vignon G, Meunier P, Vignon E, Arlot M: Le cartilage fémoral senescent et arthrosique données macroscopiques comparatives. Rev Rheum Mal Osteoartic 41: 25, 1974

Acta Morphologica Hungarica, 35 (3—4), pp. 125—133 (1987)

SUBPOPULATIONS OF T-LYMPHOCYTES IN IgA GLOMERULONEPHRITIS

T. MAGYARLAKI, JUDIT NAGY

DEPARTMENT OF PATHOLOGY AND 2nd CLINIC FOR INTERNAL MEDICINE, UNIVERSITY MEDICAL SCHOOL, PÉCS, HUNGARY

(Received 5 August 1986)

Peripheral subpopulations of T-lymphocytes were studied morphologically, cytochemically and with monoclonal antibodies (Leu 1, Leu 2a, Leu 3a) in 27 IgA glomerulonephritis cases and in 15 healthy controls. The number of helper T-lymphocytes was found significantly increased particularly in the active phase of IgA glomerulonephritis, while that of suppressor lymphocytes decreased. Thus helper/suppressor ratio increased significantly. In the inactive phase this ratio was also seen to increase but not in a significant manner. Comparing different methods used it is concluded that all of them proved to be suitable for the demonstration of altered subpopulation ratios.

Keywords: T-lymphocytes, IgA glomerulonephritis, increased helper/suppressor ratios

Introduction

Subpopulations of human T-lymphocytes play an important role in regulating immune responses. A number of techniques are available to identify lymphocyte sunpopulations such as IgG-, IgM or occasionally IgA—Fc fragment-binding receptors, morphology, enzyme reactions and monoclonal antibodies. Human T-lymphocytes form E-rosettes and react with OKT 3 and Leu 1 monoclonal antibodies. The suppressor-cytotoxic T-cells posses an IgG—Fc receptor, they are OKT 8 (Leu 2a)-positive, yield a multifocal acid phosphatase reaction and contain a typical azurophilic granulation in their cytoplasm (large, granular lymphocytes, LGL). Inducer-helper T-cells have IgM—Fc receptors, react with OKT 4 (Leu 3a) monoclonal antibodies and give unifocal acid phosphatase reaction.

IgA glomerulonephritis (IgA GN, 2) belongs to the chronic immune-complex GNs. Its pathogenesis is still obscure but data suggest that there exists a disturbance in the regulatory function of T-lymphocyte subpopulations with a concomitant rise in serum IgA levels and an appearance of circulating, partly IgA-containing ICs. [7, 8, 9, 10, 17, 18, 21, 22, 25]

Send offprint requests to Dr. T. Magyarlaki, Dept. of Pathology Szigeti 12, 7643 Pécs, Hungary

The present paper is an account of our observations on the T-lymphocyte subpopulations of IgA GN patients. We were interested in the following questions:

1. Are the morphological, cytochemical and monoclonal marker techniques suitable to differentiate between various T-lymphocyte subpopulations in clinical practice? Are the results divergent with different methods?

2. Is there a difference in IgA GN patients as compared to the controls between T-lymphocyte subpopulations demonstrated with different methods? (Difference in percentage, and in the helper/suppressor ratio).

Materials and methods

We have studied 27 IgA GN patients (8 female, 19 male, age: 18 to 51) and 15 healthy controls (6 female, 9 male, mean age: 26). Diagnosis was in all cases established by kidney biopsy [16]. On the basis of clinical symptoms observed at the time of examination patients were divided into two groups. In the active state of the disease were patients with proteinuria higher than 700 mg/day and haematuria higher than 10 million as determined according to Addis. Patients with lower values or without proteinuria or haematuria were considered as being in the inactive phase. On the basis of these criteria 11 of our patients were in the active, while 16 in the inactive phase at the time of examination.

To determine the percentage distribution of T-lymphocyte subpopulations lymphocytes were isolated from peripheral blood as described by Boyum [6].

Monoclonal antibodies

To demonstrate the surface-antigens of T-lymphocytes Leu 1, Leu 2a and Leu 3a monoclonal antibodies (Beckton-Dickinson) were used. For indirect immunofluorescence, FITC-labelled heterologous anti-mouse serum (GRUB FMo-1) was used as second antibody. To 100 μl 4×10^6/ml lymphocytes 5 μl Leu antibody was applied incubated at $+4$ °C for 30 min. Non-binding antibodies were removed by rinsing three times.

The second phase consisted of a 30 min incubation at 4 °C with 100 μl at 1 : 20 dilution of a second antibody added to the same amount of cell suspension. After three rinses cells were dropped onto a glass slide. In each case 200 cells were evaluated determining the % of fluorescent cells, i.e. how many of them belong to the lymphocyte subpopulation studied.

Cytomorphological and cytochemical studies

Morphological properties and cytochemical reactions of IgG GN patients and controls were studied in peripheral blood-smears and in pellets of peripheral lymphocytes isolated on a Ficoll-gradient using a cytocentrifuge (Shandon Southern). Cell morphology was evaluated in May-Grünwald-Giemsa preparations searching for the "large granular lymphocytes" (LGL) described by Timonem et al [23]. Acid phosphatase reaction was carried out according to Savage et al [22]. Acid esterase reaction was made using the method of Ranki and Häyri [18], slightly modified as described earlier [14].

Statistical methods

The means of T-lymphocyte subgroups in control, active and inactive groups were determined with different methods. The mean scatter (s) was calculated and the two-sampled student's *t*-test was employed. This method was also used when evaluating statistically the helper/suppressor ratios.

Results

In Fig. 1. T-lymphocyte subpopulation determined by monoclonal antibodies are shown in active and inactive IgA GN patients as compared to the controls. T-lymphocyte number increased in the IgA GN patients only moderately, while the helper T-lymphocytes were found in significantly

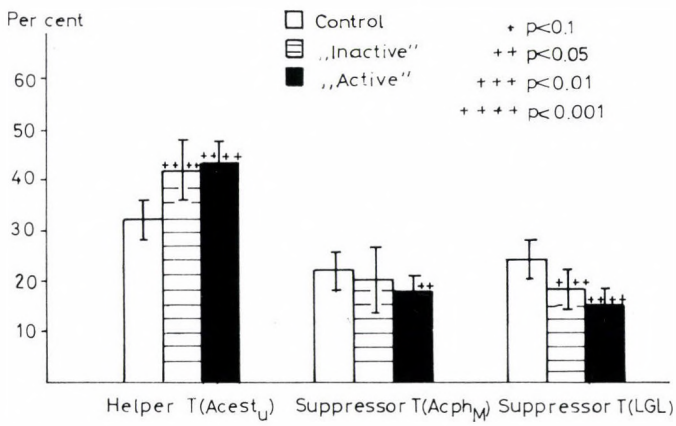

Fig. 1. Subpopulations of T-lymphocytes detected by monoclonal antibodies in IgA-glomerulonephritis. Leu 1 reaction with peripheral T-lymphocytes; Leu 3a positivity with helper and Leu 2a with suppressor T cells are demonstrated in columns. Empty columns are controls, cross-striated and black ones are IgA-glomerulonephritis patients in an "inactive" or "active" clinical stages. Standard deviations and significant levels are also shown

($p < 0.001$) higher numbers in both active and inactive IgA GN groups than in the controls. The number of suppressor T-lymphocytes increased slightly ($p < 0.05$) in the inactive group and decreased significantly ($p < 0.001$) in the active group.

In Fig. 2. lymphocyte subpopulations distinguished on the basis of their morphology and cytochemical reactions are shown. The number of helper T-lymphocytes was found to be significantly higher than in the control group ($p < 0.001$) while that of suppressor T-cells varied in the inactive group with the method applied: the number of cells displaying cytoplasmic multifocal acid phosphatase reaction decreased only moderately, while that of LGL cells decreased significantly ($p < 0.01$). In the active group the number of multifocal acid phosphatase positive cells decreased significantly ($p < 0.05$) with an even more pronounced decrease ($p < 0.001$) of LGL cells.

Figure 3. compares the helper/suppressor T-cell ratios as determined by different methods. Helper/supressor ratio determined by monoclonal antibodies was significantly higher ($p < 0.01$) in the active group. In the ratios deter-

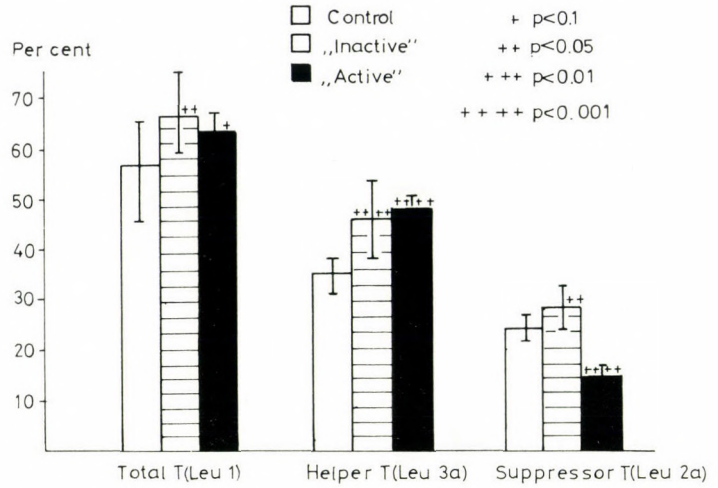

Fig. 2. Morphological and cytochemical markers of T-lymphocyte subpopulations. Helper T-lymphocytes show a unifocal pattern of acid esterase reaction ($Acest_U$); suppressor T cells are large granular lymphocytes (LGL) and have multifocal positivity of acid phosphatase enzyme reaction in their cytoplasms ($Acph_M$). Otherwise the signals are the similar to that of Fig. 1

Examined groups / helper / suppressor	Control	„Inactive"	„Active"
Leu 3a / Leu 2a	1.43 ± 1.2	1.63 ± 1.56	2.99 ± 1.15 +++
$Acest_U$ / $Acph_M$	1.96 ± 4.75	2.13 ± 5.65	2.33 ± 4.1
$Acest_U$ / LGL	2.00 ± 3.95	2.21 ± 4.45	2.55 ± 3.45

+++ p<0.01

Fig. 3. Helper/suppressor ratios in control, "inactive" and "active" clinical groups of IgA-glomerulonephritis detected by different methods. Significant elevation of ratios by using monoclonal antibodies in the "active" group of IgA-glomerulonephritis is shown first line (+++). The second and the third lines show the tendency similar to that of the first, but it is not significant

mined on morphological or cytochemical bases a similar trend could be observed but without significant alterations.

Figure 4a. is a photomicrograph of an LGL; 4b. demonstrates unifocal acid phosphatase positivity in the cytoplasm of peripheral lymphocytes; 4c.

illustrates multifocal acid phosphatase reaction in peripheral lymphocytes; In 4d. immunoreactive cells are shown reacted with Leu 2a monoclonal antibodies.

Discussion

On the basis of experimental and clinical data most GNs can be considered as being of IC origin. Temporary or permanent disturbances of the immune system may be held responsible for the development of chronic IC diseases such as the IgA GN. Increased IgA production and the appearance of IgA ICs and IgA aggregates in IgA GN are most likely due to a functional impairment of suppressor T-cells and a hyperreactivity of B-cells. The decrease in activity of IgA-specific T suppressor cells [21], the increase in number of T alpha-cells [20] and of IgA-producing peripheral B-lymphocytes [18] has also been pointed out. Endoh et al [10] claim that T alpha-cells are IgA-specific helper T-cells and probably their increased number and activity is responsible for the enhanced IgA production of B-cells [9].

There are several methods used currently to study T-lymphocyte subpopulations. Investigations with monoclonal antibodies are gaining wide application but enzyme reactions and morphology may also be used for identification. However, data are scarcely available concerning the comparison of the different methods. Matutes and Catovsky[15] have described the large cytoplasm and coarse azurophilic granulation of OKT 8 (Leu 2a) and T_G rosette positive (suppressor) cells (LGL). On the other hand OKT 4 (Leu 3a) and T_M rosette positive (helper T) cells were found to have a thin, cytoplasmic rim poor in organelles. Timonem et al [23] and Van der Loo and Meier [13] adopted the tartarate-sensitive acid phosphatase reaction to characterize suppressor and LGL cells. Bernard and Dufer [3] found an 80% acid phosphatase positivity in the OKT 8 (Leu 2a) positive subpopulation and also in other cell population although disregarding the localization pattern (uni- or multifocal) of the reaction. Bodolay et al [5] applied the multifocal acid esterase reaction parallel to T_G rosette for the determination of supressor population and found comparable results with the two methods in SLE patients. Recently, the chloroacetate esterase reaction has been described in suppressor T-cells [3, 12].

The unifocal acid esterase reaction has been described as characteristic for helper T-lymphocytes by Grossi et al [11] and Heuman et al [12]. Although this view has been challenged [1, 4], Bernard and Dufer [3] and Van der Loo and Meier [13] support it by demonstrating a significantly higher occurrence of unifocal positivity in helper populations than in other cells.

In our IgA GN patients the percentage of helper T-cells was found to be significantly elevated with both Leu 3 antibodies and unifocal acid esterase

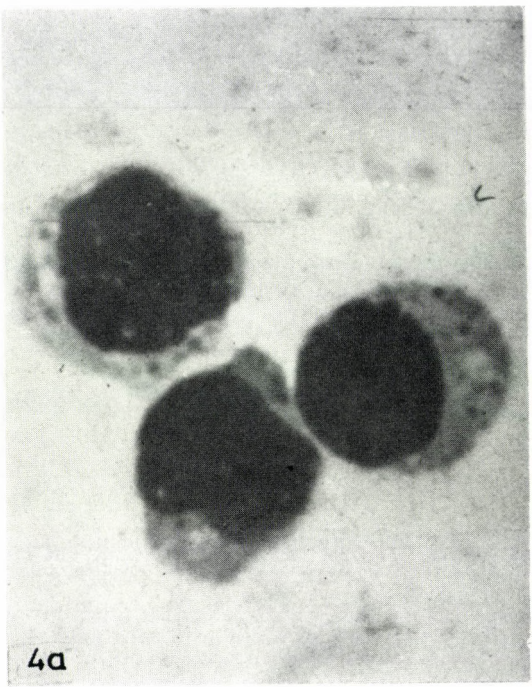
4a

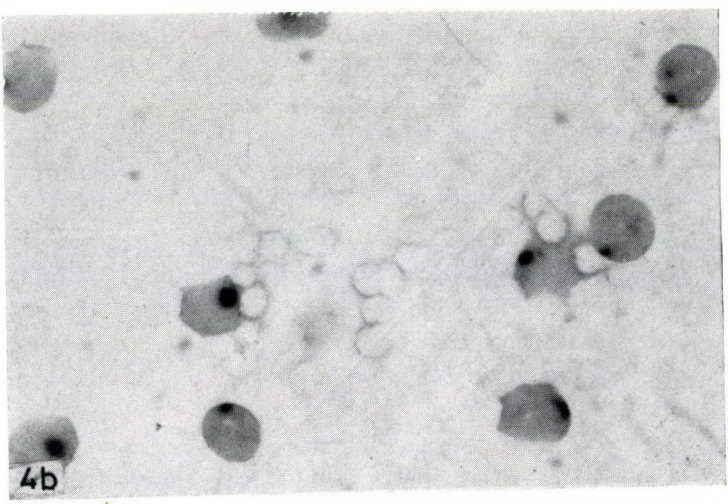
4b

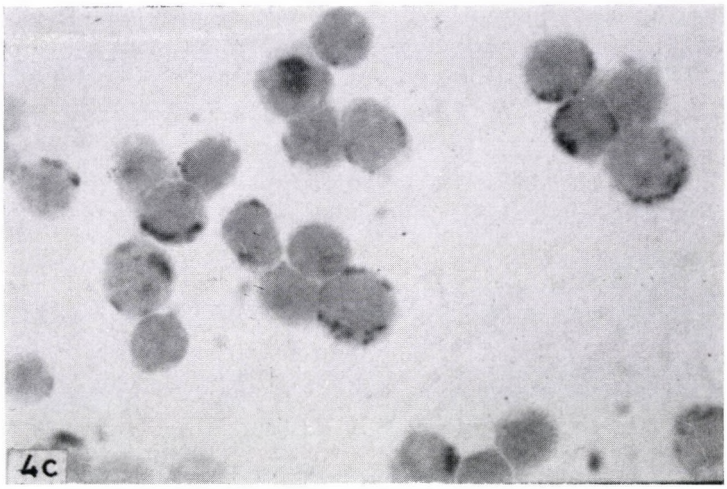

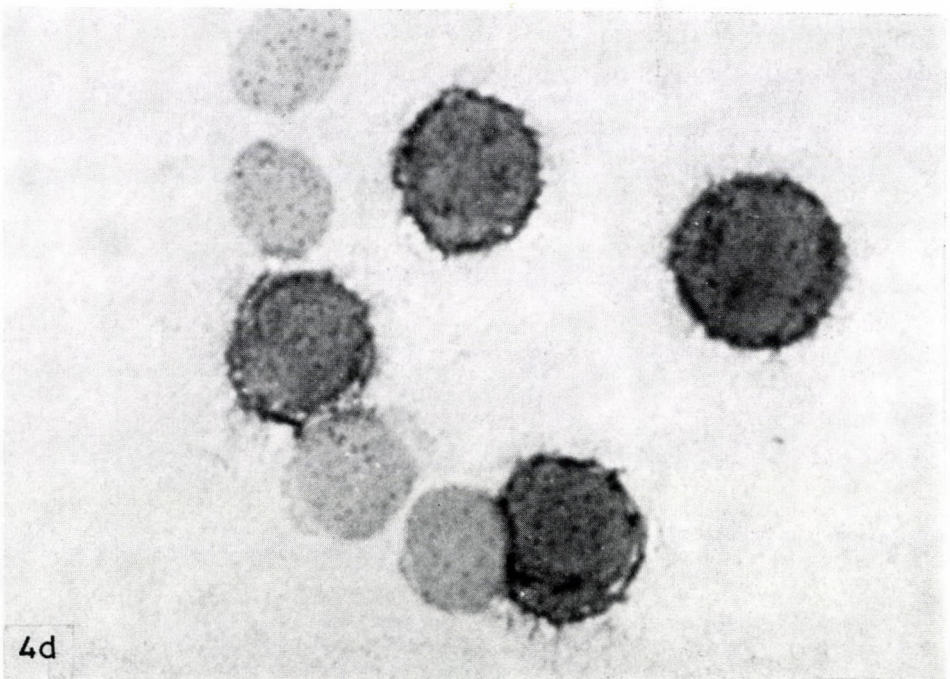

Figs 4a. Peripheral lymphocytes. Giemsa. Azurophilic granulation in the cytoplasm of three peripheral lymphocytes (×2000); *b.* Peripheral lymphocytes, acid esterase reaction. Unifocal positivity in the cytoplasm of lymphocytes (×1000); *c.* Peripheral lymphocytes, acid phosphatase reaction. Multifocal positivity in the cytoplasm of numerous lymphocytes (×1000); *d.* Peripheral lymphocytes stained by the indirect immunoperoxidase method using Leu 2a monoclonal antibodies. Four positive and four negative cells are shown (×2000)

reaction. On the other hand, the percentage of suppressor T-cells decreased, observed either by Leu 2a antibodies, or by multifocal acid phosphatase reaction or by morphological examination (LGL). An exception was the inactive group where the number of T-suppressor cells was found slightly increased with Leu 2a antibodies. However, helper/suppressor ratio was found to be increased in both patient-groups regardless to the method employed. Similar conclusions were arrived at by Chatenaud and Bach [7] and Egido et al [9] but they did not differentiate between patients according to clinical symptoms. Our results suggest that the rise in helper/suppressor ratio is typical mainly for patients in the active phase of the disease. We think therefore, that this change observed in the T-cell subpopulations, i.e. the relative dominance of helper T-cells, may be responsible for high serum IgA levels [17, 20, 24] and for the frequently seen immune complex positivity in the circulating blood [8, 24].

The comparison of different methods indicated that they yielded principally similar results. Nevertheless, cytomorphology and cytochemistry appeared to be less accurate (higher scatter, lower significance, no difference between active and inactive phases) as compared to detection with monoclonal antibodies. In spite of this, the analysis of LGL cells and of acid phosphatase and esterase reactions in peripheral blood-smear preparations may be useful as simple, rapid means to have a general assessment of T-lymphocyte subpopulations necessary for monitoring the state of the immune system in IgA GN patients.

REFERENCES

1. Amitage RJ et al.: The morphology and cytochemistry of human T-cell subpopulations defined by monoclonal antibodies and F_C receptors. Brit J Haematol 51: 605, 1982
2. Berger J, Hinglais N: Les depots intercapillaires d'IgA-IgG. J Urol Nephrol (Paris) 74: 694, 1968
3. Bernard J, Dufer J: Cytochemistry of human lymphocyte subpopulations delineated by monoclonal antibodies. Brit J Haematol 53: 351, 1983
4. Binkley B et al: Cytochemical and ultrastructural studies on human T-cell subsets separated with fluorescence activated cell sorter. Am J Clin Path 80: 121, 1983
5. Bodolay E, Boros P, Szegedi Gy: Alpha-naphthylacetat-esterase reaction for peripheral lymphocytes and monocytes of patients with SLE. Acta Med Hung 39: 145, 1982
6. Boyum A: Separation of leucocytes from blood and bone marrow. Scand J Clin Lab Invest 21: 97 (Suppl) 1968
7. Chatenaud L, Bach MA: Abnormalities of T-cell subsets in glomerulonephritis and systemic lupus erythematosus. Kidney Int 20: 267, 1981
8. Coppo R et al: IgA, IgG and IgM containing immune complexes in primary IgA nephropathy and in Schönlein-Henoch nephritis. Correlations with clinical and histological signs of activity. Clin Nephrol 18: 230, 1982
9. Egido J et al: T-cell dysfunction in IgA nephropathy: specific abnormalities in the regulation of IgA synthesis. Clin Immunol Immunpathol 26: 201, 1983
10. Endoh M et al: IgA specific helper activity of T-cells in human peripheral blood. J Immunol 127: 2612, 1981
11. Grossi CE et al: Morphological and histochemical analysis of two human T-cell subpopulations bearing F_C receptors for IgM or IgG. J Exp Med 147: 1405, 1978

12. Heuman D, Colombatti M, Mach JP: Human large granular lymphocytes contain an esterase activity usually considered as specific for myeloid series. Eur J Immunol 13: 254, 1983
13. Van der Loo EM, Meyer CJLM: Morphological aspects of T-cell subpopulations in human peripheral blood lymphocytes: characterization of the cerebriform mononuclear cells in healthy individuals. Clin Exp Immunol 43: 506, 1981
14. Magyarlaki T, Pár A: T-lymphocyta subpopulatiók systemás lupus erythematosusban. Magyar Belorvosi Arch 37: 254, 1984
15. Matutes E, Catovsky D: Fine structure of normal lymphocyte subpopulations — a study with monoclonal antibodies and immunogold technique. Clin Exp Immunol 50: 416, 1982
16. Nagy J et al: IgA glomerulonephritis: light microscopic and immunhistological studies. Acta Morph Hung 32: 143, 1984
17. Nagy J et al: Circulating immune complexes in patients with IgA glomerulonephritis. Acta Med Hung 39: 211, 1982
18. Ranki A, Häyri P: Distribution of four subclass specific markers in man. Acta Pathol Scand C 86: 63, 1978
19. Reinherz EL, Moretta L, Roper L: Human T lymphocyte subpopulations defined by F_C receptors and monoclonal antibodies. J Exp Med 151: 969, 1980
20. Sakai H et al: Increase in IgA specific helper T alpha cells in patients with IgA nephropathy. Clin Exp Immunol 50: 77, 1982
21. Sakai H et al: Decrease of IgA specific suppressor T cell activity in patients with IgA nephropathy. Clin Exp Immunol 38: 243, 1979
22. Savage RA, Valenzuela R, Hoffman GC: Acid phosphatase as staining pattern inductor of T cell acute leukemia. Am J Clin Path 76: 760, 1981
23. Timonem T, Ortaldo HR, Herberman RB: Characterisation of human large granular lymphocytes and relationship to NK and K cells. J Exp Med 153: 569, 1981
24. Woodroffe AJ et al: Immunologic studies in IgA nephropath. Kidney Int 18: 366, 1980

Acta Morphologica Hungarica, 35 (3—4), pp. 135—144 (1987)

EFFECT OF HISTAMINE ON THE ULTRASTRUCTURE OF MUCOSAL CIRCULATORY VESSELS IN RAT LARGE INTESTINE

K. Dikranian

DEPARTMENT OF ANATOMY AND HISTOLOGY, INSTITUTE OF MEDICINE, VARNA, BULGARIA

(Received 29 August 1986)

Histamine, applied intravenously at various concentrations (3 μg, 125 μg, 250 μg/100 g body weight) caused 90 and 210 s after the injection ultrastructural alterations in the endothelial cells of rat colonic mucosal microvessels. The most prominent changes occurred with the 250 μg/100 g/90 s combination, including an increase of vesicular population, formation of vacuole-like spaces, increase in the luminal evaginations of the fenestrated capillaries, as well as an increase in size of the Golgi complex. Only few gaps were distinguished in some venules after the administration of 250 μg/100 g histamine and a circulation time of 210 s. Intact vessels were detected at all concentrations. Results indicate, that histamine affects structures involved in transvascular transport, mainly by increasing the number of pinocytotic vesicles. They also suggest a possible differential response within the endothelial cell population towards histamine action.

Keywords: Histamine, capillaries, pinocytotic vesicles

Introduction

Histamine affects a number of physiologic processes. In most vascular beds it has been shown to be a vasodilator of the arteries and a constrictor of some venules and small veins [15, 16]. In the mesentery, cutaneous and muscle tissue [9, 18, 13] increase vascular permeability. Ultrastructural studies have clearly shown that the enhanced transcellular transport of macromolecules, like serum albumin occurs via gaps in leaky endothelia of postcapillary vessels [10, 15, 16]. In an elegant computer reconstruction of serial electron micrographs, it was demonstrated that histamine promotes the widening of the gaps between venular endothelial cells [10]. Many other studies have clarified the nature of histamine receptors, associated both with vasodilation and permeability in various vessels [3, 6, 11, 15, 17]. Apart from these there have been reports of increased vesiculation and other endothelial

Send offprint requests to K. Dikranian, Dept. of Anatomy and Histology, Institute of Medicine, Varna 9002, Bulgaria

changes [1, 8, 14]. It has been postulated, that an increase of internal radius of pinocytotic vesicles would lead to a manyfold increase in their volume turnover [19]. It is well known that the endothelium of mesenteric vessels is the site of storage of large amounts of endogenous histamine [12]. On the other hand, histamine, as a powerful autoregulatory tool of the mesenteric circulation, interacting with H_1 receptors, may mediate pressure-induced and in part, prostaglandine-induced haemodynamic changes [2], thus acting on the regional homeostasis. Data from both physiological and morphological studies have shown that it is difficult to determine the concentration of histamine at the actual site of permeability change. Most morphological studies are made with concentrations considerably greater than those used in physiological studies. Perhaps the most widely used route of histamine introduction is the topical application, where doses up to 100 μg/ml/min are reported [10]. Others[17] in a physiological study used intraarterial (superior mesenteric artery) dose of 10 μg/ml base 0.5 ml/min for studies in cat ileum preparations. Doses per body weight are reported by Bhargava et al. [3] — intraperitoneal application of histamine base up to 5 μg/mouse (20 g). Sparrow et al. [22] found that in order to produce equivalent extravasation, 25 times the concentration was needed, compared to guinea-pigs. This shows a relative insensitivity of the rat model to this amine. From other experiments it is evident that for the registration of constrictor response, rats require much larger doses than cats, ferrets and other species. Even the lethal doses range between 500—700 mg/kg which predicts the high degres of histamine tolerance in rats. Time course of tracer extravasation in mesenteric vessels is between 2 to 15 min. That is why in our experiments we applied doses of histamine, comparable to those mentioned above, bearing in mind also its high diffusibility, metabolism and dilution in blood. The problem requires careful re-examination in different organs in morphological as well as physiological terms. The present study is an attempt to ascertain the effect of the amine on the ultrastructure of the endothelial cells of terminal vessels in rat colonic mucosa at various concentration and time.

Materials and methods

Experiments were carried out on adult male Wistar rats. The animals were anaesthesized with Tiopental intraperitoneally. Histamine dihydrochloride (Buchs, Switzerland) was administered through the femoral vein as a single dose at three concentrations — 3 μg/100 g (equal to 1.8 μg/100 g base), 125 μg/100 g (75 μg/100 g base) and 250 μg/100 g (150 μg/100 g base) and the animals were sacrificed after 90 and 210 s intervals. Samples were taken from the colon of the control and experimental animals, according to the experimental procedure of Simionescu et al. (1972) [20]. Fixation was made in 5% glutaraldehyde at 4 °C (in 0.2 mol phosphate buffer) for two hours. Post-fixation was performed with 2% osmium tetroxide in 0.2 mol phosphate buffer (pH 7.4) for two hours at 4 °C. After dehydration in graded ethanols, samples were embedded in Durcupan ACM (Fluka). Sections were double stained with uranyl

acetate and lead citrate. Observation was made by JEM 7A electron microscope. Measurements were made on selected micrographs of capillary profiles, perpendicular to the plane of section, by Maho-N: 60 planimeter. They were performed on the peripheral zone of the endothelial cell which accounts approximately for 40% of the cell cytoplasm [21] and appears to be functionally the most important in the current transcellular transport of solutes and also of the parajunctional zone having few transport vesicles or none at all.

Results

In the following survey we focussed on the effect of histamine on the ultrastructure of the endothelial cells of the microcirculatory vessels, other than arterioles and precapillary vessels. Only true capillaries and venous limb capillaries were considered.

The minimal dose (3 μg/100 g) caused no ultrastructural changes in the vessels. The morphological picture resembled the capillary wall of the control animals (Fig. 1).

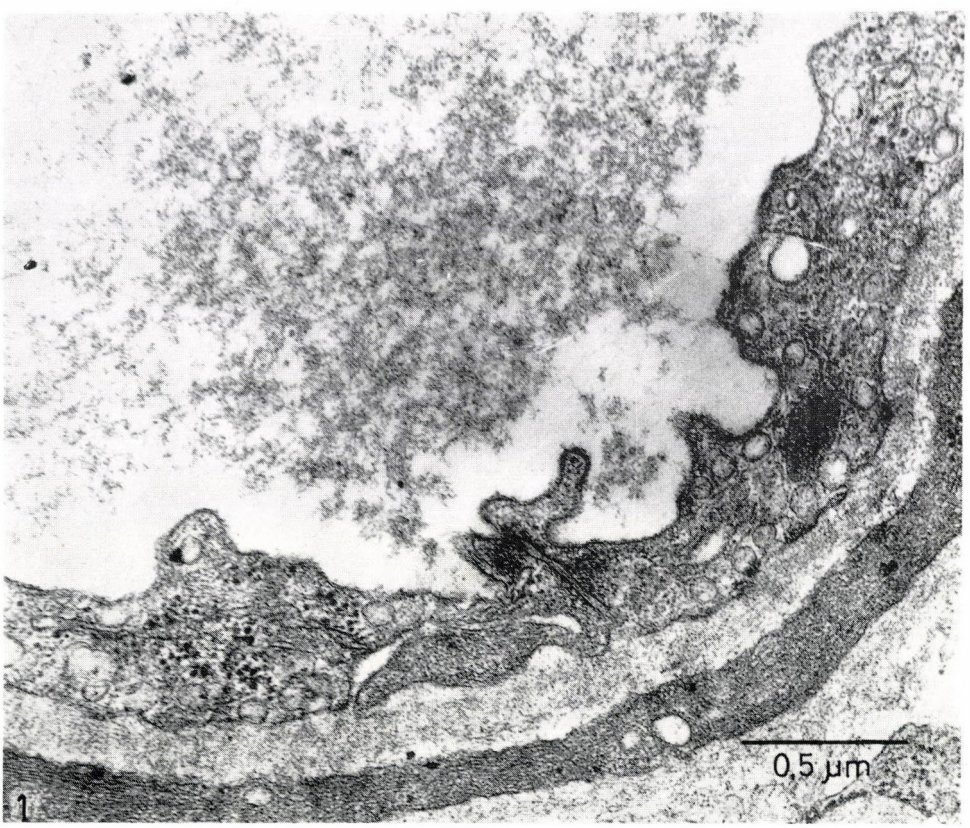

Fig. 1. Non-fenestrated capillary from the control animal. ×20 000

Table I

	Control	125 μg/100 g/90 s	250 μg/100 g/90 s
Mean values (vesicles/m²)	11.31	23.99	29.82
Number of capillary profiles	38	24	27
Standard deviation	3.12	4.80	10.87

Rise in micropinocytotic vesiculation significant after the application of histamine ($p<0.005$) Student's t test

At the 125 μg/100 g/90 s range there was an elevation of the pinocytotic vesicle population in true capillaries (Table I), as well as an increase of the number of luminal evaginations which were relatively short (Fig. 2). There was no change in the interendothelial junction in all microvessels. The basal membrane showed a normal appearance.

Fig. 2. Non-fenestrated capillary (histamine 125 μg/100 g/90 s). The endothelial cell (E) contains numerous vesicles, as well as short luminal evaginations. ×20 000

After the administration of 250 μg/100 g at the 90 s intereval, the increase of the vesicular population was much more evident (Table I.). Vesicles were distributed all over the cytoplasm (Fig. 3), including the parajunctional zone, where they are normally very scanty [21]. Besides this enhanced vesiculation, numerous vacuole-like spaces were detectable. Some of them were formed by fused pinocytotic vesicles, others were non-uniform — probably deep

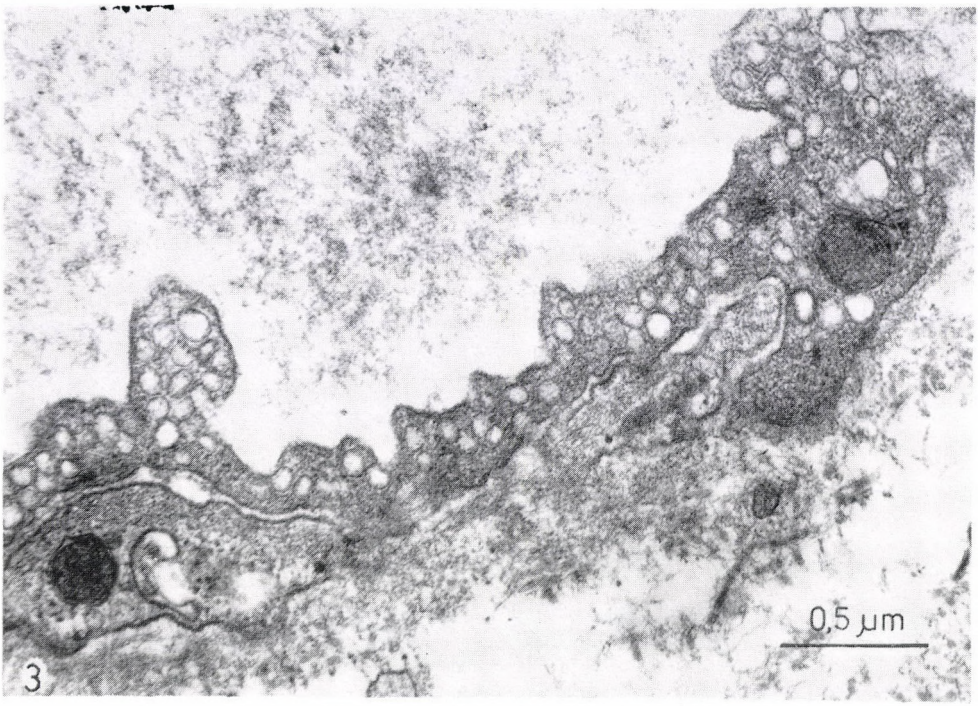

Fig. 3. Non-fenestrated capillary (histamine 250 µg/100 g/90 s). ×20 000

invaginations of the luminal surface. This picture was more pronounced in non-fenestrated capillaries (Fig. 4), while in the fenestrated and post-capillary vessels the luminal flaps were longer and more numerous (Fig. 5). Together with this, at the same plane of section we observed vessels with normal appearing endothelial lining. Almost in all paranuclear regions prominent Golgi complex associated with coated vesicles was present (Fig. 4). There was no change in the interendothelial junction and basement membrane. No gaps were distinguished. Occasionally there were local widenings of the intercellular cleft. Mostly in fenestrated vessels there were closing folds and occasional pinches of the nuclear envelope (Figs 5, 6).

At longer circulation times (210 s), at both concentrations, the above changes persisted. Weibel-Palade bodies concentrated in groups in some endothelial cells were encountered at the 125 µg/100 g group. Gaps in venules were detected only twice, together with intact junctions along the circumference of the same vessels.

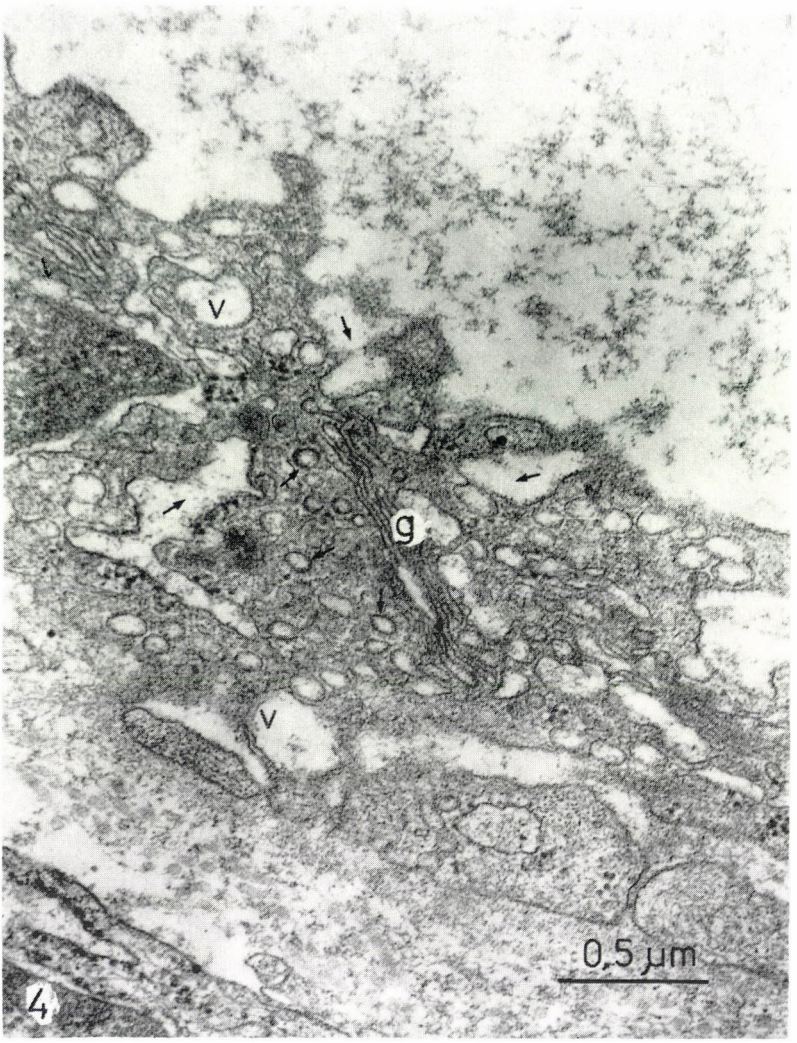

Fig. 4. Non-fenestrated capillary (histamine 250 µg/100 g/90 s). Note the vacuole-like spaces (V) or deep invaginations (arrows) and coated vesicles (arrowheads). Golgi complex (G). ×17 000

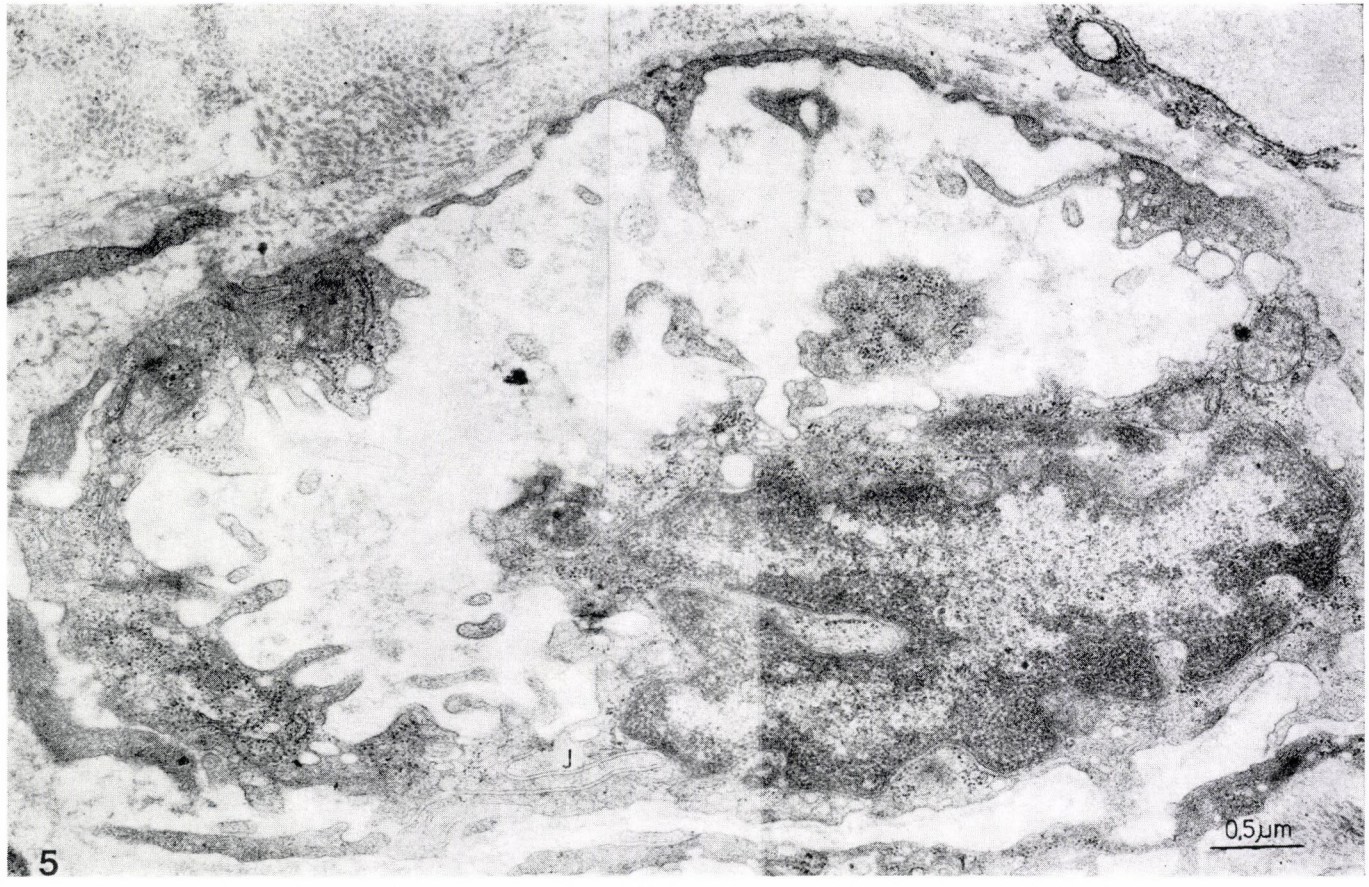

Fig. 5. Fenestrated capillary (histamine 250 µg/100 g/90 s). Intact interendothelial junction (J). ×17 000

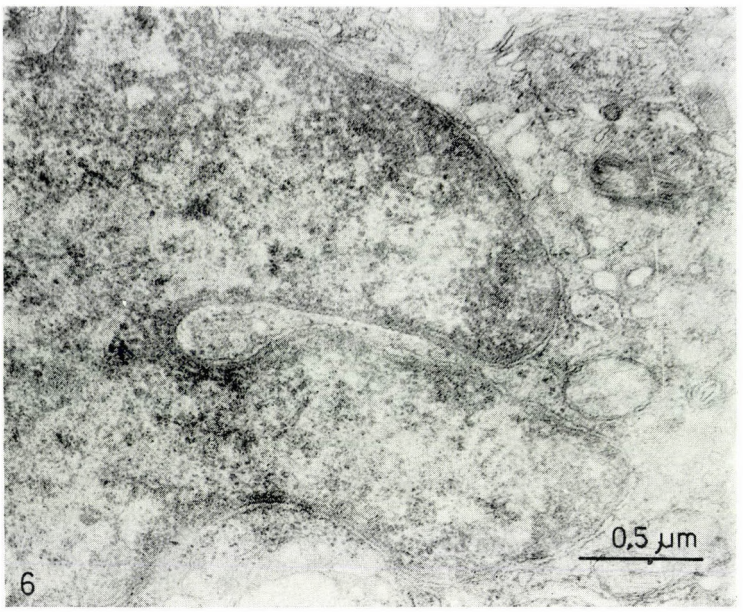

Fig. 6. Deep nuclear fold (histamine 250 µg/100 g/30 s). ×20 000

Discussion

Our data demonstrate that histamine affects the structures concerned with the permeability properties of the colonic mucosal microvessels, mainly by increasing the number of pinocytotic vesicles (Table I). Our results correlate with other morphological and physiological studies [1, 4]. Apart from this, the increase in the number of vacuoles after the administration of 250 µg of histamine, would obviously diminish the molecular selectivity and raise the turnover capacity of the vessel. In this respect the response might be considered as a dose-dependent one. The fact, that not all endothelial cells respond in the same manner and our failure to registrate gaps in post-capillary vessels at the 90 s interval, — and only few in the 210 s range — is subject to speculation, considering the nature of receptors, concerned with histamine action, onset and duration of the effect and the local conditions. It may be so that not all endothelial cells react in the same way even if they are located side by side. Electron-microscopic criteria are not sufficient to fully clarify these changes. Further studies, using histamine receptor antagonists, need to be applied too.

Moreover, if we assume, that histamine dilates the arterioles within the experimental period, it could promote the opening of large number of capillaries and this relative increase of permeable surface could lead per sec to an

enhanced passage of solutes, without involving major changes in endothelial ultrastructure, which is the alternative possibility. Another thing that comes into consideration is that autoregulatory processes in the mesenteric circulation may alter the response to the exogenously administered drug and/or a sort of "autoregulatory escape" is involved. It should be noted, that so far we cannot ascertain an endothelial contraction, only having the nuclear folds and pinches as the sole signs, without meeting the other criteria, postulated by Majno et al. [16], or findings have to be attributed to vessels with larger diameter. However, the expression of the Golgi complex at the higher concentration, which shows some endothelial activation, supports our impression that the response in this case is dose-dependent.

Finally, if we consider that the described changes provide structural evidence for a short-term autoregulatory response to the intravenously applied amine, further studies are needed to clarify the limits of this action and the chronomorphologic heterogeneity of the endothelium in the mucosal microcirculatory vessels.

Acknowledgements

We are most grateful to Dr. S. Nikolov, Dr. M. Jeliazkova and Dr. N. Temnialov for the stimulating discussion and Ms L. Pastarmadijieva for technical assistance.

REFERENCES

1. Alksne JF: The passage of colloidal particles across a dermal capillary wall under the influence of histamine. Quart J Exp Physiol 44: 51, 1959
2. Banks R, Callavan R Jr, Zinner M, Bulkey G, Harper S, Granger D, Jacobson E: Vasoactive agents in control of the mesenteric circulation. Fed Proc 44, 12: 2743, 1984
3. Bhargava KP, Nath R, Palit G: Nature of histamine receptors concerned in capillary permeability. Brit J Pharmacol 59: 349, 1977
4. Carter RD, Joyner WC, Renkin EM: Effect of histamine and some other substances on molecular selectivity of the capillary wall to plasma proteins and dextran. Microvasc Res 7: 31, 1974
5. Clementi F, Palade G: Intestinal capillaries. II. Structural effect of EDTA and histamine. J Cell Biol 42: 706, 1969
6. Cuth PH, Smith E: Histamine receptors in the mesenteric circulation of the cat and rat. Am J Physiol 234, 4: 370, 1978
7. Cuth PH, Hirabayashi K: The effect of histamine on microvascular permeability in the muscularis externa of the rat small intestine. Microvasc Res 25: 322, 1983
8. Dux E, Joo F: Morphological equivalents of macromolecular transport in the brain capillaries. Acta Biol Hung 37 (Suppl.): 256, 1986
9. Fox JR, Wayland H: Effect of doze level of histamine on mesenteric microvascular permeability. Microvasc Res 11: 118, 1976
10. Fox JR, Galey F, Wayland H: Action of histamine on the mesenteric vasculature. Microvasc Res 19: 108, 1980
11. Heltianu C, Simionescu N: Histamine receptors of the microvascular endothelium revealed in situ with histamine-ferritine conjugate. Characteristics of high-affinity binding sites in venules. J Cell Biol 93: 357, 1982
12. Howland RD, Spector S: Disposition of histamine in mammalian blood vessels. J Pharmacol Exp Ther 182: 239, 1972
13. Kozlovsky T, Raymond RM, Korthius RG: Microvascular protein efflux: interaction of histamine and H_1 receptors. Proc Soc Exp Biol Med 166: 263, 1981

14. Majno G: Ultrastructure of the vascular membrane. In: Hamilton WF, Dow P, (eds) Handbook of Physiology, Williams and Wilkins, Baltimore 1965, p. 2293
15. Majno G, Gilmore V, Leventhal M: On the mechanism of vascular leakage caused by histamine-type mediators. A microscopic study in vivo. Circ Res 21: 833, 1967
16. Majno G, Shea SM, Leventhal M: Endothelial contraction induced by histamine-type mediators. J Cell Biol 42: 647, 1969
17. Mortilaro NA, Granger D, Kvietys PR, Rutilia G, Taylor AE: Effect of histamine antagonists on intestinal permeability. Am J Physiol 240: G381, 1981
18. Owen DAA, Poy E, Woodward DF: Evaluation of the role of histamine H_1 and H_2 receptors in cutaneous inflammation in guinea-pig, produced by histamine and mast cell degranulation. Brit J Pharmacol 69: 615, 1980
19. Renkin EM, Carter RD, Joyner WL: Mechanism of the sustained action of histamine and bradykinin on the transport of large molecules across capillary walls in the dog paw. Microvasc Res 7: 49, 1974
20. Simionescu N, Simionescu M, Palade G: Permeability of intestinal capillaries. Pathway followed by dextrans and glycogens. J Cell Biol 53: 365, 1972
21. Simionescu M, Simionescu N, Palade G: Morphometric data on the endothelium of blood capillaries. J Cell Biol 60: 128, 1974
22. Sparrow EM, Wilhelm DL: Species difference in susceptability to capillary permeability factors: Histamine, 5-hydroxytryptamine and compound 48/80. J Physiol 137: 51, 1937

Acta Morphologica Hungarica, 35 (3—4), pp. 145—156 (1987)

PROTEINASE INHIBITORS WHILE INFLUENCING HORMONE RELEASE DO NOT AFFECT CELL MORPHOLOGY OF HYPOPHYSEAL CULTURES*

GY. RAPPAY[1], ILONA FAZEKAS[1], E. BÁCSY[1], GYÖNGYI GAÁL[1], MARIE ELISABETH STOECKEL[2], I. NAGY[3], ANGÉLA GYÉVAI[1], G. B. MAKARA[1]

[1]INSTITUTE OF EXPERIMENTAL MEDICINE, HUNGARIAN ACADEMY OF SCIENCES, BUDAPEST,
[2]LABORATOIRE DE PHYSIOLOGIE, UNIVERSITÉ LOUIS PASTEUR, STRASBOURG,
[3]HEIM PÁL PEDIATRIC HOSPITAL, BUDAPEST, HUNGARY

(Received 18 February 1987)

Cultured cells from adult rat anterior pituitaries and intermediate lobes were treated with proteinase inhibitor substrate analogues (Boc-DPhe-Pro-Arginal [BOC-DPPA], DPhe-Pro-Arginal [DPPA], BOC-DPhe-Leu-Lysinal [BOC-DPLL], BOC-DPhe-Phe-Lysinal [BOC-DPPL]) to elucidate their effect on cell morphology. It was established that BOC-DPPA and DPPA (which in previous studies stimulated alpha-MSH release [6]) caused a slight decrease in the number of immunoreactive secretory granules inmelanotrophs. BOC-DPLL, which inhibited growth hormone and prolactin release, did not alter the fine structural features of cultured cells. No difference was observed in the membrane turnover traced by cationic ferritin when cells were treated with BOC-DPPL.We suggest that substrate analogues used are harmless to pituitary cells.

Keywords: Pituitary cells in culture, proteinase inhibitor, hormone release membrane turnover, electron microscopy

Introduction

The recognition of the limited proteolysis as a widely occurring cellular machinery in formation of biologically active peptides and proteins lead to searching either for enzymes catalyzing partial hydrolysis of proteinaceous substrates or for inhbitors which may interfere with the catalytic processes. Up to now most enzymes are uncharted whereas enzyme inhibitors are increasingly available.

One of the best examples of limited proteolysis is the activation and the subsequent release of peptide and protein hormones produced by the hypophyseal cells [3, 10]. Chertow [3] has emphasized the use of proteinase inhibi-

* Dedicated to Professor Z. Lojda on his 60th birthday

Send offprint requests to Dr. György Rappay, Institute of Experimental Medicine, H-1083 Budapest, Szigony u. 43, Hungary

tors which may facilitate the unmasking of the nature of the activation process(es) and/or its localization within the parenchymal cells of the adenohypophysis.

In earlier experiments we found that a class of proteinase inhibitors may influence hormone release by cultured pituitary cells. Some tripeptide aldehydes which inhibit the catalytic activity of serine and thiol endopeptidases interfere with adrenocorticotropic hormone (ACTH) release by anterior pituitary cells [1], while some tripeptide aldehydes may stimulate ACTH and melanocyte stimulating hormone (alpha-MSH) release by monolayer cultures derived from rat pituitary intermediate lobes [7]. Prolactin (PRL) and growth hormone (GH) release by anterior pituitary cells in culture are inhibited with BOC-DPhe-Pro-Arginal (BOC-DPPA) and BOC-DPhe-Phe-Lysinal (BOC-DPPL) under both basal and stimulated conditions [17, 18, 19], whilst hormone synthesis remains unchanged during an 8 h treatment [13, 14].

In the present study we report on the innocuity of tripeptide aldehydes to cell morphology of anterior and intermediate lobe cultures of the rat pituitary.

Materials and methods

Cell cultures

In each experiment usually 25 anterior and/or intermediate lobes were collected under sterile conditions after decapitation of female rats weighing 200 g. The anterior pituitaries were dispersed with trypsin [16] and $5-8 \times 10^5$ cells/ml were explanted into multiwell disposotrays (24/16 LINBRO). They were maintained in an ASSAB CO_2 incubator for 7 or 8 days. The intermediate lobes were mechanically disintegrated and cultured as organotypic suspensions [6]. Both types of culture were fed every other day.

Incubations

Cultured cells were washed twice with tissue culture medium 199 (P199) containing 2.5 mg/ml bovine serum albumin (BSA) and subsequently incubated in the same medium or a medium containing one of the test substances for 2 h or for a longer period according to the protocol described in the Results. Thereafter control and test media were collected for later hormone radioimmunoassays. The cells were either homogenized for protein and/or hormone assays or fixed for electron microscopic examinations.

Electron microscopy

Control and treated cells were first fixed in 2.5% glutaraldehyde buffered at pH 7.4 with cacodylate at room temperature for 2 h. They were then washed overnight in the same buffer, post-fixed in 1% osmium tetroxide, and embedded in Durcupan ACM. For immunocytochemistry, the cells of monolayer cultures were fixed in a mixture of 4% paraformaldehyde, 1% glutaraldehyde in 0.1 M phosphate buffer of pH 7.4. or in some cases 2% paraformaldehyde, 1% glutaraldehyde in 0.1 M sodium cacodylate buffer (pH 7.4) containing 5% sucrose at 4 °C for 3 h. Some cultures were postfixed with 1% osmium tetroxide and embedded in Epon.

Ultrathin sections were mounted on bare copper or nickel grids, stained with Reynolds lead citrate and examined in a JEOL Temscan 100C electron microscope.

Radioimmunoassay and immunocytochemistry

GH and PRL in the media were assayed employing antibodies and protocols from the Rat Pituitary Distribution Program of the National Institute of Arthritis, Diabetes and Digestive and Kidney Diseases (NIADDK).

Alpha-MSH immunoreactivity was demonstrated using a protein A-colloidal gold techniqueas described by Stoeckel et al. [22].

Results

In eight-day-old suspension cultures, tissue spherules consist of tightly packed melanotrophs with pleomorphic secretory granules scattered evenly in their cytoplasm (Fig. 1). In some cells, the cytoplasm contains large mitochondria, more or less smooth and rough surfaced endoplasmic reticulum as well as seemingly empty vacuoles. The intercellular space is scarce with tiny cytoplasmic processes. Here and there cells are interconnected with stocky junctions.

The fine structure of cells incubated for 2 h in the presence of proteinase inhibitors shows similar features to the control cells. BOC-DPPA, while causing an enhanced hormone release into the medium [7] does not essentially alter cellular structures. DPhe-Pro-Arginal (DPPA), a less protected variant of the tripeptide aldehydes used, depletes slightly the secretory granules of the melanotrophs (Fig. 2), whereas well-developed Golgi regions show signs of undisturbed secretory granule formation (Fig. 3).

Alpha-MSH immunoreactivity was found over most secretory granules and in some endoplasmic reticulum cisternae in melanotrophs from the intact intermediate lobe (Fig. 4). In untreated eight-day-old suspension cultures, melanotrophs contain a large number of pleomorphic secretory granules which are highly reactive to alpha-MSH antibody (Fig. 5). Cells treated with proteinase inhibitors show fine structural features similar to their untreated counterparts. The number of immunoreactive secretory granules seems to be lower, especially in cells treated with DPPA (Figs 6 and 7). These findings are in good agreement with previous data on monolayer cultures of the intermediate lobe which released a high amount of alpha-MSH when the cells were incubated with these tripeptide aldehydes for 24 h [7].

In anterior pituitary cell cultures neither the parenchymal nor the non-parenchymal cells showed any sign of loss of their morphological integrity after having been exposed to tripeptide aldehydes for 2 or 4 h. In contrast, their hormone release into the medium was more than 50% less in comparison with control cultures as described previously [18, 19]. The same holds true

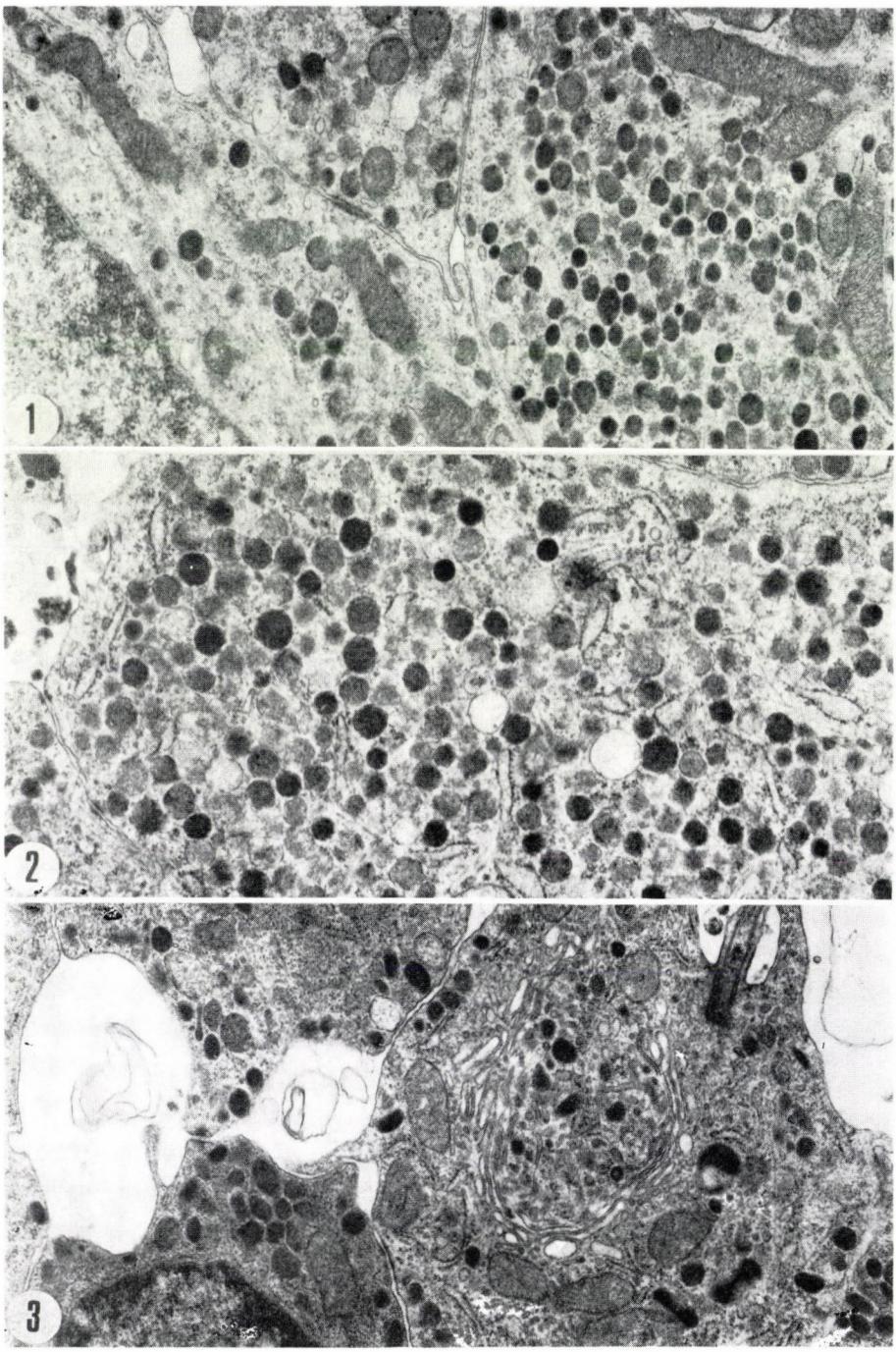

Fig. 1. Portion of untreated melanotrophs from an eight-day-old suspension culture. Note tightly packed cells with pleomorphic secretory granules. Arch. no.: 22 417. ×15 000

Fig. 2. Cytoplasmic details of two melanotrophs from an eight-day-old intermediate lobe culture treated with BOC-DPhe-Pro-Arginal (10^{-3} M) for 2 h. Arch. no.: 22 422. ×15 000

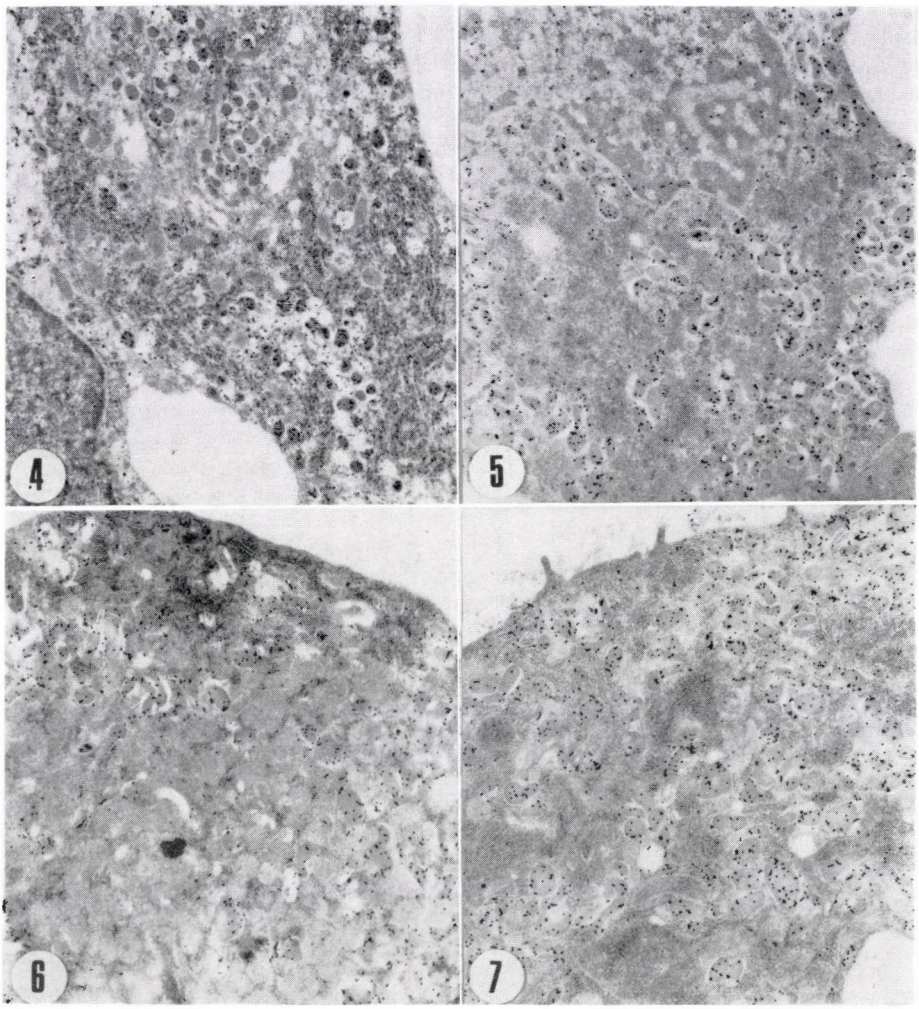

Figs 4—7. Alpha-MSH immunoreactivity in intermediate lobe cells. Fig. 4: untreated control cells before cultivation. Arch. no.: J-95 43 237/18. ×10 000. Fig. 5: portion of melanotrophic cells cultured in suspension for eight days. Note gold particles over most of the secretory granules. Arch. no.: J-95 32 235/7. ×14 000. Fig. 6: Cytoplasmic detail of a melanotroph from an eight-day-old culture treated with DPhe-Pro-Arginal (10^{-3} M) for 2 h. Moderate number of gold particles are seen over many secretory granules. Arch. no.: J-95 10 237/5. ×14 000. Fig. 7: Portion of a melanotroph from an eight-day-old culture treated with BOC-DPhe-Pro-Arginal (10^{-3} M) for 2 h. The number of gold particles over the secretory granules is similar to those of controls. Arch. no.: J-95 19 236/10. ×14 000

Fig. 3. Portion of cells from an eight-day-old suspension culture treated with DPhe-Pro-Arginal (10^{-3} M) for 2 h. Note a well-developed Golgi region with forming secretory granules. Arch. no.: 22 362. ×15 000

for cultures treated for 24 h with a potent enzyme inhibitor BOC-DPhe-Leu-Lysinal (Tab. I). The ultrastructural features after 24 h treatment with the enzyme inhibitor remained unchanged as demonstrated in Figs 8 and 9.

Table I

Inhibition of PRL and GH release into the medium by anterior pituitary cell cultures treated with BOC-DPhe-Leu-Lysinal for 24 h (n = 4)

	PRL	GH
	in μg/culture	
Control	3.51 ± 0.33*	20.6 ± 1.6
Treated	1.48 ± 0.12	9.0 ± 0.7

* mean ± SEM

In earlier experiments we suspected that the substrate analogue tripeptide aldehydes exert their hormone release inhibitory action on the cell membrane. Therefore we studied the membrane turnover of PRL and GH producing cells in anterior pituitary cell cultures in the presence of BOC-DPPL (one of the most potent inhibitor of PRL and GH release) [5] it binds to the plasma membrane of pituitary cells. The tracer (0.1—1.0 mg/ml) was applied alone or together with BOC-DPPL for up to 2 h.

In control cultures, cationic ferritin (irrespective of its concentration) labelled almost instantaneously the cell surface (Fig. 10) and was rapidly internalized in quickly formed endocytic vesicles. Within 5 min and later the endocytozed tracer was present in a variety of membrane-bound structures: in multivesicular bodies, lysosomes, tubules and Golgi saccules. Cationic ferritin was not present within the rough surfaced endoplasmic reticulum and it was not found in mature secretory granules of either mammotrophs or somatotrophs.

Thirty minutes (and later) after treatment with 10^{-4} M BOC-DPPL the secretory granules were numerous and some of them became highly amorphous in both mammotrophs (Fig. 11) and somatotrophs (Fig. 12). Tracer accumulation in vesicles could be found in between secretory granules in the parenchymal cells (Fig. 13). Within the Golgi complex small numbers of cationic ferritin molecules was frequently seen in multiple cisternae in a given stack and the largest concentrations were found in the transmost cisternae with condensing secretory granules (Figs 14 and 15).

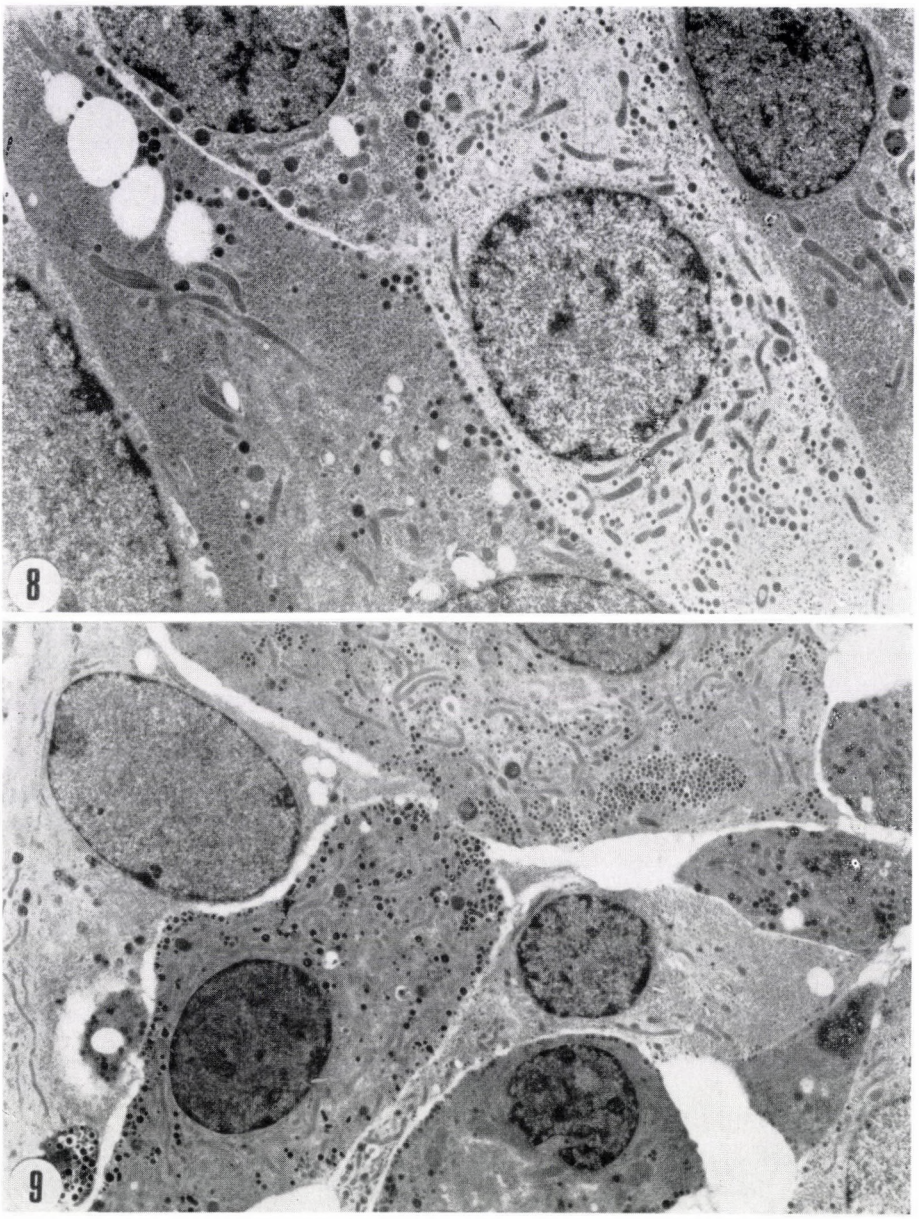

Fig. 8. Low-power electron micrograph of a monolayer culture derived from an untreated eight-day-old anterior lobe culture. Arch. no.: 16 949. ×5000

Fig. 9. Low-power electron micrograph of a monolayer culture derived from an eight-day-old anterior lobe culture treated with BOC-DPhe-Leu-Lysinal (10^{-3} M) for 24 h. Arch. no.: 16 958. ×5000

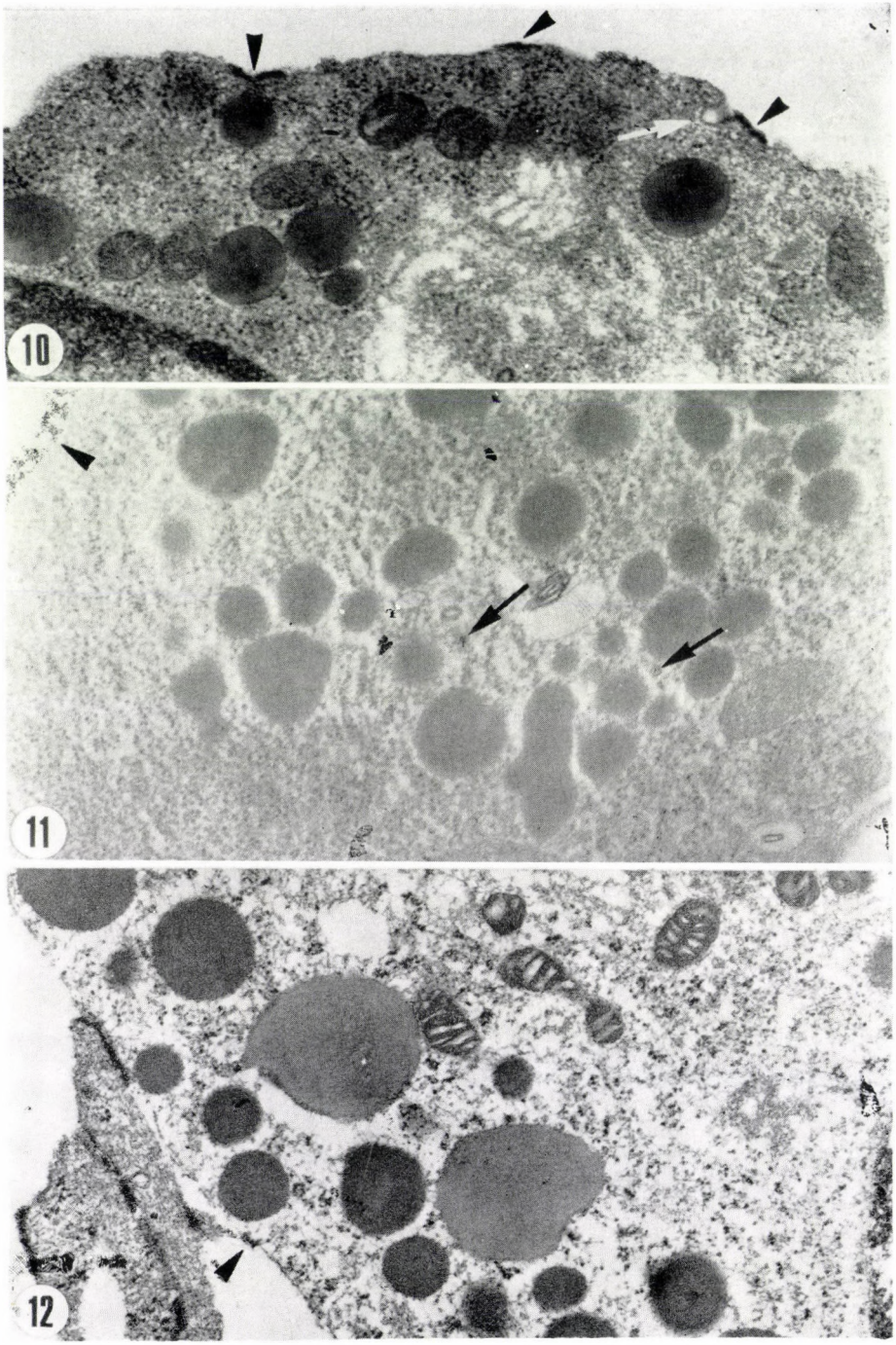

Figs 10—15. Electron micrographs taken from monolayer cultures of the anterior pituitary and labelled with cationic ferritin (CF). Fig. 10: CF (0.2 mg/ml) molecules line up on the cell surface (arrowheads) already after 20 s. Note (arrow) a coated pit without tracer. Control culture. Arch. no.: 20 685. ×30 000. Fig. 11: Prolactin secretory granules after treatment with BOC-DPhe-Phe-Lysinal (10^{-4} M) for 30 min. CF (0.5 mg/ml) is seen at the cell surface (arrowhead) and in small vesicles (arrows). Arch. no.: 26 919. ×24 000. Fig. 12: Growth hormone secretory granules after treatment with BOC-DPhe-Phe-Lysinal (10^{-4} M) for 30 min CF (0.5 mg/ml) molecules are at the cell surface (arrowheads). Arch. no.: 26 712. ×24 000.

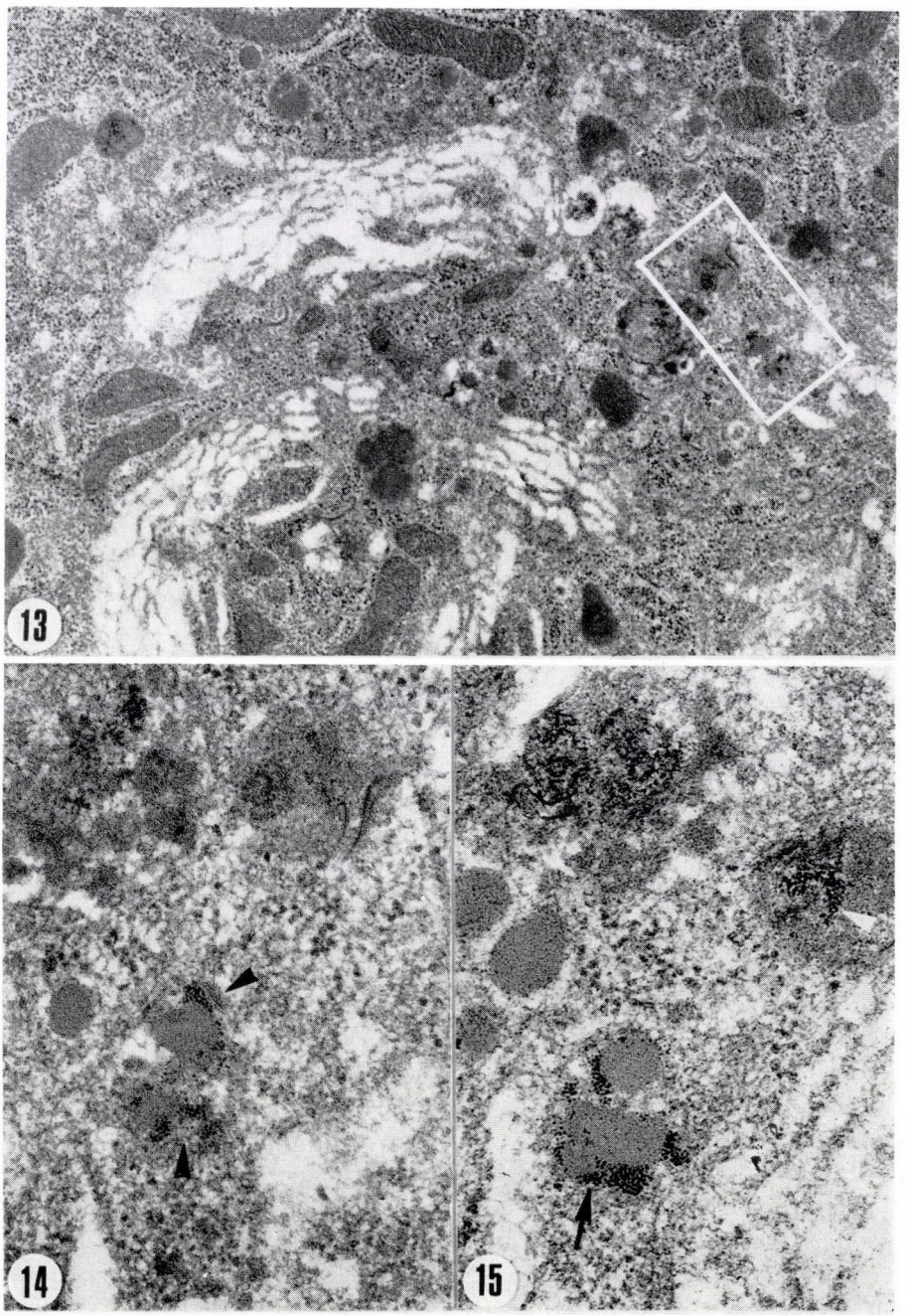

Fig. 13 Portion of the Golgi region of a pituitary cell treated with BOC-DPhe-Phe-Lysinal (10^{-4} M) for 30 min. Note undisturbed granule formation. Arch. no.: 26 723. ×16 000.

Fig. 14: A portion of the Golgi region shown in the previous figure. Note CF around forming secretory granuless (arrowheads). Arch. no.: 26 722. ×49 600.

Fig. 15: The same structures in a section adjacent to that displayed on the previous figure. CF is seen around (arrows) and within (arrowhead) secretory granules. Arch. no.: 26 721. ×49 600

Discussion

A few data presented above and a large body of evidence described earlier [18, 19] favour the view that substrate analogue tripeptide aldehydes may influence the release of at least four hormones produced by cultured hypophyseal cells. In the present study we demonstrated that some of the potent aldehydes are harmless to cells, i.e. they do not affect cellular morphology and membrane turnover. On the other hand, substances which had a stimulatory effect on ACTH and alpha-MSH release by intermediate lobe cells slightly diminish the number of alpha-MSH immunoreactive secretory granules.

Proteinase inhibitors or substrate analogues were frequently used in cell biology. According to Couch and Strittmatter [4] rat myoblast fusion requires metalloendoprotease activity. Experiments with proteinase inhibitors implicate metalloendopeptidase in synaptic transmission at the mammalian neuromuscular junction [2]. Metalloendopeptidase inhibitors prevent the release of histamine from mast cells as well as of catecholamines from adrenal chromaffin cells indicating that exocytosis may require endoproteinase activity [12]. A number of low molecular weight serine proteinase inhibitors, with differing specificities and modes of action, decrease human chorionic gonadotropin stimulation of ovarian adenylate cyclase [11, 20]. Chymotrypsin substrate analogues inhibit endocytosis of insulin and insulin receptors in adipocytes while causing a marked increase in surface-bound insulin by trapping insulin-receptor complexes on the cell surface [8]. In all these experiments the authors emphasized the non-toxic nature of the substances since cell viability tests were unaltered in their presence. To our knowledge, ultrastructural studies have not been published so far.

The possible targets of these substances are enzymes most probably localized in the cell membrane. However, until their exact demonstration the action of inhibitors and substrate analogues cannot be properly interpreted. Although target enzymes are mainly uncharted, promising experiments have been performed to show their presence in the cell membrane [9, 15]. Plasminogen activators and numerous plasminogen-independent proteases are present in ovarian membranes which may play a role in ovulation, luteolysis and mediation of hormonal stimulation [21].

The reason why relatively high concentrations of substrate analogues must be used to achieve proper effects on living cells remains to be elucidated. Nevertheless the membrane turnover using cationic ferritin as a tracer was undisturbed when BOC-DPPL was used in a concentration of 10^{-4} M. Its presence in the Golgi region, especially in the closed vicinity of the forming secretory granules, indicates that the tripeptide aldehyde treatment does not obviously interfere with hormone synthesis and packaging. In earlier studies

we have also demonstrated that the total biosynthesis of GH and PRL is slightly reduced only in the presence of the highest 10^{-3} M tripeptide aldehyde concentration, while the overall protein biosynthesis is totally unaffected [13, 14].

Acknowledgements

We thank the NIADDK and Dr. A. F. Parlow for the supply of RIA reagents, Dr. Z. Ács for supervision of hormone determinations, and Mr. I. Csapó for the photography. The skilful technical assistance of Ms. A. Deák, V. Garamvölgyi, Zs. Vadász and É. Vass is gratefully acknowledged.

REFERENCES

1. Barna I, Gráf L, Makara GB, Rappay Gy: A serine-proteinase inhibitor (BOC-D-Phe-Pro-Arg-H) inhibits the secretion of adrenocorticotropin- and endorphine-immunoreactive peptides in vitro. Neuropeptides 3: 65, 1982
2. Baxter DA, Johnston D, Strittmatter WJ: Protease inhibitors implicate metalloendoprotease in synaptic transmission at the mammalian neuromuscular junction. Proc Natl Acad Sci USA 80: 4174, 1983
3. Chertow BS: The role of lysosomes and proteases in hormone secretion and degradation. Endocr Rev 2: 137, 1981
4. Couch CB, Strittmatter WJ: Rat myoblast fusion requires metalloendoprotease activity. Cell 32: 257, 1983
5. Farquhar MG: Recovery of surface membrane in anterior pituitary cells. Variations in traffic detected with anionic and cationic ferritin. J Cell Biol R35—R42, 1978
6. Fazekas Ilona, Gyévai Angéla, Bácsy E, Rappay Gy: Rat intermediate lobe cell groups in suspension culture: morphological and functional characteristics. Acta Biol Acad Sci Hung 31: 69, 1980
7. Fazekas Ilona, Rappay Gy, Bácsy E, Medzihradszky-Schweiger H, Gyévai A, Gaál Gy: Dissimilar responsiveness of cultured corticotrophs and melanotrophs to tripeptide aldehydes. Histochem 84: 418, 1986
8. Jochen AL, Berhanu P: Chymotrypsin substrate analogues inhibit endocytosis of insulin and insulin receptors in adipocytes. J Cell Biol 103: 1807, 1986
9. Kellokumpu S, Rajaniemi H: Involvement of plasma membrane enzymes in the proteolytic cleavage of luteinizing hormone receptor. Endocrinology 116: 707, 1985
10. Loh YP, Gainer A: Characterization of pro-opiocortin converting activity of purified secretory granules from rat pituitary neurointermediate lobe. Proc Natl Acad Sci USA 79: 108, 1982
11. McIlroy PJ, Richert ND, Ryan RJ: Effects of proteinase inhibitors on adenylate cyclase. Biochem J 188: 423, 1980
12. Mundy DI, Strittmatter WJ: Requirement for metalloendoprotease in exocytosis: evidence in mast cells and adrenal chromaffin cells. Cell 40: 645, 1985
13. Nagy I, Makara GB, Horváth Gy, Rappay Gy, Kurcz M, Bajusz S: Serine protease inhibitors decrease in vitro prolactin and growth hormone (GH) secretion of the rat pituitaries. In: MacLeod, RM, Thorner, MO, Scapagnini U, (eds) Prolactin, Basic and Clinical Correlates, Fidia Res Ser., Vol. I, Liviana Press, Padova, 1985. p. 229
14. Nagy I, Makara GB, Horváth G, Rappay G, Kurcz M, Bajusz S: Tripeptide aldehyde protease inhibitors may depress in vitro prolactin and growth hormone release. Endocrinol 116: 1426, 1985
15. Orlowski M: Pituitary endopeptidases. Mol Cell Biochem 52: 49, 1983
16. Rappay Gy, Gyévai A, Kondics L, Stark E: Growth and fine structure of monolayers derived from adult rat adenohypophyseal cell suspension. In Vitro 8: 301, 1973
17. Rappay Gy, Makara GB: Release of hormonal substances: role of presumptive proteolytic enzymes in the discharge through the cell membrane. In: Röhlich P, Bácsy E (eds) Tissue Culture and RES, Akadémiai Kiadó, Budapest, 1984. p. 109

18. Rappay Gy, Nagy I, Makara GB, Horváth Gy, Kárteszi M, Bácsy E, Stark E: Inhibition of growth hormone and prolactin secretion by a serine proteinase inhibitor. Life Sci 34: 337, 1984
19. Rappay Gy, Makara GB, Bajusz S, Nagy I: Various proteinase inhibitors decrease prolactin and growth hormone release by anterior pituitary cells. Life Sci 36: 549, 1985
20. Richert ND, Ryan RJ: Proteolytic enzyme activation of rat ovarian adenylate cyclase. Proc Natl Acad Sci USA, 74: 4857, 1977
21. Roche PC, Ryan RJ: Electrophoretic analysis of membrane proteases in the luteinized rat ovary. Endocrinol 119: 495, 1986
22. Stoeckel ME, Schimechowitsch S, Garand JC, Schmitt G, Vaudry H, Porte A: Immunocytochemical evidence of intraglandular acetylation of alpha-MSH in the melanotropic cells of the rabbit. Cell Tiss Res 230: 511, 1983

Acta Morphologica Hungarica, 35 (3—4), pp. 157—174 (1987)

MORPHOLOGY OF THE HUMAN SEPTAL AREA: A TOPOGRAPHIC ATLAS

S. Horváth, M. Palkovits[1]

DEPARTMENT OF NEUROLOGY AND[1] FIRST DEPARTMENT OF ANATOMY, SEMMELWEIS UNIVERSITY MEDICAL SCHOOL, BUDAPEST, HUNGARY

(Received 13 March 1987)

The cell-groups of the human septum pellucidum are demonstrated in a series of 27 frontal sections. The basal part of the septum which contains mainly nerve cells extends 14—16 mm in the oro-caudal direction. Within this region two medial nuclei with 6 subdivisions and two lateral nuclei with 3 subdivisions were distinguished. The definition of oro-caudal coordinates and the topographical description of nuclei may be of help in localizing with sufficient accuracy clinico-pathological alterations of the septum.

Keywords: Septum pellucidum, septum verum

Introduction

Until recently a general view shared by neurologists and neuropathologists was that the septum, an important element in the limbic system of the mammalian CNS, has regressed in the human brain to an insignificant structure, hence its clinical role is also negligible. As compared to the total brain volume the volume of the septum is indeed the smallest in man among all vertebrates, still data are available [2, 3] suggesting that it is not fully justified to suppose a morphological reduction in the human septum.

The human pathological role of the septum has been underlined by recent observations. Unusually large septal nuclei were found in the New-Guinea fore-tribesmen died in kuru [3]. The significance of this finding is still unclear [15]. Septal malformations result in well-defined clinical symptoms [11, 17]. Tumours and aneurysms causing septal lesions lead to memory disturbances mainly amnestic syndrome and personality changes [1, 9, 18, 20, 24, 25, 27]. In Alzheimer's disease the early lesion of the cholinergic septo-hippocampal tract has been observed [4, 12, 26]. Septal diseases were so far related to the septum as a whole. Lacking detailed information on septal cytoarchitectonics no attempts were made to localize septal alterations to individual cell groups.

Send offprint requests to Dr. M. Palkovits, First Department of Anatomy, Semmelweis University Medical School, Budapest, Tűzoltó u. 58. H-1450, Hungary

In the rat, the septum is one of the structures richest in neurotransmitters: at about 40 neurotransmitters have been detected in septal neurons and nerve endings [21]. Currently the topographical mapping of neurotransmitters in human brains is a rapidly expanding field of research. Correlation of results with experimental data obtained in animals is possible only if detailed and accurate morphological data are available. However, little is known concerning the cytoarchitectonics and topography of the human septum [2, 6, 10]. To our knowledge, a topographical atlas describing nuclei of the human septum in a coordinate system being thus useful also in practical neuropathology has not yet been published. The present work is aimed to abridge this gap.

Materials and methods

The brain of a 40-year-old male killed in a traffic accident was fixed in 4% formaldehyde for 2 months, then sliced in the frontal plane. The septal region was excised in two blocks and embedded in paraffin. Serial sections of 10 μm thickness were cut in the frontal plane and each 40th and 41st sections were alternatingly stained with luxol fast-blue cresyl violet according to Klüver and Barrera [14] and with cresyl-violet. Linear shrinkage caused by the histochemical procedure was regarded as 30% [22]. Thus distance between two consecutive sections stained with the same method was estimated to 520 μm.

The sections were photographed and the septal nuclei were delineated and subdivisions defined on the basis of cell packing densisy; staining intensity, size of cells and cell nuclei. The topographical division obtained was correlated with the cytoarchitectonic atlas of the rat septum [13] prepared by quantitative histological analysis, to identify nuclei and nuclear groups. The atlas was also compared with the human histological preparations of the Laboratory of Neuropathology of the Neurological Clinic, Semmelweis University Medical School. Identification of septal nuclei was carried out in dozens of differently stained preparations derived from individuals of different sex and age.

Results

The human septum is found in the midline of the rostral telencephalon with some parts extending slightly laterally to the midline. Its borders are: from above, the corpus callosum, from lateral the lateral ventricles, from oral, the subcallosal gyrus, from ventrolateral, the nucleus accumbens and the interstitial nucleus of the stria terminalis, ventrally the preoptic region, anterior hypothalamus and the anterior commissure. It can be divided into two parts: the dorsally located septum pellucidum containing in its caudal part a few neurons in addition to myelinated fibres and glial cells, and the ventral area termed by Andy and Stephen as "septum verum" [2] containing predominantly nerve cells. As compared to other species, the human septum is markedly elongated in the dorsoventral direction.

For orientation we have used the frontal plane of the septum and the oro-caudal coordinates as related to the plane of the bregma, a reference-line

used often in rat and in a number of other mammals. This plane is defined by the level of encounter of fornical fibres and the crossing anterior commissural fibres. Both structures are easy to recognize even in unstained sections. In our coordinate system this plane was regarded as "0-plane", structures located orally to it were designated with A (anterior), the caudal ones with P (posterior).

The so-called „septum verum" containing mainly nerve cells begins 7800 μm orally to the 0-plane (A7800) and with some individual variations extends to 6 to 8000 μm caudally to it. Thus its total length is 14 to 16 mm. Its largest dorsoventral diameter is 12 mm, its thickest part is about 8.2 mm wide.

The pellucidal part has a much larger oro-caudal span: it can be followed from the genu of the corpus callosum to the meeting of the fornical bundles with the corpus callosum. Its dorso-ventral span is caudalwards gradually decreasing. Caudally, along the myelinated fibres more and more neurons appear scattered between the glial cells. Dorsally they reach the lower level of the corpus callosum.

In the human septum all four nuclei determined by the quantitative study of the rat septum [13] as well as the nucleus of the diagonal band (of Broca) are to be found and delineated (Figs 1—7). Grouping of nuclei of the human septum is summarized in Table I, their oro-caudal extension is shown in Fig. 8.

Table I

Nuclei and subdivisions of the human septum

Nuclei and subdivisions of the medial area
Medial septal nucleus
pars dorsalis
pars ventralis
pars fimbrialis
pars intermedia
pars posterior
Triangular nucleus
Nucleus of the diagonal band (of Broca), vertical part
Nuclei and subdivisions of the lateral area
Dorsal septal nucleus
Lateral septal nucleus
pars anterior
pars dorsalis
pars ventralis

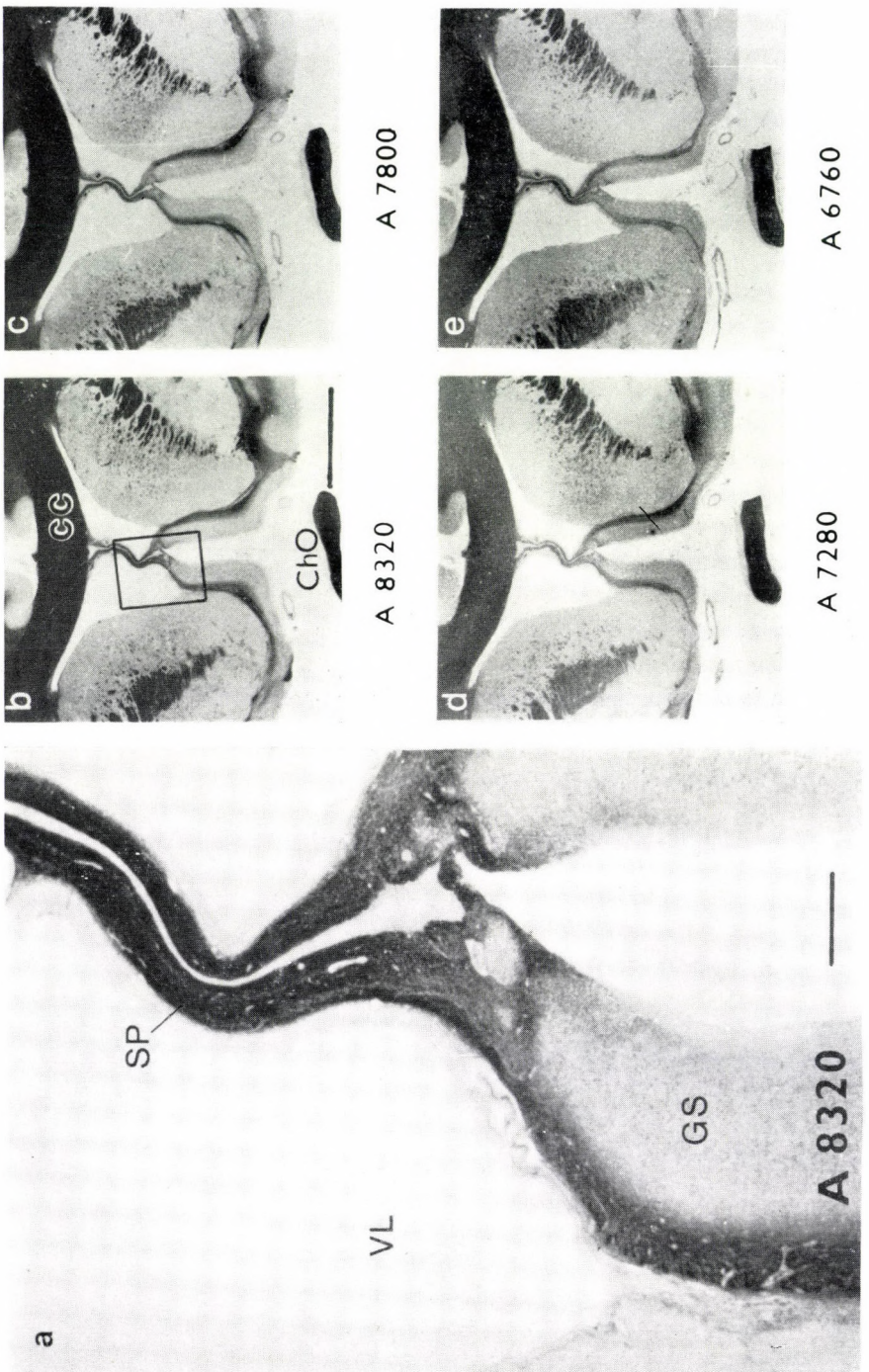
a
SP
VL
GS
A 8320
b
cc
ChO
A 8320
c
A 7800
d
A 7280
e
A 6760

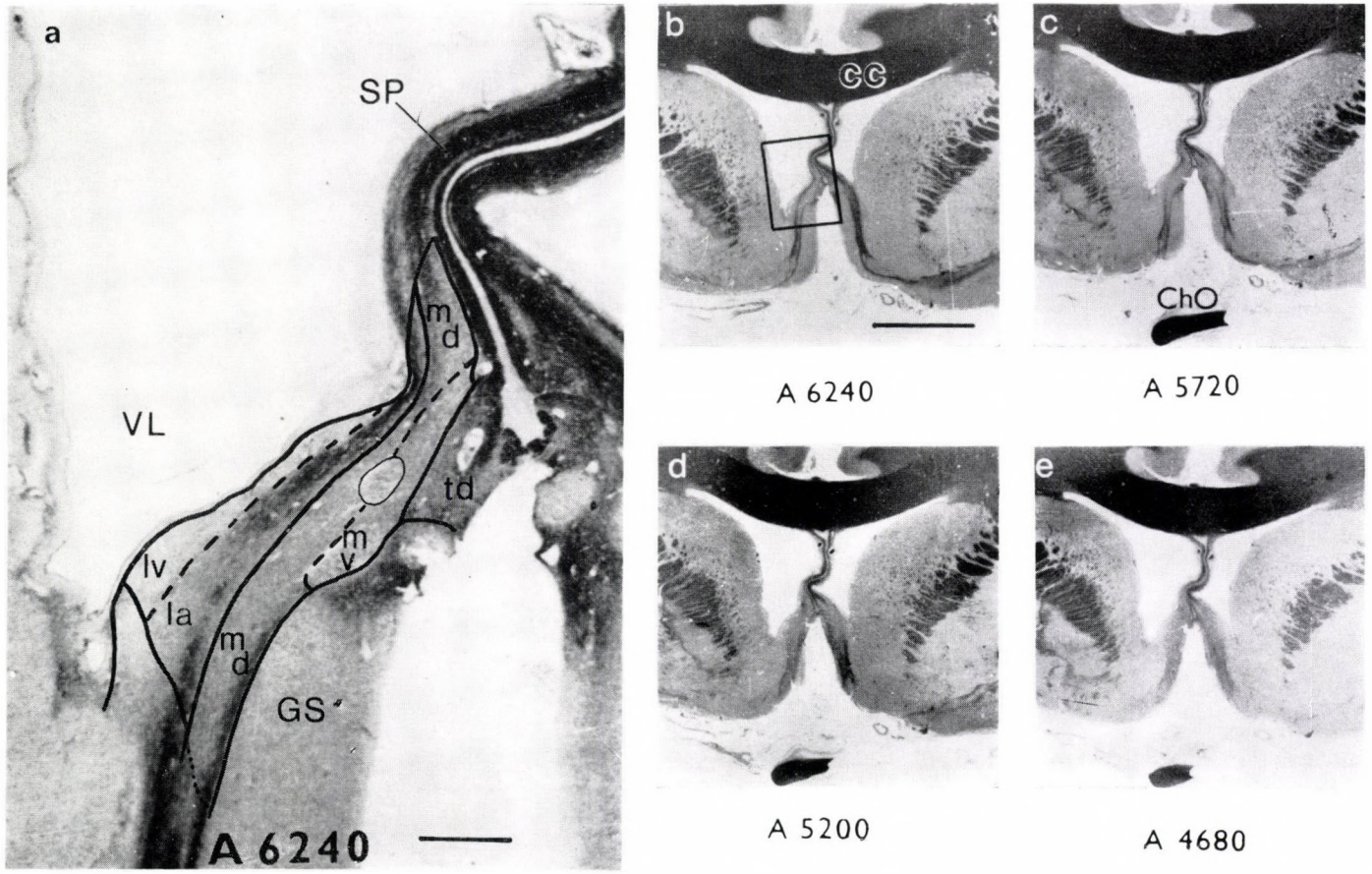
a
SP
md
VL
td
mv
lv
la
md
GS
A 6240
b
CC
A 6240
c
ChO
A 5720
d
A 5200
e
A 4680

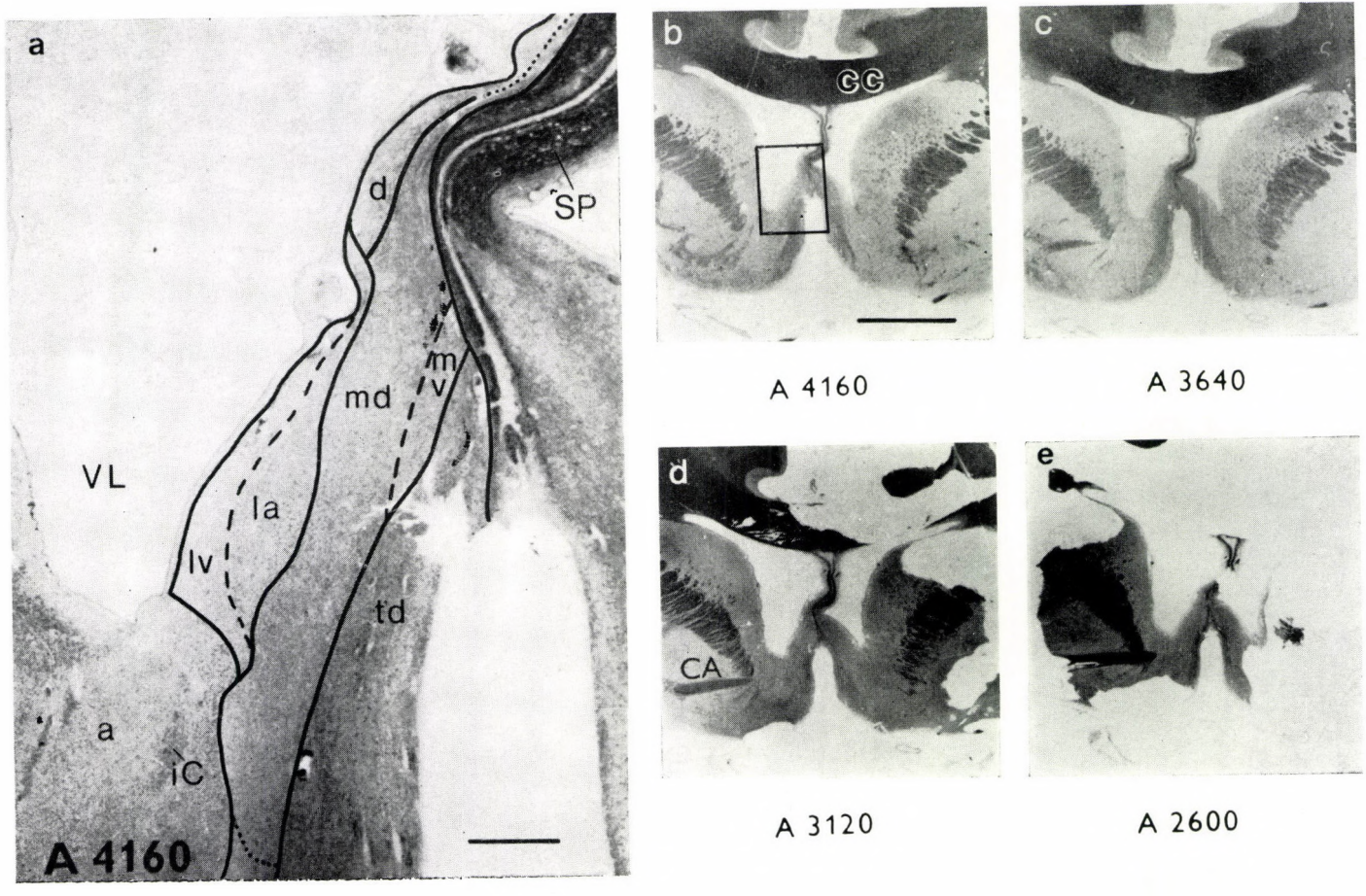
a
d
SP
m
v
md
VL
la
lv
td
a
ic
A 4160
b
cc
A 4160
c
A 3640
d
CA
A 3120
e
A 2600

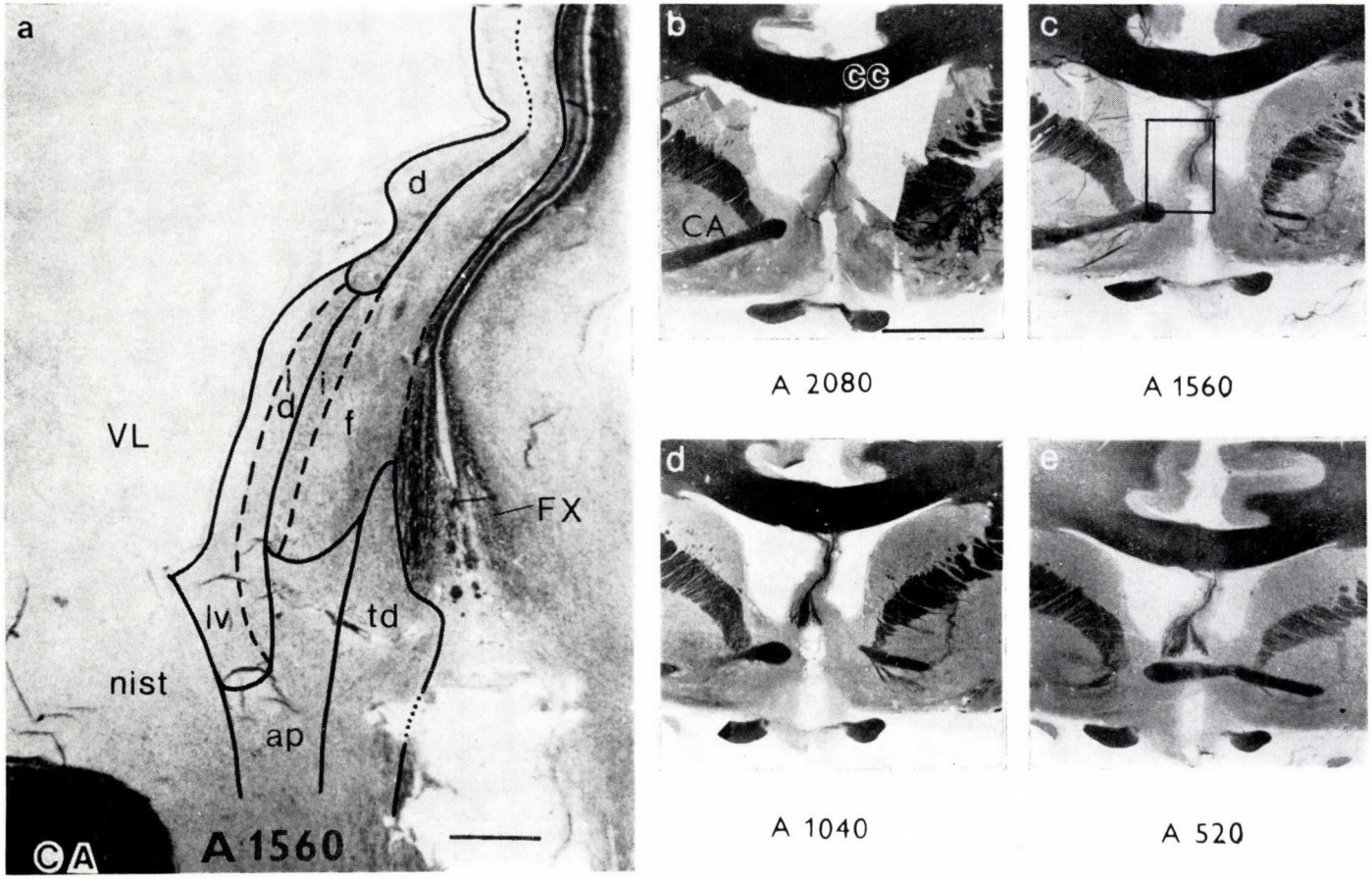
a
d
d
f
VL
FX
lv
td
nist
ap
CA
A 1560
b
CC
CA
A 2080
c
A 1560
d
A 1040
e
A 520

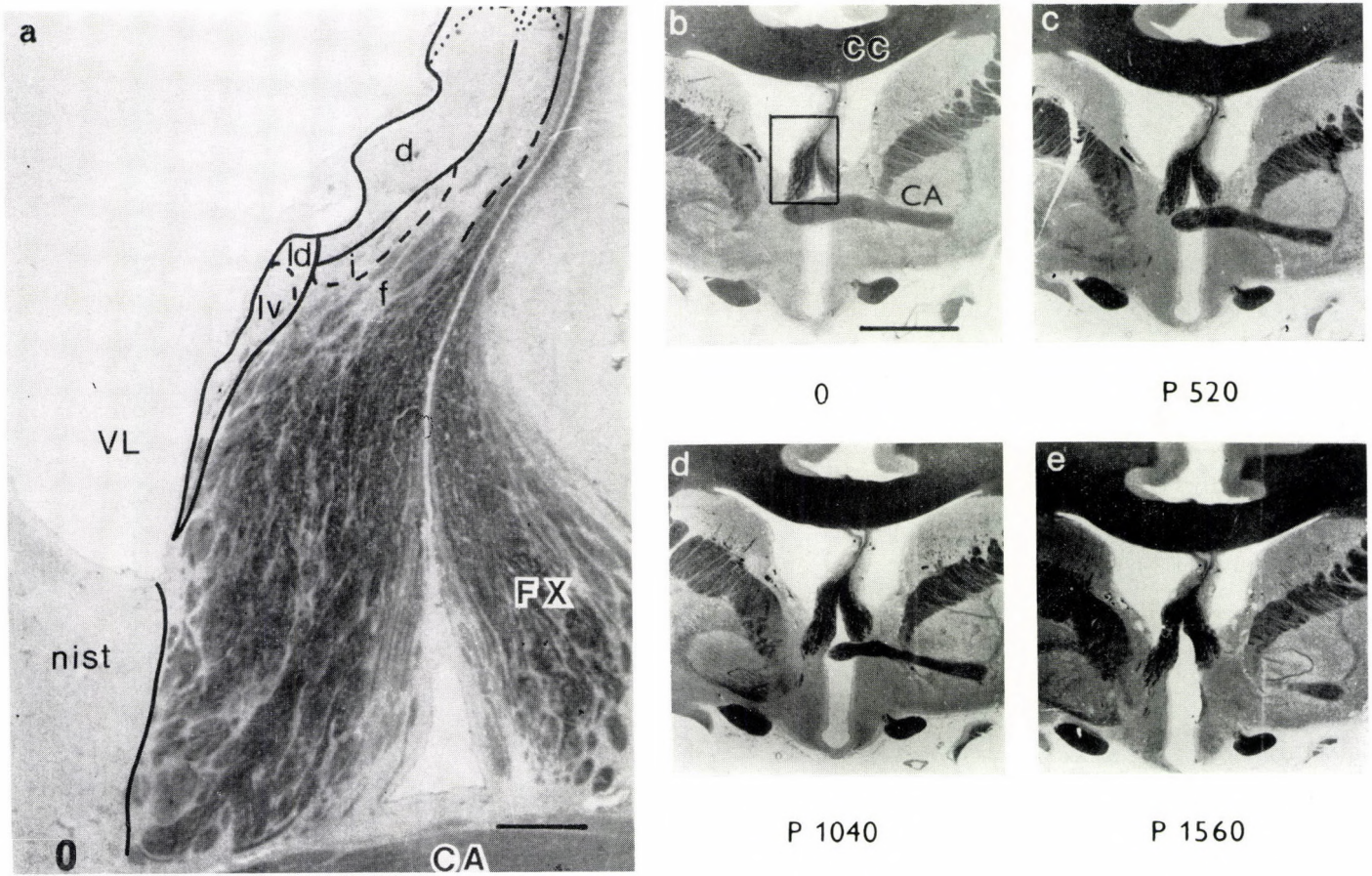
a
d
ld
i
lv
f
VL
FX
nist
0
CA
b
cc
CA
0
c
P 520
d
P 1040
e
P 1560

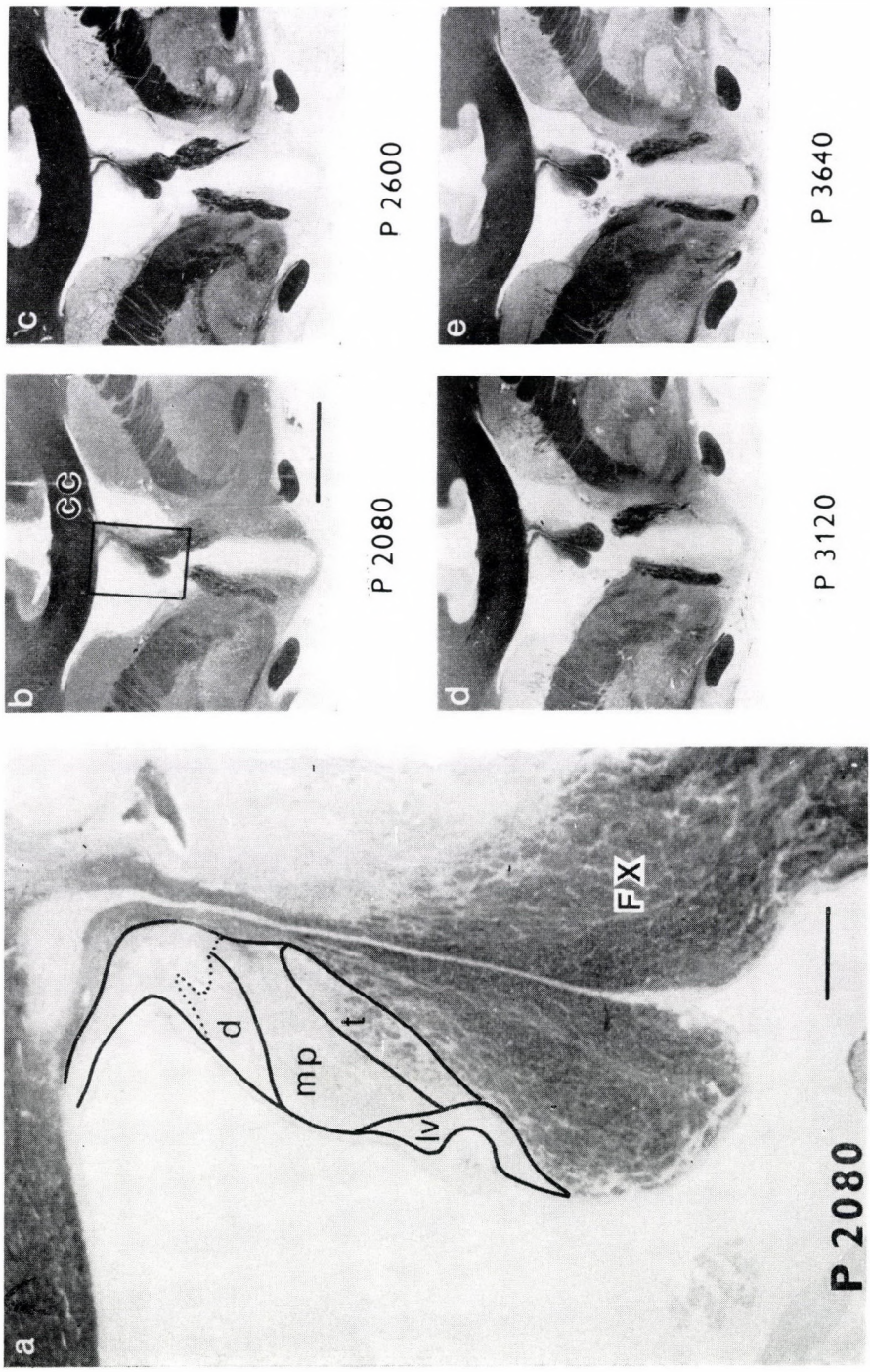
a
d
mp
t
lv
FX
P 2080
b
cc
P 2080
d
P 3120
c
P 2600
e
P 3640

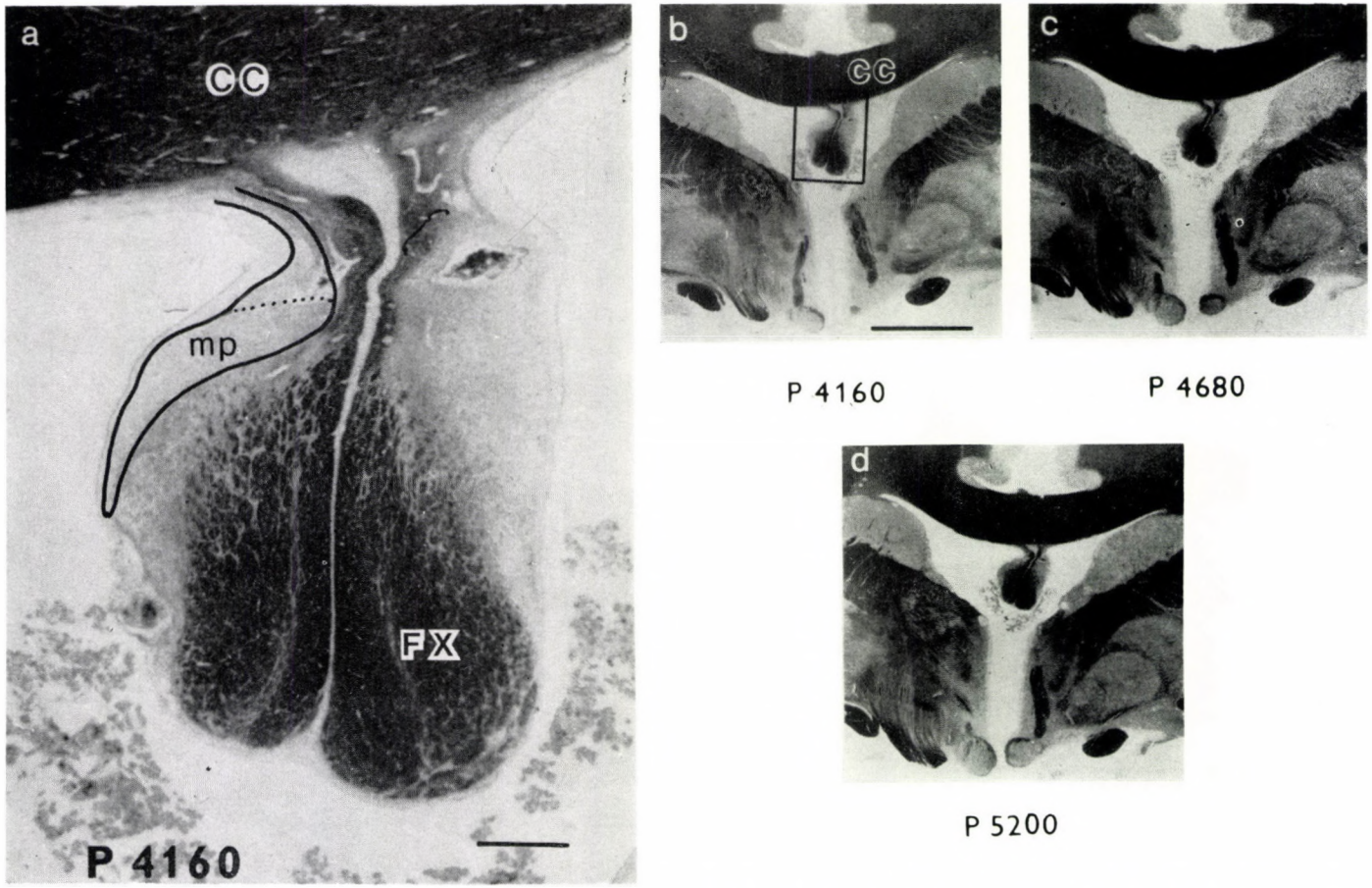

Figs 1—7. Topography of nuclei and subdivisions of the human septum as seen in photographs of frontal serial sections from 8320 μm oral to the 0-plane (A = anterior) to 5200 μm caudal to the 0-plane (P = posterior). 0-plane = the frontal plane at the level of the encounter of anterior commissure fibre-crossing and the diverging fornix-stems. Klüver—Barrera staining [14]. (a) Borders of nuclei and subdivisions. Bar scale: 1 mm. For abbreviations see list. (b—e) Photographs of frontal serial sections. Square shows the position of (a). Bar scale: 1 mm

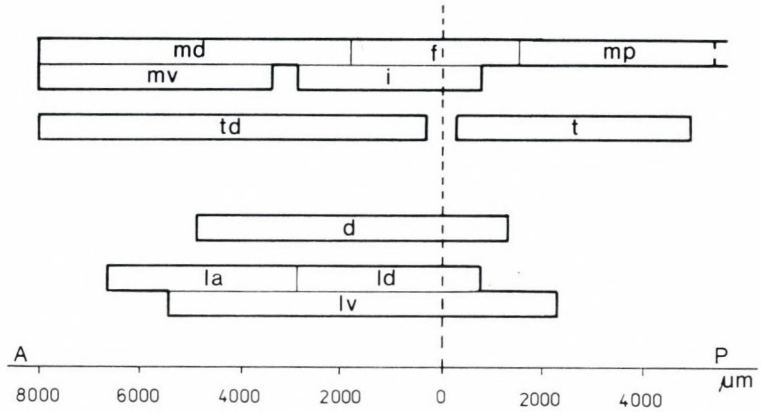

Fig. 8. Oro-caudal coordinates of nuclei and subdivisions of the human septum. Coordinates: see Figs 1—7; for abbreviations see list

I. Medial cell group

The medial cell group of the septum comprises the medial and triangular septal nuclei and the nucleus of the diagonal band.

(1) Within the medial septal nucleus (m), similar to the rat septum, five subdivisions are to be discerned:

Pars dorsalis of medial septal nucleus(md). This cell group is located in the oral and middle thirds of the so-called "septum verum" (Fig. 8). In the oro-caudal direction its cells are first apparent at A7280 μm, dorsally in the midline, ventrally along the diagonal band (of Broca) and the lateral edge of subcallosal gyrus (Figs 2, 3). To caudal it can be followed to A2080 μm. From lateral it is bordered in oro-caudal order by the lateral septal nucleus, the pars intermedia of the medial nucleus and the dorsal nucleus (Figs 2, 3). Its cells are large, slightly elongated or multipolar with medium light staining. At some places they form groups of higher packing density (Fig. 9). From the nuclei of the lateral septum and the ventral cell group of the medial nucleus, it can be distinguished by its larger cells, while from the dorsal septal nucleus it differs in the higher packing density of its cells. On the other hand, its cells are not as densely packed as those of its caudal neighbour, the pars intermedia, and does not contain giant cells typical for its medial neighbour, the nucleus of the diagonal band. To caudal the volume of this subdivision increases but it is there replaced by the pars fimbrialis.

The *pars ventralis of medial septal nucleus (mv)* is an orally bigger, caudally thinning cell group. It is situated between A7800 and A3640, laterally to the nucleus of the diagonal band and the subcallosal gyrus (Fig. 8). From lateral, it is bordered by the pars dorsalis of the medial nucleus (Figs 2, 3) of which it is well demarcated by its smaller and irregularly shaped cells.

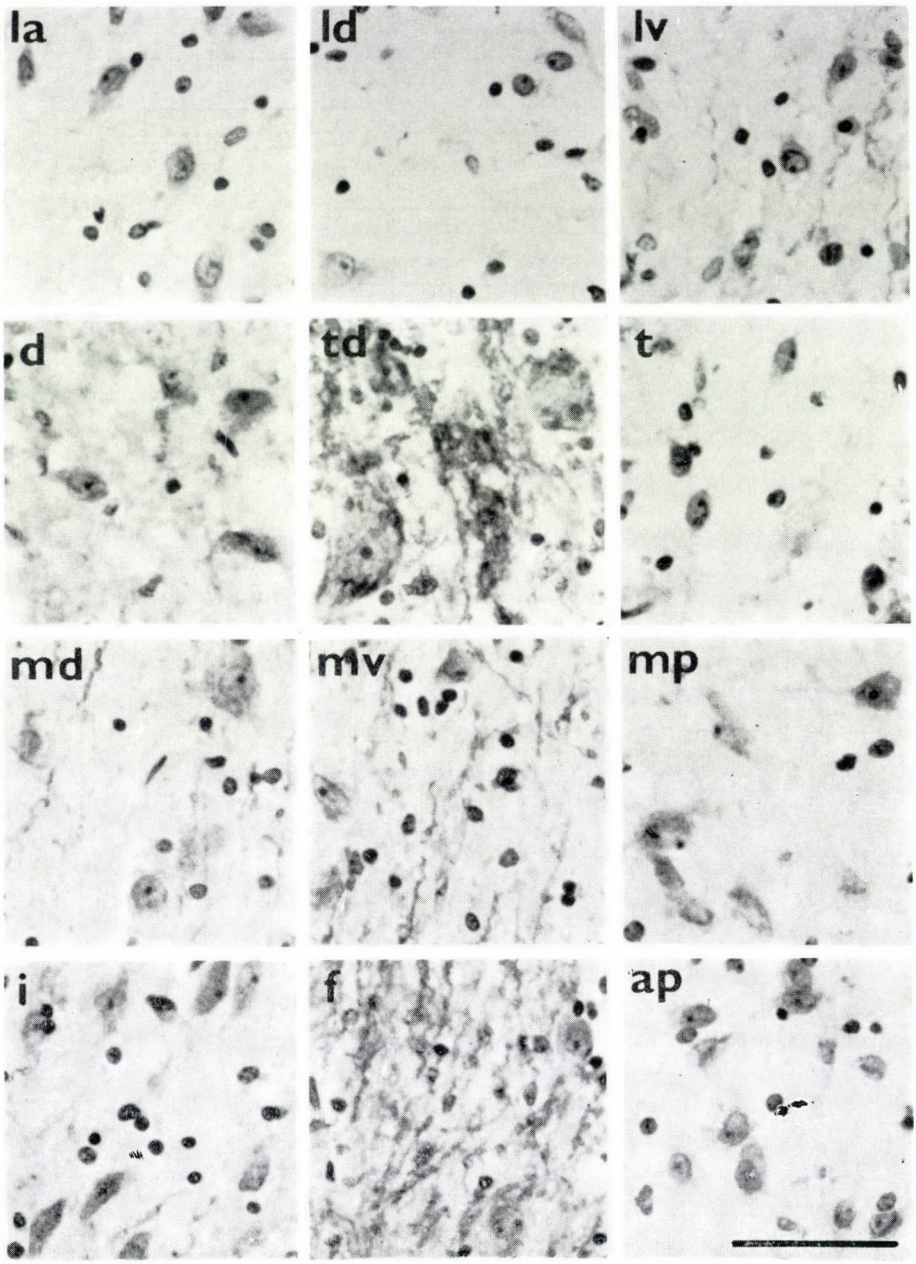

Fig. 9. Characteristic cell-types of nuclei and subdivisions of the human septum. Klüver—Barrera staining [14]. Bar scale: 50 μm; for abbreviations see list

These cells stain medium light (Fig. 9). Its hind border is vague by the mixing of its cells with those of the dorsal subdivision of the nucleus.

Pars fimbrialis of medial septal nucleus (f). The beginning of this subdivision is marked by the appearance of fibres of the fimbria septi, at A1560 (Fig. 4). Its cells are scattered between fimbrial fibres. They resemble the dorsal subdivision cells but a few solitary large cells and some groups of small cells between the fibres are also to be observed (Fig. 9). This subdivision extends caudally to P1040 μm (Fig. 8).

Pars intermedia of medial septal nucleus (i). This is a dorsoventrally extended narrow cell-column between A2600 and P520 μm (Figs 4, 5). Its cells are elongated and relatively darkly stained (Fig. 9). It appears to be the cell group of the human septum having the highest packing density. From lateral, the lateral and dorsal septal nuclei, from medial and ventral, the dorsal and fimbrial parts of medial nucleus form its borders.

Pars posterior of medial septal nucleus (mp). It is found in the hind portion of the septum, dorsolaterally from the triangular nucleus and from the fibres of the formix and fimbria septi, between P2080 and P5200 μm (Figs 6—8). The caudal extension of this cell group shows substantial individual variations, in some cases it reaches to P6000—8000 μm. Concerning its position and cell types it corresponds to the pars interstitialis commissurae fornicis of the rat medial septal nucleus.

(2) *Triangular nucleus (t).* This nucleus is found dorsolaterally to the fibres of the fornix and fimbria septi, between P520—P4680 μm (Figs 6, 8). A cell group of relatively high packing density with medium darkly staining, usually small and irregular cells (Fig. 9). Upon inspection it appears to be smaller relative to the whole septum in man than in rat.

(3) *Nucleus of diagonal band (of Broca ; td).* This nucleus does not belong to the septal nuclei, not even in species where both the septum and this nucleus are particularly well-developed. However, a part of the nucleus, the vertically situated cells extend to the territory of the septum therefore, it is generally mentioned when surveying the topography of the septum. The vertical cell group entering from below the septum, appears first orally at A7800 μm, above the subcallosal gyrus. Caudally it can be followed for A520 μm (Figs 2—4, 8). This midline nucleus contains both small and giant cells (Fig. 9). Due to the latter its identification and demarcation is rather obvious. From lateral it is bordered by the dorsal and ventral subdivisions of the medial nucleus.

II. The lateral cell group

In the lateral part of the septum, the dorsal and lateral nuclei and the 3 subdivisions of the latter can be distinguished.

(1) *Dorsal septal nucleus (d).*As it is indicated by its name, this nucleus occupies the dorsal, dorsolateral edge of the septum between A4680 and P1040 μm (Figs 3—6, 8). Its cells and cell nuclei are mostly large, pale and slightly more elongated than the cells of the adjacent dorsal subdivision of medial nucleus (Fig. 9). Sporadic giant cells are to be observed. However, the delineation of a magno-cellular subdivision, unlike to that in the rat septum, is not possible.

(2) *Lateral septal nucleus (l).* Similarly to the lateral septal nucleus of the rat, its human analogue contains also three nuclear groups:

Pars anterior of lateral septal nucleus (la) occupies the oral part of lateral corner of "septum verum", between A6240 and A3120 μm (Figs 2—3, 8). Its relatively small, pale cells having lightly stained nuclei can readily be distinguished from the dorsal subdivision of the medial nucleus lying medially to it (Fig. 9).

The *pars dorsalis of lateral septal nucleus (ld)* is found caudally to the pars anterior, between A2600 and P520 μm, at the upper region of the lateral area (Figs 4, 5, 8). It differs from the other two subdivisions of the lateral nucleus by its cells larger than those of the ventral subdivision and more darkly stained than those of the anterior subdivision (Fig. 9).

Pars ventralis of lateral septal nucleus (lv) is distinguished from its surrounding by its close topographic relationship to the ventral edge of the ventricle rather than by its cellular packing density (Figs 2—6). It reaches over a long distance between A520 and P2080 μm (Fig. 8), its cells are most compact between A1560 and A1040 μm; while its oral segment is rather poor in cells.

Discussion

The septal area in man consists of two parts, from the dorsally located so-called "septum pellucidum" and the ventrally located so-called "septum verum" [2]. The septum pellucidum is a phylogenetically new plate-like structure extending from the ventral aspect of the corpus callosum. It separates the lateral ventricles and contains mainly fibres and glial cells. Its position is defined by the corpus callosum growing rapidly due to the extensive development of the cortex and by the relatively lesser volume-increase of the ventral septum [2, 16]. Under the septum pellucidum is found the "septum verum" which corresponds to the septum in animals.

Previous studies and definitions of septal nuclei both in man and in animals, involved a great deal of subjective assessment. As a result, a diversity exists in terminology and the delineation of nuclear borders is often somewhat arbitrary. In rats we were able to introduce a computer-analysis technique

[13] by which 4 septal nuclei with 10 subdivisions could objectively be distinguished and borders safely be determined. A similar study of the human septum revealed also 4 nuclei with 9 subdivisions, all well recognizable and cytoarchitectonically discernible. Nevertheless, orientation in terminology, identification of synonymous terms presented a considerable difficulty. The value of a number of relevant observations and descriptions was reduced by the difficulty of correlation due to the lack of the use of a coordinate system and to the diversity of terminology.

Medial septal nuclei and their subdivisions

The dorsal, fimbrial and posterior subdivisions show a cytomorphological similarity: cells are mainly medium-sized and stain medium light; they are round or slightly elongated. Their differentiation is primarily topographical. By contrast, the medial subdivision contains smaller cells, while those of the pars intermedia are more elongated, more densely packed and darkly stained as compared to the other subdivisions of this nucleus. The dorsal subdivision corresponds to the pars posterior of medial septal nucleus of Andy and Stephan [2], and to the pars intermedio-lateralis of Gaspar et al. [10].

With the appearance of fimbrial fibres caudally from the oro-caudal plane equal to A1560 μm, the dorsal subdivision of medial nucleus continues into the cell group of the pars fimbrialis. Their cellular patterns differ by the heterogeneity of the cell population of pars fimbrialis. This latter contains a mixed population of small and large cells with a few giant cells. Small cells are arranged in groups between fimbrial fibres. This subdivision corresponds to the septo-fimbrial nucleus of Andy and Stephan [2] and Gaspar et al. [10].

The pars intermedia is a compact cell column mostly composed of elongated cells situated laterally to the pars dorsalis and pars fimbrialis of the nucleus. In the rat this subdivision shows the highest cell nucleus/neurophil ratio [13]; also in man this is the structure of the septum richest in cells. Andy and Stephan [2] termed it as the dorsal septal nucleus, while Gaspar et al [10] called it the pars interna of the dorsolateral nucleus.

The ventral subdivision of the medial nucleus is rather difficult to delineate either in the rat or in man. It can be identified with the medial part of the pars anterior of medial septal nucleus of Andy and Stephan [2].Gaspar et al [10] make no mention of this cell group.

As to its position, the pars posterior of the medial nucleus corresponds to the pars (nucleus) interstitialis of the commissure of the fornix. Due to its larger cells it can be distinguished from the triangular nucleus, while the darkly staining cytoplasm and nucleus of its cells it differ markedly from the dorsal nucleus. Andy and Stephan [2] do not describe this as a distinct cell group. In their work quoted this area is called the dorsal nucleus but they do

not identify it with any of our four subdivisions. Nor do Gaspar et al [10] describe this cell group. Although from the cytoarchitectonical point of view they are identical the use of the mammalian term interstitial nucleus of the commissure of the fornix is thought to be not quite appropriate for the human septum as the hippocampal (fornical) commissure is far to ventral from the cell group proper, hence the term "interstitial nucleus" makes no topographical sense.

The septal triangular nucleus is found dorsolaterally to the fimbria septi and the fornix. Along these structures it can readily be distinguished as a caudally extending cell group containing small, darkly staining cells which render it different from the overlying pars posterior of medial nucleus. Concerning the topography of this nucleus views are divergent both for the rat and man. Andy and Stephan [2] describe as triangular nucleus a cell group above the hippocampal commissure and underneath the fibres of the fornix containing a few round cells. They note that it is a cell group difficult to define and its volume is small as compared to other septal nuclei. Crosby et al [8], Nauta and Haymaker [19] and Brown [7] use the term "triangular nucleus" to denote a cell group above the fornix, i.e. much more rostral than in our interpretation. This cell population, according to Swanson and Cowan [23] corresponds in the rat to the median cell group of the preoptic nucleus. This is suggested for the human septum by the documentation of Andy and Stephan [2] and this view is shared by Gaspar et al [10].

The nucleus of the diagonal band (of Broca) can be divided also into a ventrical and a horizontal cell group extending into the septum and the preoptic area, respectively. The typical giant cells are of help in distinguishing this nucleus from its surrounding. It corresponds to the similarly termed cell group of Andy and Stephan [2], while Gaspar et al [10] call it medial septal nucleus.

Lateral septal nuclei and their subdivision

The lateral part of "septum verum" is occupied dorsally by larger, in the centre and ventrally by smaller cells.

In terms of cytoarchitectonical division of the rat septal region, the dorsolateral area of the human septum containing mainly large cells is considered as the dorsal septal nucleus. The upper part of the ventrolateral region containing small and medium-sized cells is considered by Andy and Stephan [2] and by Gaspar et al. [10] as belonging to the dorsal nucleus. Andy and Stephan [2] distinguish four subdivision within the dorsal nucleus of which only the pars externa containing relatively large cells corresponds to our dorsal nucleus. On the other hand, the pars intermedia of dorsal septal nucleus is in our terminology identical with the pars dorsalis of the lateral nucleus.

Within the human dorsal septal nucleus we failed to delineate the magno- and parvocellular subdivisions described for the rat [13].

Similarly to the rat septum [13], three subdivisions were distinguished in the human septum. Cell nuclei of the pars anterior are paler than those of the pars dorsalis, while its cells are larger than those of the ventral subdivision. Thi slatter is separated by a cell-poor zone from the nucleus accumbens and the bed nucleus of the stria terminalis.

Andy and Stephan [2] have divided the lateral nucleus into two subdivisions. Their pars externa corresponds to our pars ventralis whereas their pars interna, as suggested by their description, might be identical with a portion of the pars dorsalis of the lateral nucleus. Our third subdivision, the pars anterior is analogous to the lateral part of the pars anterior of medial nucleus of Andy and Stephan [2].

List of abbreviations

ap — area parolfactoria
CA — anterior commissure
CC — corpus callosum
ChO — optic chiasma
d — dorsal septal nucleus
dm — dorsal septal nucleus, magnocellular part
dp — dorsal septal nucleus, parvocellular part
f — medial septal nucleus, fimbrial part
FX — fornix
GS — subcallosal gyrus
i — medial septal nucleus, pars intermedia
iC — insula magna (of Calleja)
la — lateral septal nucleus, pars anterior
ld — lateral septal nucleus, pars dorsalis
lv — lateral septal nucleus, pars ventralis
md — medial septal nucleus, pars dorsalis
mp — medial septal nucleus, pars posterior
mv — medial septal nucleus, pars ventralis
nist — bed nucleus of the stria terminalis
t — septal triangular nucleus
td — nucleus of the diagonal band (of Broca)
VL — lateral ventricle

REFERENCES

1. Alexander M–P, Freedman M: Amnesia after anterior communicating artery aneurysm rupture. Neurology 33 (Suppl 2): 104, 1983
2. Andy OJ, Stephan H: The septum in the human brain. J Comp Neurol 133: 383, 1968
3. Andy OJ, Stephan H: Septum development inprimates. In: DeFrance JF (ed.) The Septal Nuclei. Plenum Press, New-York 1976, p. 3.
4. Arendt T, Bigl V, Arendt A, Tennstedt A: Loss of neurons in the nucleus basalis of Meynert in Alzheimer's disease, Paralysis agitans and Korsakoff's disease. Acta Neuropathol (Berl) 61: 101, 1983
5. Beck E, Gajdusek DC: Variable size of the septal nuclei in man. Nature 210: 1338, 1966
6. Brockhaus H: Zur feineren Anatomie des Septum und des Striatum. J Psychol Neurol 51: 1, 1942

7. Brown JW: Early prenatal development of the human precommissural septum. J Comp Neurol 215: 331, 1983
8. Crosby EC, Humphrey T, Lauer EW: Correlative Anatomy of the Nervous System. MacMillan, New York, 1962
9. Damasio AR, Graff-Radford NR, Eslinger PJ: Amnesia following basal forebrain lesions. Arch Neurol 42: 263, 1985
10. Gaspar P, Berger B, Alvarez C, Vigny A, Henry JP: Catecholaminergic innervation of the septal area in man: Immunocytochemical study using TH and DBH antibodies. J Comp Neurol 241: 12, 1985
11. Griffiths P, Hunt S: Specific spatial defect in a child with septo-optic dyspalsia. Dev Med Child Neurol 26: 395, 1984
12. Henke H, Lang W: Cholinergic enzymes in neocortex, hippocampus and basal forebrain of non-neurological and senile dementia of Alzheimer-type patients. Brain Res 267: 281, 1983
13. Horváth S, Palkovits M: Septal nuclei of the rat: a cytoarchitectonic map. (in prep.)
14. Klüver H, Barrera E: A method for the combined staining of cells and fibers in the nervous system. J Neuropathol Exp Neurol 12: 400, 1953
15. Koch F, Schuz A, Kariks J: Comparison of the septal areas in New Guinean and European brains. Am J Phys Anthropol 67: 259, 1985
16. Kuhlenbeck H: Some comments on the development of the human corpus callosum and septum pellucidum. Acta Anat Nippon 44: 1245, 1969
17. Lewis SW, Mezey GC: Clinical correlates of septum pellucidum cavities: an unusual association with psychosis. Psychol Med 15: 43, 1985
18. Lindquist G, Norlén G: Korsakoff's syndrome after operation on ruptured aneurysm of the anterior communicating artery. Acta Psychiatr Scand 42: 24, 1966
19. Nauta WJH, Haymaker W: Hypothalamic nuclei and fiber connections. In: Haymaker W, Anderson E, Nauta WJH (eds) The Hypothalamus. Thomas, CC, Springfield, 1969
20. Norlén G, Olivecrona H: The treatment of aneurysms of the circle of Willis. J Neurosurg 10: 404, 1953
21. Palkovits M: Distribution of neuropeptides in the central nervous system: A review of biochemical mapping studies. Progr Neurobiol 23: 151, 1984
22. Palkovits M, Magyar P, Szentágothai J: Quantitative histological analysis of the cerebellar cortex in the cat. I. Number and arrangement in space of the Purkinje cells. Brain Res 32: 1, 1971
23. Swanson LW, Cowan WM: The connections of the septal region in the rat. J Comp Neurol 186: 621, 1979
24. Taren JA: Anatomical pathways related to the clinical findings in aneurysms of the anterior communicating artery. J Neurol Neurosurg Psychiat 28: 228, 1965
25. Volpe BT, Hirst W: Amnesia following the rupture and repair of an anterior communicating artery aneurysm. J Neurol Neurosurg Psychiat 46: 704, 1983
26. Whitehouse PJ, Price DL, Struble RG, Clark AW, Coyle JT, DeLong MR: Alzheimer's disease and senile dementia: loss of neurons in the basal forebrain. Science 215: 1237, 1982
27. Zeman W, King FA: Tumors of the septum pellucidum and adjacent structures with abnormal affective behavior: an anterior midline structure syndrome. J Nerv Ment Dis 127: 490, 1958

Acta Morphologica Hungarica, 35 (3—4), pp. 175—181 (1987)

REED-STERNBERG LIKE CELLS IN CULTURES OF MONONUCLEAR BLOOD CELLS INFECTED BY EPSTEIN-BARR VIRUS

P. Bucsky[1, 3], W. Hampl[1], N. Frickhofen[2], G. Gaedicke[3]

[1]DEPT. OF VIROLOGY (MICROBIOLOGY) I, [2]CENTER OF MEDICINE III
[3]UNIVERSITY CLINIC OF PAEDIATRICS, DEPT. PAEDIATRICS II,
UNIVERSITY OF ULM, FRG

(Received 27 May 1986)

The origin of Reed-Sternberg cell is still unresolved. It is known that in the cultures of mononuclear blood cells stimulated by pokeweed mitogen, Reed-Sternberg like cells occur. Most of these cells have the phenotype of T lymphocytes. To investigate the fusion theory, as one of the possibilities for the origin of Reed-Sternberg cells, we have infected mononuclear blood cells from normal donors by Epstein-Barr virus as a T cell independent B lymphocyte stimulator. In these cell cultures, large multinucleated cells resembling Reed-Sternberg cells were found. These cells usually have the phenotype of B lymphocytes, some of them, however, also have markers of monocytes/macrophages. The possibility of an in vitro fusion between B lymphocytes and monocytes induced by Epstein-Barr virus may be assumed. As to the origin of Reed-Sternberg cells, an in vivo fusion between B-lymphocyte and monocyte/macrophage is proposed.

Introduction

The origin of Hodgkin cells and Reed-Sternberg cells in Hodgkin's disease remains obscure in spite of intensive investigations. There are different theories favouring their origin from macrophages/histiocytes [15, 19, 37], B lymphocytes [2, 17, 24, 39], T lymphocytes [3], plasmacytes [40], dendritic reticulum cells [10] or from interdigitating reticulum cells [16]. They are also suggested to be the tumorous counterpart of a newly discovered cell type, found in normal lymph nodes [36]. In addition, the possibility of cell fusion is also mentioned [5, 35, 41]. The presence of Reed-Sternberg like cells have been described in short term cultures of normal donors, stimulated repeatedly with pokeweed mitogen (PMW) [38].

To investigate the fusion hypothesis for the in vivo origin of Reed-Sternberg cells — reported previously [5] — we infected mononuclear blood cells by Epstein-Barr virus (EBV) to induce fusion [1] between B lymphocytes and monocytes, in long-term cultures of mononuclear blood cells from normal donors, stimulated by EBV.

Send offprint requests to Dr. Péter Bucsky, Medizinische Hochschule Hannover, Abteilung Kinderheilkunde IV, Pädiatrische Hämatologie/Onkologie, Konstanty-Gutschow Str. 8. D-3000 Hannover 61, FRG

Materials and methods

Mononuclear blood cells from six normal donors obtained by Ficoll-Paque (R) (Pharmacia Fine Chemicals AB, Uppsala, Sweden) centrifugation (400 *g* for 30' at 20 °C were cultured in RPMI 1640 medium supplemented with 10% heat-inactivated fetal calf serum, 2 mM glutamine, streptomycin (100 μg/ml) and penicillin (100 U/ml) at 37 °C) in an air atmosphere containing 5% CO_2.

Starting cell density was $2.6-5.7\times10^6$ cell/ml, starting volume was 2.5 ml/culture in Falcon tubes. At the beginning of culturing the cells were infected with EBV, which had been harvested from supernatants of B95—8 marmoset cell cultures at growth saturation [28]. The cells were re-fed twice weekly.

The cultures were investigated two to three times weekly under phase contrast microscope. After three months of culture, some cells were removed, mounted on bio-Merieux slides and were stained by May-Grünwald-Giemsa (MGG) for light microscopic morphology. Cell surface markers were determined with a panel of the following monoclonal antibodies: a cocktail of Leu 4 and Leu 9, which is specific for T cells [23, 25], RFB 4 and RFB 6 (kindly provided by G. Janossy to N. F.), which are both specific for B cells, VIM-2, which is specific for granulocytes/monocytes [27], KI-M6 (kindly provided by H. J. Radzun to N. F.), which is specific for macrophages, OKM-1, VIM-D5, S-HCL-3, which all are specific for granulopoesis/monocytes [4, 21, 34] and anti-Ia [32]. The alkaline phosphatase-anti alkaline phosphatase method was performed [12]. Cell suspensions from the cell cultures of three donors were also analyzed for esterase isoenzymes as described [7]. Briefly, enzymes were extracted and analysis was done by analytical isoelectric focusing on thin layer polyacrylamide gels and subsequent staining using alpha-naphthyle-acetate as a substrate and Fast Blue RR as a coupling salt.

For cytochemical analysis the naphtol-AS-acetate esterase reaction was done [26].

The detection of EBV-associated nuclear antigen (EBNA) was performed according to Reedman and Klein [31] using controls for both positive and negative reactions.

Results

All of the infected cell cultures began to grow and after some days typical cell aggregates appeared. In contrast, non-infected cell cultures from the same donors died within three weeks.

Using phase contrast microscopy we observed among the cell aggregates and lymphoblastoid cells also large multinucleated cells occurring with a frequency of less than 1%. To characterize these cells, after three months of culture some cells were removed for light microscopic morphology, surface marker analysis and cytochemical and biochemical characterization. By light microscopy they had a diameter of 40—60 μm and contained 2—3 nuclei. Some of the multinucleated cells resembled the typical Reed-Sternberg cells with their large — sometimes mirror image — nuclei, having a reticular chromatin pattern as well as prominent nucleoli (Fig. 1).

Cytochemically some of the large multinucleated cells reacted positively with the naphtol-AS-acetate esterase.

The biochemical characterization of cells in suspension provided evidence that monocytes were present in the cell cultures since monocyte specific isoenzymes were clearly seen (Fig. 2).

The results of reactions performed with a panel of monoclonal antibodies were as follows: with pan-B nearly every cell stained positively; with pan-T

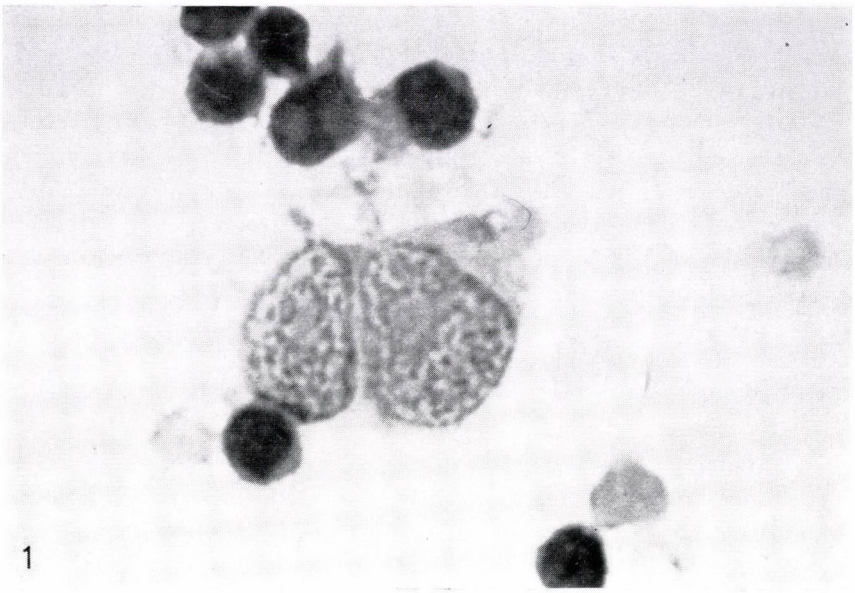

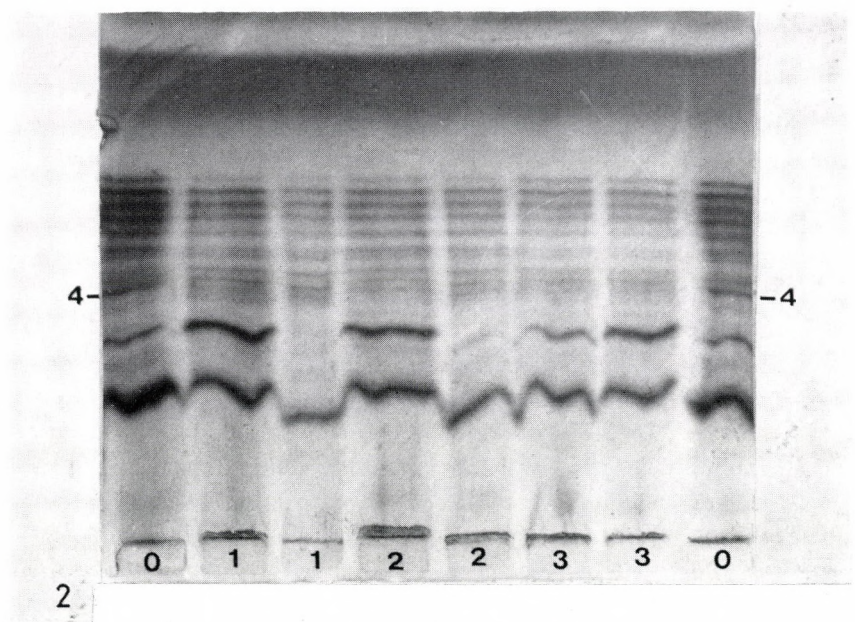

Fig. 1. Binucleated Reed-Sternberg like cell (MGG, ×1000)
Fig. 2. Esterase isoenzyme pattern. 1, 2, 3: cultures investigated; 4: monocyte specific isoenzymes; 0: control cell suspension from tonsilla

the number of positive cells was less than 1%; with VIM-2 and KI-M6 some of the large multinucleated cells stained positively, VIM-D5, OKM-1, S-HCL-3 were all negative, whereas anti-Ia was strongly positive.

Nearly all of the mononucleated cells were EBNA positive. Also, the nuclei in the multinucleated cells were EBNA positive. We have only rarely seen EBNA negative cells, and when multinucleated, all nuclei were negative.

According to these results, the cell cultures represented B lymphocyte populations, some of the large multinucleated cells, however, also had markers of monocytes/macrophages.

Discussion

The question concerning the origin of Reed-Sternberg cells is not yet resolved. Similarly, the aetiology and pathomechanism of the disease are also poorly understood and infectious agent(s) causing the disease has not been ruled out [13, 14]. The connection between Hodgkin's disease and EBV infection is discussed, too [8, 9, 22, 29]. To answer the question as to the origin of the neoplastic cells remains difficult because at present no cell cultures exist originating undoubtedly from Reed-Sternberg cells. The results of investigations done on cells from cultures derived presumably from the neoplastic cells are inconsistent [6, 18, 30].

Their origin from B lymphocytes [2, 17, 24, 39], T lymphocytes [3], macrophages/histiocytes [15, 19, 37], dendritic cells [10], plasmocyte derivates [40], interdigitating reticulum cells [16] is discussed. Some authors favour the hypothesis, that these cells might be the neoplastic variants of a cell type newly discovered in normal lymp nodes [36]. Theories have also been mentioned, linking the origin of Reed-Sternberg cells to cell fusion, e.g. fusion between B lymphocytes and "reticulum cells" [41], between B and T lymphocytes [35] or between B immunoblasts and monocytes/macrophages induced by a (pathogenic?) virus [5]. It is also assumed, that the origin of Hodgkin cells and Reed-Sternberg cells is not quite identical [5]. Stimulating repeatedly mononuclear blood cells of normal donors in short-term cultures by PWM as a T cell dependent B lymphocyte stimulator, cells resembling Reed-Sternberg cells can be found. After exposure to Hodgkin tissue, the frequency of these cells is increased. The majority of large, bizarre cells disclosed the phenotype of T lymphocytes, while some showed a character for B cells and only a few had marker for monocytes/macrophages [38].

Investigating the possibility of an in vitro fusion between B lymphocytes and monocytes caused by a virus as a possible in vivo origin for Reed-Sternberg cells, we have infected mononuclear blood cells by EBV. At present EBV is the only T cell independent B lymphocyte stimulator. This close

restriction is determined at the receptor level. The receptor of B cells for EBV is related to [20] and perhaps identical [11] with the C3d receptor, which is specific for B lymphocytes. Several days after infection, the typical cell aggregates appeared. Among the lymphoblastoid cells we have observed large multinucleated cells, some of them strongly resembling Reed-Sternberg cells. In contrast to the results obtained in cultures of lymphocytes stimulated by PWM, the Reed-Sternberg like cells in our cultures stimulated by EBV have a phenotype of B lymphocytes, e.g. they are EBNA positive. Investigating them by monoclonal antibodies, some of the large multinucleated cells, however, also had markers for monocytes/macrophages. The esterase isoenzyme analysis made from suspension of cultured cells showed the presence of monocytes in the cultures, too. Positivity of naphtol-AS-acetate esterase reaction in few multinucleated cells was also observed.

Taking into consideration the possibility of cell fusion between B cells and monocytes in our cell cultures, it can be assumed that at least one of the nuclei of a fused cell (originating from a monocyte) should be negative for EBNA. But all of the nuclei of the multinucleated cells investigated were EBNA positive.

We think that the nuclei of monocytes become EBNA positive following fusion with B cells which have receptors for EBV. This presumably is also the case in nasopharyngeal carcinoma. These neoplastic epithelial cells are also positive for EBNA, although they do not have receptors for EBV. It is assumed that these cells obtain their EBNA positivity by in vivo fusion with EBNA positive B lymphocytes in the pharynx [33].

On the basis of marker studies most of the theories favour the origin of the Reed-Sternberg cells as either from macrophages/histiocytes/monocytes or from B lymphocytes. An in vivo fusion between these two cell types (induced by a virus?) could well explain the "double" phenotype, the rarity and the lack of mitotic forms of Reed-Sternberg cells in Hodgkin tissue. The preliminary investigations reported here might also suggest such a mechanism.

Acknowledgement

This work was supported by the Alexander von Humboldt Foundation. We thank Prof. Dr. A. K. Kleinschmidt and Prof. Dr. E. Kleihauer for their critical and helpful comments.

REFERENCES

1. Bayliss GJ, Wolf H: An Epstein-Barr virus early protein induces cell fusion. Proc Natl Acad Sci USA 78: 7162, 1981
2. Bernuau D, Feldmann G, Vorhauer W: Hodgkin's disease: Ultrastructural localization of intracytoplasmic immunoglobulins within malignant cells. Brit J Haematol 40: 51, 1978

3. Biniaminov M, Ramot B: Possible T-lymphocyte origin of Reed-Sternberg cells. Lancet 1: 368, 1974
4. Breard J, Reinherz EL, Kung PC, Goldstein G, Schlossman SF: A monoclonal antibody reactive with human peripheral blood monocytes. J Immunol 124: 1943, 1980
5. Bucsky P: Origin of Hodgkin's and Reed-Sternberg cells. N Engl J Med 303: 284, 1980
6. Diehl V, Kirchner HH, Schaadt M, Fonatsch C, Stein H, Gerdes J, Boie C: Hodgkin's disease: Establishment, characterisation of four in vitro cell lines. J Cancer Res Clin Oncol 101: 111, 1981
7. Drexler HG, Gaedicke G: Isoenzyme studies in human leukemia-II. Carboxylic esterase (E.C.3.1.1.1.1.). Leuk Res 7: 599, 1983
8. Evans AS, Comstock GW: Presence of elevated antibody titres to Epstein-Barr virus before Hodgkin's disease. Lancet 1: 1183, 1981
9. Evans AS, Gutensohn NM: A population-based case-control study of EBV and other viral antibodies among persons with Hodgkin's disease and their siblings. Int J Cancer 34: 149, 1984
10. Fisher RJ, Bates SE, Bostick-Bruton F, Tuteja N, Diehl V: Neoplastic cells obtained from Hodgkin's disease function as accessory cells for mitogen-induced human T cell proliferative responses. J Immunol 132: 2672, 1984
11. Frache R, Barel M, Ehlin-Henriksson B, Klein G: gp 140, the C3d receptor of human B lymphocytes, is also the Epstein-Barr virus receptor. Proc Natl Acad Sci USA 82: 1490, 1985
12. Frickhofen N, Bross KJ, Heit W, Heimpel H: Modified immunocytochemical slide technique for demonstrating surface antigens on viable cells. J Clin Pathol 38: 671, 1985
13. Gallo RC, Gelmann EP: In search of a Hodgkin's disease virus. N Engl J Med 304: 169, 1981
14. Gutensohn N, Cole P: Childhood social environment and Hodgkin's disease. N Engl J Med 304: 135, 1981
15. Kadin ME, Stites DP, Levy R, Warnke R: Exogenous immunoglobulin and the macrophage origin of Reed-Sternberg cells in Hodgkin's disease. N Engl J Med 299: 1208, 1978
16. Kadin ME: Possible origin of the Reed-Sternberg cell from an interdigitating reticulum cell. Cancer Treat Rep 66: 601, 1982
17. Hayhoe FGJ, Burns GF, Cawley JC, Stewart JW: Cytochemical, ultrastructural and immunological studies of circulating Reed-Sternberg cells. Brit J Haematol 38: 485, 1978
18. Kaplan HS, Gartner S: "Sternberg-Reed" giant cells of Hodgkin's disease: Cultivation in vitro, heterotransplantation, and characterisation as neoplastic macrophages. Int J Cancer 19: 511, 1977
19. Kaplan HS: Hodgkin's disease: Biology, treatment, prognosis. Blood 57: 813, 1981
20. Klein G, Klein E: The changing faces of EBV research. Prog Med Virol 30: 87, 1984
21. Knapp W, Majdic O, Stockinger H, Bettelheim P, Liszka K, Köller U, Peschel C: Monoclonal antibodies to human myelomonocyte differentiation antigens in the diagnosis of acute myeloid leukemia. Med Oncol Tumor Pharmacother 1: 257, 1984
22. Lange B, Arbeter A, Hewetson J, Henle W: Longitudinal study of Epstein-Barr virus antibody titers and excretion in pediatric patients with Hodgkin's disease. Int J Cancer 22: 521, 1978
23. Ledbetter IA, Evans RL, Lipinski M, Cunningham-Rundles C, Good RA, Herzenberg LA: Evolutionary conservation of surface molecules that distinguish T lymphocyte helper/inducer and T cytotoxic/suppressor subpopulation in mouse and man. J Exp Med 153: 310, 1981
24. Linch DC, Berliner N, O'Flynn K, Kay LA, Jones MM, MacLennan K, Huehns ER, Goff K: Hodgkin-cell leukaemia of B-cell origin. Lancet 1: 78, 1985
25. Link M, Warnke R, Finlay J, Amylon M, Miller R, Dilley J, Levy R: 4H9, a single monoclonal antibody identifying acute lymphoblastic leukemia and lymphoma of T cell type. Blood 62: 722, 1983
26. Löffler H: Cytochemischer Nachweis von unspezifischer Esterase in Ausstrichen. Klin Wochenschr 23: 1220, 1961
27. Majdic O, Bettelheim P, Stockinger H, Abere W, Liszka K, Luth D, Knapp W: M2, a novel myelomonocytic cell surface antigen and its distribution on leukemic cells. Int J Cancer 33: 617, 1984
28. Miller G, Lipman M: Release of infectious Epstein-Barr virus by transformed marmoset leukocytes. Proc Natl Acad Sci USA 70: 190, 1973
29. Munoz N, Davidson RJL, Witthoff B, Ericsson JE, De-The G: Infectious mononucleosis and Hodgkin's disease. Int J Cancer 22: 10, 1978

30. Olsson L, Behnke O, Pleibel N, D'Amore F, Werdelin O, Fry KE, Kaplan HS: Establishment and characterization of a cloned giant cell line from a patient with Hodgkin's disease. JNCI 73: 8093, 1984
31. Reedman BM, Klein G: Cellular localization of an Epstein-Barr virus (EBV)-associated complement-fixing antigen in producer and non-producer lymphoblastoid cell lines. Int J Cancer 11: 499, 1973
32. Reinherz EL, Kung PC, Pesando IM, Ritz J, Goldstein G: Ia determinants on human T-cell subsets defined by a monoclonal antibody. J Exp Med 150: 1472, 1979
33. Rickinson A: Epstein-Barr virus in epithelium. Nature 310: 99, 1984
34. Schwarting R, Stein H, Wang CY: The monoclonal antibodies alpha-S-HCL-1 (alpha-Leu-14) and alpha-S-HCL-3 (alpha-Leu-M5) allow the diagnosis of hairy cell leukemia. Blood 65: 974, 1985
35. Sinkovics JG, Schullenberger CC: Hodgkin's disease. Lancet 2: 506, 1975
36. Stein H, Gerdes J, Schwab U, Lemke H, Mason DY, Ziegler A, Schienle W, Diehl V: Identification of Hodgkin and Reed-Sternberg cells as a unique cell type derived from a newly-detected small-cell population. Int J Cancer 30: 445, 1982
37. Strauchen JA: Lectin receptors as markers of lymphoid cells II. Reed-Sternberg cells share lectin-binding properties of monocyte macrophages. Am J Pathol 116: 370, 1984
38. Stuart AE: The production of abnormal cells and Reed-Sternberg-like cells from normal lymphocytes. Brit J Cancer 47: 731, 1983
39. Stuart AE, Volsen SG, Zola M: The reactivity of Reed-Sternberg cells with monoclonal antisera at thin section and ultrastructural levels. J Pathol 141: 71, 1983
40. Umihara J, Tanaka M, Tanaka H, Saito K, Ishikawa E: Hodgkin's disease. A histochemical study with special emphasis on the character of Hodgkin's cell and Reed-Sternberg cell. Acta Pathol Jpn 33: 751, 1983
41. Warner TFCS: Origin of the Reed-Sternberg cell. Lancet 2: 511, 1973

Acta Morphologica Hungarica, 35 (3—4), pp. 183—187 (1987)

EFFECT OF CADMIUM ON THE SPERMATOGENESIS OF *RANA HEXADACTYLA* LESSON

S. KASINATHAN, K. VEERARAGHAVAN, S. RAMAKRISHNAN

DEPARTMENT OF BIOLOGY AND BIOCHEMISTRY, JAWAHARLAL INSTITUTE OF POSTGRADUATE MEDICAL EDUCATION AND RESEARCH, PONDICHERRY, INDIA

(Received 26 June 1986)

A single subcutaneous injection of 0.5 mg cadmium chloride in Amphibian Ringer solution caused a significant decrease in secondary spermatogonial and primary spermatocytic stages in the semineferous tubules of frogs in 7 days. B_3 cells of adenohypophysis and the activities of Δ^5-3β-hydroxy steroid dehydrogenase and 17β-dehydrogenase in the Leydig cells were significantly increased in the same period. There were no significant changes in 3 days.

It has been reported that a single subcutaneous injection of cadmium chloride at subtoxic level produced a rapid and irreversible degeneration of germinal epithelium associated with temporary damage to interstitial Leydig tissue in rats [14]. Cadmium produced deleterious effects also in birds [12, 19] and toads [3]. However, histological studies on the abdominal testes on Suncus [6] and frog [4] did not support the above observations as there was no testicular degeneration . In view of the conflicting reports, the present study was undertaken in South Indian green frog *Rana hexadactyla* Lesson to find out the effect of cadmium chloride on the testes.

Materials and methods

Adult male frogs, *Rana hexadactyla* Lesson, weighing 50—65 g and 70—90 mm snout to vent length were selected for the study. They were kept in the laboratory for a few days prior to experimentation. The frogs were divided into following groups (1) control groups receiving 0.2 ml of Amphibian Ringer injection, (2) two groups received 0.5 mg of cadmium chloride dissolved in Amphibian Ringer solution. All animals were fed with earthworms *ad libitum*. The animals were sacrificed 3 days and 7 days after cadmium injection with an equal number of Placebo control frogs. The testes of all animals were removed, fixed in Bouin sectioned at 7 μm and stained with Haematoxylin and Eosin. Quantitative assessment of spermatogenetic stages was done adopting Van Oordt's classification [20]. Pituitaries were fixed in Bouin, embedded in paraffin, sectioned in 3 μ and stained with Clevel and Wolfe's trichrome stain. For histochemical localization of the 3β-HSD enzyme, fresh frozen cryostat sections of the testis (20 μm) were incubated in an appropriate medium for 30 min by the method of Deane et al [5]. The enzyme 17β-HSD was demonstrated in the same way using

Send offprint requests to S. Kasinathan, Department of Biology and Biochemistry; Jawaharlal Institute of Postgraduate Medical Education and Research, Pondicherry 60 5006, India

testosterone as the substrate in a different incubation medium according to Pearson and Grose [17]. Parallel sections were incubated in substrate-free medium for each type of enzyme and the sections after incubation were fixed and mounted in glycerine jelly.

These enzymes were estimated quantitatively by biochemical methods [2, 13]. The quantitative estimation of testosterone was done by the method of Romulo Garza [18].

Testes (100 mg) were homogenized in Krebs-Ringer biocarbonate buffer, pH 7.4. The homogenate was mixed with 1.0 ml of methanol and mixed in a vortex for 30 s. 5 ml of diethyl ether was added and again mixed in a vortex for 2 min. The solution was allowed to settle in ice and the ether layer was separated. The aqueous solution was washed twice with ether and the ether extract was pooled. The ether extract was evaporated to dryness at 45 °C in a water bath. The dried ether extract was reconstituted with GPBS (0.15 molar) (Gelatin 0.4% phosphate, 10 mm buffer pH 7.2) buffered saline and aliquots were taken for testosterone assay.

Testosterone was assayed by RIA using (^{3}H) testosterone (6000 cpm) and antiserum (1 : 5000). The bound serum was separated by Dextran-coated charcoal and the counts were measured in an automatic liquid scintillation system. (Electronic Corporation of India) with a counting efficiency of about 50%. The specific binding was 26% and non-specific binding was 1.5%.

Results

The testis of Placebo controls showed normal spermatogenesis. No significant changes were observed in the testis of frogs treated with cadmium chloride in 3 days. But in 7 days, there was a marked decrease in primary and secondary spermatogonial stages O, I and II and primary spermatocytic stage III (Table I). The decrease of stage IV was also statistically significant

Table I

Effect of cadmium chloride on the spermatogenetic stages and B_3 cells of *Rana hexadactyla* Lesson
(Number of frogs per group: 10)

Days	Dose administered	Spermatogenetic stages					Percentage of B_3 cells o pituitary
		0	I	II	III	IV	
Control	—	1.98 ±0.03	1.82 ±0.04	2.44 ±0.02	3.69 ±0.08	1.84 ±0.05	7.2
After 3 days	0.5 mg/day	2.01 ±0.09	1.75 ±0.22	2.19 ±0.84	3.59 ±0.02	1.78 ±0.04	6.8
7 days	0.5 mg/day	1.62 ±0.20	0.86 ±0.02	0.92 ±0.05	1.12 ±0.09	1.29 ±0.16	13.3
P value cont vs	3 days	NS	NS	NS	NS	NS	NS
P value cont vs	7 days						
Mean ± S.D.		0.01	0.001	0.01	0.001	0.001	0.001

(Table I). In addition, it was observed that in the control animals sperms remained scattered in the tubular lumen aggregated near the Sertoli cells. But in the cadmium treated animals, both free and aggregated sperms were found to be markedly reduced in 7 days.

Histological studies on the anterior pituitary showed proliferation of B_3 cells in 7 days after treatment with cadmium.

Histochemical and biochemical studies revealed a marked increase in the activities of enzymes Δ^5-3 β hydroxy steroid dehydrogenase (Δ^5-3 β-HSD) and 17β hydroxy steroid dehydrogenase (17β-HSD) in the Leydig cells of cadmium-treated animals after 7 days compared to controls (Table II). Correspondingly, the concentration of testosterone was found to be greater in the testes of the experimental group at the same period (Table III).

Table II

3 β-HSD and 17 β-HSD in control and cadmium chloride treated frogs

Enzymes	Control	Experimental
3 β-HSD Units/gm	24×10^{-5}	12.6×10^{-4}
17 β-HSD Units/gm	4.1×10^{-4}	17.2×10^{-4}

3 β-HSD = 1 Unit = 1 micromole of progesterone formed per min at 37°C under laboratory condition.
17 β-HSD = 1 Unit = 1 micromole of testosterone formed per min at 37 °C under laboratory condition.

Table III

Effect of cadmium chloride on the concentration of testosterone in the testis of frog

Control	Cd treated
24 ± 1.2 μg	55 ± 1.7* μg

* $P<0.001$

Discussion

The present study demonstrated that testes do not show any histological changes in 3 days after cadmium administration. This confirms the work of Chiquoine [4] and Biswas et al [3].

Spermatogenesis is reported to decrease in toad [3] ringdove [12], pigeon [19] and transplanted testis of rat [11].

Evidence is strong that pituitary B_3 cells are concerned with the elaboration of ICSH. Homoplastic transformation of adenohypophyses leads to a regression of B_1, B_2 and B_3 cells in the pituitary and also affects the interstitial tissue of the testes and the secondary sexual characters of the recipient frogs. Van Oordt [21] suggested a correlation between B_3 cells and the cycle

of interstitial cells in the testis of common frog. On this basis, Van Oordt and Lofts [22] and independently Pasteels [15, 16] concluded that B_3 cells were the source of ICSH in both normal and experimental conditions. Proliferation of B_3 cells is therefore suggestive of increased ICSH activity.

Hyperplasia and tumour formation in the Leydig cells have been shown by Gunn et al. [7, 8] in mice and rats treated with cadmium for one year. Sarkar and Mondal [19] have observed Leydig cell hypertrophy in cadmium-treated pigeon while Biswas et al. [3] made a similar observation in *Bufo melanostictus*. The latter workers reported an increased Δ^5-3 β HSD also in the same organism. In our work both Δ^5-3 β-HSD and 17β-HSD were found to be elevated in the testes, in 7 days, after Cd treatment, suggesting augmented testosterone synthesis. The increased levels of testosterone in testes corroborate this conclusion.

The sequence of events in 7 days after Cd treatment in *Rana hexadactyla* Lesson appears to be as follows: There is an increase in the pituitary B_3 cells. This leads to an increase of ICSH. The trophic hormone stimulates the Leydig cell activity and particularly the enzymes Δ^5-3 β-HSD and 17β-HSD. Increased enzyme levels cause augmented synthesis of testosterone (Table II). Once the androgen is in excess, it exercises a negative feed-back on the pituitary and inhibits spermatogenesis (Fig. 1). It is well-documented that while optimum levels of testosterone are needed for proper spermatogenesis, increased production of testosterone has actually an opposite effect. In fact, exogenous administration of testosterone inhibits spermatogenesis in intact but hypophysectomized frogs [1, 10]. In our work, profound increase in B_3 cells due to Cd after 7 days has actually disturbed the normal biological function of the same and led to a marked decrease in spermatogenetic stages O, I, II, III and IV.

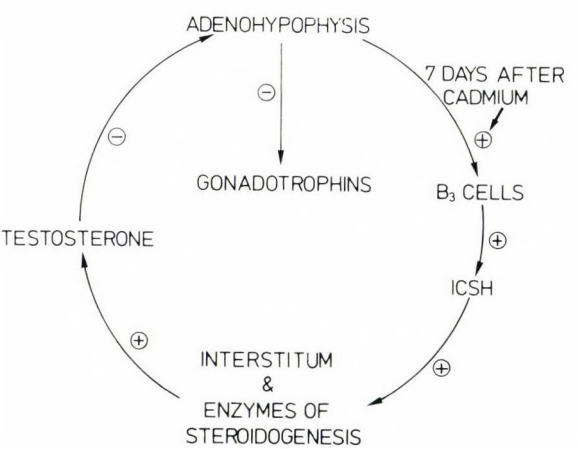

Fig. 1. Schematic representation of the mode of action of cadmium chloride

REFERENCES

1. Basu SL, Nandi J: Effects of testosterone and gonadotropins on spermatogenesis in *Rana pipiens* Schreber. J Exp Zool 159: 493, 1965
2. Bayer KF, Samuels LT: Distribution of steroid. 3-B-OL-dehydrogenase in cellular structures of the adrenal gland. J Biol Chem 219: 69, 1956
3. Biswas NM, Chandra S, Gosh A, Chakrabarthy J: Effect of cadmium on spermatogenesis in toad *(Bufo melanostictus)*. Endocrinologie 68 (3): 349, 1976
4. Chiquoine AD: Observation on the early events of cadmium necorsis of the testes. Anat Rec 149: 23, 1964
5. Deane HW, Rubin BL, Driks EC, Lober BL, Leipsner G: Trophoblastic giant cells in placentas of rats and mice and their probable role in steroid hormone production. Endocrinology 70: 407, 1962
6. Dryden GL, McAllister HY: Sustained fertility after Cd Cl_2 injection by a non-scrotal mammal *Sincus murinus* (Insectivora: Sorcidae). Biol Reproduction 2: 23, 1970
7. Gunn SA, Gould TC, Anderson WAD: Cadmium induced interstitial tumors in rats and mice and their prevention by zinc. J Natl Cancer Inst 31: 745, 1963
8. Gunn SA, Gould TC, Anderson WAD: Comparative study of interstitial cell tumors of rat's testis induced by cadmium injection and vascular ligation. J Natl Cancer Inst 35: 329, 1965
9. Kar AB, Dasgupta PR, Das RP: Effect of a low dose of cadmium chloride on the genital organs and fertility of male rats. J Sci Ind Res (India) 20C: 322, 1973
10. Kasinathan S, Basu SL: Effect of hormones on spermatogenesis in hypophyzectomised *Rana hexadactyla* Lesson. Acta Morph Acad Sci Hung 21 (3): 249, 1973
11. Mackawa K: The destructive effect of cadmium on rat testis. J Tokyo Med Coll 23: 413, 1965
12. Mackawa K, Suzuki T, Tsunenari Y: Damage of the gonads produced by cadmium in male and female ring doves *(Streptiopelia risoria)*. Acta Anat Nippon 39: 294, 1964
13. Marcus PI, Talalay P: Induction and purification of α- and β-hydroxysteroid dehydrogenase. J Biol Chem 218: 661, 1956
14. Parizek J, Zahor Z: Effect of cadmium salt on testicular tissue. Nature New Biol 177: 1036, 1956
15. Pasteels JL: Recherches experimentales sur la role de l'hypotalamus dans la differentiation cytologique de l'hypophyse chez *Pleurodeles waltlii*. Arch Biol (Liege) 68: 65, 1957
16. Pasteels JL: Etude experimentale des differentes categories d'elements chromophiles de l'hypophyse adulte de *Pleurodeles waltlii*. Arch Biol (Liege) 71: 409, 1960
17. Pearson B, Grose F: Histochemical demonstration of 17β-hydroxysteroid dehydrogenase by use of Tetrazolium. Proc Soc Exp Biol Med 100: 636, 1959
18. Romulo Garza: Radio immunoassay of steroids. In: Abraham GE (ed.): Handbook of Radioimmunoassay. Marcel Dekker Inc. New York and Basel, 1977
19. Sarkar AK, Mondal R: Injurious effect of cadmium on the testis of domestic pigeons and its prevention by zinc. Ind J Exp Biol 11: 108, 1973
20. Van Oordt PGWJ: Regulation of the spermatogenetic cycle in the common frog *(Rana temporaria)* Thesis. Utrecht University G. W. Van der Weil and Company, Arnhem, Holland, 1: 116, 1956
21. Van Oordt PGWJ: The analysis and identification of hormone producing cells of the adenohypophysis. In: Jorgensen CB, Barrington EJW, (eds) Perspectives of Endocrinology — Hormones in the Life of Lower Vertebrates. 1968
22. Van Oordt PGWJ, Lofts B: The effects of high temperature on gonadotrophin secretion in the male common frog *(Rana temporaria)* during autumn. J Endoc 27: 137, 1963

Acta Morphologica Hungarica, 35 (3—4), pp. 189—198 (1987)

ATHEROSCLEROTIC LESION OF THE AORTA: ITS STUDY APPLYING A BIOMETRIC SYSTEM USING MULTIVARIATE STATISTICAL TECHNIQUES

J. E. Fernandez-Britto[1], J. Bacallao[1], P. V. Carlevaro[2], A. S. Koch[3], H. Guski[4]

[1]HIGHER INSTITUTE OF MEDICAL SCIENCE OF HABANA, CUBA, [2]FACULTY OF MEDICINE, UNIVERSITY OF REPUBLIC, MONTEVIDEO, URUGUAY, [3]SECOND DEPARTMENT OF PATHOLOGY, SEMMELWEIS MEDICAL UNIVERSITY, BUDAPEST, HUNGARY, [4]INSTITUTE OF PATHOLOGY, HUMBOLDT UNIVERSITY OF BERLIN (CHARITÉ), GDR

(Received 25 August 1986)

To study the atherosclerotic lesion (a.l.) in the two aorta segments (thoracic and abdominal) in a given set of autopsies (total 2043) performed during five years (1981—85) in one of the principal general hospitals in the city of Havana, a set of five variables was used as part of a new biometric system (BS), to characterize the a.l. in any vascular sector. Three of these variables represent the main types of a.l., fatty streaks (X), fibrous plaques (Y) and severe (complicated and calcified) plaques (Z), while the others were indices of stenosis (P) and benignity (B). Classical dissection and pathological laboratory procedures were performed. Qualitative and quantitative gross morphometric analyses were done by a digitilizer joined to a NEC (9801) personal microcomputer (Japan). These data were processed in a medium size computer EC-1040 (GDR). The multivariate statistical techniques, the principal component analysis (PCA) and the discriminant analysis (DA), were used applying the "SPSS" programme. Conclusions: (1) PCA revealed in the two aorta segments studied a first component of benignity, fatty streaks (X) and benignity index (B) and a second component of severity, severe plaques (Z) and stenosis number (P). Because of the dimensions of the two aorta segments (width and length) the dominant, first component, is benignity. So the BS is useful in characterizing and describing the lesional state of any aorta segments; (2) DA and BS proved to be useful to distinguish between the high atherosclerotic group (HAG) and the low atherosclerotic group (LAG). The correct classification rate exceed in all cases 70%. The three components of the lesional state vector (X, Y, Z) distinguish the groups. The stenosis (P) and benignity (B) indices proved to be most relevant. The sign of benignity index is always the same as that of the LAG. Thus this variable truly represents benignity. The coherence and consistency of the BS was also proved by DA.

Introduction

The aorta's atherosclerotic lesions have been in the focus of research since many years [20, 30]. Early in 1908 the archeologist Dr. C. Elliot Smith unwrapped the mummy of Pharaoh Menephtah (Pharaoh of the Hebrew Exodus) and sent a specimen of the aorta to Dr. S. C. Shattok (London) [20],

Send offprint requests to J. E. Fernandez-Britto, Higher Institute of Medical Science of Habana, Cuba

whose conclusion after microscopical study was: "advanced atherosclerosis of aorta with extensive deposition of calcium phosphate". During the period 1910—1911, Sir Marc Armand Ruffer [19], at the Cairo Medical School (Egypt) did an extensive study on the field of atherosclerosis in several Egyptian mummies, of a period of about 2000 years (1580 B. C.—525 A. D.). His most relevant finding was, among others, the presence of calcified plaques in the aorta.

Since that time extensive work has been done in this field, applying various different techniques from the simplest [21] to the most sophisticated ones [12].

In animals [14] the aorta was the subject to study the induced atherosclerotic lesions, mainly because its being a target organ and because its convenient size (length and width). Comparison of and correlations between the atherosclerotic lesions of aorta and many other arteries (coronaries, cerebral, iliac, femoral renal, etc . . .) have been recently the topic of numerous publications [5—8, 17, 23—25].

The present paper is a report on the study of the atherosclerotic lesions of the aorta applying a BS (developed to characterize this lesion in any vascular sector in a suitable manner) using two highly sophisticated multivariate statistical techniques: the PCA [16] and the DA [15].

Materials and methods

In the present study a total of 2043 autopsies were included, that were performed at the Pathology Department of Dr. C. J. Finlay, Military Central Teaching Hospital, Havana, between 1981—85. Some essential facts had to be considered to include a case in this study, viz. more than 15 years of age and natural death. The patients were classified according to the primary cause of death, as belonging to HAG or LAG, comprizing 1171 and 872 cases respectively [4, 29]. The arteries were processed according to the traditional methods established by WHO in 1958 [28]. The following techniques were applied: the Holman staining techniques [13], Sudan IV, the qualitative analysis of each lesion type, fatty streak, fibrous plaque, and sever (complicated and calcified) plaques, and the quantitative gross morphometric analysis (measure in mm^2) the total end arterial surface of each endarterial lesion.

A BS for characterization of the a.l. in any vascular sector introduced by Carlevaro and Fernandez-Britto in 1982 [2, 3] was applied to all arteries, and the data were collected according to a specially designed protocol. The a.l. of the arteries were registered by a digitilizer joined to a NEC 9801 microcomputer (Japan). Data were processed in a medium size computer EC-1040 (GDR) of 1024 K byte internal memory. For the statistical analysis, the commercial package "SPSS" [22], was utilized. In this BS, the a.l. was specified on the basis of the three main types of lesions, fatty streak, fibrous plaques, and severe (complicated-and calcified) plaques, as a three dimensional vector. The "lesional state" was defined by coordinates representing the three kinds of lesions. The total endarterial surface and the areas occupied by the different types of lesions, were measured in mm^2. The variables of BS used here are defined as follows: X = fatty streak; Y = fibrous plaque; Z = severe (complicated and calcified) plaques, and the total area of endarterial surface = (S). Normalized surface were obtained as: (X) = X/S; (Y) = Y/S; (Z) = Z/S. Then $\Sigma = (X+Y+Z)$, is the total relative surface of atherosclerosis present in a given artery. To conserve the total information content of each variable, a vector representation was introduced as follows: $(\vec{V})$ = vector "lesional state" has the (X, Y, Z) coordinates as its components $(\vec{V} = X, Y, Z)$.

Another and very useful form of representation is through the module and the cosines of slopes of the lesional state coordinator. The $|\vec{V}|$ module was obtained as follows: $|\vec{V}| = \sqrt{X^2+Y^2+Z^2}$ and the cos $\alpha = X/|\vec{V}|$; cos $\beta = Y/|\vec{V}|$; cos $\gamma = Z/|\vec{V}|$. Other further indices were also used: (Ω). Obstruction index, (P) stenosis number (index) and (B) benignity index. The (Ω) is the measure of reduction of the vascular lumen due to the protrusion of endarterial fibrous and severe plaques. This is obtained as ($\Omega = 2Y+3Z$). If the obstruction were referred to the arterial radius, we obtained the stenosis number ($P = 4\Omega/r$). This variable is also a measure of the relative increase of resistance to blood flow: $P = \Delta R/R$, where (ΔR) = increased of resistence to blood flow, and (R) = resistence to blood flow. Since fatty streak is considered as innocuous a.l. never protruding into the vascular lumen, an index of benignity can be defined as ($B = X/\Sigma$).

The following conclusions were obtained from the "SPSS": (I) [16]: "The DA beginning with the desire to statistically distinguish between two or more groups of cases. These groups are defined by the particular research situation. To distinguish between the groups the researchers select a collection of "discriminating variables" that measure characteristics in which the groups are expected to differ. The mathematical objective of DA is to weigh and linearly combine the discriminating variables in some fashion so that the groups are forced to be as statistically distinct as possible. By taking several issues and mathematical combining them; we would hope to find a single dimension on which the members of one group are clustered at one end and the members of the other in the opposite end. Once the discriminant function has been derived, we are able to pursue the two research objectives of this technique, namely analysis and classification. (II) [15]: "The PCA is a relatively straightforward method of transforming a given set of variables into a new set of composite variables of principal component that are orthogonal (uncorrelated) to each other. No particular assumptions about the underlying structure of the variables is requiered. One simply asks what the best linear combinations of variables, would be best in the sense how the particular combination of variables would account for more of the variance in a set of data as a whole than any other linear combination of variables. The first principal component, therefore may be viewed as the single best summary of linear relationships exhibited in the data. The second component is defined as the second best linear combination of variables, under the condition that the second component is orthogonal to the first. To be orthogonal to the first component the second one must account for the proportion of the variance not accounted for by the first one. Thus the second component may be defined as the linear combination of variables that account for the most residual variance affect the effect of the first component is removed for the data. Subsequently components are defined similarly until all variance in the data is exhausted.

Results and discussion

A) *The principal components analysis*

Applying the PCA to the aortic sector (thoracic and abdominal) the following results were obtained: the first component is a benign one, and there is a strong association between the relative area of fatty streaks ($X = -$ -0.351) and the index of benignity ($B = 0.381$) for the thoracic segments and ($X = 0.391$) and ($B = 0.431$) in the abdominal segment (Table I and Fig. 1). Meanwhile the second is a severe one, the relative area of severe plaque ($Z = 0.619$) and the stenosis number ($P = 0.421$) in the thoracic segment and ($Z = 0.528$) and ($P = 0.269$) in the abdominal sector, in both cases there are in a very strong correlation and dominate this second component. This points out the real value of (X) fatty streaks and (B) benignity index (always associated) to characterize the existing variability between the individuals of the data set of autopsies studied. In these aorta segments the first component

Table I

Principal components analysis of the thoracic and abdominal aorta segments

	Thor. aorta		Abd. aorta	
	1	2	1	2
X	−0.351	.042	.391	.053
Y	.157	−0.271	−0.295	−0.251
Z	.198	.619	−0.073	.528
P	−0.053	.421	.228	.269
B	.381	−0.067	.431	.050
	51.9%	26.7%	48.4%	29.7%
	78.6%		78.1%	

explained the 51.9% in the thoracic and 48.4% in the abdominal while the second explained the 26.7% and the 29.7% in the thoracic and abdominal sectors respectively (Table I). In the coronary sector [11] in the two principal arteries responsible for miocardial infarction, right coronary and left anterior descending, the first component was severity (severe plaque Z and stenosis number P), while the second component was benignity (fatty streaks X and benignity index B).

In our opinion, these results have made evident the analitical potential the solidity and coherence of this multivariate technique in characterizing the lesional profile through the system of variables defined in this work.

The PCA revealed that the component of severity and stenosis (in the graphs representation) together with the component of benignity represent in most cases a satisfactory explanation of the diversity existing between the individuals studied. The PCA had also shown the analitical efficiency coherence and consistence of the BS used in the quantitative description and characterization of the atherosclerotic lesions.

The five different variables used, (X, Y, Z, P, B) represent the three coordinates of the atherosclerotic lesional state vector (fatty streaks, fibrous plaques and severe plaques) and the two extreme weighting indices, (B) benignity and (P) stenosis (Table I and Fig. 1). In the aortic sectors the distribution of components is in full accordance with the diameter of these two aorta segments [9, 18]. The results presented, show the metric consistency and the use of the BS in characterizing the atherosclerotic lesions, and in assessing the differences between individuals and between different sectors of the vessels. It is a good example for the use of mathematical and statistical methods to discover hidden factors present in the basic set of data.

This is a new approach, making use of and extending the available methodology for the study of the morphology and morphometry of atherosclerosis, by applying multivariate statistical techniques.

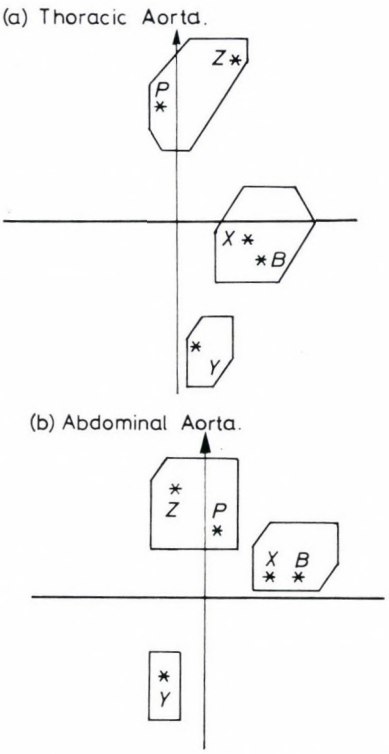

Fig. 1. Principal components analysis. a) Thoracic aorta; b) Abdominal aorta

B) *The discriminant analysis*

The clinical diagnosis and the anatomico-pathological findings at autopsy, were used to classify the patients into two groups, high and low atherosclerosis [4, 29]. To examine the validity of such a classification on an exact basis five variables, (X, Y, Z, P, B) of the BS [2, 3] were used in this research, to classify the two segments of aorta (TA, AA). This is shown in Tables II and III and Figs 2—5.

To both aorta segments, the percentage of correct classification (HAG or LAG) is higher than 70%. Also the Wilks criterion used to differentiate the two groups is always significant ($p < 0.001$). The average incidence of error in correct classification is very small for both segments of the aorta (Tables II and III). The best results were obtained in these aorta sectors (Tables II, III and Figs 3, 5) when the indices (P) stenosis number and (B) benignity index were also considered, this resulted in a high efficiency of discrimination between the two groups (Tables II, III and Figs 3, 5). The (P) stenosis number, presented itself as one of the best variables in the two aorta segments and it was ulti-

Table II

Thoracic aorta. Results of the discriminant analysis (DA)

X, Y, Z		X, Y, Z, P, B
X, Y, Z	Variables used	X, Y, Z, P, B
3	No. of variables in the DA	2
X, Y, Z	Variables included in the DA	P, B
—	Variables non-included in the DA	X, Y, Z
$\alpha_x = 0.1583$ $\alpha_y = -0.6700$ $\alpha_z = -0.7901$	Coefficients of the variables	$\alpha_p = -0.7123$ $\alpha_B = 0.4235$
HAG = −0.3792 LAG = 0.5502	Groups' position	HAG = −0.3605 LAG = 0.5787
Z, Y	Best variables	P, B, Z
$\lambda = 0.8012$ ($p<0.001$)	Wilks criterion	$\lambda = 0.7893$ ($p<0.001$)
HAG = 81.8% LAG = 55.2% Average = 72.1%	% of correct classification	HAG = 92.1% LAG = 50.3% Average = 76.1%

α = discriminant coefficients

Table III

Abdominal aorta. Results of the discriminant analysis (DA)

X, Y, Z		X, Y, Z, P, B
X, Y, Z	Variables used	X, Y, Z, P, B
3	No. of variables in the DA	4
X, Y, Z	Variables included in the DA	Y, Z, P, B
—	Variables non-included in the DA	X
$\alpha_x = 0.1902$ $\alpha_y = -0.5212$ $\alpha_z = -1.0023$	Coefficients of the variables	$\alpha_y = -0.4593$ $\alpha_z = -1.0051$ $\alpha_p = -0.1172$ $\alpha_B = 0.2901$
HAG = −0.3843 LAG = 0.5693	Groups' position	HAG = −0.3724 LAG = 0.5911
Z, Y	Best variables	P, B, Z
$\gamma = 0.7931$ ($p<0.001$)	Wilks criterion	$\gamma = 0.7876$ ($p<0.001$)
HAG = 84.1% LAG = 49.9% Average = 71.2%	% of correct classification	HAG = 85.7% LAG = 48.1% Average = 71.3%

α = discriminant coefficients

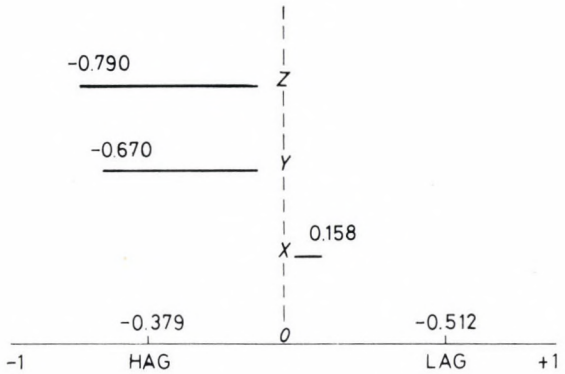

Fig. 2. Thoracic aorta. Results of the discriminant analysis (X, Y, Z). Wilks criterion $\lambda = 0.8012$ ($p < 0.001$). Per cent of correct classification = 72.1% best variables = Z, Y

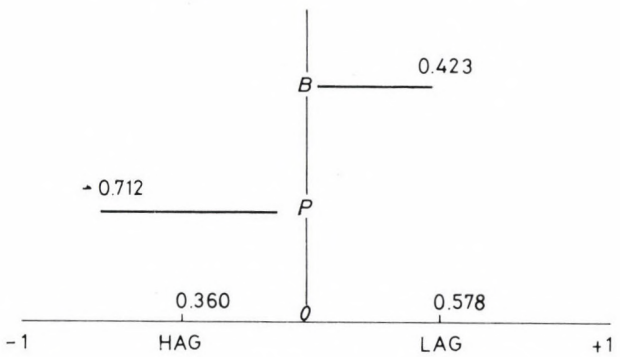

Fig. 3. Thoracic aorta. Results of the discriminant analysis (X, Y, Z, P, B). Wilks criterion $\lambda = 0.7693$ ($p < 0.001$). Per cent of correct classification = 76.1% best variables = P, B, Z

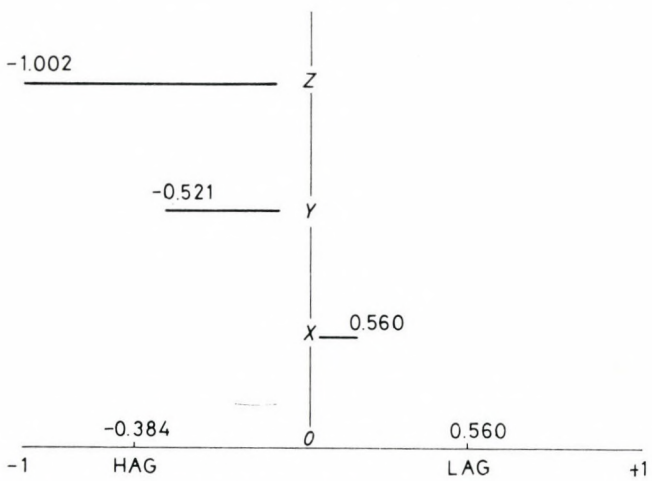

Fig. 4. Abdominal aorta. Results of the discriminant analysis (X, Y, Z). Wilks criterion $\lambda = 0.7931$ ($p < 0.001$). Per cent of correct classification = 72.1% best variables = Z

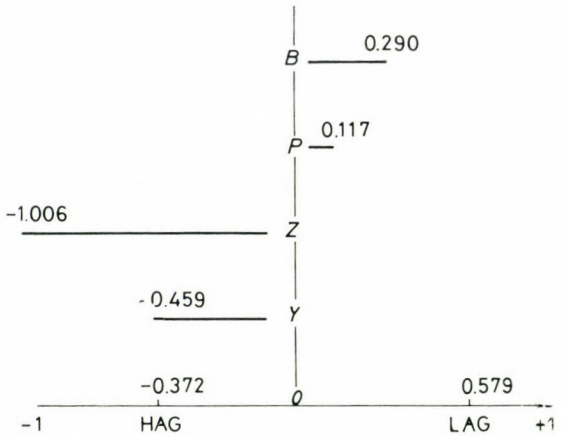

Fig. 5. Abdominal aorta. Results of the discriminant analysis (X, Y, Z, P, B). Wilks criterion $\lambda = 0.8213$ ($p<0.001$). Per cent of correct classification = 71.3%, best variables = P, Z, B

mately the very best one, here. (TA, $\alpha_p = -0.7123$ and AA, $\alpha_p = -0.1172$). Both in the thoracic and abdominal segments of the aorta the index of benignity (B) appeared as one of the best variables (TA, $\alpha_B = 0.4235$; AA, $\alpha_B = 0.2901$). It should be observed that the sign of the benignity index (B) is always positive like it is in the LAG, this means that (B) does in fact represent benignity. Similar results were reported for the coronary sector [10]. This confirms that (B) is a true measure of benignity, as best observed in these aorta segments. Here its high values mean a favourable prognosis for the patients. Considering the results shown in Tables II and III and graphs 3–5 the major errors of classification are present in the LAG. As already reported [10] this suggests the possibility that the DA classified patients into the wrong groups in these cases. Why does this happen in the LAG? Apparently because some patients with atherosclerotic lesions sufficient to classify them as belonging to HAG do actually die of some other disease (e.g. cancer) independent of the grade of their actual atherosclerosis. Such patients are classified clinically as belonging to LAG since their immediate cause of death was not atherosclerosis. In both aorta segments the (X) fatty streak is associated with LAG which shows the benignity of this atherosclerotic lesion. The highest contribution to discriminating between HAG and LAG comes from the relative surface of the severe plaques (Z) in both aorta sectors, as it is in the coronary sector [10]. A comparative study was done to establish, the discriminating contributions of each lesional state vector coordinate (X, Y, Z) in classifying a patient into HAG and LAG, the results are presented as follows: In both aorta segments the discriminating values of fatty streaks is less than that of fibrous plaques, and this is always less than that of severe plaques.

These facts are in accordance with the very strong correlation already reported in some earlier papers [1, 5—8, 23, 24, 26, 27].

Finally the use of the multivariate techniques (DA) should be emphasized, applied in this study to establish the validity consistency and coherence of the BS. The results presented have shown that the use of the anatomico pathological classification into HAG and LAG, according the basic cause of death is correct.

Conclusions

The variables (X, Y, Z, P, B) of the BS used in this work are useful in characterizing and describing the lesional state of the two aorta segments studied (thoracic and abdominal), and in distinguishing between the HAG and the LAG groups. They are also consistent with the criterion used to differenciate these groups on the basis of the direct cause of death.

In the two aorta segments studied, the following factors were identified a) a first component, benignity (fatty streaks (X) and benignity index (B) and b) a second component, severity (severe plaques (Z) and stenosis number (P)).

The variables (X, Y, Z), as components of the lesional state vector are sufficient to distinguish between the HAG and the LAG, while the stenosis number (P) and the benignity index (B) appear frequently as the most important variables in the discriminating functions.

The sign of the benignity index (B) is always the same as that of the LAG in the factorial axis of the discriminant analysis. Thus (B) is a true benignity variable.

The two multivariate statistical techniques PCA and DA have shown the scientific value, consistency and coherence of the BS developed to characterize the a.l. of the two aorta segments studied (TA and AA) The PCA revealed some important hidden components or factors characterizing this arterial region with only an "a posteriori" logically and very useful reduction of the primary data. The DA has shown that the criterion based on the direct cause of death to classify the patients (at autopsy) into HAG and LAG is correct and useful.

REFERENCES

1. Campos R: Aterosclerosis y cancer: Estudio anatomopatologico de las arterias coronarias: aorta y cerebrales. Tesis de Especializacion en Anatomia Patologica Hosp. Militar Central La Habana, Cuba, 1980
2. Carlevaro PV, Fernandez-Britto JE: Bases metricas para la caracterizacion de la lesion aterosclerotica. Actualidades en Anatomia Patologica. Serie de Informacion Tematica, Minsap. 4: 8, 1982
3. Carlevaro PV, Fernandez-Britto JE: Algunos criterios biometricos de ponderacion de gravedad en las lesiones ateroscleroticas. Actualidades en Anatomia Patologica. Serie de Informacion Tematica, Minsap, 4: 29, 1982

4. Fernandez-Britto JE, Bielokrinitzki V, Morgalo R, Candas A, Dujarric R, Candas M: Diseno experimental de la investigacion "estudio de la aterosclerosis coronaria, aortica y cerebral". Rev Cub Hig Epid 19: 137, 1981
5. Fernandez-Britto JE, Carlevaro PV, Bacallao J, Dujarric R: Analisis del grado de asocoacion existente entre la lesion aterosclerotica de las arterias coronarias y de la aorta. Rev Cub Invest Biom 1: 348, 1982
6. Fernandez-Britto JE, Carlevaro PV, Bacallao J, Dujarric R: La aterosclerosis de las arterias coronarias y su forma de asociacion con la aterosclerosis de la aorta. Rev Cub Invest Biom 1: 385, 1982
7. Fernandez-Britto JE, Carlevaro PV, Bacallao J, Dujarric R: Analisis del grado de asociacion existente entre la lesion aterosclerotica de las arterias cerebrales y de la aorta. Rev Cub Invest Biom 1: 385, 1982
8. Fernandez-Britto JE, Carlevaro PV, Bacallao J, Dujarric R: La aterosclerosis de las arterias cerebrales y su forma de asociacion con la aterosclerosis de la aorta. Rev Cub Invest Biom 1: 412, 1982
9. Fernandez-Britto JE, Carlevaro PV, Bacallao J: The atherosclerotic lesion. A Biometric System for its description and characterization in any vascular sector. Acta Morph Hung 32: 3, (Abstr) 1984
10. Fernandez-Britto JE, Bacallao J, Carlevaro PV, Campos R, Falcon L, Dujarric R: Coronary atherosclerotic lesion: its characterization applying a Biometric System using Discriminant Analysis. Exp Path (in press).
11. Fernandez-Britto JE, Bacallao J, Carlevaro PV, Campos R, Falcon L, Dujarric R: Coronary atherosclerotic lesion: its characterization applying a Biometric System using Principal Components Analysis. Exp Path (in press).
12. Gotto AM Jr: Directions of atherosclerosis research in the 1980s and 1990s. Circulation 70: (Suppl III), 1984
13. Holman RL, McGill HC Jr, Strong JP, Geer JC: Technics for studying the atherosclerotic lesions. Lab Invest 7: 42, 1958
14. Jellinek H, Detres Z, Veress B: Transmural Plasma Flow in Atherogenesis. Akadémiai Kiadó. Budapest 1983
15. Kim K-O, Nie NH, Hull CH, Jenkins JG, Steinbrenner K, Bent H: Factor Analysis "SPSS" Statistical Package For Social Sciences Vol. 24. (2nd ed.) McGraw-Hill, 1975, p. 468
16. Klecka WR: Discriminant Analysis. "SPSS", Statistical Package For Social Science. Vol. 23. (2nd ed.) McGraw-Hill, 1975, p. 434
17. McGill HC Jr, (ed): The Geographic Pathology of Atherosclerosis. Baltimore, Williams and Wilkins, 1968
18. Pena A: La aterosclerosis de la aorta. Estudio de una serie consecutiva de 173 necropsias del Hospital Militar Central Dr. C. J. Finlay, durante el ano 1978. Tesis de Especializacion en Anatomia Patologica. La Habana, 1979
19. Ruffer MA: On arterial lesions found in Egyptian Mummies (1580 BC-AC 525). J Path Bact 15: 453, 1910—11
20. Shattock CG: A report upon the pathological condition of the aorta of King Menephtah, traditionally regarded as the Pharaoh of the Exodus. Proc Roy Soc Med Pathol (Section 2): 122, 1908—09
21. Sjovall HG, Wihman G: Beobachtungen über die Arteriosklerose in Schweden samt einem Beitrag zur Frage der Lipoidose der Arterien intima. Acta Path Microbiol Scand (Suppl) 20, 1934
22. "SPSS". Statistical Package For Social Sciences. (2nd ed). McGraw-Hill, 1975
23. Sternby NH: Atherosclerosis in a defined population (An autopsy survey in Malmö, Sweden). Acta Path Microbiol Scand (Suppl) 194, 1968
24. Strong JP, Restrepo C, Guzman MA: Coronary and aortic atherosclerosis in New Orleans. II. Comparison of lesions by age, sex and race. Lab Invest 39: 364, 1978
25. Tracy RE, Toca V, Lopez CR, Kissling GE, Devaney K: Fibrous intimal thickening and atheronecrosis of the thoracic aorta in coronary heart disease. Lab Invest 48: 303, 1983
26. Vihert A: Atherosclerosis of the aorta in five towns. Bull Wld Hlth Org 53: 501, 1976
27. Vihert A: High and low atherosclerosis groups. Bull Wld Hlth Org 53: 519, 1976
28. WHO: Study group on the classification of atherosclerotic lesions. Technical report series 143, 1958
29. WHO: Atherosclerosis of the aorta and coronary arteries in five towns. Bull Wld Hlth Org 53: 485, 1976
30. Zahor Z, Czabanova V: Postlathyric fibroelastosis of the rat aorta related to topical factors of experimental atherosclerosis. Path Res Pract 179: 545, 1985

Acta Morphologica Hungarica, 35 (3—4), pp. 199—206 (1987)

EFFECTS OF QUANTITATIVE UNDERNOURISHMENT, ETHANOL AND XYLENE ON CORONARY MICROVESSELS OF RATS

VERONIKA MORVAI[1], GY. UNGVÁRY[2], H.-J. HERRMANN[3], CH. KÜHNE[4]

[1]2ND DEPARTMENT OF MEDICINE, SEMMELWEIS UNIVERSITY OF MEDICINE, [2]NATIONAL INSTITUTE OF OCCUPATIONAL HEALTH, BUDAPEST, [3]CENTRAL INSTITUTE FOR HEART AND CIRCULATION RESEARCH, BERLIN, [4]CENTRAL INSTITUTE OF MICROBIOLOGY AND EXPERIMENTAL THERAPY, JENA, ACADEMY OF SCIENCES, GDR

(Received 27 October 1986)

The effect of alimentary deficiency, ethanol intake and exposure to xylene on the coronary microvessels and heart weight were investigated in rats.

The coronary microvessels of rats, which were undernourished for 5 weeks and which were fed ad libitum were studied with the histomorphometric method of Herrmann et al [19].

In another experiment a group of rats was fed a control liquid diet while another group was fed a liquid diet containing ethanol up to 36% of the total Joule intake. One-half of both groups were placed in an exposure chamber supplied with pure air; the other two half-groups were made to inhale air containing 1000 mg xylene/m^3 for 6 h daily, 5 days a week, for a period of 4 weeks.

It was found that undernourishment did not cause any morphological reactions in the microvessels and did not affect the relative heart weight. Ethanol increased the contractile activity of the wall cells of coronary microvessels, and also the relative heart weight. The effect of xylene was similar to that of the ethanol. The effect of xylene in combination with ethanol was additive on the one hand (in some parameters), on the other hand there was an inhibition between the effects of the two chemicals (in the case of the number of mv.* 10.5 $\mu m < d < 21$ μm).

It is concluded that both ethanol and xylene increase the vascular tone of coronary microvessels and this alteration causes a decrease in the nutritive myocardial blood flow. Undernourishment does not play any role in the increase of vascular tone.

Keywords: Ethanol, xylene, undernourishment, coronary microvessels

Introduction

The association between chronic alcoholism and clinical cardiac dysfunction is well known, but the mechanism of ethanol toxicity is poorly understood. It is unclear whether alcohol itself [31], or its primary metabolic product acetaldehyde[23] may be held responsible for a direct toxic effect on the heart.

Abbr.: mv. = microvessels; m.ch.l. = maximal chord length

Send offprint requests to Veronika Morvai, 2nd Dept. of Internal Medicine, Semmelweis Medical University 1088 Budapest, Szentkirályi u. 46. Hungary

The pathological changes in chronic alcoholic heart disease are not specific for alcohol toxicity, but may reflect the effect of chronic ischemia [7]. It is likely that these changes are mediated by alterations in the small coronary vessels as large coronary vessel disease is usually absent [6].

After long-term alcohol intake in rats the nutritive blood-flow of the myocardium decreases, while myocardial vascular resistance increases [26, 27]. In the elevation of coronary resistance due to chronic alcohol ingestion the increase of wall thickness of coronary microvessels may play a role [18]. However, the cause for the apparent long-term increase in contractile vascular tone remains unclear.

After 16 weeks ethanol administration to rats in a diet in which 40% of the total caloric intake originated from ethanol, Rossi [34] detected pathomorphological changes and an increase in the catecholamine concentration of the heart only in those ethanol-treated animals which had been kept on a calorically inadequate diet, whereas no such changes developed in the ad libitum fed ethanol-treated rats. Numerous studies support the hypothesis that the association between chronic ethanol consumption and cardiomyopathies is a consequence of a primary multifactorial nutritional deficiency [5, 22]. The discussion of the pros [12, 22] and cons [32, 33] of this assumption is of practical relevance, for ethanol induces disturbances in the intestinal resorption of nutrients [14, 20]. According to Hepp and Kochsiek [15], it is obvious that the lower body weights of rats observed by most authors after long-term ethanol intake, is an outcome of these resorption disturbances. Therefore, it was the first aim of the present study to answer the question whether quantitative undernourishment is able to induce the above-mentioned morphological reaction as seen in the microvessels of ethanol-fed rats.

Xylene is a widely used industrial chemical, which can induce cardiovascular disorders[25]. The effect of xylene poisoning on myocardial circulation is not known. The second aim of the present work was to investigate the effect of xylene on coronary microvessels.

The toxic effect of a number of environmental and occupational chemicals is stimulated by alcohol. The question arises whether the two substances given together have any effect on the coronary microvessels. The third aim of the present work was to obtain data bearing on this possible interaction.

Materials and methods

Six of twelve 11-week-old male Wistar rats were fed a normal laboratory diet ad libitum, the other 6 rats received only 10 g of the diet per animal per day for 5 weeks.

Thirty CFY male rats weighing 250—280 g were kept on the liquid diet of DeCarli and Lieber [11] modified by Ungváry and Hudák [37]. After a period of adaptation to this diet, 15 of these animals were fed a control diet, while the other 15 rats were given a diet of a similar Joules value for 4 weeks which, however, contained ethanol instead of some of

the carbohydrates and fat (36% of the total Joules). The animals on the alcoholic diet received 11.5—12.5 g ethanol/kg b.w. daily. To ensure the same caloric value in both groups, the animals were pair-fed according to DeCarli and Lieber [11].

Twenty-four further CFY rats weiging 250—280 g were fed in the same manner. In 12 of these animals, the above-mentioned ethanol feeding was applied. Six rats of both groups were treated daily by xylene inhalation in an exposure chamber: 1000 mg/m^3 over 6 h each day, 5 days a week. The other group of these rats were made to inhale pure air.

All the animals were killed by intracardiac KCl. For the histomorphometric and histopathological investigation of the left ventricular wall, the hearts were cut vertically in the middle so that in each heart specimens could be prepared from the same definite middle zone comprising the left and right ventricular wall as well as the septum. For further methodological details (specimen preparation, the selective visualization of microvessels by means of a special ATP-ase reaction detecting the ATP-hydrolysis of only the endothelial and muscle cells of precapillary mv. and of special endothelial cells of some capillaries, the counting, classification and measurement of the surface of these mv. by means of the automatic image analyzer QUANTIMET, for the interpretation and statistical testing of the histomorphometric data and for discussion on the reliability of this method see [16, 19].

Experiments to control value ratios (R) were calculated by dividing the parameters of the specimens of the experimental animal by the corresponding values of the simultaneously sectioned and prepared specimens of the control animals measured in the same manner. Using a 2-way analysis of variance, the mean values of these ratios and their deviations were tested against the deviations occurring between at least 20, but mostly 40 to 50, of the corresponding measurement values of heart specimens of untreated rats prepared and measured in the same manner. The mv. were classified by the QUANTIMET according to their maximal chord length (m.ch.l.) into 3 classes (class I: 6.5 μm$<$m.ch.l.$<$10.5 μm, class II: 10.5 μm$<$ $<$m.ch.l.$<$21 μm, class III: m.ch.l.$>$21 μm). Thus each class contains a number of mv. with an external transversal diameter (d) smaller than the lower class limit ($N_i^{d<i}$). The experimental to control value ratios (R) of mv.$_{10.5\mu m<d<21\mu m}$ (R_{II}^d) and of mv.$_{d>21\mu m}$ (R_{III}^d) were approximately calculated as follows:

$$R_{II}^d = \frac{R_{II} - R_I \cdot m_{II}}{1 - m'_{II}} \tag{1}$$

$$R_{III}^d = \frac{R_{III} - R_I \cdot m_{III} - R_{II} \cdot m'_{III}}{1 - m_{III} - m_{III}} \tag{2}$$

I, II, III: QUANTIMET classes

m: mean percentage of $N_i^{d<i}$ in class i/100 for mv.$_{d<10.5\mu m}$; in class II: 0.29, in class III: 0.054.

m': the same for mv.$_{10.5\mu m<d<21\mu m}$; in class III: 0.484; (for details see [37]).

Moreover, the QUANTIMET procedure was extended by measurements of the projected wall area of all the mv. ($A_{\Sigma mv.}$) and the mv. of each class ($A_{cl.i}$). By dividing the area of class (i) and the mv. number (N) of the same class, the mean mv. wall area of this class ($A_{mv.,cl.i.}$) was calculated. The statement of an increase of wall thickness of mv.$_{d<10.5\mu m}$ or of mv.$_{10.5\mu m<d<21\mu m}$ is based on a significant augmentation of the mv. number of the next higher class. A thickening of walls of mv.$_{d>21\mu m}$ is recognizable if $A_{mv.,cl.III}$ is significantly increased or if it remains in the normal range, although the number of mv. of class III is unchanged or increased, for the mean area of mv. joining class III from class II by thickening of their walls lies distinctly below the normal mean $A_{mv.,cl.III}$-value. Therefore, the $A_{mv.,cl.III}$-value would have been lower if only the "border crossers" mentioned had increased the number and total area of the mv. of class III and the walls of the pre-existing mv. of this class had not thickened.

A significant elevation of mv.$_{d<10.5\mu m}$ (N_I) demonstrates an increase in the number of mv. capable of hydrolyzing ATP; a proliferation of capillaries may contribute to such a result.

Serially sectioned specimens were stained with hematoxylin-eosin, Gomori-silver and Sudan III. Student's *t*-test was used to analyze the mean values of the absolute and relative weights of the left and right ventricular wall (weight of ventricular walls $\times$ 1000/body weight) as well as of body weights.

Results

Quantitatively undernourished rats do not show any kind of morphological mv. reactions (Table I). Ethanol feeding in animals kept likewise only in their cages, results in significant augmentation of all the parameters measured, with the exception of the mean area of mv. measured in the 3 classes ($A_{mv.,cl.I,II,III}$). This means that the wall thickness of all microcirculatory areas and the number of $mv._{d<10.5\mu m}$ which are able to hydrolyze ATP are significantly increased. Almost the same mv. reactions are seen in solely ethanol-fed "chamber"-rats, although the augmentation of $mv._{d>21\mu m}$ indicating a thickening of walls of $mv._{0.5\mu m<d<21\mu m}^{1}$ is not present. The level of significance of the increased values is less frequently reached in ethanol-fed "chamber" animals, due mostly to the lower number of rats in each group.

Table I

Experiments to control value ratios of wall area (A) and number (N) of mv. as well as

Experimental influence	A						
	Σ mv.	cl. III	cl. II	cl. I	mv. cl. III	mv. cl. II	mv. cl. I
Quantitative undernourishment (n=6)	1.06 ±0.32	—	—	—	—	—	—
Ethanol-feeding (n=15)	1.33* ±0.28	1.36* ±0.34	1.28* ±0.27	1.35* ±0.38	1.03 ±0.13	0.99 ±0.10	0.98 ±0.04
Chamber experiments:							
controls (n=6)							
Ethanol-feeding and air inhalation (n=6)	1.21 ±0.23	1.22* ±0.16	1.24 ±0.44	1.20 ±0.37	1.09 ±0.20	0.96 ±0.07	0.98 ±0.04
Control diet and xylene inhalation (n=6)	1.19 ±0.26	1.24 ±0.29	1.17 ±0.36	1.13 ±0.45	1.10 ±0.33	0.94 ±0.06	0.99 ±0.06
Ethanol-feeding and xylene inhalation (n=6)	1.27* ±0.35	1.34* ±0.20	1.18 ±0.72	1.19 ±0.88	1.17 ±0.31	1.03 ±0.09	1.01 ±0.02

* significant different from controls

Xylene inhalation induces nearly the same mv. reaction as ethanol feeding. The combination of both is in part followed by a somewhat stronger ($A_{\Sigma mv.}$, $A_{cl.III}$, $A_{mv.,cl.III}$, $N_{d>21\mu m}$) or lesser ($N_{10.5\mu m<d<21\mu m}$) increase in the values measured. But these are not significant differences. In mv. and heart muscle cells of all experimental groups there were no qualitative pathological changes. Ethanol-fed rats showed an increase in the number of interstitial cells of the heart. The body weights were reduced in all experimental animals. The same was true for the absolute heart weights with the exception of solely ethanol-fed "chamber" rats. But the heart to body weight ratios were elevated, except for the quantitatively undernourished rats which showed a slight decrease (Table I).

body weights (b.w.), heart weights (h.w.) and relative heart weights (rel.h.w.)

N				b.w.	h.w.	(rel. h.w.)
mv. d>21	mv. 10.5<d<21	mv. d<10.5	mv. d<21	(g)	(mg)	$\left(\frac{\text{h.w.}\times 1000}{\text{b.w.}}\right)$
1.01 ±0.25	—	—	1.08 ±0.26	342 ±47 (c)	84 ±108 (c)	2.49 ±0.1 (c)
				230* ±46 (e)	548* ±103 (e)	2.39 ±0.1 (e)
1.38* ±0.47	1.26* ±0.28	1.38* ±0.39		293 ±0.23 (c)	700 ±75 (c)	2.39 ±0.17 (c)
				265* ±22 (e)	655 ±68 (e)	2.51* ±0.15 (e)
				283 ±19	690 ±58	2.45 ±0.11
0.97 ±0.21	1.32* ±0.54	1.24 ±0.42		255 ±38	6.87 ±0.62	2.73 ±0.35
0.99 ±0.10	1.30* ±0.45	1.15 ±0.47		253 ±26	649 ±26	2.59 ±0.23
1.28 ±0.50	1.15 ±0.69	1.16 ±0.85		256 ±25	664 ±59	2.60* ±0.08

c: control
e: ethanol-feeding

Discussion

The undernourishment of rats failed to induce any morphological reactions in coronary microvessels. Thus, this factor can be excluded as the sole cause for the general increase in wall thickness of coronary microvasculature and the augmented ATP-hydrolysis of $mv_{d<10.5\mu m}$ which are detected without any qualitative vascular changes in ethanol-fed animals. The reason for these morphological correlates of predominantly vasotonic influences acting beyond the period of short-term regulation has to be searched for in other factors, especially in the increases observed in the synthesis, release and/or blood levels of catecholamines [4, 10, 28, 29, 30, 35], aldosterone [24], renin [21,24] and corticosterone [8, 9] as well as the effect of acetaldehyde and acetate, the metabolites of ethanol [1]. It is worth mentioning that the absolute weight of the ventricular walls was distinctly less reduced in ethanol-fed rats than in quantitatively undernourished animals. While the latter showed a tendency of decreasing relative heart weights, this parameter was significantly elevated in ethanol-fed rats. Therefore, the increase of the heart-to-body-weight ratio is attributable not only to the loss of body mass, but also in all likelihood, to anabolic effects on heart muscle cells counteracting the predominating catabolic processes, thus hampering an equal loss of body and heart mass.

It is interesting to note that in all our experiments [26, 27] the systolic blood pressure and the cardiac index decreased. Thus, an increase in the functional activity of heart muscle cells causing a hoemodinamically detectable elevation of the performance of the heart can be excluded. Therefore, the reason for the increased heart-to-body-weight ratio need to be explained.

Ethanol-fed "chamber"-rats did not show the increase in wall thickness of $mv._{10.5\mu m<d<21\mu m}$ recognizable in a significant augmentation of the number of $mv._{d>21\mu m}$ as seen in ethanol-fed animals remaining in their cages. Possibly this difference is attributable to the special conditions and influences of the chamber experiment, for repeated handling of animals only for the procedures of blood pressure measurements was sufficient for a decrease in wall thickness of microvessels both in Wistar rats [19] and in spontaneously hypertensive rats [17].

Xylene inhalation is followed by almost the same mv. reactions as ethanol intake. The increased wall area of all mv. ($A_{\Sigma mv.}$) and of mv. with maximal chord lengths (more than 21 μm, $A_{cl.III}$) distinctly exceeded the methodological error.

Xylene is a mixture of alkyl derivatives of benzene (ortho-, meta-, para-xylene and ethylbenzene). It is frequently used as organic solvent and may have biological effects. It has been shown that benzene and its alkyl derivatives, in spite of their similar chemical structures, act differently on the dopamine and noradrenaline levels and turnover in the hypothalamus, median

eminence, striatum and subcortical limbic regions as well as on the secretion of prolactin, TSH and corticosterone from the pituitary and adrenals [2, 3]. Benzene and its alkyl-derivatives cause a significant change in the density of monoaminergic nerve fibers of the iris, liver, ovarium, uterus, etc. as visualized by Falck and Hillarp's [13] catecholamine histofluorescence technique [36]. These data and the results of the present study suggest that xylene affects the contractile vascular tone of the myocardial microvasculature through a change in the local concentration of vasoactive substances. These alterations in coronary microvessels may explain the cardiac dysfunction disorders of ventricular repolarization, arrhythmias caused by subacute poisoning with xylene [25].

Combined exposure to xylene and ethanol increased the experimental to control value ratios of all wall areas as well as the number of $mv._{d>21\mu m}$. These effects were additive. The number of $mv._{10.5\mu m<d<21\mu m}$ did not change significantly under the simultaneous effect of xylene and ethanol, and the effect did not differ from the controls.

Consequently, in this case there is an inhibiting interaction between the effect of xylene and that of ethanol.

It is concluded that both ethanol and xylene increase the vascular tone of coronary microvessels and thereby they decrease the nutritive blood flow which can elicit hypoxaemic alterations. It is highly interesting that there is no addition or potentiating interaction between the similar effect of two chemicals on the vascular tone. The main effects of the two chemicals on the cardiovascular system are independent of each other.

REFERENCES

1. Altura BM, Gebrewold A: Failure of acetaldehyde or acetate to mimic the splanchnic arteriolar or venular dilator actions of ethanol: direct in situ studies on the microcirculation. Br J Pharmac 73: 580, 1981
2. Andersson K, Fuxe K, Nilsen OG, Toftgard R, Eneroth P, Gustafsson JA: Production of discrete changes in dopamine and noradrenaline levels and turnover in various parts of the rat brain following exposure to xylene, ortho-, meta-, and para-xylene and ethylbenzene. Toxicol Appl Pharmacol 60: 535, 1981
3. Andersson K, Fuxe K, Toftgard R, Nilsen OG, Eneroth P, Gustafsson JA: Toluene-induced activation of certain hypothalamic and median eminence catecholamine nerve terminal systems of the male rat and its effect on arterior pituitary hormone secretion. Toxicol Lett 5: 393, 1981
4. Baratti CM, Rubio MC, Perec CJ, Tiscornia OM: Effect of chronic alcohol feeding on adrenergic and cholinergic neurotransmission mechanism. Amer J Gastroenterol 73: 21, 1980
5. Benchimol AB, Schlesinger P: Beriberi heart disease. Amer Heart J 46: 245, 1953
6. Brigden W: Alcoholic cardiomyopathy. Cardiovasc Clin 4: 187, 1972
7. Burch GE, Cholcoldugh HL, Harb JM, Tsui CY: The effect of ingestion of ethylalcohol, wine, and beer on the myocardium of mice. Amer J Cardiol 27: 522, 1971
8. Cicero TJ: Neuroendocrinological effects of alcohol. Annu Rev Med 32: 123, 1981
9. Cobb Ch F, v. Thiel DH, Gavaler JS, Lester R: Effects of ethanol and acetaldehyde on the rat adrenal. Metabolism 30: 537, 1981

10. Cohen LB, Sellers EM, Sellers EA, Flattery KY: Ethanol and sympathetic denervation effects on rat adrenal catecholamine turnover. J Pharmacol Exp Ther 212: 425, 1980
11. DeCarli LM, Lieber CS: Fatty liver in the rat after prolonged intake of ethanol with a nutritionally adequate new liquid diet. J Nutr 91: 331, 1967
12. Factor SM: Intramyocardial small-vessel disease in chronic alcoholism. Amer Heart J 92: 561, 1976
13. Falck B, Hillarp NA, Thieme G, Thorp A: Fluorescence of catecholamines and related compounds condensed with formaldehyde. J Histochem Cytochem 10: 348, 1962
14. Frank O, Baker H: Vitamin profile in rats fed stockor liquid ethanolic diets. Amer J Clin Nutr 33: 221, 1980
15. Hepp A, Schier H, Kochsiek K: Dosisabhängige Kardiodepression bei der akuten Alkoholintoxikation der Ratte. Z Kardiol 71: 533, 1982
16. Herrmann HJ, Kühne CHR, Mühlig P, Lauter J: Zur Feststellung von wanddicken Veränderungen arterieller Endsbrombahngefässe durch das ATPase-Quantimet-Verfahren. Gegenbaurs Morph Jahrb Leipzig, 126: 2, S. 273, 1980
17. Herrmann HJ, Moritz V, Norden C, Kühne CHR: Morphologische Reaktionen und Langzeitvasotonusverhalten des mikrovascularen Koronarsystem in verschiedenen Stadien der spontanen Hypertonie der Ratte. Z Gesamte Inn Med 37: 696, 1982
18. Herrmann HJ, Morvai V, Ungváry Gy, Norden C, Mühlig P: Long-term effects of ethanol on coronary microvessels of rats. Microcirc Endothel and Lymphatics 1: 589, 1984
19. Herrmann HJ, Mühlig P, Kühne CHR, Lauter J: Automated image analysis for measurements of morphological reactions of blood vessels of the microvascular system. Exp Path 17: 215, 1979
20. Hoyumpa AM, Nichols S, Henderson GI, Schenker S: Intestinal thiamin transport: effect of chronic ethanol administration in rats. Amer J Clin Nutr 31: 938, 1978
21. Ibsen H, Christensen NJ, Rasmussen S, Hollaugel H, Nielsen MD, Giese J: The influence of chronic high alcohol intake on blood pressure, plasma noradrenaline concentration and plasma renin concentration. Clin Sci 61: 377, 1981
22. Ikram H, Maslowski AH, Smith BL, Nicholls MG: The haemodynamic, histopathological and hormonal features of alcoholic cardiac beriberi. Quart J Med New Series. N 200: 359, 1981
23. James TN, Bear ES: Effects of ethanol and acetaldehyde on the heart. Amer Heart J 74: 243, 1967
24. Linkola J, Fyhrquist F, Ylikahri R: Renin, aldosterone, and cortisol during ethanol intoxication and hangover. Acta Physiol Scand 106: 7582, 1979
25. Morvai V, Hudák A, Ungváry Gy, Varga B: ECG changes in benzene, toluene and xylene poisoned rats. Acta Med Acad Sci Hung 33: 275, 1976
26. Morvai V, Ungváry Gy: Effects of simultaneous alcohol and toluene poisoning on the cardiovascular system of rats. Toxicol Appl Pharmacol 50: 381, 1979
27. Morvai V, Ungváry Gy, Varga K, Albert K, Folly G: Effect of long-term alcohol intake on the cardiovascular system of the rat. Acta Physiol Acad Sci Hung 54: 369, 1979
28. Motoyama K: Change in catecholamine level in rabbit blood caused by acute alcoholism. Chem Abstr 58: N 10 650, 1968
29. Perman ES: The effect of ethyl alcohol on the secretion from the adrenal medulla in man. Acta Physiol Scand 44: 241, 1958
30. Pohorecky LA: Influence of alcohol on peripheral neurotransmitter function. Fed Proc 41: 2452, 1982
31. Regan TJ: Ethyl alcohol and the heart. Circulation 44: 957, 1971
32. Regan TJ, Ettinger PO: Alcohol and the heart. In: Hurst JW (ed.), The Heart, McGraw-Hill Book Comp New York, 1979, p. 259
33. Regan TJ, Haider B: Ethanol abuse and heart disease. Circulation 64 (Suppl. III. 14, 1981
34. Rossi MA: Alcohol and nutrition in the pathogenesis of experimental alcoholic cardiomyopathy. J Pathol 130: 105, 1980
35. Siegel JH: The effect of enteric ethanol on arterial and portal venous catecholamines. Clin Res 12: 213, 1964
36. Ungváry Gy, Donáth T: Effect of benzene and its methyl-derivatives (toluene, paraxylene) on postganglionic noradrenergic nerves. Z Mikorsk Anat Forsch Leipzig 98: 5, S. 755, 1984
37. Ungváry Gy, Hudák A: Hosszan tartó nagy dózisú orális alkohol kezelés módjai és ezek gyomor-bél tractusra és a májra kifejtett hatásának összehasonlítása CFY patkányokban. Kíséerl Orvostud 29: 86, 1977

Acta Morphologica Hungarica, 35 (3—4), pp. 207—210 (1987)

THE CHRONICALLY FUROSEMIDE-TREATED MOUSE AS A POSSIBLE ULTRASTRUCTURAL MODEL FOR CYSTIC FIBROSIS

G. T. Szeifert, Éva Varga, L. Damjanovich Sz. Gomba

DEPARTMENT OF PATHOLOGY, UNIVERSITY MEDICAL SCHOOL OF DEBRECEN, HUNGARY

(Received 4 November 1986)

The effect of chronic furosemide treatment on the structure of the secretory cells in the mouse pancreas was studied using electron microscopy. The number of the zymogen granules increased in the cytoplasm of acinar cells; they were more densely packed and had a less electron-dense appearance than the controls. Because these ultrastructural findings resemble the changes observed in exocrine glands of patients with cystic fibrosis, the chronic furosemide-treated mouse is proposed as an experimental model for this disease.

Keywords: Cystic fibrosis, furosemide, chloride transport

Introduction

Cystic fibrosis (CF) is the most common lethal genetic disorder affecting Caucasians, characterized by obstructive lesions throughout multiple organ-systems and disturbances of mucus and electrolyte secretion [2, 9]. The primary cause of the disease remains unknown, but it is generally accepted that it results from a single gene defect [8]. Although the gene remains to be identified, at least it is now certain that it resides in the middle of the long arm of chromosome 7 [5]. Recently, however, some investigators suggested that it might be a gene which affects chloride ion transport in cell membranes [1, 7]. Martinez and Cassity have demonstrated that furosemide reduces saliva and Cl secretion in the isolated, perfused rat submandibular gland by effecting acinar cells [3]. We have studied the ultrastructural changes of secretory cells induced by chronic furosemide treatment in the mouse pancreas. These alterations resembled the lesions observed in exocrine glands of patients with CF, and therefore the chronically furosemide-treated mouse is proposed as an experimental model for this disease.

Send offprint requests to L. Damjanovich, Department of Pathology, University Medical School of Debrecen, H-4012, P.O.B. 23., Hungary

Materials and methods

Adult male CFLP mice (30 g) were used in these experiments. Furosemide (330 mg/kg body weight) was administered daily for 50 days by intraperitoneal injections. Non-treated mice served as controls. All animals were supplied with food and water ad libitum. Although the daily dose administered i.p. by us corresponded to the i.v. DL50 for mouse, the treatment was well tolerated by the animals, no signs of sickness or decreased physical activity were detectable. The pancreas was removed after aether anaesthesia and processed immediately. A portion of each pancreas was fixed in 8% formaldehyde and processed in the routine manner for light microscopy. Tissue samples were cut into cubes of 1 mm^3, fixed in 3% glutaraldehyde, postfixed with 1% osmium tetroxide, dehydrated in graded ethanol and embedded in Araldite. Thin sections were stained with uranyl acetate and lead citrate and evaluated by a Tesla BS 513A transmission electron microscope.

Results and discussion

Light microscopic examination has not revealed any remarkable changes in the furosemide-treated animals.

Ultrastructurally the secretory cells of the pancreas in the untreated control animals contained conspicuous, electron-dense, single membrane-bound zymogen granules (Fig. 1). Chronic treatment with furosemide moderately enlarged the size and diameter of the acinar cells. The number of the zymogen granules increased remarkably; they were more densely packed and had a less electron-dense appearance compared to the controls. Plications of the lateral cell membrane of the acinar cells occurred in the furosemide-treated animals (Fig. 2). These could not be observed in the control pancreas.

The transepithelial movement of Cl in salivary acinar cells is necessary for salivary fluid secretion. This implies entry of Cl, which occurs in part by means of a furosemide-sensitive co-transport system, and also an efflux of Cl [4]. Patients with CF have reduced salivary secretion. It may be the result of a defective transepithelial transport of Cl in secretory cells affecting either the diuretic-sensitive Cl uptake or the Cl efflux. Quinton demonstrated that the abnormality in CF is almost certainly due to an impairment of Cl permeability of the cell membrane [7]. Salivary fluid volume and Cl transport in acinar cells were greatly decreased by furosemide in isolated, perfused rat submandibular glands [3]. The results of our experiments indicate that the morphological changes in the mouse pancreas after chronic treatment with furosemide are compatible with those seen in other experimental models for CF [5]. The increased number of the zymogen granules in the secretory cells suggests an accumulation of secretory material in the cells, and consequently a reduced salivation. These ultrastructural findings could support the previous theories that the abnormality of Cl transport might play an important role in the pathogenesis of cystic fibrosis.

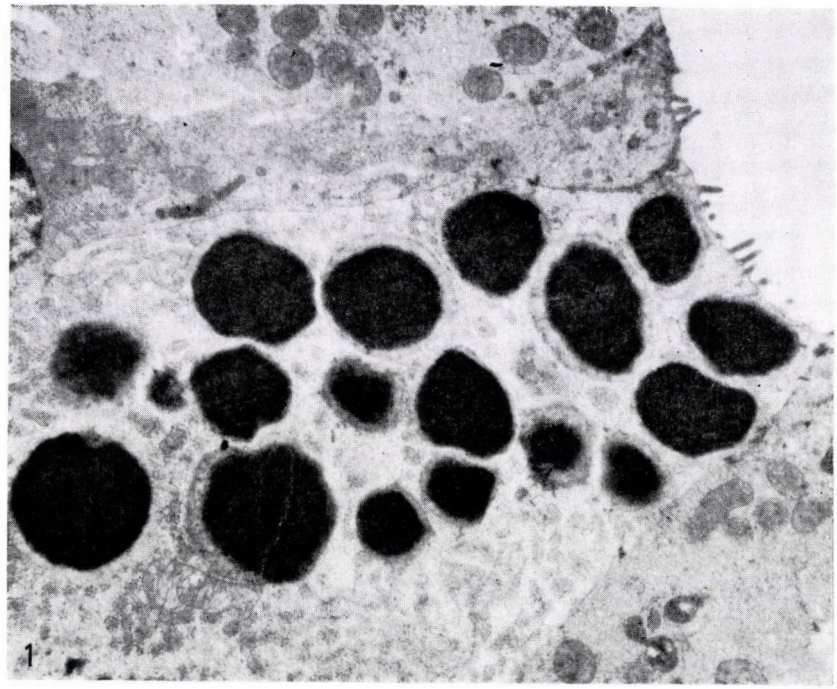

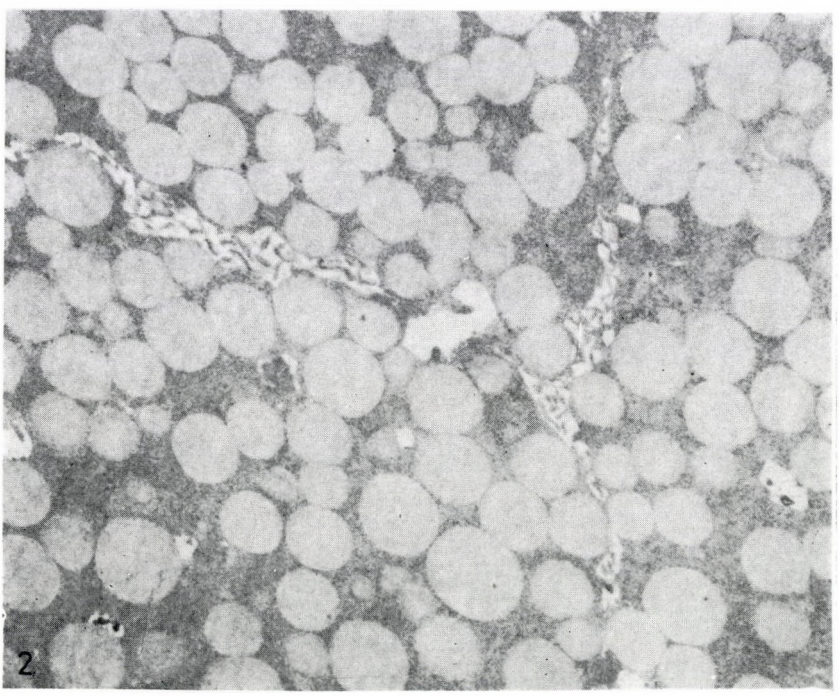

Fig. 1. Secretory cell of the pancreas in an untreated mouse. ×5600
Fig. 2. Acinar cells of the pancreas in a chronically furosemide-treated mouse. ×5600

REFERENCES

1. Kolata G: A new approach to cystic fibrosis. Science 228: 167, 1985
2. Lobeck C: Cystic fibrosis. In: The Metabolic Basis of Inherited Diseases. McGraw-Hill, New York, 1972. p. 1683.
3. Martinez JR, Cassity N.: Effects of ouabain and furosemide on saliva secretion induced by sympathomimetic agents in isolated, perfused rat submandibular glands. Experientia 40: 357, 1984
4. Martinez JR, Cassity N: The chronically reserpinized rat as a model for cystic fibrosis: abnormal Cl transport as the basis for reduced salivary fluid secretion. Pediatr Res 19: 711, 1985
5. Müller RM, Kuijpers GAJ, Bardon A, Ceder O, Roomans GM: The chronically pilocarpine-treated rat in the study of cystic fibrosis: investigations on submandibular gland and pancreas. Exp Mol Pathol 43: 97, 1985
6. Newmark P: Testing for cystic fibrosis. Nature 318: 309, 1985
7. Quinton PM: Chloride impermeability in cystic fibrosis. Nature 301: 421, 1983
8. Szabó M, Teichmann F, Szeifert GT, Tóth M, Török O, Papp Z: Prenatal diagnosis of cystic fibrosis by trehalase enzyme assay in amniotic fluid. Clin Genet 28: 16, 1985
9. Wood R, Boat T, Doershuk C: Cystic fibrosis. Am Rev Respir Dis 113: 833, 1976

Acta Morphologica Hungarica, 35 (3—4), pp. 211—218 (1987)

DIETHYL-NITROSAMINE HEPATOCARCINOGENESIS IN CIRRHOTIC RATS

A. Zalatnai, K. Lapis

FIRST INSTITUTE OF PATHOLOGY AND EXPERIMENTAL CANCER RESEARCH, SEMMELWEIS MEDICAL UNIVERSITY, BUDAPEST, HUNGARY

(Received 19 March 1987)

The aim of this study was to clarify how the CCl_4-induced cirrhosis modifies the process of diethylin-nitrosamine hepatocarcinogenesis. Two strains of rats (CFY and F-344) were used. CFY rats proved to be resistant toward both the cirrhogenic effect of CCl_4 and carcinogenic effect of DEN. In the F-344 rats, on the other hand, a large number of foci, neoplastic nodules and hepatocellular carcinomas occurred following DEN treatment only and fullblown liver cirrhosis did develop in the CCl_4-treated group. In F-344 rats with cirrhotic liver, foci and neoplastic nodules appeared in the usual number and at the usual time following DEN treatment, but — opposite to the expectations — much less carcinomas developed than in the rats receiving DEN only. When, however the CCl_4-treatment was applied following the DEN administration, a promoting effect was seen. The mechanism of the inhibitory effect of the CCl_4-induced liver cirrhosis upon hepatocarcinogenesis is not clarified, similarly to the mechanism of of the promoting effect of the CCl_4-treatment applied following the DEN administration.

Keywords: Diethyl-nitrosamine, hepatocarcinogenesis, CCl_4-induced cirrhosis

Introduction

In Europe and North America the majority of the human hepatocellular carcinomas (HCCs) develop in cirrhotic livers [1, 2], but the mechanism of the malignant transformation in cirrhotic liver is still unclear [3].

In the known rodent hepatocarcinogenesis models used all over the world [4] the HCCs generally develop in non-cirrhotic liver, and the preneoplastic lesions occur at the early stage of the experiment [5, 6]. These protocols therefore are not suitable for modeling the liver carcinogenesis taking place in cirrhotic human liver.

Our purpose therefore was to establish an experimental model for studying the role of the liver cirrhosis in the process of hepatocarcinogenesis induced by diethylnitrosamine (DEN). The fundamental question was whether the chronic carbon tetrachloride (CCl_4)-pretreatment or rather the CCl_4-induced liver cirrhosis is enhancing or diminishing the hepatocarcinogenic effect of DEN. We have also studied the effect on hepatocarcinogenesis of CCl_4 administered following the treatment with hepatocarcinogen.

Send offprint requests to A. Zalatnai, 1st Institute of Pathology and Experimental Cancer Research, Semmelweis Medical University, Budapest, Üllői út 26, H-1085, Hungary

Materials and methods

A total of 88 male Fischer-344 inbred and 66 male CFY outbred rats (obtained from LATI, Hungary), weighing about 130 g were used in the experiments. The experimental schedule and the groups are seen in Fig. 1.

Hepatic cirrhosis was induced by repeated doses of CCl_4, because the hepatocarcinogenic potential of this compound is known to be very low [7]. CCl_4 was administered at a dose of 0.5 ml/kg b.w. dissolved in corn oil (0.5 ml by gavage), 3 times a week for three months. At the end of the third month CCl_4-treated rats were killed in both strains to see whether liver cirrhosis has developed or not. Two weeks after the last CCl_4 dose, DEN was administered (purchased from SERVA, Heidelberg, FRG) intraperitoneally dissolved in 0.9% of sterile saline. The single dose of DEN was 200 mg/kg b.w., while the repeated doses were 10 mg/kg b.w. 3 times a week to reach a total dose of 200 mg/kg b.w.

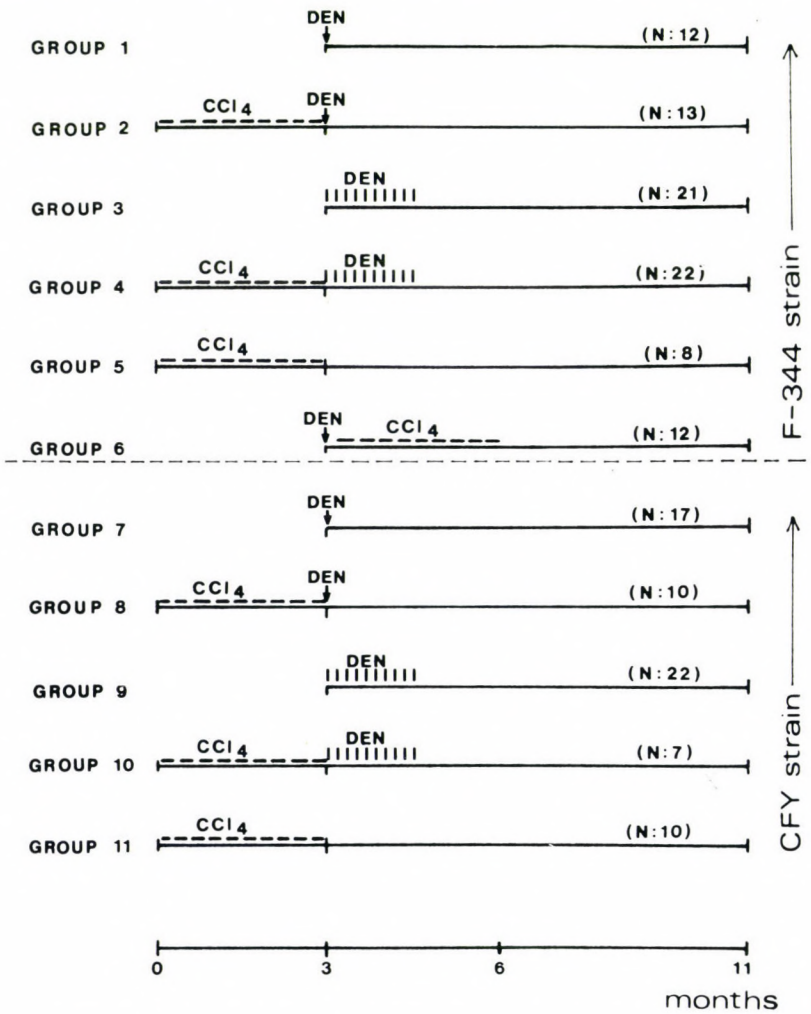

Fig. 1. The experimental schedule and the groups. CCl_4 = carbon tetrachloride, DEN: diethyl-nitrosamine

Experiments were ended 8 months after starting the carcinogenic treatment and 11 months after beginning of CCl_4 administration, when all animals were killed by exsanguination under a light aether anaesthesia. The removed livers were fixed in 8% buffered formalin, samples were embedded in paraffin and section of 5 μg thickness were cut. In addition to the routine HE staining and PAS (periodic acid-Schiff) reaction, a Picrosyrius red staining was also performed for the demonstration of the collagen [8]. Foci, neoplastic nodules and hepatocellular carcinomas were classified according to the recommendation of the international workshop [9].

Results

As it is seen in Fig. 2, the sensitivity of the F-344 and CFY strains was totally different to the carcinogenic potential of DEN.

	Cirrhosis	Focus	Neopl. nodulus	HCC
1→	-/12	5/12	2/12	-/12
2→	-/13	2/13	-/13	-/13
3→	-/21	12/21	8/21	18/21
4→	17/22	9/22	10/22	3/22
5→	7/8	1/8	-/8	-/8
6→	7/12	5/12	5/12	3/12
7→	-/17	3/17	-/17	-/17
8→	-/10	-/10	-/10	-/10
9→	-/22	4/22	1/22	-/22*
10→	-/7	1/7	-/7	-/7
11→	-/10	-/10	-/10	-/10

*1 angiosarcoma

Fig. 2. The lesions in the experimental groups. Numbers with arrows indicate the number of the corresponding groups

Histopathological findings in CFY rats

The CFY strain proved to be much less sensitive: apart from a single case of a hepatic angiosarcoma (group 9) no HCCs developed either with or without CCl_4 pretreatment. Only a small number of foci and neoplastic nodules

appeared in the animals treated with DEN (groups 7 and 9). It is also noteworthy, that the chronic CCl_4 treatment failed to produce liver cirrhosis by 3 months, only hepatic fibrosis and fatty degeneration developed (group 11). Similarly, no cirrhotic changes occurred upon the combined effect of CCl_4 + DEN administration.

Histopathological findings in F-344 rats

F-344 male rats proved to be sensitive both to the cirrhogenic effect of the CCl_4 and to the carcinogenic effect of DEN. Seven out of 8 animals showed hepatic cirrhosis in the CCl_4-treated group and in one only fibrotic changes were seen (group 5). The hepatocarcinogenic potential of the chronic CCl_4 treatment proved to be negligible: only in one out of the 8 rats with liver cirrhosis was a single basophilic cell-focus observable. There were no preneoplastic lesions in the rats with hepatic fibrosis either.

The single necrogenic dose of DEN induced many foci and some neoplastic nodules but no HCCs (group 1). When repeated doses of DEN were administered (group 3), the frequency of HCCS was very high (18 out 21). Moreover, the liver of a great number of animals contained foci and neoplastic nodules.

As the results of the group 2 show, the chronic CCl_4 pretreatment did not increase the incidence of the preneoplastic and neoplastic liver lesions, even some "protective" effect could be observed: altered cell foci and neoplastic nodules occurred in fewer animals than in the respective control group (group 1). Moreover, as the results obtained in the group 4 are showing, when chronic CCl_4-treatment preceded the repeated doses of DEN, there was a high reduction in the number of the HCCs: cancer developed only in 3 out of the 22 animals while 18 out of 21 rats were observed in the respective control group (group 3). There was no meaningful change however in the number of the putative preneoplastic lesions.

It is a very interesting finding, that in group 2, in which a high necrogenic dose of DEN was applied at the end of the experiments no signs of cirrhosis were found, only fibrosis were seen. In group 4, on the other hand, where several small doses of DEN followed the chronic CCl_4-treatment, liver cirrhosis was still present in the majority of the animals.

In group 6 a single necrogenic dose of DEN was applied first, which was followed by chronic CCl_4-treatment. In this experimental group only 5 months have passed between the stopping of the CCl_4-administration and the end of the experiment. The hepatocarcinogenic process, however, seemed to be significantly enhanced. More neoplastic nodules and HCCs occurred in this group and they appeared earlier than in the group receiving a single DEN dose not followed by CCl_4 post-treatment (group 1) (Table I).

Table I

Groups	Mean body weight at start, g	Mean body weight at the end, g	Mean liver weight at the end of experiments, g
1.	176	360.4	8.46
2.	183	418	10.14
3.	178	367.6	10.52
4.	174	354.4	11.72
5.	178	381.2	11.5
6.	165	303	9.41
7.	135	552.8	16.6
8.	130	532	15.3
9.	135	563	14.5
10.	145	613	13.7
11.	148	650	15.3

Discussion

In Europe and North America most liver cancers develop in cirrhotic livers [1]. This is why the liver cirrhosis is regarded as a preneoplastic alteration in human pathology [10]. Kew an Popper studying the relationship between hepatocellular carcinomas and cirrhosis stated that the hepatocytes in cirrhotic liver may become more sensitive to the environmental carcinogenic effects or compounds [11].

The CCl_4-induced cirrhosis as a morphological model of the human cirrhosis has always been a matter of debate. Apart from a number of differences it proved to be a useful experimental approach [12] but the true relationship between these conditions is still not clear.

In most rodent hepatocarcinogenesis models the HCCs develop in non-cirrhotic livers. Bannasch [14] and Williams [15] concluded that in the experimental models of hepatocarcinogenesis the liver cirrhosis and HCCs were not causally related lesions. Bannasch even went futher [14] saying that the "induction of hepatocellular tumours by chemical carcinogens is independent of liver cirrhosis" [14]. Williams on the other hand, admitted [15] that the mechanism by which cirrhosis might predispose for the development of carcinoma, is rather obscure.

In our view, the problem of the relationship between liver cirrhosis and liver cancer cannot be regarded as settled. We cannot disregard the fact that we see the majority of liver cancer cases in cirrhotic livers. This is why we tried to study this problem in animal experiments. Although it is still controversial whether the CCl_4-induced cirrhosis is the proper model of human liver cirrhosis or not, we have chosen this route because at least the hepatocarcinogenic potential of the CCl_4 itself is known to be very low in rats with the exception of the Buffalo inbred strains [16].

DEN administered intraperitoneally causes no liver cirrhosis, this compound proved to be cirrhogenic by gavage [17]. So in our experimental regimen where CCl_4 was administered by gavage and the DEN by ip., the pure cirrhogenic effect of the CCl_4 and the pure carcinogenic effect of DEN may prevail separately.

Our results showed, that the CCl_4 pretreatment-induced liver cirrhosis had no enhancing effect on the DEN hepatocarcinogenesis, but there was a marked inhibitory effect on the formation of HCCs. For the moment being it is difficult to explain these findings, as the mechanism may be rather complex. It seems likely that in addition to the pathological alterations (for instance alterations in the hepatic circulation), biochemical events (e.g. altered metabolism of carcinogen in the cirrhotic liver) may have an important role.

The biochemical events and the metabolism of the CCl_4 and DEN have been investigated extensively [18]. It is generally accepted that these compounds require metabolic activation for exerting their necrogenic, cirrhogenic and carcinogenic effects. The converting enzymes involved are mainly located in the microsomal fraction of the hepatocytes, so the cytochrome P-450 — monooxygenase system serves as a common target both for DEN and CCl_4. In *acute* experiments the amount and the activity of the cytochrome P-450 decreased rapidly following administration of CCl_4 [18, 19, 20] or DEN [21]. The activation or inhibition of the cytochrome-system is known to lead to modification of the effects of the compound involved via altered metabolites [22].

The effect of CCl_4 pretreatment on the carcinogenicity of nitrosamines has been studied mostly in *acute* conditions. In the catalytic activity of the low K_m N-nitroso-dimethylamin demethylase a 50% loss was observed 3 h after giving 10 μl CCl_4 [23]. Similarly, CCl_4-treatment before dimethylnitrosamine administration resulted in a complete inhibition of the electrophilic intermediate capable of methylating DNA, and 7-methylguanin and O^6-methylguanin were not detectable [24]. However, in spite of these biochemical results, the CCl_4 administered 24—28 h prior to DEN enhanced the formation of liver and kidney tumours in mice [25]. Similarly, rats given dimethyl-nitrosamine 42 or 60 h after a single necrogenic dose of CCl_4, an increased number of liver tumours has been observed [26]. According to Taylor

et al [27] in chronic experiments the combined CCl_4 + sodium nitrite + aminopyrine treatment resulted also much more hepatocellular tumours than the aminopyrine + sodium nitrite combination or the dimethyl-nitrosamine alone. Thus, in the experiments of Taylor et al [27] the chronic CCl_4-treatment has increased the tumour formation. In one of our animal groups (group 6) where CCl_4 was administered after DEN treatment-similarly an enhancing effect was seen.

In our main experimental groups (groups 2 and 4), however, the chronic CCl_4-treatment did not enhance but on the contrary decreased the rate of cancer formation.

Although chronic CCl_4-treatment was applied by Taylor et al. [27] as well as by us, there are striking differences between the two treatment schedules. In the work of Taylor et al. [27] the initiator and promoter i.e. the carcinogen and CCl_4 was administered stimultaneously and no cirrhosis did develop in their animals, not even in the ones treated with CCl_4 alone. In our main experimental groups on the other hand, animals with fullblown cirrhotic liver were treated with carcinogen i.e. initiation should have taken place in cirrhotic livers. The precise mechanism of the inhibitory effect of the CCl_4-induced liver cirrhosis on the DEN-hepatocarcinogenesis is not known. It may be that the modulation of the microsomal converting enzyme system is responsible for the decreased tumour incidence. According to the few data available in the literature [28, 29, 30] the microsomal cytochrome P-450 content of the cirrhotic liver in rats is significantly lower than that of the control animals. In addition no signs of recovery were seen during 8 weeks after cessation of CCl_4-treatment [28]. So it is possible that the decreased hepatocarcinogenetic effect of DEN cirrhotic rats is related with this permanently low cytochrome content of the liver, i.e. with the reduced metabolism of the carcinogen which results in a decreased initiation. The suggested role of the CCl_4-induced modification of the cytochrome P-450 system in hepatocarcinogenesis is under further investigation at our Institute.

REFERENCES

1. Nagashue N: The epidemiology and etiology of primary liver cancer: A current trend. Fukuoka Acta Med 73: 281, 1982
2. Gall EA: Primary and metastatic carcinoma of the liver. Relationship to hepatic cirrhosis. Acta Pathol 70: 226, 1960
3. Cameron HM, Linsell DA, Warwick GP (eds) Liver cell cancer. Elsevier Scientific Publ. Co. Amsterdam, New York, Oxford. 1976
4. Farber E: Neoplastic transformation. In: Arias I, Popper H, Schachter D, Shafritz DA (eds). The liver: Biology and Pathobiology. Raven Press, New York, 1982, p. 811
5. Scherer E: Neoplastic progression in experimental hepatocarcinogenesis. Biochim Biophys Acta 738: 219, 1984
6. Bannasch P, Moore MA, Klimek F, Zerban H: Biological markers of preneoplastic foci and neoplastic nodules in rodent liver. Toxicol Pathol 10: 19, 1982
7. Clayson DB: Chemical Carcinogenesis. J. and A. Churchill, London, 1962

8. Szendrői M, Vajta G, Kovács L, Schaff Zs, Lapis K: Polarization colours of collagen fibres: a sign of collagen production activity in fibrotic process. Acta Morphol Hung 32: 47, 1984
9. Stewart HL, Williams G, Keysser CH, Lombard LS, Montali RJ: Histologic typing of liver tumors of the rat. J Natl Cancer Inst 64: 179, 1980
10. Shikata T: Primary liver carcinoma and liver cirrhosis. In: Okuda K, Peters RL (eds) Hepatocellular Carcinoma. John Wiley and Sons, New York, London, Sydney, Toronto 1976 p. 53,
11. Kew M, Popper H: Relationship between hepatocellular carcinoma and cirrhosis. Seminars in: Liver Dis 4: 136, 1984
12. Tamayo RP: Is cirrhosis of the liver experimentally produced by CCl_4 an adequat model of human cirrhosis? Hepatology 3: 112, 1983
13. Ito N, Tatematsu M, Nakanishi K, Hasegawa R, Takano T, Imaida K, Ogiso T: The effects of various chemicals on the development of hyperplastic liver nodules in hepatectomized rats treated with N-nitrosodiethylamine or N-2-fluorenylacetamide. Gann 71: 832, 1980
14. Bannasch P: Cellular and subcellular pathology of liver carcinogenesis. In: Remmer H, Bolt HM, Bannasch P, Popper H (eds). Primary Liver Tumors. Falk Symposium 25. MTP Press Ltd. Int. Med. Publ., London, 1978 p. 87,
15. Williams, GM: The pathogenesis of rat liver cancer caused by chemical carcinogens. Biochem Biophys Acta 605: 167, 1980
16. Reuber MD, Glover EL: Hyperplastic and early neoplastic lesions of the liver in Buffalo strain rats of various ages given subcutaneous carbon tetrachloride. J Natl Cancer Inst 38: 891, 1967
17. Steinhoff D: Effect of diethylnitrosamine on the livers of rats after a high oral doses administered at intervals varying between three and twenty-four days. Acta Hepato-Gastroenterol 22: 72, 1975
18. Slater TF: Biochemical studies on liver injury. In: Slater TF (ed.) Biochemical Mechanisms of Liver Injury. Academic Press London, New York, SanFrancisco 1978 p. 2,
19. Recknagel RO: Minireview: A new direction in the study of carbon tetrachloride hepatotoxicity. Life Sci 33: 401, 1983
20. Reynolds ES, Treinen RJ, Farrish HH, Molsen MT: Metabolism of (^{14}C) carbon tetrachloride to exhaled, excreted and bound metabolites. Dose-response, time-course and pharmacokinetics. Biochem Pharmacol 33: 3363, 1984
21. Remmer H: Metabolism of carcinogens: its significance for the initiation of liver tumors. In: Remmer H, Bolt HM, Bannasch P, Popper H (eds). Primary Liver Tumors. Falk Symposium 25. MTP Press Ltd. Int. Med. Publ., London, 1978 p. 31,
22. Kunz W, Appel KE, Rickart R, Schwarz M, Stöckle G: Enhancement and inhibition of carcinogenic effectiveness of nitrosamines. In: Remmer H, Bolt HM, Bannasch P, Popper H (eds). Primary Liver Tumors. Falk Symposium 25. MTP Press Ltd. Int. Med. Publ. London, 1978 p. 261,
23. English C, Anders MW: Evidence for the metabolism of N-nitrosodimethylamine and carbon tetrachloride by a common isozyme of cytochrome P-450. Drug Metab Disposition 13: 449, 1985
24. Ruchirawat M, Mostafa MH, Shank RC, Weisburger EK: Inhibitory effects of carbon tetrachloride on dimethylnitrosamine metabolism and DNA alkylation. Carcinogenesis 4: 537, 1983
25. Pound AW: Influence of carbon tetrachloride on induction of tumours of the liver and kidney in mice by nitrosamine. Brit J Cancer 37: 67, 1978
26. Pound AW, Lawson TA, Horn L: Increased carcinogenic action of dimethylnitrosamine after prior administration of carbon tetrachloride. Brit J Cancer 27: 451, 1973
27. Taylor HW, Lijinsky W, Nettesheim P, Snyder CM: Alteration of tumor response in rat liver by carbon tetrachloride. Cancer Res 34: 3391, 1974
28. Marshall WJ, McLean AEM: The effect of cirrhosis of the liver microsomal detoxication and cytochrome P-450. Brit J Cancer 50: 578, 1969
29. Farrell GC, Zaluzny L: Hepatic heme metabolism and cytochrome P_{450} in cirrhotic rat liver. Gastroenterology 89: 172, 1985
30. Murray M, Farrell GC: Different effects of carbon tetrachloride toxicity and cirrhosis on substrate binding to rat hepatic microsomal cytochrome P-450. Biochem Pharmacol 33: 687, 1984

Acta Morphologica Hungarica, 35 (3—4), pp. 219—224 (1987)

COMPARATIVE MORPHOLOGICAL STUDY OF AGE RELATED MITOCHONDRIAL CHANGES OF THE LYMPHOCYTES AND SKELETAL MUSCLE CELLS

EDIT BEREGI, O. REGIUS

GERONTOLOGY CENTER OF THE SEMMELWEIS MEDICAL UNIVERSITY, BUDAPEST, HUNGARY

(Received 18 March 1987)

The age dependent electron microscopic changes of the mitochondria in a mitotic cell (lymphocyte) were compared with those of a postmitotic cell (skelatal muscle cell) in humans and in CBA/Ca mice. Two types of age related changes could be observed in the mitochondria of lymphocytes and skeletal muscle cells: (i) degenerative changes; (ii) giant mitochondria. The frequency of the mitochondrial changes increased with age and were more frequent in the skeletal muscle cells than in the lymphocytes.

Keywords: Aging in lymphocytes, aging in skeletal muscle cells, age changes in mitochondria

Introduction

In most countries the number of aged individuals in the total population increases. Aging is one of the most critical issue facing mankind in the 20th century, either in medical and social, or in economical aspects. Enhanced interest in diseases and disabilities associated with aging has led to careful investigation of many biological systems with the hope that methods will be found for delaying the onset of aging, lessening its severity, or perhaps preventing some of the age-dependent pathologic changes.

Aging is characterized by a diminished ability to adapt to environmental changes. The immune system has an important role in adaptation.

Several data indicate that aging is associated with immune dysfunction both in humans and in experimental animals [13]. We were interested weather the functional changes have a morphological basis or not. In our previous work, therefore we examined the morphological changes in the mitochondria of popliteal lymph node and spleen lymphocytes of CBA/Ca mice, Wistar rats and in the peripheral lymphocytes of humans [2]. It is also well known that muscular strength is decreasing with aging, for that reason mitochondria of skeletal muscle cells were examined in CBA/Ca mice and in humans [4]. In the present work we have compared the age dependent changes of mitochondria by electron microscopy in a mitotic cell (lymphocyte) with those of a postmitotic cell (skeletal muscle cell).

Send offprint requests to Edit Beregi, Gerontology Center of The Semmelweis Medical University, Budapest, Somogyi B. u. 33. 1085 Hungary

Materials and methods

Humans peripheral lymphocytes and skeletal muscle cells of both sexes were examined. The lymphocytes were separated by Böyum's method [5] from healthy individuals. 57 subjects were 36—50 years of age (control group) and 364 subjects over 71 years of age.

Biopsy material of musculus (m) rectus abdominis was obtained from a surgical department. 5 patients were 36—50 years of age and 15 were 71 years and over. Out of the 20 patients 13 were operated on hernia, 6 on cholelithiasis and 1 on duodenal ulcer [4].

Spleen lymphocytes from 51 CBA/Ca mice, mm. gastrocnemius and rectus abdominis from 62 mice were examined. 17 mice were between the age of 301—600 days and the remaining over 601 days of age.

Peripheral lymphocytes, small parts of the spleen and skeletal muscle were freshly fixed in cold glutaraldehyde, then in osmium tetroxide and embedded in Araldite. Ultrathin sections were prepared using an LKB Ultratome III., contrasted with lead citrate, and studied in a JEM 100 C electron microscope.

Results

Two types of age related changes could be observed in the mitochondria of lymphocytes and skeletal muscle cells, as well: (i) Degenerative changes, the density of cristae increased (Fig. 1) and in some cells the cristae of the mitochondria disappeared and were replaced by a lamellar structure resembling myelin (Fig. 2), sometimes electron-dense or electron-translucent substance was visible. The structure of this material is comparable to lipofuscin. (ii) The size of mitochondria proved to be changed, giant mitochondria could be observed (Fig. 3).

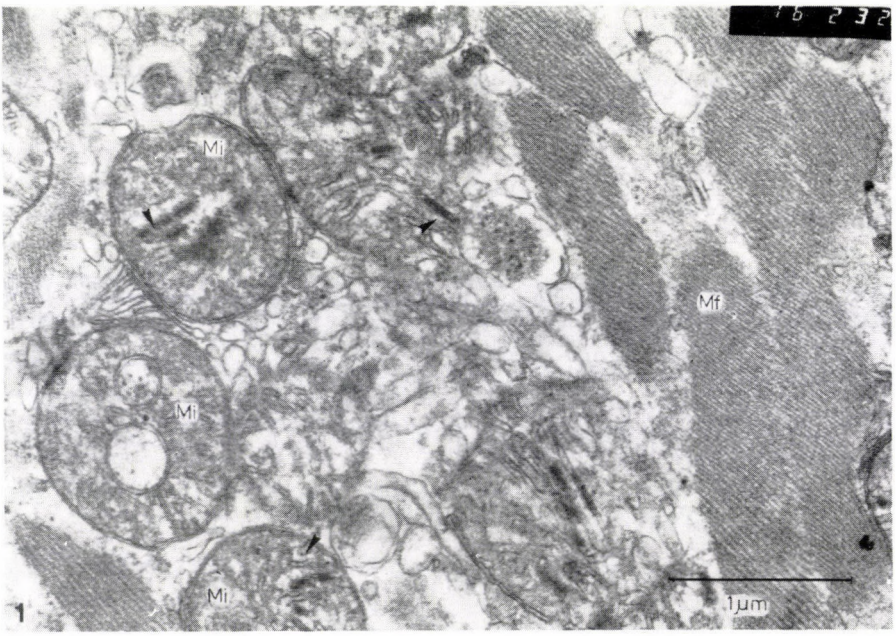

Fig. 1. In old human the density of mitochondrial cristae of the skeletal muscle cells increased (×16 000) (Abbreviations: Mf = myofibrils; Mi = mitochondria; ↗ = dense cristae)

Fig. 2. Myelin-like lamellar structure and electron dense material in the mitochondria of peripheral lymphocyte of old human. Lipofuscin granule near the mitochondria. (×30 000) (Abbreviations: D = electron dense material; L— = lipofuscin; Mi = mitochondria; My = myelin-like material; N = nucleus)

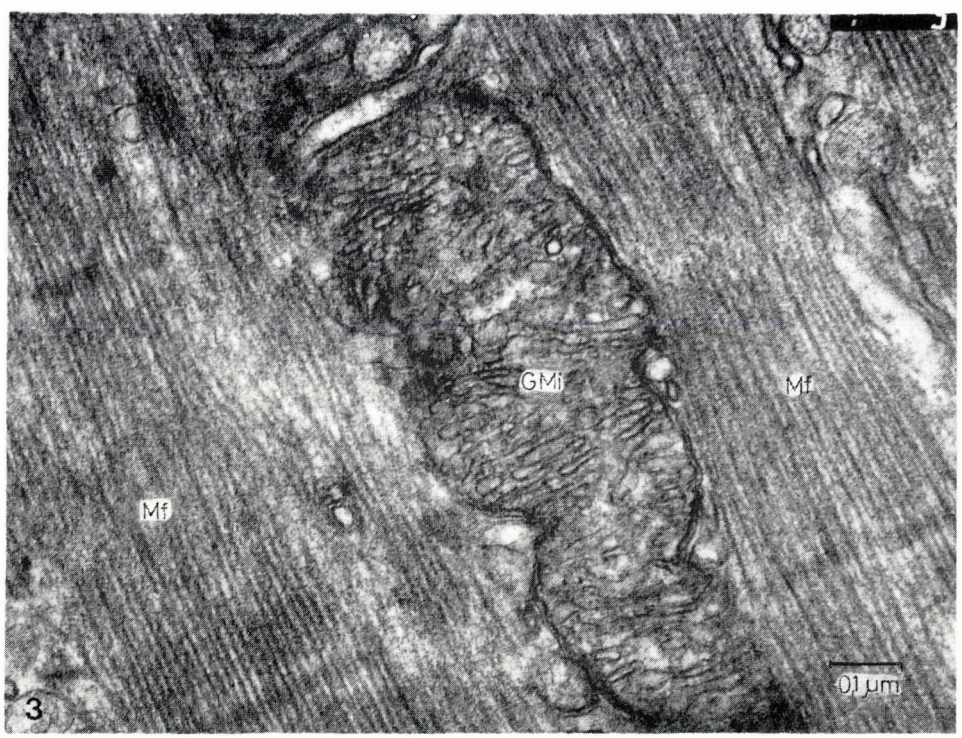

Fig. 3. Giant mitochondria in the gastrocnemius muscle cell of CBA mice (×50 000). (Abbreviations: Mf = myofibrils; GMi = giant mitochondria)

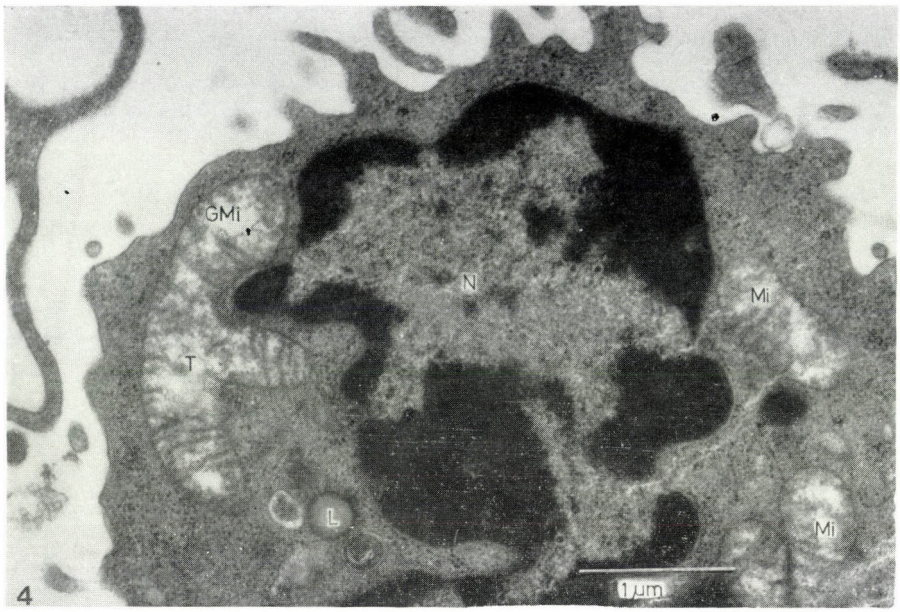

Fig. 4. Giant mitochondria in the peripheral lymphocyte of old human. Disruption of mitochondrial cristae and electron translucent material (× 20 000). (Abbreviations: GMi = giant mitochondria; Li = lipid drop; Mi = mitochondria; N = nucleus; T = electron translucent material)

In some cases degenerative changes were observed in the giant mitochondria, too (Fig. 4).

The frequency of these mitochondrial changes increased significantly with age. We have compared the frequency of the mitochondrial changes of human lymphocytes with those of skeletal muscle cells.

In the peripheral lymphocytes of humans between 36—50 years of age only 5% while in those over 71 years of age 60% of the subjects examined proved to have these mitochondrial changes.

We have found no mitochondrial changes in the muscle cells of the subjects between 36—50 years of age, but they could be demonstrated in 73% of patients over 71 years of age (Table I).

The presence of giant mitochondria proved to be significantly more frequent in human skeletal muscle cells (47%) than in lymphocytes (17%). The density of mitochondrial cristae increased only in the muscle cells.

Comparing the frequency of mitochondrial changes in the lymphocytes and skeletal muscle cells of CBA/Ca mice, we have found an increase in frequency of these changes with age in both cell types, but they were more frequent in the muscle cells — similarly with the findings in humans — than in the lymphocytes (Table II). The alterations were mostly of degenerative character and giant mitochondria could be found only in a few mice. The changes in m. rectus abdominis and m. gastrocnemius proved to be identical.

Table I

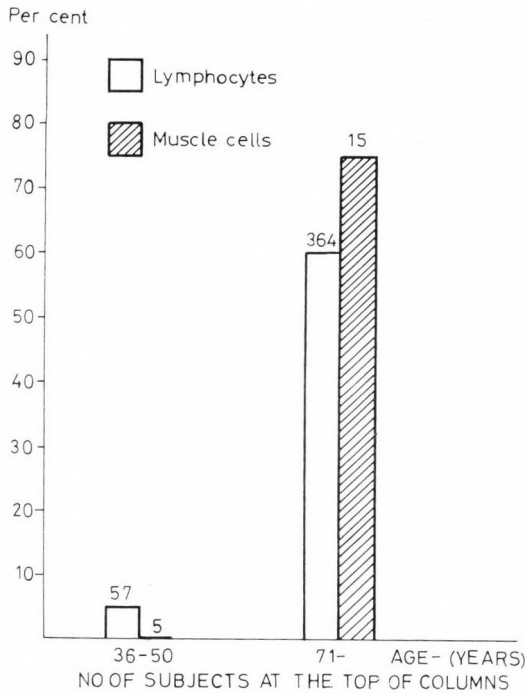

Table II

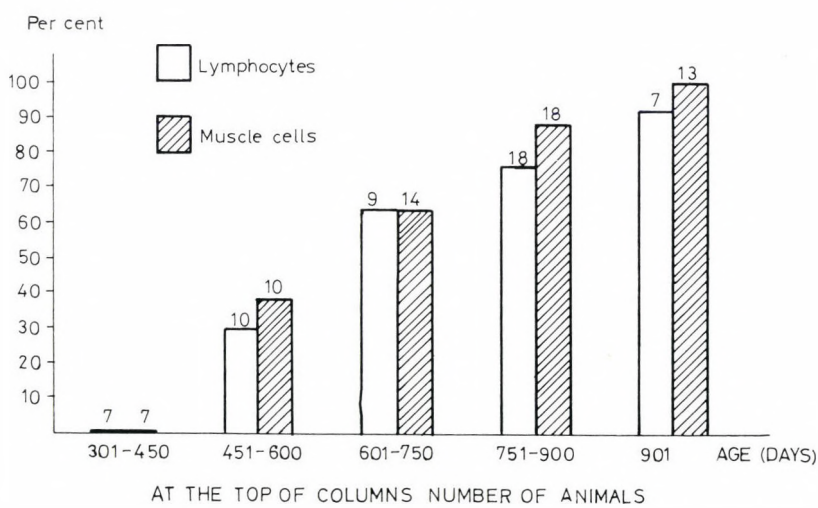

Discussion

Age related mitochondrial alterations were compared in mitotic (lymphocytes) and postmitotic cells (skeletal muscle cells) of humans and CBA/Ca mice. It could be stated that the mitochondrial changes increased with age in both cell types and they were seen more frequently in skeletal muscle cells than in lymphocytes.

Degenerative changes in the mitochondria of flight muscle cells of aged insects [9, 11] and in the skeletal muscle cells of mice and rats have been described [8], and we have published data of age related alteration in the mitochondria of lymphocytes [2]. An increased size of hepatic cell mitochondria were also described by morphometric studies [10, 12] but not in lymphocytes and skeletal muscle cells.

The role of mitochondria in the aging process has been widely discussed. Some of the authors consider aging of mitochondria as a possible causative factor in cell aging [6, 7]. It is well known that mitochondrial DNA synthesis takes place on the inner membrane of the mitochondria, and the inner membrane is the main site of free radical production. As free radicals may have serious damaging effect on biological membranes, it is possible that the degenerative changes observed develop as a consequence of this effect [1, 6].

As mitochondria are energy-centers of cells, it can be hypothesized that the morphological changes described result in a diminished functional capacity of lymphocytes and skeletal muscle cells leading to insufficiency of immune functions and declining of muscular strength.

REFERENCES

1. Albring M, Griffith J, Attardi G: Association of a protein structure of probable membrane derivation with HeLa cell mitochondria. DNA near its origin of replication. Proc Natl Acad Sci USA 74: 1348, 1977
2. Beregi E, Biró J, Regius O: Age-related morphological changes in lymphocytes as a model of aging. Mech Ageing Develop 14: 173, 1980
3. Beregi E, Regius O: Relationship of mitochondrial damage in human lymphocytes and age. Act Gerontol 13: 226, 1983
4. Beregi E, Regius O, Hüttl T, Göble Zs: Age- related changes in the skeletal muscle cells. Zschr Gerontol 18: 260, 1986
5. Böyum A: Separation of lymphocytes from blood and bone marrow. Scand J Clin Lab Invest 21: 97, 1968
6. Fleming JE, Miquel J, Cottrell SF, Yengoyan LS, Economos AC: Is cell aging caused by respiration-dependent injury of the mitochondrial genome? Gerontology 28: 44, 1982
7. Harman D: The biologic clock: the mitochondria? J Am Geriatr Soc 20: 145, 1972
8. Ludatscher R, Silbermann M, Gerson D, Reznick A: The effect of enforced running on the gastrocnemius muscle in aging mice. Exper Geront 18: 113, 1983
9. Miquel J, Economos AC, Fleming J, Johnson JE: Mitochondrial role in cell aging. Exp Gerontol 15: 575, 1980
10. Rockstein M, Miquel J: Aging in insects. In: Rockstein M (ed.) The Physiology of Insecta. 2nd ed. Vol 1. Academic Press, New York 1973
11. Schal RS: Aging changes in insect flight muscle. Geront 22: 317, 1976
12. Tauchi H, Sato T: Age changes in size and number of mitochondria of human hepatic cells. J Gerontol 23: 454, 1968
13. Wecksler ME, Siskind GW: The cellular basis of immune senescence. Monogr Devel Biol. Vol 17. 1984 p. 110,

Book reviews

G. BEKÉNY: *Klinik der Muskelkrankheiten*

Akadémiai Kiadó, Budapest, 1987. (422 pages, 29 figures.)

The author of this book spent decades on clinical studies in muscle diseases.

This book summarizes his rich experience in this field. The structure of the book is clear and very didactic. Each chapter contains a brief summary of pathomorphological changes, description of clinical symptoms, diagnostic possibilities and therapy. A separate chapter deals with the up-to-date concepts of the structure of the motoric unit, the diagnostic methods and the distinction between the neurogenic and myogenic disorders. An emphasis is given to the diagnostic value of muscle biopsy. A good survey is given about the classification of neuromuscular diseases. Chapters are dealing with the various forms of muscular dystrophies, with the ocular myopathies, with the congenital and childhood myopathies, with the metabolic myopathies, with the family periodic paralysis and with myotonia. The chapters on myasthenia gravis and on inflammatory muscle diseases are the most elaborate ones. Very useful knowledge is summarized in the chapter "Neuromuscular disorders connected with malignant tumors". Neuropathies of genetic origin, progressive spinal and bulbar muscular atrophies and amyotrophic lateral sclerosis are also described in detail.

The illustrations are informative in general, but some of the histological pictures are of low technical value.

The literature is comprehensive till the early 80s, and covers 82 pages.

The book provides most up-to-date information and instructions for neurologists but it is also useful for internists and pathologists too.

B. SZENDE

J. G. SINKOVICS: *Medical Oncology*

An advanced course. A self-assessment guide for subspecialty board examinations and practice. 2nd ed. Revised and expanded Marcel Dekker Inc. NewYork and Basel. Two volumes, 2062 pages.

The two main purposes of this single authored textbook are: to help residents in preparing for subspecialty board examinations and to serve as a guide for all the physicians dealing with cancer patients.

The author — thanks to his comprehensive experience — succeeded in fulfilling these goals. Almost all fields of clinical oncology are dealt with and the various types of malignomas are discussed according to their importance, but generally in details.

Since the book is intended for physicians, the author does not deal with the definition of individual forms of diseases. These definitions are easily available from textbooks. Instead of this the most recent information on pathology, etiology, immunology of malignomas are widely discussed, and the recent developments in their diagnostics and treatment are presented. A large amount of information is presented on the basis of more than 8000 original publications.

The book is divided into six main parts. In the first part the haematologic malignancies are discussed. This part introduces the new concepts of classification and therapy of malignant lymphomas. The new achievements in the field of leukemia and AIDS-research, including information about the role of oncogens in human tumours can also be found in this part.

The second part is dealing with the tumours of mesenchymal origin, while in the third one the neuroectodermal and neurogenic tumours are discussed. The discussion of the classification of the pigment cell tumours and APUD-omas in this chapter is reflecting the author's modern concepts.

Carcinomas are described in part four. Obviously, the largest scope is devoted to this most frequent and most significant group of malignomas. In connection with the epithelial tumours of different organs their incidence and the recent knowledge related to their etiology are consistently discussed. Detailed information is given concerning their most significant histological forms, clinical signs and staging the new diagnostic and therapeutic procedures are discussed critically.

The fifth part is a kind of summary on the principle and practice of modern cancer therapy. Particularly the chemotherapy and the immunotherapy are thoroughly reviewed. The successes achieved in treatment of malignant melanomas, breast, lung cancers, gastrointestinal tumours and gynecological malignancies are emphasized by presenting the internationally accepted and used protocols. The infectious complications and their treatment possibilities are also exhaustively discussed in this part.

Chapter six is a unique part of the book. The author has reached his goal indeed. This part will provide inestimable help to residents preparing themselves for board examination. This part contains carefully selected self-assessing tests. The right answers to questions are also included giving even references in some instances.

The text is well written and clear, the chapters are well structured. The style of the book is concise, for the sake of brevity — according to the author's words — it is almost telegraphic. Concerning many diseases, entities, tables showing the most important characteristics of the disease are also included. The well composed tables help the quick and yet thorough orientation of the reader so the book can easily be used in every-day practice.

From editorial aspects the classification of some of the diseases could be debated. E.g. mononucleosis infectiosa does not seem to belong to the category of malignant lymphomas. Although this EB virus induced disease is producing lymphoproliferation, this has however reactive characteristics — according even to the author's opinion, and patients are generally recovering without any treatment. It would have been more suitable to discuss this condition under the previous subchapter (related conditions). Amyloidosis, which — as the author describes — may be a consequence of certain malignomas but is not a tumour, itself is dealt with in a subchapter on plasma cell neoplasias. It would have been better to discuss it together with other gammopathies as possible consequence of plasma cell tumours.

Taking into consideration that the author wrote his book for residents who are aware of the basic nature of the various disease-entities, the above mentioned and some other disputable classification however cannot cause significant misunderstandings.

These bulky but well edited volumes contain an enormous amount of information critically selected and presented by an author with great experience both in the fields of theoretical and clinical oncology. The book is going to be an excellent manual for doctors specializing in clinical oncology and training for taking examination, but it is promising for practicians giving a versatile review about various types of malignancies. It can also be a useful reference book for theoretical experts.

K. Lapis and K. Simon

J. H. Langdon: *Functional Morphology of the Miocene Hominoid Foot*

Karger, Basel, 1986, 225 pages with 69 figures and 22 tables. Price: SFr 98.—,

This book is the 22nd volume of the series of Karger "Contributions to Promatology" edited by F. S. Szalay (New York). It is divided into 4 chapters: the introduction gives a survey of literature on the studies of antropoid foot bones available in museums and of fossile skeleton findings. The second chapter describes morphological methods by which Langdon compared the foot bones of 19 recent species and fossile findings. The third chapter contains the detailed morphometric data and functional anatomical conclusions. In addition to body structure the author stresses the features, similarities and differences in posture and locomotion. Understandably, the longest chapter of all is the fourth, a descriptive anatomical one, amounting to more than 100 pages. The conclusions also point out the role of environmental factors.

The description follows the principles of classical comparative anatomy, i.e. it operates with uniform nomenclature, order, typing etc. It is of great help to the interested reader to find this wealth of metric and descriptive data collected in one volume, everything that

has been published in this field till 1985. The author is a co-worker of the Anthropology Department of Yale University and collected his material from different parts of the world. All who provided help or data are mentioned in acknowledgements, among them the Hungarian Miklós Kretzoi making his observations on the finding of Rudabánya accessible for Langdon.

There are regretfully few photographic illustrations in the book and even these are far from being flawless. This is due to the fact that the author did not use his own material but second copies. The reference list is comprehensive containing more than 350 items. This volume fits in well with the series and can be used as an excellent sourcebook.

L. HARSÁNYI

Lehrbuch der allgemeinen Pathologie und der pathologischen Anatomie. Eds: M. EDER und P. GEDICK

Springer, Berlin, Heidelberg, New York, London, Paris, Tokyo 1986.

This bulky volume of 937 large-formate pages contains the principles of general and special pathological anatomy that students are supposed to learn at least in the FRG. The textbook reached now its 32th edition which is 26 pages longer than the previous one. The structure of the book follows the classical pattern of education in pathological anatomy, i.e. it contains chapters of general as well as of special pathology.

Apart from the extension of the text, some chapters show considerable alterations compared to the previous edition. For instance the chapter on immunopathology describes now the most up-to-date knowledge about the production and diagnostic value of monoclonal antibodies. The chapter "Pathology of Growth and Differentiation" contains in this new edition a separate subdivision for Invasion and for Metastasis, allowing the author to give more details about the mechanism and significance of metastasis of malignant tumours.

The same chapter is now completed with the basic knowledge about oncogens. This enables students to apply the rapidly increasing data about the role of oncogens in oncogenesis and probably the diagnosis of cancer in their future practice.

In special pathology the chapter "Pathology of the Skeletal-system" is extended by 8 pages and the subjects considered in the previous edition are dealt with in greater detail. Particularly in this chapter, but also in the whole textbook, the proportion of high quality colour illustrations are increased in number as compared to the previous edition.

The textbook gives a clear and comprehensive as well as a most didactic description of the modern knowledge in pathological anatomy. The information meets the requirements of the medical curriculum and it may well serve as a basis of clinical studies.

The book is also useful for medical doctors who are preparing themselves for specialization in pathology.

K. LAPIS, and B. SZENDE

Die Stellung des Makrophagen im Immunsystem. Ed.: J. H. SCHARF

Nova Acta Leopoldina, No. 263, Band 59, J. A. Barth Verlag und Deutsche Akademie der Naturforscher Leopoldina, Halle (Saale), 1986. (80 pages, 28 figures, 13 tables. Price: 45.— DM (Available from J. A. Barth, DDR 7010 Leipzig, Pf. 109.)

This issue contains the Proceedings of a Leopoldina-meeting hold in Halle, 3. 12. 1983. The scientific editor is G. Geiler (Leipzig).

The following lectures are published: Phylogenesis of the immune system wiih special attention to macrophages (H. Ambrosius, Leipzig); The mononuclear phagocyte system (J. W. M. Van der Meer and R. Van Furth, Leiden); Morphology of macrophages and the stages of their differentiation (H. K. Müller-Hermelink, M. R. Parwaresch and H. J. Radzun, Würzburg, Kiel); Function of macrophages with special respect on immunoregulation (R. Kraft and H. Cottier, Bern); The macrophage as cytotoxic effector cell (M. L. Lohmann-Matthes, Freiburg i. Br.).

A basic knowledge about macrophages can be obtained from this issue. The literature is covered up to 1983.

The booklet can be useful for pathologists, immunologists and histologists.

K. LAPIS and B. SZENDE

ERRATA

The correct order of figures to M.A. Doroshenko and P.A. Motavkin's article entitled "Olfactory epithelium of marine fishes in scanning electron microscopy", and published in Acta Morphologica (34/3, pp. 143—155, 1986) should be read as follows:

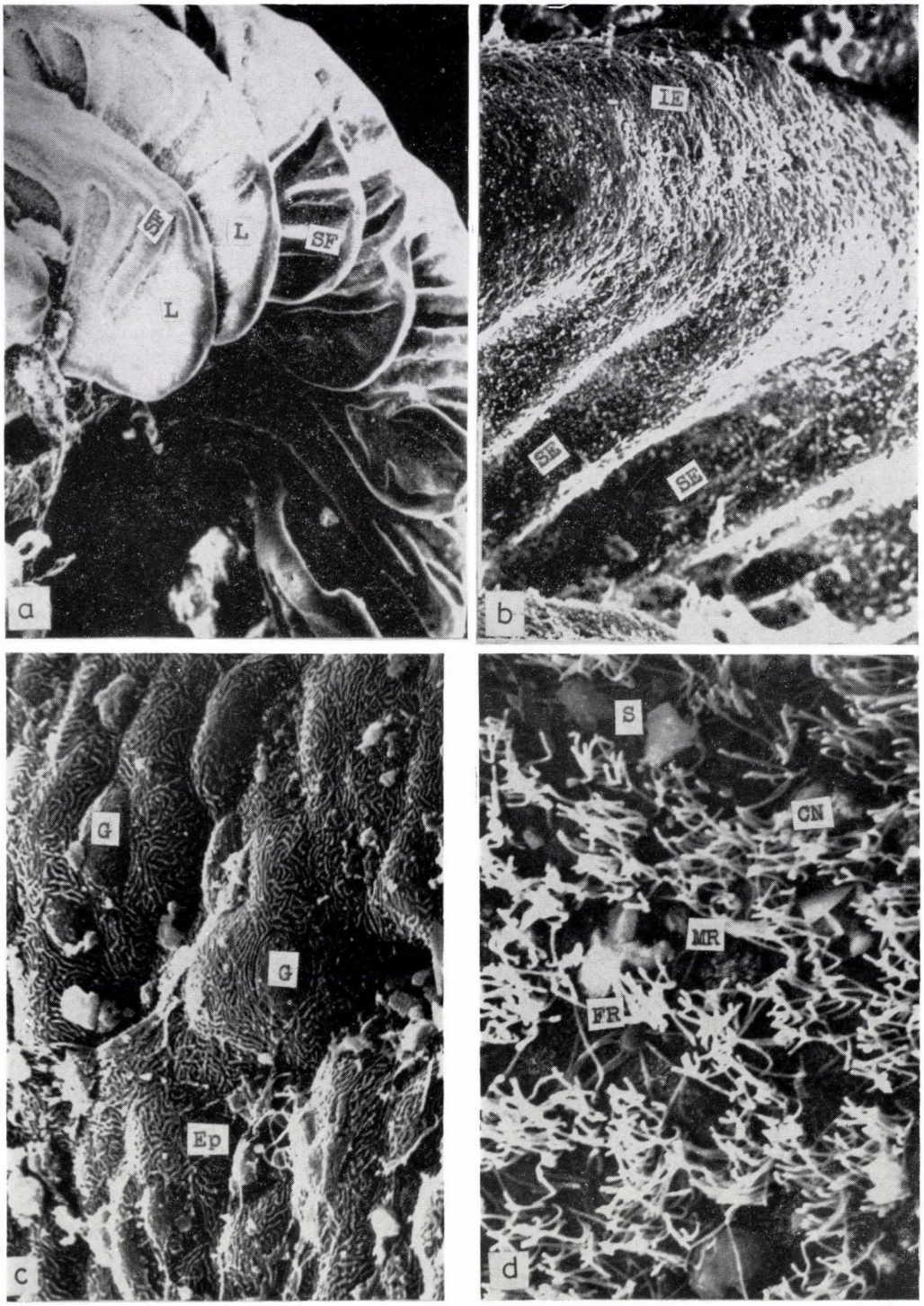

Fig. 1. Structure of the olfactory surface in *Oncorhynchus keta* and *O. gorbuscha*. (a) General view of olfactory lamella in *O. gorbuscha*, ×300. (b) Secondary folding on surface of the olfactory lamella in *O. gorbuscha*, ×1500. (c) IE at margin of olfactory lamella in *O. gorbuscha*, ×2500. (d) SE in *O. keta*, ×3000

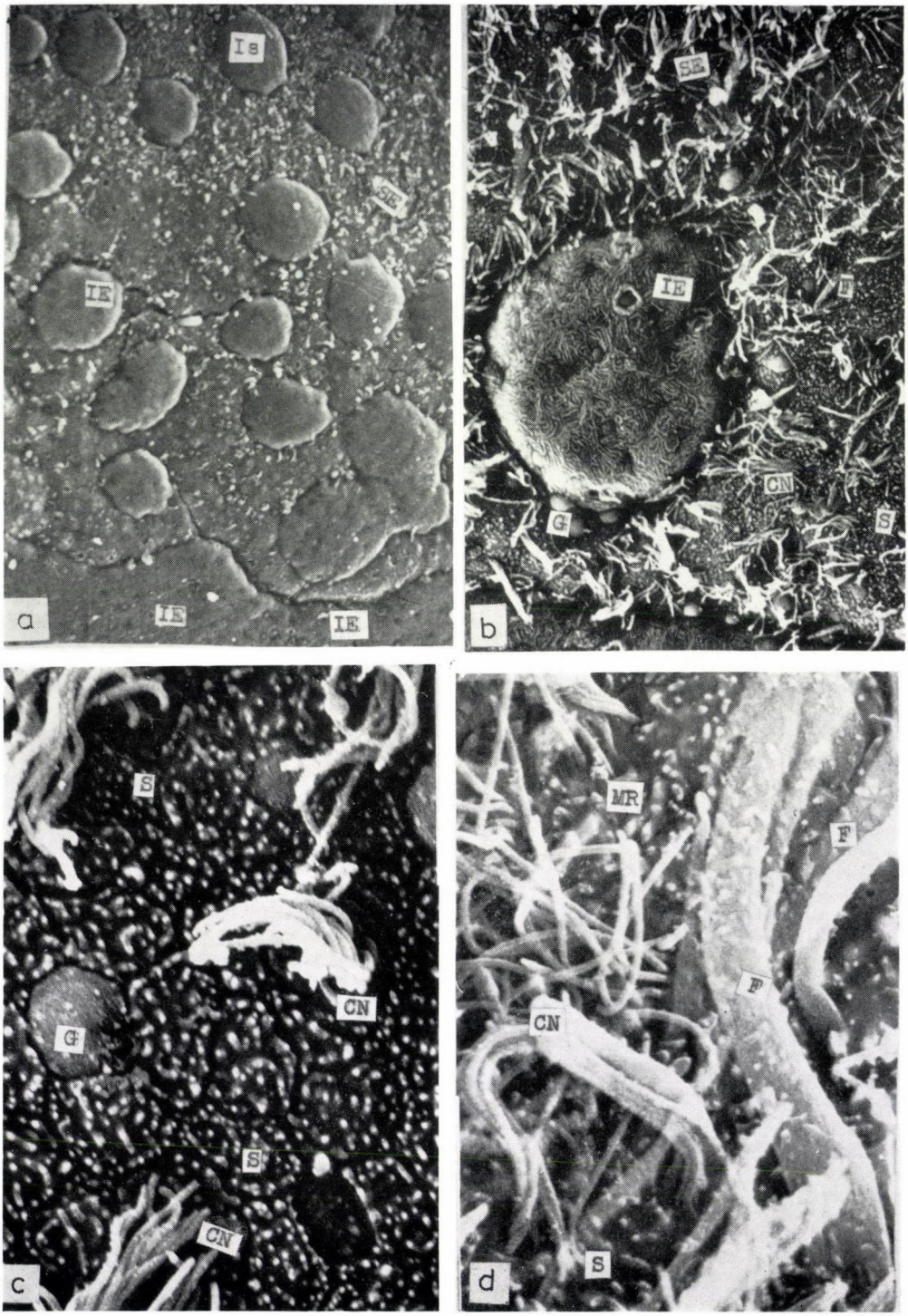

Fig. 2. Surface of olfactory lamella in *Limanda yokohamae*. (a) Islets of of IE located on olfactory lamella, ×300. (b) An islet of IE surrounded by sensory epithelium, ×1000. (c) Ciliated and secretory cells in intermediate epithelial belt, ×6000. (d) Flagella and cilia in SE, ×6000

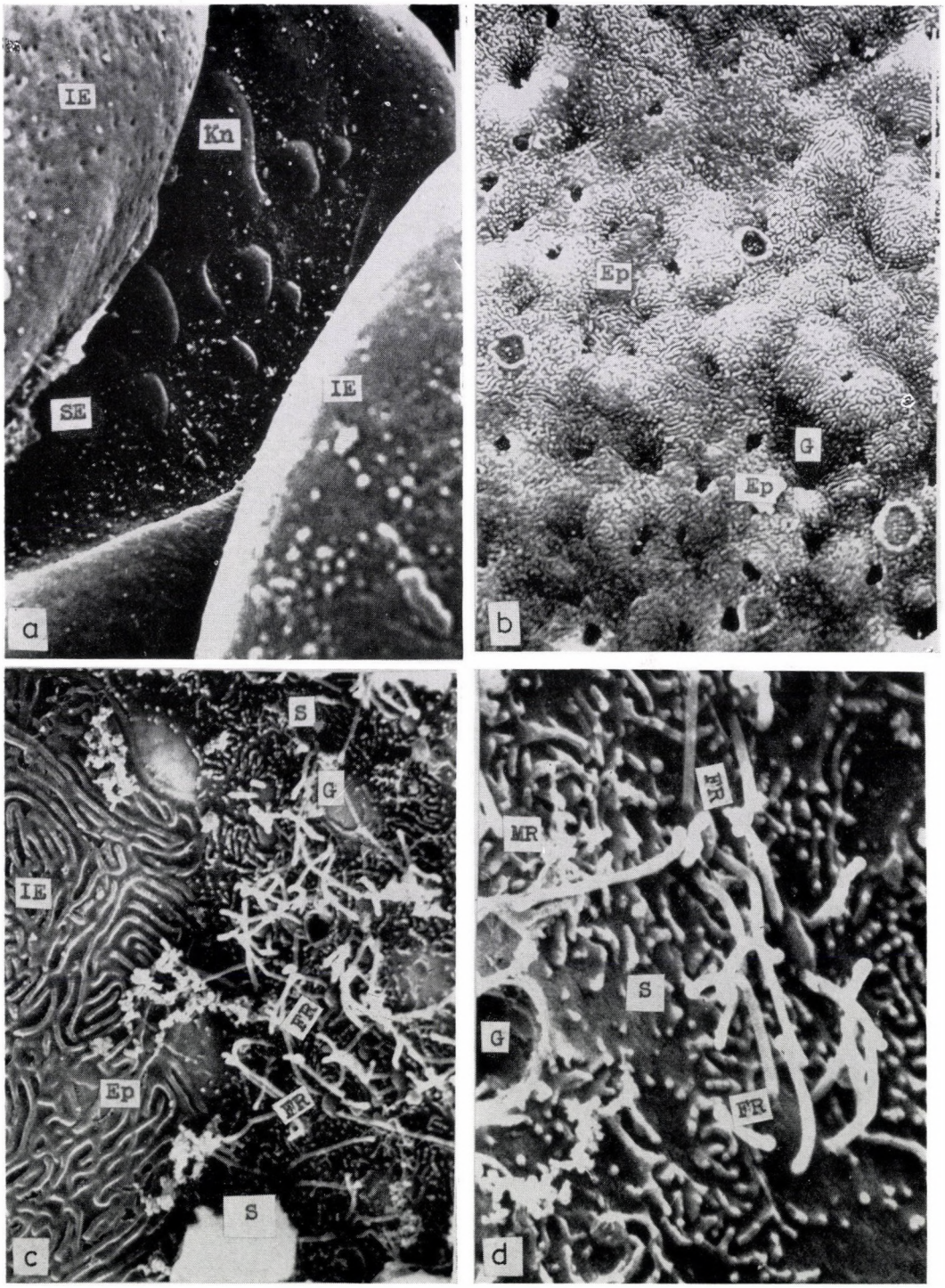

Fig. 3. Structure of surface of olfactory lamella in *Pleurogrammus azonus*. (a) General view of lamella in olfactory rosette, ×200. (b) IE on top of olfactory lamella, ×5000. (c) SE, bordering a knoll of IE, ×4000. (d) SE, ×10 000

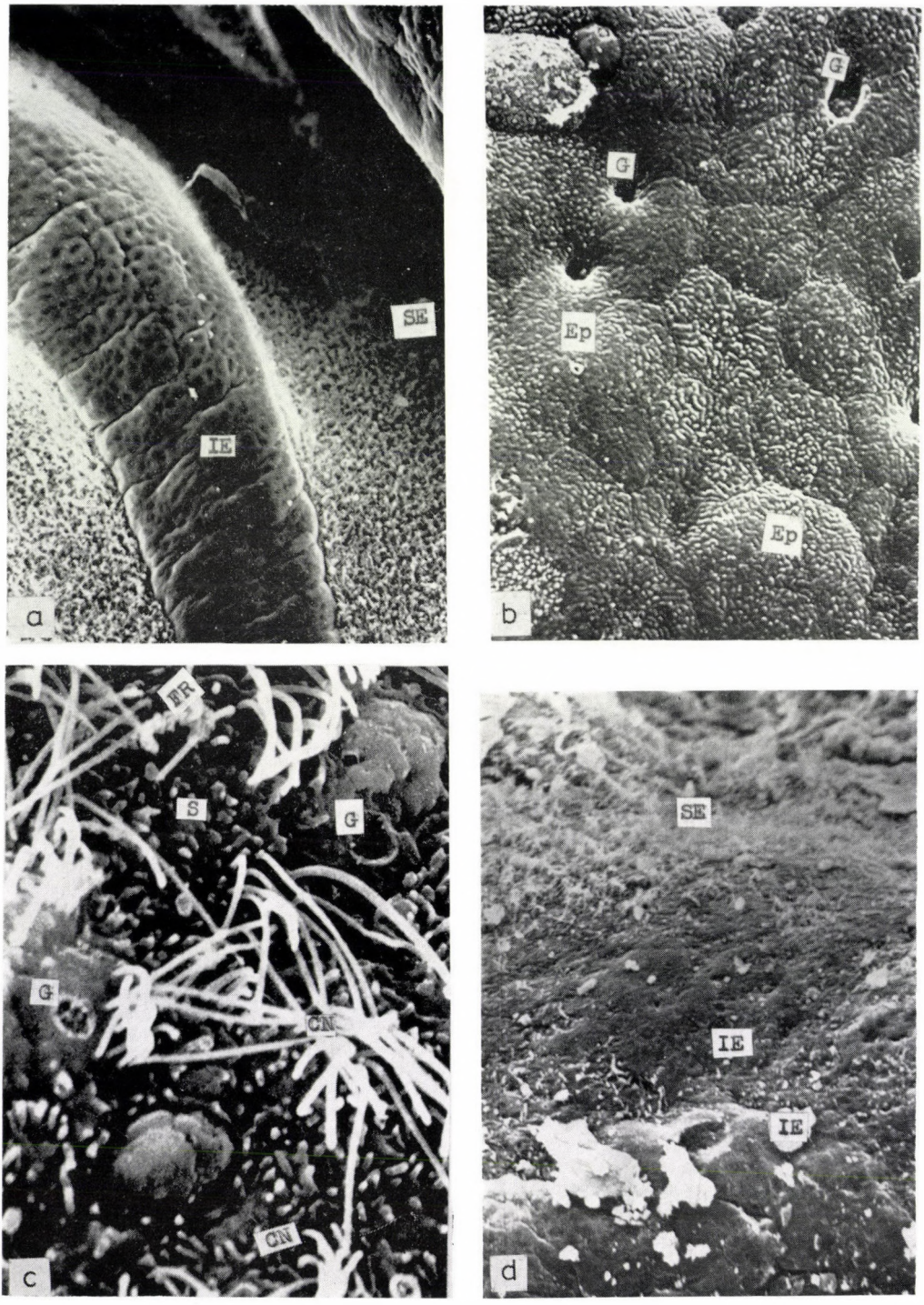

Fig. 4. Structure of surface of olfactory lamella in *Teleostomi*. (a) IE and SE on lamella of olfactory organ in sea bullhead, ×300. (b) IE on margin of olfactory lamella in sea bullhead, ×2500. (c) SE on olfactory lamella in flounder, ×6000. (d) SE and IE on olfactory lamella in filefish, ×500

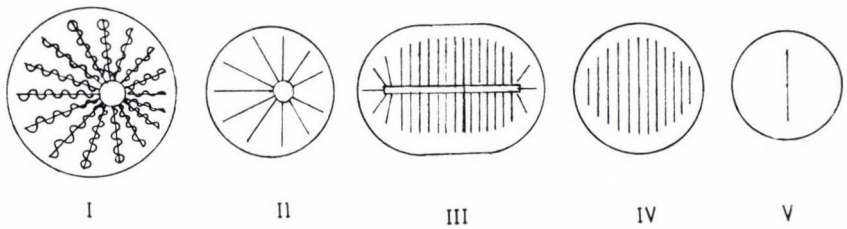

Fig. 5. Scheme of arrangements of lamellae in olfactory rosette of marine fish species. (I) Radial arrangement of lamellae around central raphe, complicated by secondary folding (salmons). (II) Simple radial arrangement of lamellae around central raphe without secondary folding. (III) Transverse and longitudinal arrangement of olfactory lamellae around elongated raphe (greenling). (IV) Parallel arrangement of lamellae without central raphe (flounder). (V) Longitudinally oriented olfactory lamella (filefish)

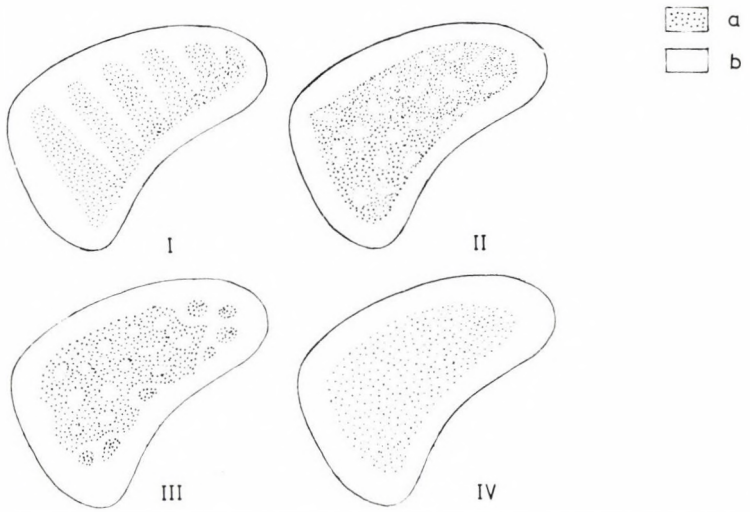

Fig. 6. Scheme of arrangements of SE over olfactory lamella. (a) SE, (b) IE. (I) SE separated by secondary folds into large continuous areas (salmons). (II) SE with irregular islets of IE (greenling). (III) SE and IE irregularly mixed (flonder). (IV) Continuous SE not reaching the margins of the olfactory lamella (see bullhead, filefish)

PRINTED IN HUNGARY
Akadémiai Kiadó és Nyomda Vállalat, Budapest

INSTRUCTIONS TO AUTHORS

Form of manuscript

Contributors are requested to supply two complete copies of the manuscript including all tables and illustrations. Manuscripts should be typed double-spaced with margins of at least 4 cm. Pages should be numbered consecutively.

The *headline* should include the title of the paper, authors' names, and name and short postal address of the institute where the work was done.

An *abstract* of not more than 200 words should be supplied typed before the text. It should briefly describe the purpose of the investigations, the methods utilized, the results obtained, and the authors' principal conclusions.

Abbreviations and symbols

Abbreviations should be spelled out when first used in the text or, alternatively, a list of abbreviations might be given. The *International System of Units (SI)* should be used for all measurements. Symbols for physical quantities are to be printed in italics and should, therefore, be underlined in the manuscript. Unusual symbols should be identified on the margin.

References

References should be numbered in alphabetical order, and these numbers only should be inserted in the text (in parentheses). In the reference list each item should include the names and initials of all authors; the title of the article; the title of the journal abbreviates according to the style used in *Index Medicus* (a list of the journals indexed is printed annually in the January issue); the volume number; the first page number; and the year of publication.

Kaplan AP, Kay AB, Austen KF: A pre-albumin activator of prekallikrein. J Exp Med 135:81, 1972

Titles of books should be followed by the publisher; place of publication; and the year.

Oláh I, Röhlich P, Törő I: Ultrastructure of Lymphoid Organs. Akadémiai Kiadó, Budapest 1975

Halász B: The endocrine effects of isolation of the hypothalamus from the rest of the brain. In: Frontiers in Neuroendocrinology, eds Ganong WF, Martini L, Oxford University Press, Oxford 1969, p. 307

Tables and illustrations

Tables should be comprehensible to the reader without reference to the text. The headings should be typed above the table. Tables should be numbered with Roman and illustrations with Arabic numerals.

Figures should be identified by number and authors' name written lightly in pencil on the back. The top should be indicated on the back of prints. The letters a, b etc. should be placed in the lower left-hand corner of prints. Staining techniques and the original magnification of photomicrographs should be stated. Figure captions should be typed on a separate sheet. The approximate place of figures and tables in the text should be indicated in the manuscript on the left-hand margin.

Proofs and reprints

Reprints and proofs will be sent to the first author unless otherwise indicated. A hundred reprints of each paper will be supplied free of charge.

Periodicals of the Hungarian Academy of Sciences are obtainable at the following addresses:

AUSTRALIA
C.B.D. LIBRARY AND SUBSCRIPTION SERVICE
Box 4886, G.P.O., *Sydney N.S.W. 2001*
COSMOS BOOKSHOP, 145 Ackland Street
St. Kilda (Melbourne), Victoria 3182

AUSTRIA
GLOBUS, Höchstädtplatz 3, *1206 Wien XX*

BELGIUM
OFFICE INTERNATIONAL DES PERIODIQUES
Avenue Louise, 485, *1050 Bruxelles*
E. STORY-SCIENTIA P.V.B.A.
P. van Duyseplein 8, *9000 Gent*

BULGARIA
HEMUS, Bulvar Ruszki 6, *Sofia*

CANADA
PANNONIA BOOKS, P.O. Box 1017
Postal Station "B", *Toronto, Ont. M5T 2T8*

CHINA
CNPICOR, Periodical Department, P.O. Box 50
Peking

CZECHOSLOVAKIA
MAD'ARSKA KULTURA, Národní třida 22
115 66 Praha
PNS DOVOZ TISKU, Vinohradská 46, *Praha 2*
PNS DOVOZ TLAČE, *Bratislava 2*

DENMARK
EJNAR MUNKSGAARD, 35, Nørre Søgade
1370 Copenhagen K

FEDERAL REPUBLIC OF GERMANY
KUNST UND WISSEN ERICH BIEBER
Postfach 46, *7000 Stuttgart 1*

FINLAND
AKATEEMINEN KIRJAKAUPPA, P.O. Box 128
00101 Helsinki 10

FRANCE
DAWSON-FRANCE S.A., B.P. 40, *91121 Palaiseau*
OFFICE INTERNATIONAL DE DOCUMENTATION ET LIBRAIRIE, 48 rue Gay-Lussac
75240 Paris, Cedex 05

GERMAN DEMOCRATIC REPUBLIC
HAUS DER UNGARISCHEN KULTUR
Karl Liebknecht-Straße 9, *DDR-102 Berlin*

GREAT BRITAIN
BLACKWELL'S PERIODICALS DIVISION
Hythe Bridge Street, *Oxford OX1 2ET*
BUMPUS, HALDANE AND MAXWELL LTD.
Cowper Works, *Olney, Bucks MK46 4BN*
COLLET'S HOLDINGS LTD., Denington Estate,
Wellingborough, Northants NN8 2QT
WM DAWSON AND SONS LTD., Cannon House
Folkstone, Kent CT19 5EE
H. K. LEWIS AND CO., 136 Gower Street
London WC1E 6BS

GREECE
KOSTARAKIS BROTHERS INTERNATIONAL BOOKSELLERS, 2 Hippokratous Street, *Athens-143*

HOLLAND
FAXON EUROPE, P.O. Box 167
1000 AD Amsterdam
MARTINUS NIJHOFF B. V.
Lange Voorhout 9–11, *Den Haag*
SWETS SUBSCRIPTION SERVICE
P.O. Box 830, 2160 Sz Lisse

INDIA
ALLIED PUBLISHING PVT. LTD.
750 Mount Road, *Madras 600002*
CENTRAL NEWS AGENCY PVT. LTD.
Connaught Circus, *New Delhi 110001*
INTERNATIONAL BOOK HOUSE PVT. LTD.
Madame Cama Road, *Bombay 400039*

ITALY
D. E. A., Via Lima 28, *00198 Roma*
INTERSCIENTIA, Via Mazzé 28, *10149 Torino*
LIBRERIA COMMISSIONARIA SANSONI
Via Lamarmora 45, *50121 Firenze*
SANTO VANASIA, Via M. Macchi 58
20124 Milano

JAPAN
KINOKUNIYA COMPANY LTD.
Journal Department, P.O. Box 55
Chitose, *Tokyo 156*
MARUZEN COMPANY LTD., Book Department
P.O. Box 5050 Tokyo International, *Tokyo 100-31*
NAUKA LTD., Import Department
2-30-19 Minami Ikebukuro, Toshima-ku, *Tokyo 171*

KOREA
CHULPANMUL, *Phenjan*

NORWAY
TANUM-TIDSKRIFT-SENTRALEN A.S.
Karl Johansgata 43, *1000 Oslo*

POLAND
WĘGIERSKI INSTYTUT KULTURY
Marszalkowska 80, *00-517 Warszawa*
CKP I W, ul. Towarowa 28, *00-958 Warszawa*

ROUMANIA
D. E. P., *Bucuresti*
ILEXIM, Calea Grivitei 64–66, *Bucuresti*

SOVIET UNION
SOYUZPECHAT — IMPORT, *Moscow*
and the post offices in each town
MEZHDUNARODNAYA KNIGA, *Moscow G-200*

SPAIN
DIAZ DE SANTOS Lagasca 95, *Madrid 6*

SWEDEN
ESSELTE TIDSKRIFTSCENTRALEN
Box 62, *101 20 Stockholm*

SWITZERLAND
KARGER LIBRI AG, Petersgraben 31, *4011 Basel*

USA
EBSCO SUBSCRIPTION SERVICES
P.O. Box 1943, *Birmingham, Alabama 35201*
F. W. FAXON COMPANY, INC.
15 Southwest Park, *Westwood Mass. 02090*
MAJOR SCIENTIFIC SUBSCRIPTIONS
1851 Diplomat, P.O. Box 819074,
Pallas, Tx. 75381-9074
READ-MORE PUBLICATIONS, INC.
140 Cedar Street, *New York, N. Y. 10006*

YUGOSLAVIA
JUGOSLOVENSKA KNJIGA, Terazije 27, *Beograd*
FORUM, Vojvode Mišića 1, *21000 Novi Sad*

Index: 26.017